

# **HYDRAULIC PROCESSES CONTROLLING RECHARGE THROUGH GLACIAL DRIFT**

by

**MARK CUTHBERT**

A thesis submitted to  
The University of Birmingham  
for the degree of  
**DOCTOR OF PHILOSOPHY**

School of Geography, Earth and  
Environmental Sciences  
The University of Birmingham  
October 2005

UNIVERSITY OF  
BIRMINGHAM

**University of Birmingham Research Archive**

**e-theses repository**

This unpublished thesis/dissertation is copyright of the author and/or third parties. The intellectual property rights of the author or third parties in respect of this work are as defined by The Copyright Designs and Patents Act 1988 or as modified by any successor legislation.

Any use made of information contained in this thesis/dissertation must be in accordance with that legislation and must be properly acknowledged. Further distribution or reproduction in any format is prohibited without the permission of the copyright holder.

# ABSTRACT

The research aims to further the understanding of hydraulic processes governing recharge through glacial drift (superficial deposits) at a range of scales by investigating the Potford Brook catchment, Shropshire, UK. At the local scale (10s m to km), an original application of the electrical resistivity tomography (ERT) method and coring have enabled a better understanding of the drift architecture and conceptual hydraulic models of recharge to be derived. At the site scale (cm to 10s m) hydraulic and hydrochemical/tracer test data suggest that recharge occurs through preferential pathways in variably saturated till. Furthermore, near-vertical hydraulically active fractures, thought to result from desiccation/freeze thaw processes and infilled with material derived from clasts in the till, have been observed. This is some of the first evidence of hydraulically significant fracturing in British glacial till. The permeability of a 6 m thick till deposit is thus approximately one order of magnitude greater than the matrix permeability. Potential travel times of contaminants to the till water table (<2 mbgl) may be as high as 1 cm/d. In glaciofluvial deposits, preferential flow is also shown to be significant and lateral flow is caused by perching on underlying glaciolacustrine materials. The vertical flow to the sandstone aquifer through the glaciolacustrine deposits has been shown, for the first time, to be just a few mm/a. Aquifer recharge may be enhanced locally in areas of patchy till/glaciolacustrine deposits due to the delayed infiltration of lateral subsurface flows and runoff. Temperature effects on the resistivity of the shallow subsurface can be very significant complicating the interpretation of time series ERT images. The results have important implications for sustainable catchment management and aquifer vulnerability.

“I have yet to see any problem, however complicated, which when looked at in the right way, did not become still more complicated.”

Paul Anderson

# ACKNOWLEDGEMENTS

Thank you to the Natural Environment Research Council for funding this project.

Sincere thanks to my supervisors Rae Mackay and John Tellam for their encouragement, thoughtful advice and commitment throughout the project. Thanks to Ron Barker and Andy Baker for helpful advice on geophysics and tracers respectively. Many thanks to Richard Greswell and Roger Livesey for support on a whole range of practical issues, time in the field and hours spent slaving in front of a hot soldering iron. Thanks to Jon Weller, Ian Morrissey and Tabitha Sudworth for graciously bearing with urgent data requests, to the MSc students and undergraduates who supported various aspects of laboratory and fieldwork, to my fellow PhD students for the general banter and advice.

Thanks to staff at BGS, particularly Adrian Humpage for helping with core-logging and general wisdom regarding Quaternary geology, but also Adrian Lawrence, George Darling, John Bloomfield and Emma Tribe on a range of other issues. I also acknowledge support of Martin Shepley, Dave Johnson and Steve Fletcher from the Environment Agency and Mike Streetly from ESI in the opening stages of the project. Thank you to the landowners who kindly gave access to their land for fieldwork, in particular to Mr Udale and Mr Bromley, for allowing installation and access to the fieldsites.

Without the support of my family and friends I may have lost the plot by now. Particular thanks to Mum and Dad for putting me up (or should I say putting up with me?) on frequent stop-overs in Birmingham; Andy for your inspiration in many ways, not least that there is indeed life after a PhD. Tam you've been a constant source of support and encouragement. Thank you for the sacrifices you've made in letting me do this degree – you're the best. Gracie, what a wonderful gift you are too, thanks for bringing me back down to earth when hydrogeology seemed to be taking over my world.

Finally, thanks to the one 'in whom we live and move and have our being'. Without you there would be nothing to be curious about in the first place.....

# TABLE OF CONTENTS

<b>1</b>	<b>INTRODUCTION.....</b>	<b>1</b>
1.1	Context.....	1
1.2	Research Aims, Approach and Thesis Structure.....	3
1.3	Definitions.....	5
1.4	Previous research.....	6
1.4.1	Introduction.....	6
1.4.2	Glacial Till.....	6
1.4.3	Glaciofluvial Sediments.....	11
1.4.4	Glaciolacustrine Sediments.....	13
1.4.5	Preferential Flow in the Vadose Zone.....	13
1.4.6	Drainage and Interflow.....	14
1.4.7	UK Research.....	17
1.5	Looking Ahead.....	21
<b>2</b>	<b>THE HYDROGEOLOGY OF THE POTFORD BROOK CATCHMENT .....</b>	<b>23</b>
2.1	Introduction.....	23
2.2	Location, Topography and Drainage.....	23
2.3	Soils and Landcover.....	27
2.3.1	Landcover 2000.....	27
2.3.2	Soils.....	28
2.4	Geology.....	30
2.4.1	Introduction.....	30
2.4.2	Regional Geology.....	31
2.4.3	Brief Geological History: Solid Formations.....	31
2.4.4	Brief Geological History: Drift Deposits.....	35
2.4.5	Geology of the Potford Brook catchment.....	35
2.5	Meteorology.....	38
2.5.1	Rainfall.....	38
2.5.2	Evapotranspiration.....	41
2.5.3	Long Term Average Rainfall and PEt.....	44
2.6	Hydrogeology.....	45
2.6.1	Hydrogeological Map.....	45
2.6.2	The Permo-Triassic Sandstone Aquifer.....	45
2.6.3	Drift Properties.....	46
2.6.4	Groundwater Recharge.....	47
2.6.5	Groundwater – Surface water Interaction.....	51
2.6.6	Abstractions and Discharges.....	52
2.6.7	Groundwater Chemistry.....	54
2.6.8	Groundwater Hydrographs.....	54

2.7	<b>Hydrology</b> .....	59
2.8	<b>Summary</b> .....	63
2.9	<b>Conclusion</b> .....	64
<b>3</b>	<b>LOCAL SCALE INVESTIGATIONS</b> .....	<b>66</b>
3.1	<b>Aim</b> .....	66
3.2	<b>Experimental Design and Methodology</b> .....	66
3.2.1	Introduction .....	66
3.2.2	Geophysical Surveys .....	67
3.2.3	Invasive Sampling .....	73
3.2.4	Laboratory Analysis of Hydraulic Properties .....	78
3.3	<b>Results</b> .....	<b>84</b>
3.3.1	ERT Surveys .....	84
3.3.2	Augering and Sonic Drilling .....	96
3.3.3	Summary of Laboratory Results .....	98
3.3.4	Presentation and Discussion of Results for Main Drift Units .....	100
3.4	<b>Conceptual Recharge Models</b> .....	<b>112</b>
3.5	<b>Adequacy of Existing Drift Mapping</b> .....	<b>114</b>
3.5.1	Introduction .....	114
3.5.2	Comparison of Existing Mapping and Research Results .....	114
3.6	<b>Conclusions and Way Ahead</b> .....	<b>117</b>
<b>4</b>	<b>SITE SCALE INVESTIGATIONS 1: SITE INSTRUMENTATION AND MONITORING</b> .....	<b>119</b>
4.1	<b>Aim</b> .....	119
4.2	<b>Site Selection</b> .....	119
4.3	<b>Instrumentation</b> .....	<b>120</b>
4.3.1	Introduction .....	120
4.3.2	Piezometers .....	122
4.3.3	Tensiometers .....	125
4.3.4	Data Loggers .....	128
4.3.5	Soil Moisture Measurement .....	129
4.3.6	ERT Arrays .....	133
4.4	<b>Experimentation</b> .....	<b>145</b>
4.4.1	Introduction .....	145
4.4.2	Applied Tracer Experiments .....	145
4.4.3	Environmental Tracer Measurement .....	153
4.4.4	Infiltrometer Tests .....	155
4.4.5	Piezometer Hydraulic Tests .....	156
4.5	<b>Summary</b> .....	<b>157</b>

<b>5</b>	<b>SITE SCALE INVESTIGATIONS 2: SITE 1 RESULTS AND MODELS .....</b>	<b>158</b>
5.1	<b>Aim .....</b>	<b>158</b>
5.2	<b>Results .....</b>	<b>158</b>
5.2.1	Geology .....	158
5.2.2	Pressures .....	159
5.2.3	Moisture Content .....	169
5.2.4	Infiltrometer Tests .....	175
5.2.5	Piezometer Tests .....	177
5.2.6	Tracer Test .....	179
5.2.7	Hydrochemistry .....	180
5.2.8	ERT .....	186
5.2.9	Test Pit .....	196
5.3	<b>Conceptual Model of Hydraulic Processes .....</b>	<b>208</b>
5.4	<b>Numerical Models .....</b>	<b>210</b>
5.4.1	Introduction .....	210
5.4.2	1-D Single Porosity Model .....	212
5.4.3	2-D Fracture Block Model .....	213
5.4.4	1-D Equivalent Porous Media Model .....	219
5.5	<b>Conclusion .....</b>	<b>225</b>
<b>6</b>	<b>SITE SCALE INVESTIGATIONS 3: SITE 2 RESULTS AND MODELS .....</b>	<b>228</b>
6.1	<b>Aim .....</b>	<b>228</b>
6.2	<b>Results .....</b>	<b>228</b>
6.2.1	Geology .....	228
6.2.2	Pressures .....	230
6.2.3	Moisture Content .....	237
6.2.4	Infiltrometer Tests .....	246
6.2.5	Piezometer Tests .....	247
6.2.6	Tracer Test .....	252
6.2.7	ERT .....	254
6.2.8	Tritium Analysis .....	267
6.3	<b>Conceptual Model of Hydraulic Processes .....</b>	<b>267</b>
6.4	<b>Numerical Models .....</b>	<b>269</b>
6.4.1	Variable Saturation Model of Glaciolacustrine, Till and Sandstone Deposits .....	269
6.4.2	Model of Tritium Transport in Clay .....	275
6.4.3	Model of Outwash Deposits .....	278
6.5	<b>Conclusion .....</b>	<b>294</b>
<b>7</b>	<b>CONCLUSIONS AND RECOMMENDATIONS .....</b>	<b>296</b>
7.1	<b>Introduction .....</b>	<b>296</b>
7.2	<b>Discussion of Main Findings .....</b>	<b>296</b>
7.2.1	Site Scale (cm to 10s m) .....	296

7.2.2	Local Scale (10s m to km).....	300
7.2.3	Catchment Scale (km to 10s km).....	302
<b>7.3</b>	<b>Appraisal of Research Methodology and Contribution.....</b>	<b>303</b>
7.3.1	Methodology.....	303
7.3.2	Contribution.....	304
<b>7.4</b>	<b>Recommendations .....</b>	<b>306</b>
	<b>REFERENCES .....</b>	<b>309</b>
	<b>APPENDICES .....</b>	<b>325</b>

# LIST OF FIGURES

<b>Figure 2.1</b> Simplified geology map of the UK indicating the location of the study area and major aquifers	24
<b>Figure 2.2</b> Location map of the River Tern and Potford Brook catchments	25
<b>Figure 2.3</b> Digital terrain model of the Potford Brook catchment with draped geology	26
<b>Figure 2.4</b> Landcover 2000 map of the Potford Brook catchment at 25 m resolution	27
<b>Figure 2.5</b> Hydrogeological Map of the Potford Brook Catchment	29
<b>Figure 2.6</b> Solid geology of the River Tern catchment	32
<b>Figure 2.7</b> Drift geology of the River Tern catchment	34
<b>Figure 2.8</b> Cross sections A-A' and B-B' as shown in Figure 2.5	37
<b>Figure 2.9</b> Double mass plot for rainfall at Peplow (431312) and Shawbury (433710)	39
<b>Figure 2.10</b> Double mass plot for rainfall at Peplow (431312) and Bowling Green (T10)	41
<b>Figure 2.11</b> Double mass plot for PEt at Oakley Folly (T17) and Bowling Green (T10)	43
<b>Figure 2.12</b> Comparison of 2004 PEt for Oakley Folly (T17) and MORECS (sq 114 and 124)	43
<b>Figure 2.13</b> Annual total PEt (MORECS grass, sq 114 and 124) and Rainfall	44
<b>Figure 2.14</b> Groundwater abstraction (GWABS), surface water abstractions (SWABS) and surface water discharges (SWDIS) in the Potford Brook catchment	53
<b>Figure 2.15 A to B</b> Groundwater hydrographs in the Potford Brook catchment (monthly data)	56
<b>Figure 2.15 C to D</b> Groundwater hydrographs in the Potford Brook catchment (monthly data)	57
<b>Figure 2.16</b> Comparison of Radmoor and Hopton Corner hydrographs	58
<b>Figure 2.17</b> Mean daily stream flow for the Potford Brook at Sandyford Bridge with baseflow separations and groundwater levels at Wood Mill Farm (445)	60
<b>Figure 3.1</b> Photographs of the ERT equipment	71
<b>Figure 3.2</b> Sensitivity of ERT inversion to parameter variation	74
<b>Figure 3.3</b> Photographs of the Minute-Man auger (A) and drive-sampler (B)	77
<b>Figure 3.4</b> Photograph of the sonic drilling rig at Site 1	78
<b>Figure 3.5</b> Locations of ERT survey lines A to M	85

<b>Figure 3.6</b> Locations of augerholes around Hazles Farm (geology as for Figure 3.5)	85
<b>Figure 3.7</b> Locations of augerholes around Wood Farm and Site 1 (geology as for Figure 3.5)	86
<b>Figure 3.8</b> Locations of augerholes around Whitegates Farm and Site 2 (geology as for Figure 3.5)	86
<b>Figure 3.9</b> Interpreted ERT inversions with locations of augerholes	87-93
<b>Figure 3.10</b> Frequency distribution of Permo-Triassic sandstone resistivity at depth from resistivity depth soundings	94
<b>Figure 3.11</b> Summary of borehole logs	97
<b>Figure 3.12</b> Summary of permeameter tests for horizontal (H) and vertical (V) sample orientations	99
<b>Figure 3.13</b> Ternary diagram representing grainsize distribution by proportion of fine ( $<63 \mu\text{m}$ ), sand ( $63 \mu\text{m}$ to $2 \text{mm}$ ) and gravel+ ( $>2 \text{mm}$ ) size particles for different drift types	100
<b>Figure 3.14</b> Core from borehole S2_4 showing the transition from gravely sand (glacial outwash) into the underlying glaciolacustrine clay	101
<b>Figure 3.15</b> Exposure of glacial outwash material overlying Permo-Triassic sandstone at NGR SJ 582236	102
<b>Figure 3.16</b> Core from borehole S1_1 showing head, lodgement till and a sandstone cobble	105
<b>Figure 3.17</b> PSD data for the $<2 \text{mm}$ fraction of 12 till samples	105
<b>Figure 3.18</b> Photomicrographs of vertical (A) and horizontal (B) thin sections from S1_3 (crossed polars)	106
<b>Figure 3.19</b> Correlation between hydraulic conductivity and percentage of fines for 43 till samples	107
<b>Figure 3.20</b> Fracture in till within core from borehole S1_3	108
<b>Figure 3.21</b> Laminations in glaciolacustrine clay within core from borehole S2_4	110
<b>Figure 3.22</b> PSD data for the $<2 \text{mm}$ fraction of 6 glaciolacustrine clay samples	110
<b>Figure 3.23</b> Photomicrograph of a vertically oriented thin section from S2_4 (crossed polars)	111
<b>Figure 3.24</b> Conceptual recharge model schematics	112
<b>Figure 3.25</b> Hydrogeological drift domain map. Reproduced from Bridge <i>et al</i> (2002).	115
<b>Figure 4.1</b> Site 1 location plan	121
<b>Figure 4.2</b> Site 2 location plan	122
<b>Figure 4.3</b> Piezometer installation materials	124
<b>Figure 4.4</b> Photograph showing a tensiometer installation at Site 2	128

<b>Figure 4.5</b> TRIME TDR T3 probe and access tube	130
<b>Figure 4.6</b> Permanent ERT array (A) being installed (B)	135
<b>Figure 4.7</b> Volumetric water profiles used as forward model inputs	139
<b>Figure 4.8</b> Comparison of forward model inputs and inverted outputs	140
<b>Figure 4.9</b> Comparison of changes in forward model inputs and inverted outputs to the baseline model (a)	142
<b>Figure 4.10</b> Comparison of changes in predicted moisture contents between forward model inputs and inverted outputs and the baseline model (a) with no temperature correction applied	143
<b>Figure 4.11</b> Comparison of changes in predicted moisture contents between forward model inputs and inverted outputs and the baseline model (a) with a temperature correction applied	144
<b>Figure 4.12</b> Setting up the tracer experiment at Site 1	147
<b>Figure 4.13</b> Spectrophotometer calibrations for amino G acid	150
<b>Figure 4.14</b> Spectrophotometer calibrations for fluorescein	150
<b>Figure 4.15</b> EEM at PMT voltage of 725 for soil sample (20 to 30 cmbgl) in S2H1	153
<b>Figure 5.1</b> Schematic geological cross section of Site 2	159
<b>Figure 5.2</b> Time series of total pressure heads recorded at Site 1 piezometers and tensiometers	161
<b>Figure 5.3</b> Time series of groundwater levels recorded at Site 1 piezometers	162
<b>Figure 5.4</b> Time series of groundwater levels recorded at Site 1 piezometers from 1/11/04 to 11/03/05 alongside rescaled atmospheric pressure	163
<b>Figure 5.5</b> Soil tension recorded at Site 1 tensiometers at 5 minute intervals between 7/12/04 to 11/01/05	164
<b>Figure 5.6</b> Time series of average daily pressure heads recorded at Site 1 tensiometers	165
<b>Figure 5.7</b> Comparison of TDR and gravimetric moisture contents at Site 1	171
<b>Figure 5.8</b> TDR data for S1_M2 and S1_M3	172
<b>Figure 5.9</b> TDR data for S1_M1	173
<b>Figure 5.10</b> Relationship between moisture content and standard deviation in the three moisture content readings taken at each depth at different orientations at S1_M1	174
<b>Figure 5.11</b> Gravimetric moisture content profile for S1_1 and S1_2	176
<b>Figure 5.12</b> Infiltrometer tests results for Site 1	177

<b>Figure 5.13</b>	Piezometer falling head test results for S1_3	178
<b>Figure 5.14</b>	Piezometer falling head test results for S1_4	178
<b>Figure 5.15</b>	Tracer distributions at Site 1 after 108 days (S1_H2) and 126 days (S1_H3 and H4) since tracer application	180
<b>Figure 5.16</b>	Major ion, pH and TON profile for TE32	182
<b>Figure 5.17a</b>	ERT inversions for Site 1 survey line 1R	188
<b>Figure 5.17b</b>	ERT inversions for Site 1 survey line 1R	189
<b>Figure 5.18a</b>	ERT difference from 21/07/04 for Site 1 survey line 1R	190
<b>Figure 5.18b</b>	ERT difference from 21/07/04 for Site 1 survey line 1R	191
<b>Figure 5.19</b>	Relationship between moisture content and resistivity for a sample of till taken from an adjacent field to Site 1 (from Russell and Barker 2005)	192
<b>Figure 5.20</b>	Observed and modelled air and ground temperatures at Site 1 and T17 Oakley Folly	193
<b>Figure 5.21</b>	Sketch of west face of test pit	197
<b>Figure 5.22</b>	Sketch of north face of test pit (key as for Figure 5.21)	198
<b>Figure 5.23</b>	Sketch of south face of test pit (key as for Figure 5.21)	199
<b>Figure 5.24</b>	Photograph of features 1 and 2 shown in Figure 5.21	200
<b>Figure 5.25</b>	Photograph of feature 3 shown in Figure 5.21	200
<b>Figure 5.26</b>	Photograph of feature 4 shown in Figure 5.21	201
<b>Figure 5.27</b>	Photograph of feature 5 shown in Figure 5.21	202
<b>Figure 5.28</b>	Photograph of feature 6 shown in Figure 5.22	202
<b>Figure 5.29</b>	Perspective sketch of fractures in north face and base of test pit	205
<b>Figure 5.30</b>	Photograph showing the connectivity of fractures in north face and base of test pit	205
<b>Figure 5.31</b>	Schematic cross section of fracture distribution with depth	206
<b>Figure 5.32</b>	Sketch of fracture distribution in 3-dimensions	207
<b>Figure 5.33</b>	Photograph showing seepage from fracture in base of test pit	208
<b>Figure 5.34</b>	Initial conditions and results of 1-D single porosity model (S1_A)	214
<b>Figure 5.35</b>	Discretisation of model S1_B	214
<b>Figure 5.36</b>	Soil moisture characteristic curves and van Genuchten parameters for FAT3D-UNSAT models	215

<b>Figure 5.37</b> Initial conditions and results of 2-D model S1_B	216
<b>Figure 5.38</b> Results of 1-D equivalent porous medium model S1_C	222
<b>Figure 6.1</b> ERT survey across Site 2	229
<b>Figure 6.2</b> Schematic geological cross section of Site 2	229
<b>Figure 6.3</b> Soil tension recorded at Site 2 tensiometers at 5 minute intervals between 8/11/04 and 13/12/04	231
<b>Figure 6.4</b> Time series of average daily pressure heads recorded at Site 2 tensiometers	232
<b>Figure 6.5</b> Time series of average daily total pressure heads recorded at Site 2 piezometers and tensiometers	233
<b>Figure 6.6</b> Water table position (cmbd) within glacial outwash materials at Site 2 on 6/12/04	235
<b>Figure 6.7</b> Comparison of TDR and gravimetric moisture contents at Site 2	238
<b>Figure 6.8</b> Monthly TDR results from S2_M1	239
<b>Figure 6.9</b> Monthly TDR results from S2_M1	240
<b>Figure 6.10</b> Monthly TDR results from S2_M3	241
<b>Figure 6.11</b> Soil moisture (from nearby TDR) versus soil tension for Site 2 tensiometers	244
<b>Figure 6.12</b> Gravimetric moisture contents for Site 2 core samples	245
<b>Figure 6.13</b> Infiltrometer tests results for Site 2	247
<b>Figure 6.14</b> Piezometer falling head test results for S2_5	248
<b>Figure 6.15</b> Piezometer falling head test results for S2_6	249
<b>Figure 6.16</b> Piezometer falling head test results for S2_7	249
<b>Figure 6.17</b> Piezometer falling head test results for late time at S2_3	251
<b>Figure 6.18</b> Piezometer falling head test results for late time at S2_4	251
<b>Figure 6.19</b> Piezometer falling head test results for late time at S2_8	252
<b>Figure 6.20</b> Tracer distributions at Site 2 after 108 days (S2_H1) and 120 days (S2_H2 and H3) since tracer application	253
<b>Figure 6.21a</b> ERT inversions for Site 2 survey line 2W	255
<b>Figure 6.21b</b> ERT inversions for Site 2 survey line 2W	256
<b>Figure 6.22a</b> ERT difference from 23/07/04 for Site 2 survey line 2W	258
<b>Figure 6.22b</b> ERT difference from 23/07/04 for Site 2 survey line 2W	259

<b>Figure 6.23</b> Relationship assumed between volumetric water content and bulk resistivity based on Archie's law for $\varphi = 0.4$ , $m = 1.5$ , $a = 0.1$ and $n = 2$	260
<b>Figure 6.24a</b> ERT inverted moisture content for Site 2 survey line 2W	262
<b>Figure 6.24b</b> ERT inverted moisture content for Site 2 survey line 2W	263
<b>Figure 6.25a</b> ERT inverted moisture content changes from 23/07/04 for Site 2 survey line 2W	264
<b>Figure 6.25b</b> ERT inverted moisture content changes from 23/07/04 for Site 2 survey line 2W	265
<b>Figure 6.26</b> Results of 1-D variably saturated models of the lower part of the Site 2 drift profile	273
<b>Figure 6.27</b> Results of a 2-D variably saturated model of the lower part of the Site 2 drift profile	274
<b>Figure 6.28</b> Historic data for tritium in precipitation for the UK area. Data courtesy of IAEA (2004) Isotope Hydrology Information System (ISOHIS) Database: <a href="http://isohis.iaea.org">http://isohis.iaea.org</a> .	276
<b>Figure 6.29</b> Predicted tritium distribution within the glaciolacustrine clay for all model runs at the time of drilling (2004)	278
<b>Figure 6.30</b> Soil moisture characteristic curves for models s2upper1 and s2upper2	283
<b>Figure 6.31</b> Results of models s2upper1 and s2upper2	285
<b>Figure 6.32</b> Results of models s2upper3 and s2upper4	288
<b>Figure 6.33</b> Results of models PG1 and PG2	292

# LIST OF TABLES

<b>Table 2.1</b> Lithostratigraphy for the solid geology of the River Tern catchment	33
<b>Table 3.1</b> Synthetic groundwater recipe	79
<b>Table 3.2</b> Ionic concentration of synthetic groundwater as calculated from the recipe in Table 3.1	80
<b>Table 3.3</b> Phase proportions (values in weight %) determined by XRD analysis	106
<b>Table 3.4</b> Description of hydrogeological drift domains	115
<b>Table 4.1</b> Piezometer construction details	125
<b>Table 4.2</b> Tensiometer installation depths	127
<b>Table 4.3</b> TDR tube depths	132
<b>Table 4.4</b> Model parameters for layer 1	138
<b>Table 5.1</b> CFC results for TE32 at Site 1	184
<b>Table 6.1</b> van Genuchten parameters used in variably saturated models of the lower part of the Site 2 drift profile	271
<b>Table 6.2</b> Root zone parameters for model s2upper 1 and s2upper2	282
<b>Table 6.3</b> Root constant and wilting points for models PG1 and PG2	293

# 1 INTRODUCTION

## 1.1 Context

Understanding the processes involved in groundwater recharge is crucial to both water resources studies and aquifer vulnerability assessments (Robins 1998). Estimation of recharge is essential in water balance and modelling approaches to quantify groundwater resource availability (Jackson and Rushton 1987; Rushton *et al.* 1988; Bradbury and Rushton 1998). Furthermore, knowledge of recharge flux and velocity can be integrated with other data to assess the vulnerability of an aquifer unit to recharge-mediated contamination (Sears 1998; McMillan *et al.* 2000).

Fundamental to the estimation of recharge for these applications is the understanding of a complex set of hydraulic processes which control subsurface flows. In order to understand these processes some knowledge of meteorology, soil physics, land use, plant physiology, topography, drainage and the influence of any drift (superficial) deposits is required (Hulme 2002). Although these aspects have been addressed in existing literature (Rushton and Ward 1979; Lerner *et al.* 1990; Hulme *et al.* 2001; Hulme and al 2002; Scanlon *et al.* 2002), many authors note the difficulties in recharge estimation due to uncertainties in measured climatological variables, the lack of data to understand soil zone processes and the unknown influence of drift deposits (Lloyd 1980; Lerner *et al.* 1990). It is the influence of the drift on groundwater recharge that is the subject of this thesis.

A covering of drift deposits of variable lithology is found across much of the mid-latitudes as a result of glacial, periglacial and fluvial deposition over the last several thousand years (Lloyd 1983). These deposits often have hydrogeological importance in terms of influencing runoff and evaporative processes, and in modifying the timing, magnitude and chemistry of

recharge reaching underlying aquifers. Although recent research has begun to address the issue, what is currently not well understood is the field-scale flow regime in drift deposits (particularly in heterogeneous and clay-rich deposits) and the relative importance of various pathways (e.g. fractures, sedimentary structures) in contributing to horizontal and vertical groundwater fluxes. Regional groundwater studies often rely on simple assumptions about recharge in drift-covered areas based on field mapping and data from widely spaced boreholes. However, this is frequently because the processes operating at the local scale are poorly understood and suitable measurements are not collected. Current mapping of drift deposits does not often enable an understanding of the subsurface hydraulic processes controlling recharge to be developed.

Clearly if the flow processes are not well understood then this can lead to significant uncertainty in groundwater resource assessment in drift covered areas. Furthermore, contaminant transport calculations can become even more problematic making decisions about aquifer vulnerability harder to justify.

A recent driver for the research is the implementation of the EU Water Framework Directive (Official Journal (OJ L 327), 22 December 2000) which stipulates in Section 2.1 “Initial Characterisation” that member states should identify:

“the general character of the overlying strata in the catchment area from which the groundwater body receives its recharge,”

Furthermore in Section 2.2 “Further Characterisation” is required:

“...of those groundwater bodies or groups of bodies which have been identified as being at risk in order to establish a more precise assessment of the significance of such risk and

identification of any measures to be required under Article 11. Accordingly, this characterisation shall include relevant information on the impact of human activity and, where relevant, information on.....characteristics of the superficial deposits and soils in the catchment from which the groundwater body receives its recharge, including the thickness, porosity, hydraulic conductivity, and absorptive properties of the deposits and soils”.

A better understanding of the hydraulic processes governing recharge and the relationship between flow behaviour and geological structure is needed to meet the requirements of the directive.

The research presented in this thesis is funded by the Natural Environment Research Council (NERC) as part of the LOCAR (Lowland Catchment Research) thematic programme. LOCAR is a five-year programme of research into key water resource issues in three areas, the Pang and Lambourn catchments in Berkshire, the Frome and Piddle catchments in Dorset and the Tern catchment in Shropshire. The research for this thesis was carried out in the catchment of the River Tern, a tributary to the River Severn.

## **1.2 Research Aims, Approach and Thesis Structure**

The research aims to further the understanding of hydraulic processes governing recharge through glacial drift at a range of scales by pursuing the following objectives:

- To ascertain the hydrogeological significance of glacial drift on recharge within the Potford Brook catchment
- To assess the current uncertainty in estimating the distribution and magnitude of recharge through drift at the catchment scale (km to 10s km) and to identify the main causes of this uncertainty

- To define the geometry and hydraulic properties of, and spatial relationships between, the main structural elements of the glacial drift within the catchment with the purpose of identifying recharge pathways at the local scale (10s m to km)
- To quantitatively describe the hydraulic processes controlling recharge through till, glaciolacustrine and glaciofluvial outwash deposits at the site scale (cm to 10s m)

The research strategy has been to focus on a small drift covered catchment in Shropshire, UK, in 3 stages of progressive scale refinement from the catchment scale, through the local scale to the site scale.

The structure of the thesis reflects the staged approach to the research and begins with an introduction to the study area in Chapter 2. As well as giving a context to the rest of the thesis, this chapter is focussed on ascertaining the hydrogeological significance of the drift on recharge and hence on the catchment water balance by bringing together existing data and observations from the literature. The climatological features of the area are also introduced here for use in later modelling work.

Chapter 3 describes the methods and results of field and laboratory work carried out to define the main structural elements of the drift at the local scale in terms of geometry and hydraulic properties. Local scale conceptual recharge models are also presented.

Chapter 4 introduces the research carried out at the site scale by describing the geology, instrumentation and experimental methods used at two fieldsites located in contrasting geological environments. Chapters 5 and 6 then describe the results and models derived for each site respectively. The hydraulic processes operating at each site are quantitatively described but upscaling to the local and catchment scale has not been attempted.

Chapter 7 draws together the main findings of the thesis, discusses their implications and recommends areas for further research.

The remainder of this chapter, however, concerns the context of the present research in the general corpus of knowledge in the field.

### **1.3 Definitions**

Since the topic of recharge is the focus of the thesis it is appropriate to define the term at the outset. A general definition of recharge is ‘the flow of water forming an addition to a groundwater reservoir’ (Lerner *et al.* 1990; Vries and Simmers 2002). Hence the word recharge may need to be prefixed as necessary by the hydrogeological unit into which water is entering. For example, ‘glacial outwash recharge’ or ‘sandstone aquifer recharge’.

In the UK hydrogeological community it is common for the terms potential and actual recharge to be used. Potential recharge is normally defined as the amount of water that is available for recharge from the soil zone, and equates to rainfall less runoff less evapotranspiration (Rushton *et al.* 1988). This amount may be greater than the actual recharge if, for instance, the aquifer in question is ‘full’ or significant lateral interflow takes place before water reaches the water table.

The term drift is commonly used in the UK due to the historic use of the word by the British Geological Survey (BGS). Both glacial and alluvial deposits have been traditionally referred to as drift, a term first introduced early in the nineteenth century. However, BGS now uses this term to represent all superficial deposits including man made (artificial) deposits (McMillan *et al.* 1999). This is the sense in which the word drift will be used in this thesis.

## **1.4 Previous research**

### **1.4.1 Introduction**

The pioneering work into the hydrogeological significance of glacial deposits was carried out in the 1960s. Since then a large body of literature has been generated. Much of the energy has been concentrated on glacial till deposits due to their dominance in terms of areal coverage, and since their significance as potential aquitards for aquifer protection and their potential to limit aquifer recharge have become increasingly important issues.

### **1.4.2 Glacial Till**

#### **1.4.2.1 Introduction**

Debris deposited directly by a glacier is known as ‘till’. Till is a diamicton which is a non-genetic term for a non-sorted or poorly sorted unconsolidated sediment that contains a wide range of particle sizes (Bennett and Glasser 1996). An over-consolidated mass of sediment deposited by slow incremental build up of basal glacial debris is known as ‘lodgement till’. Melting of ice at the glacier margins causes debris to be deposited as ‘flow till’ whereas the slow melting of buried ice beneath such tills leads to in situ deposition of what are known as ‘melt-out tills’ (Catt 1986).

Till genesis influences the geotechnical properties of tills through its control, for example, on grain-size distribution, stress history and jointing. Post-depositional processes are also important (Boulton and Paul 1976). These factors influence the bulk permeability which is a major geological control on recharge through such deposits. The quantification of this parameter is thus the focus of most research in this area.

#### **1.4.2.2 Fracturing**

Early research quickly identified the issue of scale dependence of hydraulic conductivity in till deposits. Many studies report the results of core-scale laboratory tests on samples of

glacial tills yielding hydraulic conductivity sometimes as low as  $1 \times 10^{-10}$  m/s (Keller *et al.* 1986; Fredericia 1990; Jensenn 1990; McKay *et al.* 1993; Klinck *et al.* 1996; Klinck *et al.* 1997; Gerber and Howard 2000; Gerber *et al.* 2001). Field measurements of hydraulic conductivity (e.g. slug tests) are also reported alongside core-scale laboratory values and often produce results several orders of magnitude greater than laboratory values measured at equivalent locations (Keller *et al.* 1986; Fredericia 1990; McKay *et al.* 1993; McKay and Fredericia 1995; Klinck *et al.* 1996; Klinck *et al.* 1997; Gerber *et al.* 2001).

An early publication giving evidence for the influence of fractures on the movement of groundwater through glacial till was by Williams (1967). The presence of fractures which provide pathways for preferential flow has been used to explain this scale dependence of hydraulic conductivity measurement ever since. It should be noted that where this effect is not observed it cannot be taken as reliable evidence of the absence of such pathways or fractures for two main reasons. First, the sampled volume is small and may happen to not intersect such a feature (Ortega-Guerrero *et al.* 1999). Second, smearing due to drilling techniques may mask the effects of such features (D'Astous *et al.* 1989). Since drilling is an inefficient method of investigating fractures due to the small volume sampled, test pits of a variety of sizes and designs have been excavated by many researchers to allow a more detailed fracture mapping to be carried out (Christy *et al.* 2000). Very detailed fracture distributions have been obtained using large excavations such as those described by Jakobsen and Klint (1999) and Klint and Gravesen (1999).

The only reliable visual evidence of hydraulically active fractures is the presence of secondary minerals on the fracture faces forming cements and coatings. In some cases, such

mineralization may potentially decrease the permeability of the fracture and provide additional surface reactivity for potential contaminant retardation (Corrigan *et al.* 2001).

Possible mechanisms for the origin of fractures within till units are desiccation, freeze-thaw cycles, shearing in response to overriding ice, stress relief due to removal of ice loading, crustal rebound, regional tectonic stresses and volume changes due to geochemical processes (Haldorsen and Kruger 1990; McKay and Fredericia 1995). Although the most intense fracturing is often associated with the oxidised weathered zone of the upper few metres, fractures have been found to extend significantly deeper than this zone to depths greater than 10 m (Ruland *et al.* 1991) and as deep as 21 m (Grisak *et al.* 1976).

Further evidence for preferential flow pathways has come from the use of applied and environmental tracers, in particular the presence of tritiated water at much greater depths than would be expected due to flow through the low permeability matrix alone (Keller *et al.* 1986; Hendry 1988; Keller *et al.* 1988; D'Astous *et al.* 1989; Ruland *et al.* 1991; Gerber *et al.* 2001). Dating of older water from aquifers underlying till sequences has also been used to assess the rate of vertical groundwater flow (Cravens and Ruedisili 1987; Hendry 1988). Stable isotopes have been used effectively to characterize the hydrogeology of a till aquitard (Remenda *et al.* 1996; Hendry *et al.* 2004).

Although the most reported method of measuring the bulk permeability of till has been short term piezometer or auger hole slug tests, it has also been investigated by a variety of different methods. For example, from the analysis of the downward propagation of pressure variations induced by seasonal water table fluctuations (Keller *et al.* 1989; Neuman and Gardner 1989), regional groundwater modelling (Gerber and Howard 2000) and pumping tests on the formation itself (Jones *et al.* 1992) or the underlying aquifer (Cartwright 2001). A useful

review of methods for determining the permeability of shallow aquitards is given by van der Kamp (2001).

Fracture flow models such as FRACTRAN have been applied to modelling flow through till in saturated conditions (Klinck *et al.* 1996; Gerber *et al.* 2001). Unsaturated preferential flow modelling has also been successfully attempted for glacial till soils (Villholth and Jensen 1998b; Gerke and Kohne 2004).

#### **1.4.2.3 Other controls on permeability**

In addition to fractures the literature points towards other structural factors in controlling the hydraulic conductivity of tills such as the depositional mode and post-depositional processes (Haldorsen and Kruger 1990). Directional relations between sorted lenses and bands which have higher permeability may define preferential flow routes through the sample. Furthermore, hydraulic conductivity may be greater in the direction parallel to the dominant long axis orientation of till clasts. It is noted that such relationships between fabric and permeability in glacial deposits are simply a special case of similar phenomena reported for a range of other geological strata (Rowe 1972).

Whereas previous work had concentrated on fracture flow in tills, Gerber *et al.* (2001) showed the importance of aquifer heterogeneity and stratigraphic architecture in controlling vertical flow paths. Vertically oriented sedimentary structures such as sand dykes and dipping erosional surfaces along with fractures may provide the primary vertical interconnecting pathways between interbeds. This is a long established conceptual model based on borehole cores, geophysics and observations of drift outcrops.

There are clearly links between the genesis of drift deposits and their hydrogeological properties (Boulton and Paul 1976; Nyborg 1989; Haldorsen and Kruger 1990). However,

no-one has yet developed a genetic model of sedimentary processes for glacial drift deposits that can generate facies for hydrogeological modelling. Indeed, simulations of fluvial sedimentary processes are still in their infancy and realistic modelling of the flow of water and sediment transport in streams over thousands of years is only just becoming possible (Bunch *et al.* 2004). The complications of sediment deposition in the glacial environment are surely even more challenging and it remains to be seen whether genetic models can be of use in understanding drift hydrogeology.

Certain studies have shown the potential use of applying lithofacies descriptions and architectural element analyses to understanding the hydraulic processes relevant to recharge which may operate within till sequences (Anderson 1989; Haldorsen and Kruger 1990; Boyce and Eyles 2000). However, it must be noted that such approaches require very extensive multi-parameter subsurface and outcrop datasets and thus are not possible within the budgets and timescales of many studies (Boyce and Eyles 2000). A study of the Lower Mersey Basin by the University of Birmingham (1981) is an early example of a relatively low cost investigation involving drift lithofacies distributions.

In addition to structural controls on the hydraulic conductivity of till, it is thought that weathering processes contribute to the development of preferential pathways for groundwater recharge. A weathering scheme for lodgement tills was defined by Eyles & Sladen (1981) who distinguished four weathering zones. They divided weathering action into chemical processes (oxidation, hydration, leaching of carbonates and soluble salts) and mechanical processes (disintegration and breakdown of particles, change of till structure by fracturing and downward movement of fine particles) (Klinck *et al.* 1997). Burrowing and root-hole development may be other contributing factors (Klint and Gravesen 1999).

Several studies have found that weathered till may be several orders of magnitude more permeable than equivalent unweathered till (Cravens and Ruedisili 1987; D'Astous *et al.* 1989; Klinck *et al.* 1996; Klinck *et al.* 1997). This more permeable weathered zone may extend as far as 18 m in the Prairie region of Canada (Hendry 1988) although depths of less than 8 m are more commonly reported in other areas (Cravens and Ruedisili 1987; Ruland *et al.* 1991; McKay *et al.* 1993; Klinck *et al.* 1996; Klinck *et al.* 1997).

The importance of macropores in soils, such as fractures, root holes and burrows, was outlined by Beven and Germann (1982). They showed that their presence may lead to spatial concentrations of water flow through soil that will not be described well by a Darcy approach and that this has important implications for the rapid movement of solutes and pollutants through soils.

### **1.4.3 Glaciofluvial Sediments**

Glaciofluvial deposition occurs where sediment is laid down by streams above, within or beneath a glacier or along meltwater discharge routes beyond the ice margin. Outwash plains (or sandar) are deposited by braided systems of meltwater streams which migrate to and fro and can build up extensive gravel, sand and silt accumulations with gently sloping surfaces (Catt 1986).

Although much of the literature focuses on the role of till in controlling recharge in glaciated areas, there has been increasing scientific attention in the past ten years on the hydrogeological modelling of fluvial sediments (Heinz *et al.* 2003).

Since the pioneering work by Anderson (1989) and Fogg (1986) many papers have been produced on the hydraulic modelling of heterogeneous sediments drawing on the sedimentological work of, for example, Allen (1983) and Miall (1984).

A range of methodologies have been developed for understanding heterogeneity in fluvial sediments and many applications made in glacial contexts. Koltermann and Gorelick (1996) give an extensive review of methods choosing to divide simulation tools into three categories: structure-imitating, process-imitating and descriptive. From a hydrogeological perspective useful overviews of many of these methods for representing the heterogeneity of geological properties are given in Fraser and Davis (1998), de Marsily (1998) and Mackay and O'Connell (1991).

A popular approach is to integrate available field data to gain an appreciation of the 3-D architecture of the various elements of a drift sequence. The application of geophysical techniques can greatly enhance such architectural definition (Aspiron and Aigner 1999; Beres *et al.* 1999; Ekes and Hickin 2001). When carried out alongside an appreciation of the original deposition environment and subsequent post-depositional processes, an understanding of the potential pathways for flow and permeability contrasts can be gained contributing to a robust conceptual model for flow and hence recharge processes.

Such an approach has been taken by, for example, Iversen *et al.* (2004). They defined lithofacies for glaciofluvial deposits on the basis of texture, sorting, bedding style and external boundaries and related these to hydrofacies having relatively homogeneous hydrogeological properties. This has enabled them to derive realistic 2-D numerical models for flow in the unsaturated zone to study the recharge processes and the potential leaching of pesticides through glaciofluvial material. An important result from this study is that features such as inclined coarse gravel/sand lenses can generate preferential flow patterns with obvious implications for contaminant migration. This modelling work illustrates the concept of funnelled flow, a preferential flow mechanism described by Kung (1990a) based on field

observations from dye tracing experiments conducted in layered glacial outwash deposits (Kung 1990b).

#### **1.4.4 Glaciolacustrine Sediments**

Lakes may occur beneath, within or above glaciers and others may form at or beyond the ice margin. The latter may be dammed by the ice itself or by morainic ridges. Glaciolacustrine sediments are often fine grained and are deposited by either slow settling from suspension in the lake water or more rapidly when inflows of cold detritus-laden meltwater spread over the lake floor (Catt 1986).

Glaciolacustrine sediments often have limited areal extent and possibly as a result they have received relatively little direct attention in the literature. Owing to the low energy depositional environment they are often dominated by silt and clay grade particles and can have vertical hydraulic conductivities as low as  $6 \times 10^{-11}$  m/s (Wealthall *et al.* 1997). A recent study into TCE diffusion through a 20 m thick clayey silt aquitard of glaciolacustrine origin showed low groundwater velocities of just 2 to 3 cm/a (Parker *et al.* 2004). However, coarser glaciolacustrine deposits may also occur with hydraulic conductivities as high as  $1.4 \times 10^{-4}$  m/s (McMillan *et al.* 2000). The consideration of glaciolacustrine sediments as a component part of wider studies within drift covered catchments shows that they can be associated with perched water tables (Artimo *et al.* 2003) consistent with their low permeability.

#### **1.4.5 Preferential Flow in the Vadose Zone**

The idea of non-uniform flow through the vadose zone goes back at least to comments about soil macropores by Schumacher (1864) (cited in Beven and Germann (1982)). Over time, the body of literature on the subject of preferential flow (as opposed to uniform flow) has steadily grown, and various mechanisms suggested for how water can move rapidly through the unsaturated zone while bypassing a proportion of the porous matrix. At least three main types

of phenomena can be distinguished. The first is non-capillary flow in continuous structural voids (root holes, burrows, fractures and other discontinuities) that has already been mentioned (Beven and Germann 1982), or through locally high conductivity in capillary sized pores. The second type is the funnelling effect due to, for example, inclined coarse sand layers in interbedded soil profiles which can result in irregular concentrations of flow (Kung 1990a; Kung 1990b) as described above. In fractured media, a similar effect can also occur at the intersection of fractures as described by Pruess (1999). The third type is related to flow instabilities of wetting fronts under certain conditions, most usually in layered soils, during infiltration. A useful review of unstable flow in layered soils is given by Hillel (1987) of which the following is a brief summary. The wetting front, instead of remaining horizontal, may form bulges called fingers, which may propagate downwards to become vertical pipes. Profile layering is not a pre-requisite for wetting front instability which may be due to increased air pressure ahead of the wetting front or to water repellency of the soil. However, fingering behaviour is particularly associated with transitions from finer to coarser textured layers. Under natural conditions the non-uniform nature of flow in the vadose zone may be compounded by non-uniform inputs to the soil as a result of, for example, stem-flow and concentrations of surface water (Beven 1991).

The result of these widely reported preferential flow phenomena is the movement of water (and solutes) to greater depths at greater speeds than would be predicted by theory based on the Richards equation (Richards 1931), applied on the basis of area averaged moisture content and potential variables (Beven 1991).

#### **1.4.6 Drainage and Interflow**

Water held up in the upper parts of a sediment profile can be lost through a combination of capillary and evaporative effects (Hendry 1988). However, local lateral flow to streams,

ditches and ponds is also likely in certain contexts (Cravens and Ruedisili 1987; McKay *et al.* 1993).

These observations are consistent with the interpretation of surface water hydrographs from rivers and streams draining drift covered catchments. It is commonly seen that components of flow exist over timescales ranging from almost immediate surface runoff (assumed to include overland flow and rapid throughflow) to the much slower aquifer response to groundwater recharge (Soley and Heathcote 1998). Intermediate between these end members is an ill-defined component sometimes termed interflow which includes water draining from superficial drift deposits commonly on a timescale of several days to weeks. In drift covered catchments it is assumed that this flow is caused by some mechanism within the drift to divert water laterally into streams without it reaching the underlying aquifer (Hinton *et al.* 1993; Heathcote *et al.* 2003).

In many catchments this may be a legitimate process to incorporate into a groundwater model. However, caution is required to make sure that the magnitude of such interflow is physically plausible considering the horizontal hydraulic gradient and hydraulic conductivity of the location in question. The reason this is sometimes overlooked is that ‘potential recharge’ (in the sense of Rushton, Kawecki *et al.* (1988)) may be calculated using a soil zone model. At certain times this quantity may be greater than can infiltrate into the underlying formation and interflow may be generated as an amount of ‘rejected recharge’.

Research has shown that in an area covered by drift deposits there are several ways by which land drainage activities may influence the natural recharge to an underlying aquifer. Holman *et al.* (2002) have shown that:

- Drainage may lower perched water tables hence reducing vertical gradients driving groundwater recharge into the underlying aquifer. This effect may be greater where low permeability drift is thinner and/or the underlying aquifer has a relatively high piezometric surface, since a change in water table will lead to a relatively greater change in the vertical hydraulic gradient.
- Land use conversion made possible by improved drainage may lead to a change in the rate of evapotranspiration and hence water available for recharge.
- Moling and subsoiling may affect the flow regime in the unsaturated zone by increasing fracturing. Moling is carried out by forming a channel using a piece of 75-mm diameter bullet-shaped metal mounted at the end of a leg which is towed through the soil. Subsoiling is the act of loosening the subsoil with a suitably shaped tine pulled horizontally through the subsoil and is normally carried out at a very frequent spacing of 60 to 100 cm.
- Lower water tables due to drainage may lead to an increase in available storage in the unsaturated zone. This may reduce the rate of runoff and the timing of infiltration to the water table.
- Soakaway drainage may increase the infiltration of runoff by providing a more permeable pathway to the underlying aquifer in areas of thin drift.

Overall it is commonly found that improved drainage leads to a reduction in surface runoff with a concomitant increase in ‘baseflow’ to streams. This baseflow may more helpfully be termed interflow or ‘drift baseflow’ since it is not necessarily discharge from the underlying

aquifer. This equates to a smoothing of the stream hydrograph due to the greater storage and travel times of water passing through the system.

#### **1.4.7 UK Research**

##### **1.4.7.1 Focussed field investigations**

The first substantial investigation into drift hydrogeology in the UK was carried out in a small experimental catchment in the Holderness area of East Yorkshire in the late 1960s by M. Bonell. The following summary is based on the series of papers and reports generated from the study (Bonell 1972a; Bonell 1972b; Bonell 1973; Visvalingham 1974; Bonell 1976; Bonell 1978). Data from textural analysis, temporal hydrograph responses and spatial head distributions, meteorological measurements and hydraulic well tests were integrated to characterise the shallow groundwater movement within weathered till materials (down to around 5 m depth) and associated patches of glacial outwash. The weathered till was found to be vertically jointed with an average bulk hydraulic conductivity of around 1.3 cm/d ( $1.5 \times 10^{-7}$  m/s) overlying an unweathered parent till thought to be practically impermeable.

The most notable result of the study was the surprisingly quick and high magnitude response of shallow boulder clay wells to rainfall events even during times of substantial soil moisture deficit. The dominant mechanism thought to explain this response was a temporary perching of water in the soil A horizon leading to quick lateral flow into the well. The relatively slow recession then seen in the well hydrograph is explained by gradual drainage from the well into the till formation. In the absence of a well it is hypothesised that water infiltrating the soil perches in the A horizon temporarily before gradually draining through the underlying clay pan into the permanently saturated C horizon (weathered till). Overland flow was not observed in the catchment and interflow was thought to be negligible due to the low hydraulic conductivity and insufficient room for the development of the head gradients to drive such

lateral flows. Another important observation made in the study was the lack of correlation between saturated hydraulic conductivity and texture of the boulder clay (Bonell 1976).

Although this pioneering work took important first steps in understanding the hydraulic processes operating in glacial till, as retrospectively appreciated by Bonell (1978), the conclusions were limited by a lack of tension and soil moisture content measurements which could have greatly enhanced the conclusions drawn by the study. Also, since the study was restricted to the shallow groundwater system little consideration was given to recharge to the underlying Chalk aquifer.

Since the 1970s there have been several other focussed investigations on recharge through drift in the UK. A study of Hall Farm, Norfolk was undertaken using cored boreholes, trial pits, field and laboratory permeability testing and geochemistry to investigate the hydrogeology of till overlying Chalk (Klinck *et al.* 1996; Klinck *et al.* 1997). They found that there were upper and lower oxidised zones (5 to 6 m thick) and a central 7 m unoxidised zone within the till. Fracturing was evident through the profile being less dense but still evident in the unoxidised zone. The upper weathered till hydraulic conductivity was found to be 2 to 3 orders of magnitude greater than that of the unweathered till, the density of fractures being used to explain this result. Recharge through the till was estimated to be around 29 to 40 mm/a based on analytical and numerical modelling using FRACTRAN (Klinck *et al.* 1996).

Further investigation in East Anglia has recently been carried out using cored boreholes, groundwater level monitoring and hydrochemistry including tritium and CFC analysis (Marks *et al.* 2001; Marks *et al.* 2004). This work indicates that the till has a significant impact on Chalk recharge quantity and distribution with recharge through the interfluvial areas being

probably less than 20 mm/a and possibly as low as 5 mm/a. Recharge at the edge of the till sheet however is thought to be enhanced by recharge of runoff water generated over till cover. This conceptual model is in broad agreement with earlier work based on hydrochemical facies analysis (Lloyd *et al.* 1981; Jackson and Rushton 1987; Lloyd and Hiscock 1990; Hiscock 1993) which makes use of the significance of drift deposits (in this and other areas of the country) in modifying groundwater chemistry in regional aquifers (Spears and Reeves 1975; Sage and Lloyd 1978; Heathcote and Lloyd 1984).

As part of the British Geological Survey's (BGS) Hydrogeological Classification of Superficial Clays programme, a series of investigations were made into the characterisation of till and glaciolacustrine clays in Shropshire (Wealthall *et al.* 1997). The programme was very successful in terms of characterising the geology at several sites and quantifying the hydraulic and hydrochemical characteristics of the deposits. There was also an attempt to quantify the recharge through the drift to the underlying sandstone aquifer at the Bacon Hall site (McDonald 1996) (see Figure 2.7 for location). However, the conclusions of this study are uncertain as the frequency of data to which the zero-flux method were applied were inadequate and no account was taken of lateral flows within the 2 m thick upper sand horizon lying above the till which seem likely to have been occurring (see Section 2.6.4 for further discussion).

As part of the assessment of the performance of a potential deep repository for radioactive waste at Sellafield, investigations into the nature and significance of the overlying Quaternary deposits were carried out. Baker (1994) carried out slug tests, fracture mapping of test pits and infiltration tests and suggested a hierarchy of approaches for examining groundwater flow and transport in a clay unit. On a larger scale McMillan *et al.* (2000) rationalised the complex

sequence of drift deposits into a series of domains each with their own upscaled hydrogeological properties for use in a groundwater model. They found that in some areas there was no significant impediment to recharge to (or discharge from) the underlying aquifer but in local areas recharge (or discharge) is considerably impeded.

#### **1.4.7.2 Regional groundwater modelling studies in drift covered areas**

Regional groundwater models have been developed in many areas in the UK that are covered or partially covered by glacial drift and it is noted that for many studies recharge through drift is poorly understood and represents an area of major uncertainty. Many of these models work on the basis of calculating groundwater recharge outside of the groundwater flow model using a soil moisture accounting model such as Penman-Grindley (Lerner *et al.* (1990) and references therein), FAO (Rushton 2000; Hulme *et al.* 2001; Hulme 2002) or FLRM (Ragab *et al.* 1997) to calculate a value for ‘potential recharge’. If the bulk permeability of any intervening drift between the soil zone and the aquifer is low enough the resulting ‘actual recharge’ may be less than the potential amount. Hulme *et al.* (2001) and Hulme (2002) provide good overviews of this type of approach.

The way in which the potential recharge signal is thought to be modified in the presence of drift varies. A common approach taken in regional studies in the past is the use of so called ‘recharge factors’ as described for the Lincolnshire Limestone by Rushton (1975). The potential recharge is multiplied by a factor between 0 and 1 depending on how much the underlying geology is thought to impede recharge to the aquifer. A commentary of this method is given by several authors describing work done on the Lower Mersey Basin, Cheshire/Lancashire (University of Birmingham 1981; Lloyd 1983; Rushton *et al.* 1988; Hulme *et al.* 2001; Hulme 2002) which also included the dependence of recharge on head gradients across the drift. Recharge factors have also been applied successfully to the drift

covered Chalk catchment around Redgrave Fen, East Anglia (Soley and Heathcote 1998) and used in a variety of other regional water resource studies (SRA 1974). In other cases a unit hydraulic gradient has been assumed and recharge set equal to the bulk permeability of the drift materials overlying the aquifer. Another more complex approach is the use of stores with associated daily flow limits and decay constants which has recently become standard practice for calculating recharge for use in regional water resources models used by the Environment Agency. The potential recharge is sent to an interflow store (representing the drift) which restricts the amount of recharge to the groundwater model via a daily recharge limit nominally based upon the vertical permeability of the drift deposits. This interflow store may drain laterally to become surface water for example under a linear decay constant. The Environment Agency has recently introduced the idea of an overflow limit for the interflow store (based on the fact that the drift may 'fill up' with water under certain conditions). If the interflow store is full any subsequent potential recharge becomes surface water flow (Whittaker 2004).

The amount of potential recharge left over once the actual recharge has been subtracted is then assumed to discharge to drains and surface watercourses. In some catchments it is thought that runoff-recharge (equivalent to the runoff-runon phenomenon in hydrological literature e.g. Smith *et al.* (2002)), for instance at the edge of a till sheet, may represent a significant part of the total recharge (Jackson and Rushton 1987; Cuthbert and Soley 2000). This process, along with the calculation of actual recharge, may be calculated using a recharge code such as that described by Heathcote *et al.* (2003).

## **1.5 Looking Ahead**

What stands out from the literature is that much of the research in the area falls into two groups. Firstly, some studies focus on the saturated zone flows through drift materials with

relatively little attention being paid to the unsaturated zone processes. The popularity of flooding tracer experiments is an example of this (e.g. Nilsson *et al.* (2001); McKay *et al.* (1999)), from which it is impossible to discern the likely flow pathways and timescales under natural gradients in the unsaturated zone. Secondly the unsaturated zone processes are often studied in detail by soil scientists but with little attention given to the fate of water once it has left the shallow soil zone (Villholth *et al.* 1998a; Villholth and Jensen 1998b; Jansson and Jansson 2003; Gerke and Kohne 2004). What is needed is a more holistic consideration of the whole system from the ground surface to the aquifer. The research presented in this thesis attempts such an approach.

The increased understanding of the hydrogeology of glacial materials which started in a concerted way in the 1960s has been concurrent with the maturing of other fields relevant to the subject of recharge through drift. For example, unsaturated zone flow theory and modelling techniques, the increased awareness of the significance of non-equilibrium and preferential flow and the application of geophysics to hydrological problems. As such we are in an excellent position to further our understanding of the hydraulic processes controlling recharge through drift by integrated research drawing on developments across these disciplines. This thesis hopes to make a contribution in this regard.

## **2 THE HYDROGEOLOGY OF THE POTFORD BROOK CATCHMENT**

### **2.1 Introduction**

As part of the LOCAR programme, it was stipulated that the research area must be within the catchment of the River Tern, a tributary of the River Severn in Shropshire, UK. The whole Tern catchment covers approximately 880 km<sup>2</sup>. Furthermore, the distribution of the drift cover and of existing hydrological monitoring locations across the catchment is very variable. It was necessary therefore, for practical reasons, to choose an area smaller than the whole Tern catchment for detailed study and fieldwork. The catchment of the Potford Brook, a tributary of the River Tern, was chosen as it has variable drift cover in terms of lithology and thickness and is underlain by Permo-Triassic sandstone, an important regional aquifer. The catchment is equipped with hydrological monitoring locations for rainfall, climate, groundwater levels and stream flows and has a reasonable coverage of boreholes with available geological logs. In addition it was found that most of the landowners in the area would grant land access for fieldwork.

The rest of this chapter introduces the main features of the catchment hydrogeology pertinent to the research topic to give a context for the rest of the thesis. This work is mainly based on a collation and critical review of existing data sets, papers and reports but original field observations and data analysis have also been undertaken.

### **2.2 Location, Topography and Drainage**

The location of the study area is shown on a simplified geological map of the UK in Figure 2.1.

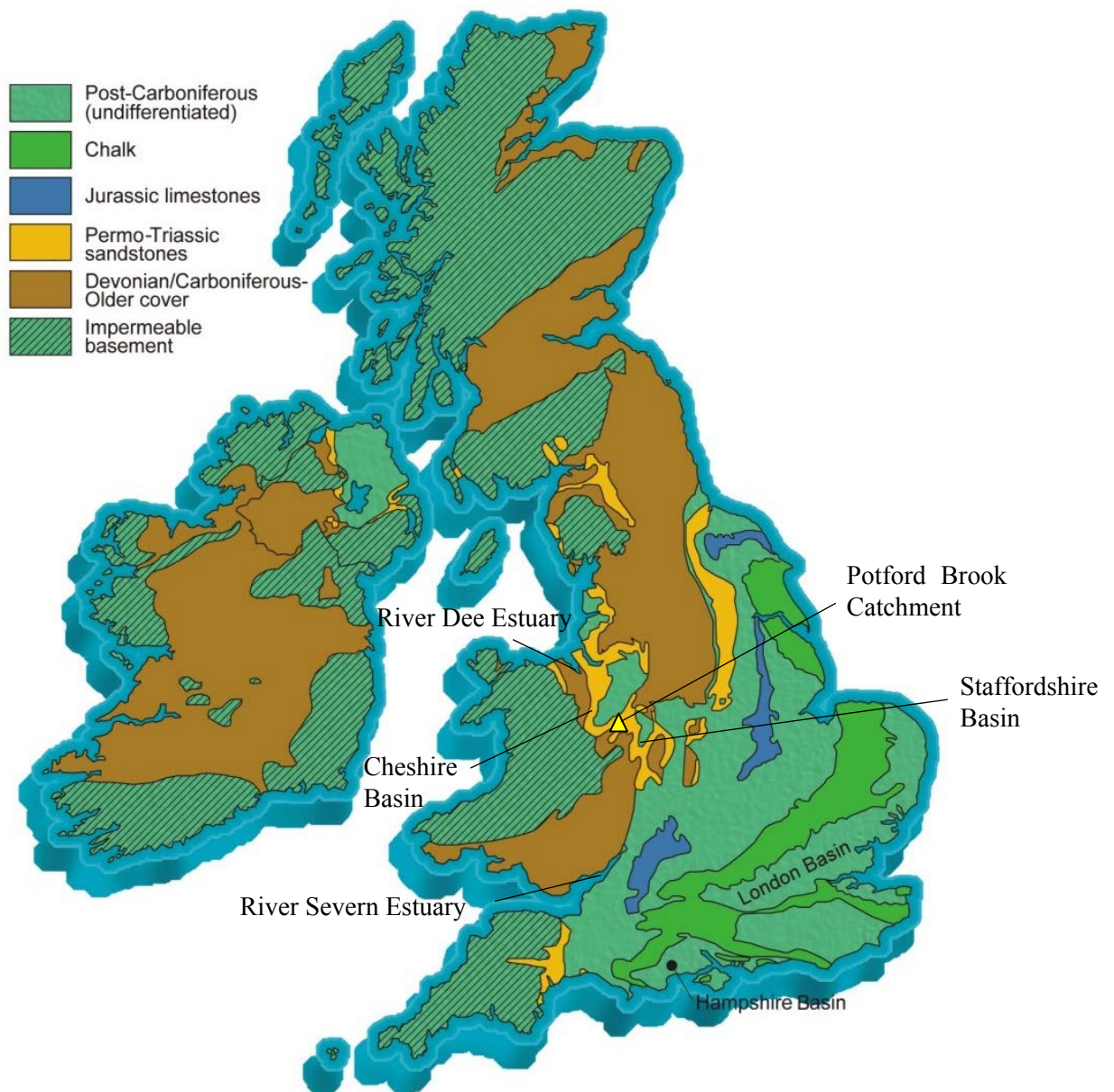


**Figure 2.1** Simplified geology map of the UK indicating the location of the study area and major aquifers (modified from a map posted by the UK Groundwater Forum:

[http://www.groundwateruk.org/archive/the\\_aquifers\\_of\\_the\\_uk.pdf](http://www.groundwateruk.org/archive/the_aquifers_of_the_uk.pdf))

The location of the Potford Brook catchment within the wider catchment of the River Tern is shown in Figure 2.2. The Potford Brook and its tributary the Platt Brook have a combined catchment area of around 22.5 km<sup>2</sup> and form a confluence with the River Tern near Cold Hatton Heath, NGR SJ 639 208.

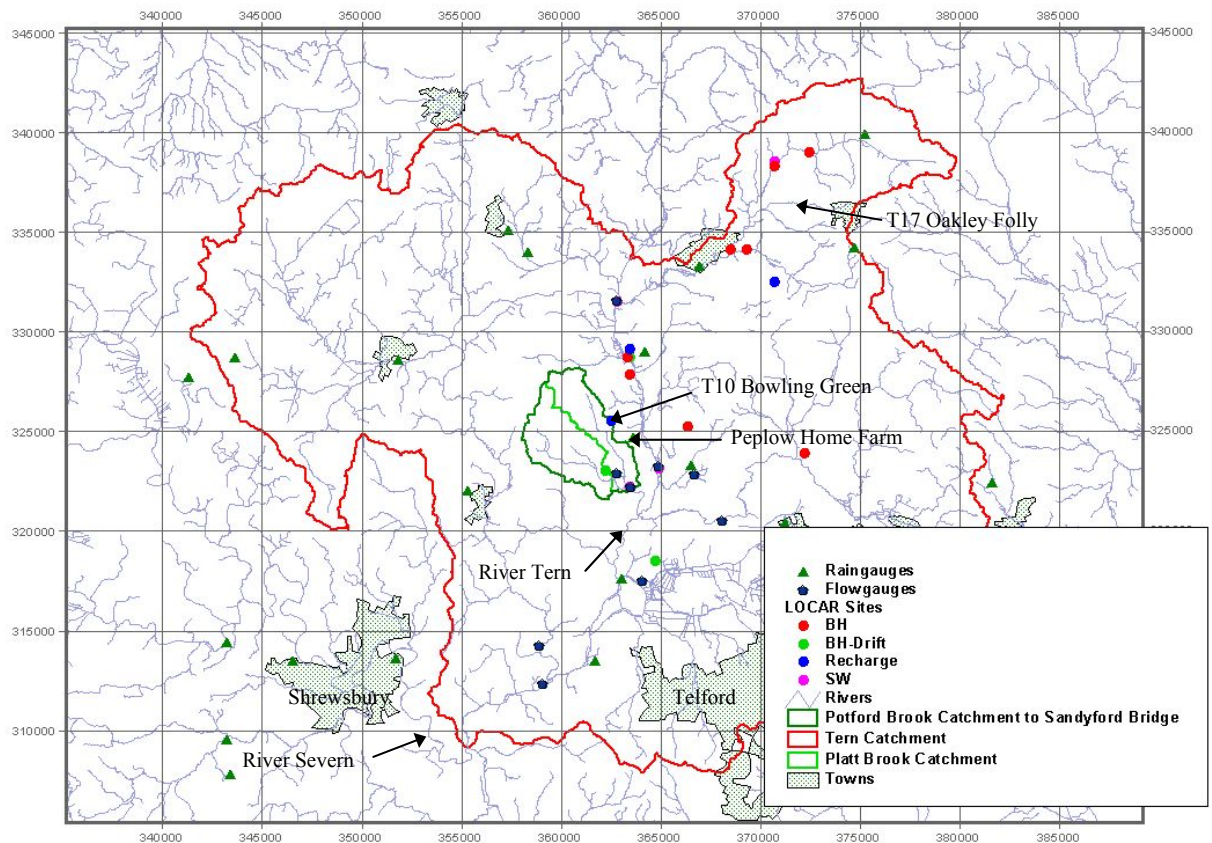


**Figure 2.2** Location map of the River Tern and Potford Brook catchments

It is a lowland catchment with a gently undulating terrain. The land rises gently from 55 mAOD in the southeast to 90 mAOD in a north-westerly direction before rising steeply to nearly 200 mAOD in the extreme north of the area. The topography is shown with significant vertical exaggeration in Figure 2.3 along with the draped geology map. This map is based on a Digital Terrain Model (DTM) at a 50 m spatial resolution (Morris and Flavin 1990). The contrast between the steep escarpment in the north of the catchment (the line of the Hodnet Fault) and the gently undulating valley/interflue topography can be clearly seen. The terrain is generally relatively flat with a small degree of valley incision due to erosion by the Potford and Platt Brooks.

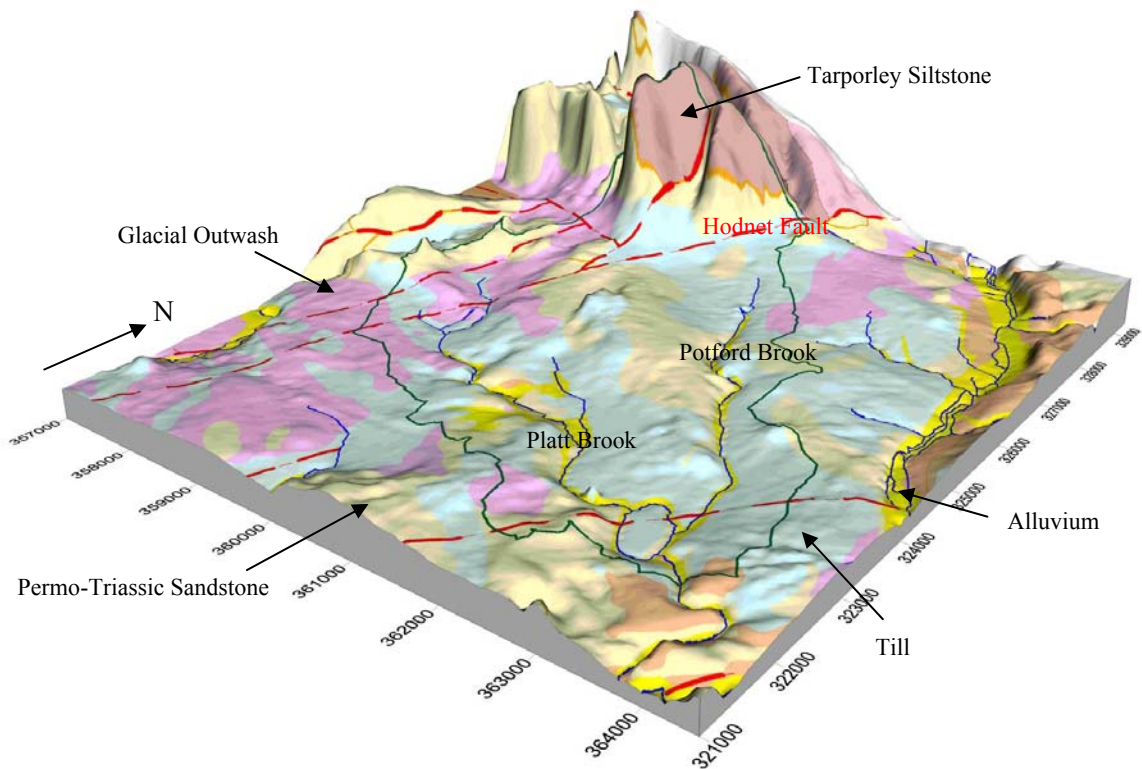


**Figure 2.3** Digital terrain model of the Potford Brook catchment with draped geology (key as for Figure 2.5)

In the wider area, the present drainage pattern which developed post-glacially is a significant modification of the pre-glacial system. In particular, the River Severn (to which the River Tern drains) formerly flowed east from its source in Wales before turning northwards to join the River Dee (see Figure 2.1 for locations). During the Pleistocene the Irish Sea ice blocked this drainage route and water is thought to have ponded in temporary lake basins in the area around Shrewsbury and the lower Tern catchment. The Iron Bridge gorge (just south of Telford) may have been cut as an overflow channel draining the area. The resulting drainage route, lower than the original course of the Severn, is still followed in the present day (Wills 1924; Worsley 1975).

Small ponds occur in clusters across the catchment, their distribution correlating strongly with areas mapped as underlain by glacial till. Many of these are believed (by local farmers) to be man made depressions mined for clay. These ponds are often linked by pipes and integrated with land drainage systems.

## 2.3 Soils and Landcover

### 2.3.1 Landcover 2000

Landcover 2000 data (Fuller *et al.* 2002) for the area are shown in Figure 2.4. Land cover is predominantly arable (55%) and grassland (37%) with a small amount of woodland and heath (6%) and urban areas (2%). Although Landcover data from 1990 are also available, due to differences in the classification used it is not possible to directly compare the 1990 and 2000 surveys to derive changes in land cover over the intervening period of time.

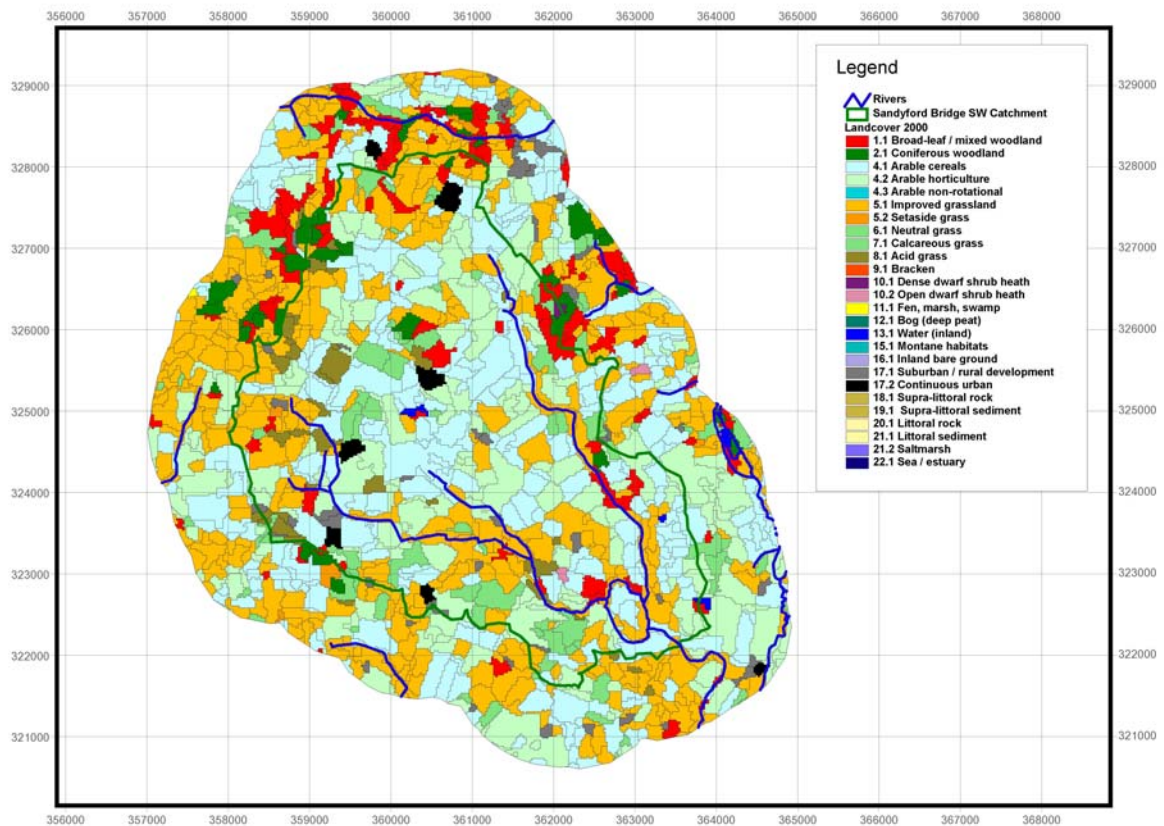


**Figure 2.4** Landcover 2000 map of the Potford Brook catchment at 25 m resolution

(Copyright NERC, Acknowledgment: CEH Monks Wood)

## **2.3.2 Soils**

### **2.3.2.1 Introduction**

A detailed soil survey of the upper Tern valley, including much of the Potford Brook Catchment, was carried out by Severn Trent Water Authority in 1982 (STWA 1982). The following section is a summary of the findings of this report which found a clear link between the underlying geology and derived soils. The digital drift geology map of the Potford Brook catchment is shown as part of the hydrogeological map in Figure 2.5.

### **2.3.2.2 Soils developed principally in reddish sandstones**

In drift free areas the soils are predominantly under agriculture with all soil types being coarse and permeable. They are easily cultivated but can have problems of compaction and erosion due to weak surface structure. Most soils tend to be droughty, retaining only small amounts of water for plant growth during the summer months. Drainage is only necessary in such soils where groundwater levels are high as in the Radmoor area (NGR SJ 628 248).

### **2.3.2.3 Soils developed principally within till or glaciolacustrine deposits**

These soils are predominantly under agriculture but permanent grassland occurs more frequently than on soil types over sandstone or glaciofluvial deposits. All the soil types contain dense, impermeable layers that impede the downward percolation of excess water causing periodic surface waterlogging. As a result, topsoils remain wet for a number of days after rain and cultivations need to be carefully timed to avoid the formation of pans. Dense subsoil horizons are difficult for roots to exploit and the soils retain only moderate amounts of water that are readily available for growing plants. The soils generally need to be underdrained and most fields containing these soils have had a systematically spaced underdrainage system installed.

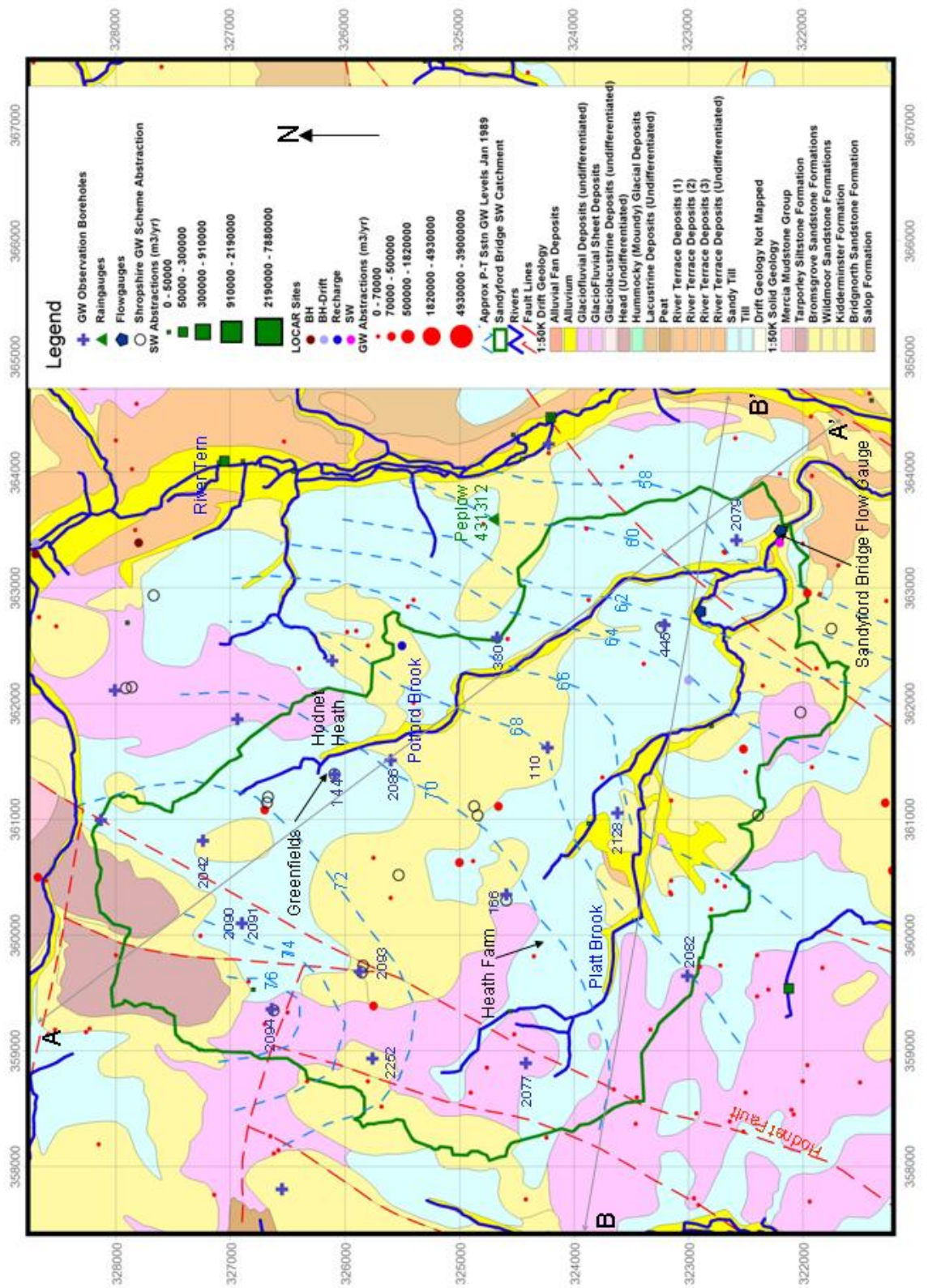


**Figure 2.5** Hydrogeological Map of the Potford Brook Catchment (see Section 2.6.1 for explanation of source data)

#### **2.3.2.4 Soils developed principally in glaciofluvial deposits**

These soils are predominantly under agriculture with grassland being uncommon. All the soil types are coarse and permeable to depth retaining low to moderate amounts of available water. Problems due to weak topsoil structure are common. These soils are often underdrained but normally on an ad-hoc basis designed to deal with localised areas of high groundwater levels.

#### **2.3.2.5 Soils developed principally in alluvium or peat**

Peat soils are dominant in the valleys of the Potford and Platt Brooks. They are frequently water logged within 1 m of their surface for much of the year and may be subject to seasonal floods. As a result most are under permanent grass and rough grazing. Underdrainage has been carried out in many areas, most schemes being ad hoc arterial systems linked to the adjacent water courses and are limited by the depth of the available outfall.

### **2.4 Geology**

#### **2.4.1 Introduction**

Many authors have described aspects of the geology of the area in the past (Wills 1924; Boulton and Worsley 1965; Yates and Moseley 1967; Worsley 1975). In terms of the drift geology the study by Thomas (1989) has not since been bettered. However, the geology has been studied in detail recently as part of the Environment Agency's East Shropshire Permo-Triassic Sandstone Groundwater Modelling Project (Bridge *et al.* 2002). This study provides an excellent background, both for the solid and drift geology, and makes a link to hydrogeological aspects of the catchment. Furthermore, as part of the LOCAR programme the BGS have produced a 3-D model of the study area based on existing geological logs using the software GSI-3D. The following summary is taken partly from these recent studies but also draws on previous work in the literature.

### **2.4.2 Regional Geology**

As shown in Figure 2.6 Jurassic and Permo-Triassic rocks, preserved in a series of half-grabens, dominate the solid geology of the River Tern catchment. These are associated with the Wem and Church Stretton Fault Systems and the succession thickens eastwards into the Stafford Basin and north-westwards into the Cheshire Basin. The Hodnet fault is taken as the dividing line between these two basins which each have their own nomenclature for the Permo-Triassic sequences. Palaeozoic and Pre-Cambrian rocks also crop out in the area in fault-controlled inliers. The lithostratigraphy is summarised in Table 2.1.

As shown in Figure 2.7, glacial deposits cover the northwest part of the Tern catchment. Over the rest of the area, including the Potford Brook catchment, the glacial drift cover is patchy. River Terrace deposits, peat and alluvium also crop out, mostly confined to the river valley areas.

### **2.4.3 Brief Geological History: Solid Formations**

During the Permian and earliest Triassic the West Midlands experienced an arid, aeolian environment. Regional crustal extension due to North Atlantic rifting created a series of north-south trending troughs across the West Midlands. Extensional movement initiated basin development in the region during the Permian with the accumulation of predominantly wind-blown sands.

During the Triassic northerly flowing braided streams deposited conglomeratic and pebbly sandstones followed by the deposition of finer grained fluvial material and local aeolian deposits. Intra-Triassic regional uplift resulted in a period of erosion followed by further deposition of fluvial and aeolian sandstones and then in the late Triassic the restricted saline playa lake deposits of the Mercia Mudstone Group.

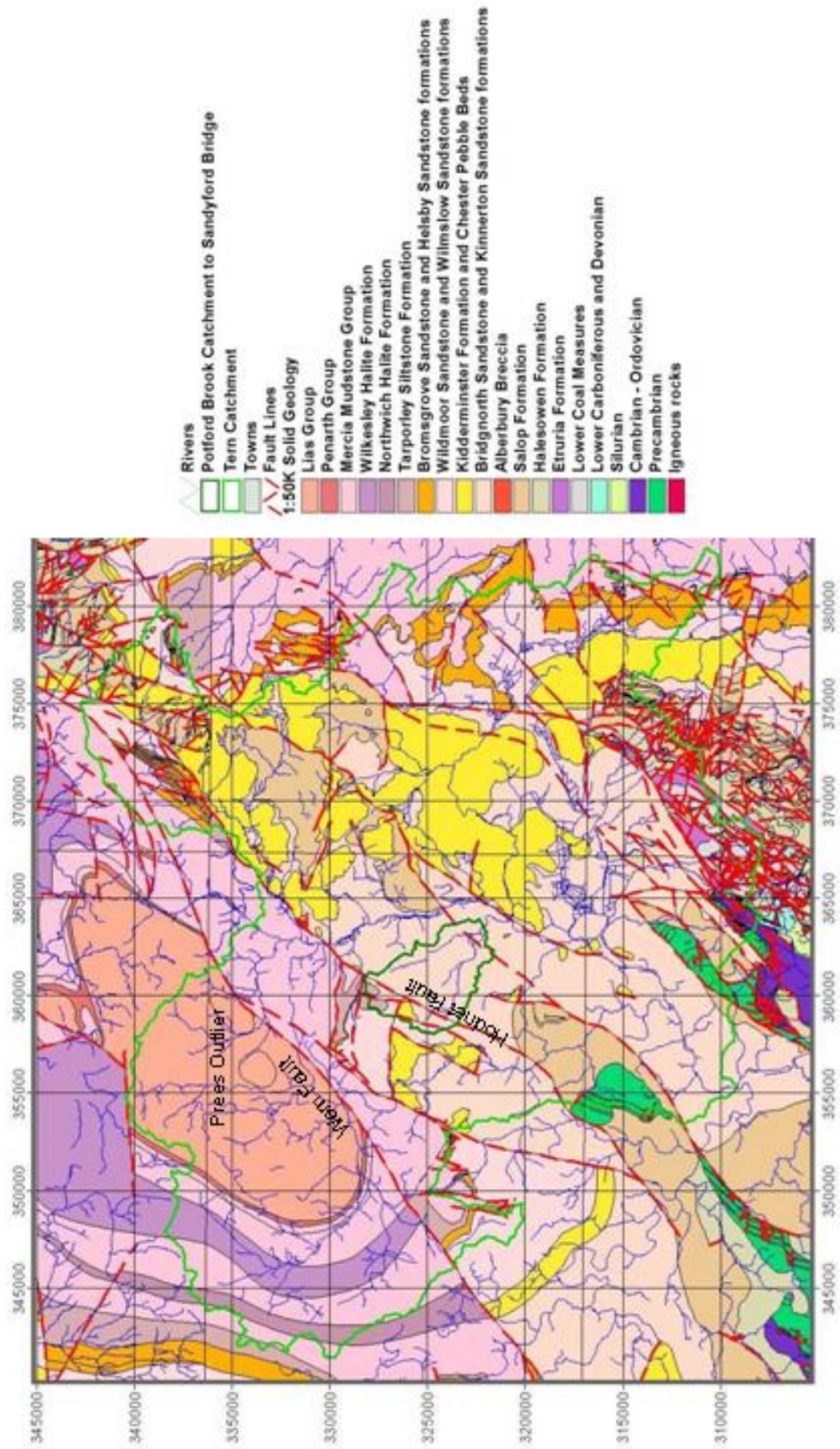


**Figure 2.6** Solid geology of the River Tern catchment (BGS Sheet 138, Wem, Solid)

Period	Stage	Group	Formation Names	Facies
Jurassic	Hettangian	Lias Group		Calcareous mudstones and limestones.
Triassic	Rhaetian	Penarth Group		Mudstones, silty limestones and fine-grained sandstones.
	Ladinian-Norian	Mercia Mudstone Group	Including <i>Tarporley Siltstone Formation</i> at base, <i>Northwich Halite</i> and <i>Wilkesley Halite</i>	Hard, red marls and siltstones, including two saliferous formations in the Cheshire Basin.
	Anisian		Bromsgrove Sandstone Formation <i>Helsby Sandstone Formation</i>	Hard, pale grey to reddish-brown micaceous sandstone, locally pebbly; subordinate mudstone.  Fluvial facies dominant in the Stafford Basin, fluvial and aeolian facies recognised in the Cheshire Basin.
	Induan-Olenekia	Sherwood Sandstone Group	Wildmoor Sandstone Formation <i>Wilmslow Sandstone Formation</i>	Friable, red sandstone with subordinate siltstones; pebble-free.  Wildmoor Sandstone dominantly fluvial.  <i>Wilmslow Sandstone</i> dominantly aeolian in the upper part and fluvial in the lower part.
			Kidderminster Formation <i>Chester Pebble Beds</i>	Conglomerates and pebbly sandstones, with subordinate sandstones and mudstones.
			<i>Kinnerton Sandstone Formation</i>	Red, fine-grained sandstones, generally pebble free, dominantly aeolian.
Permian	Undivided		Bridgnorth Sandstone Formation	
Carboniferous		Warwickshire Group	Salop Formation (formerly Enville Formation and Keele Formation)	Red-brown mudstone and sandstone with minor conglomerate and sparse thin limestones.
			Halesowen Formation (Coed-yr-Allt Beds)	Grey-green and red sandstone and mudstone with thin coals and sparse thin limestones.
			Etruria Formation	Variegated mudstone with subordinate pebbly sandstones

**Table 2.1** Lithostratigraphy for the solid geology of the River Tern catchment (Cheshire basin nomenclature in italics)

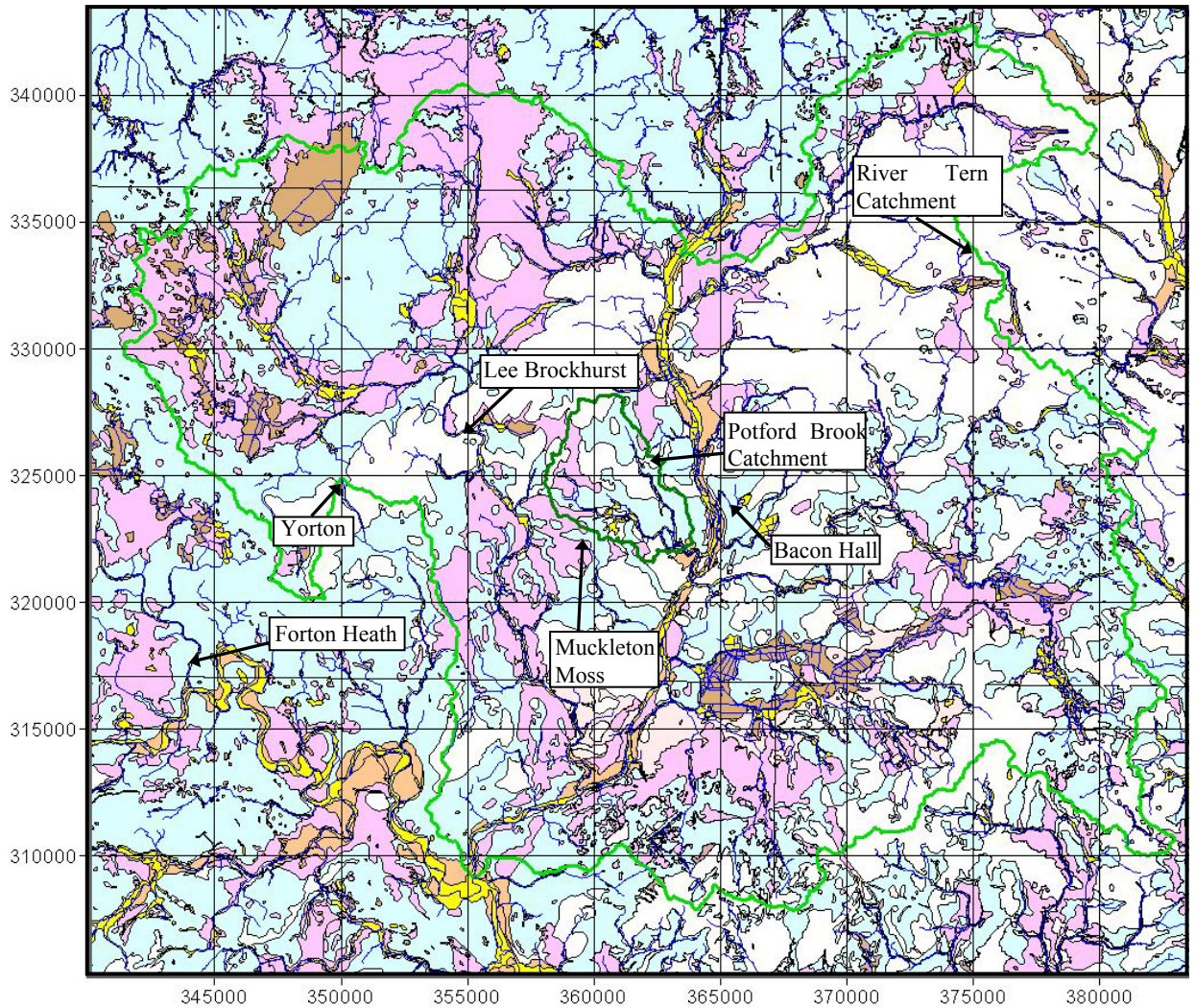


**Figure 2.7** Drift geology of the River Tern catchment (BGS Sheet 138, Wem, Drift)

(key as for Figure 2.5 but white areas are drift free)

Tethyan transgression during the latest Triassic is marked by deposition of calcareous marls followed by quasi-marine argillaceous limestones and mudstones. Further inundation of the West Midlands during the Jurassic led to the development of Liassic limestone-shale facies preserved in the Prees outlier (Figure 2.6)

#### **2.4.4 Brief Geological History: Drift Deposits**

The drift deposits in the Tern catchment are associated with the Late Devensian glaciation and subsequent Holocene deposition. The following history is based on Thomas (1989).

In the Late Devensian the Welsh ice sheet arrived in the region from the west but was rapidly overwhelmed by Irish Sea ice advancing from the north. The two ice masses coalesced to the west of Shrewsbury with the maximum extent at around 22 000 years BP just south of Wolverhampton. During ice advance till was deposited by subglacial lodgement and the permanent diversion of drainage lines was accomplished by subglacial fluvial erosion.

Some time after 13 000 years BP, the ice margin had retreated to the extent that the ice sheets began to uncouple just to the west of Shrewsbury. Outwash ridges were deposited along the drainage lines and meltwater was impounded in temporary lake basins during this time with glaciolacustrine sedimentation occurring in much of the Tern catchment. Further retreat of the ice resulted in discharge of meltwater southwards through rock channels in the Triassic escarpment around Yorton and Lee Brockhurst (Figure 2.7) creating outwash fan deposits. Subsequent melting led to a complex topography of till ridges and pitted and kettled outwash surfaces in some areas.

Since the ice retreat, silts, sands and gravels have been reworked and incorporated into river terrace deposits and alluvium. Peat commonly infills glacial drainage channels and is typically one to two metres thick.

#### **2.4.5 Geology of the Potford Brook catchment**

A simplified geology of the Potford Brook catchment is shown in Figure 2.5. Most of the catchment is underlain by Permian Bridgnorth Sandstone which thickens from around 100 m in the southeast to more than 200 m towards the Hodnet fault in the northwest of the

catchment. The bulk of the Bridgnorth sandstone sequence is represented by red to red-brown, fine to medium grained, pebble-free, dune bedded sandstones of aeolian origin.

Across the Hodnet fault to the west a series of smaller fault blocks juxtapose combinations of younger Permian Kinnerton Sandstone, Triassic Chester Pebble Beds and Wilmslow Sandstone alongside Bridgnorth Sandstone. Tarporley Siltstones of the Mercia Mudstone Group overlie Wilmslow Sandstones and crop out on the hills in the far northwest of the catchment.

With regard to drift covering, the catchment comprises 47% till, 14% glaciofluvial deposits, 5% alluvium, 30% outcrop Permo-Triassic sandstones and 4% outcrop Tarporley Siltstone based on the digitised BGS 1:50 k Drift Geology Map (Sheet 138 Wem). Drift covering is patchy with alluvium dominating the areas adjacent to the Potford and Platt Brooks along most of their length. Drift is most notably absent from the interfluvial area between the two brooks.

Glaciofluvial deposits crop out in the west of the area around the headwaters of the Platt Brook but small patches are also found in the extreme south and north of the catchment. These deposits range in texture from coarse gravels through pebbly sands to clayey sands. The most likely explanation for their deposition is that they are outwash fans deposited as meltwater flowed through gaps in the escarpment located to the northwest of the catchment derived from the ice sheet as it retreated northwards. However there may have been a component of meltwater down the present location of the Tern valley contributing to the fluvial deposition in the east of the catchment. These matters are still open to debate (Humpage 2005). Less widespread is the occurrence of glaciofluvial deposits underlying till

which are thought to have been laid down in front of the glacier during ice advance. An example of such a deposit is shown in the cross section in Figure 2.8 B.

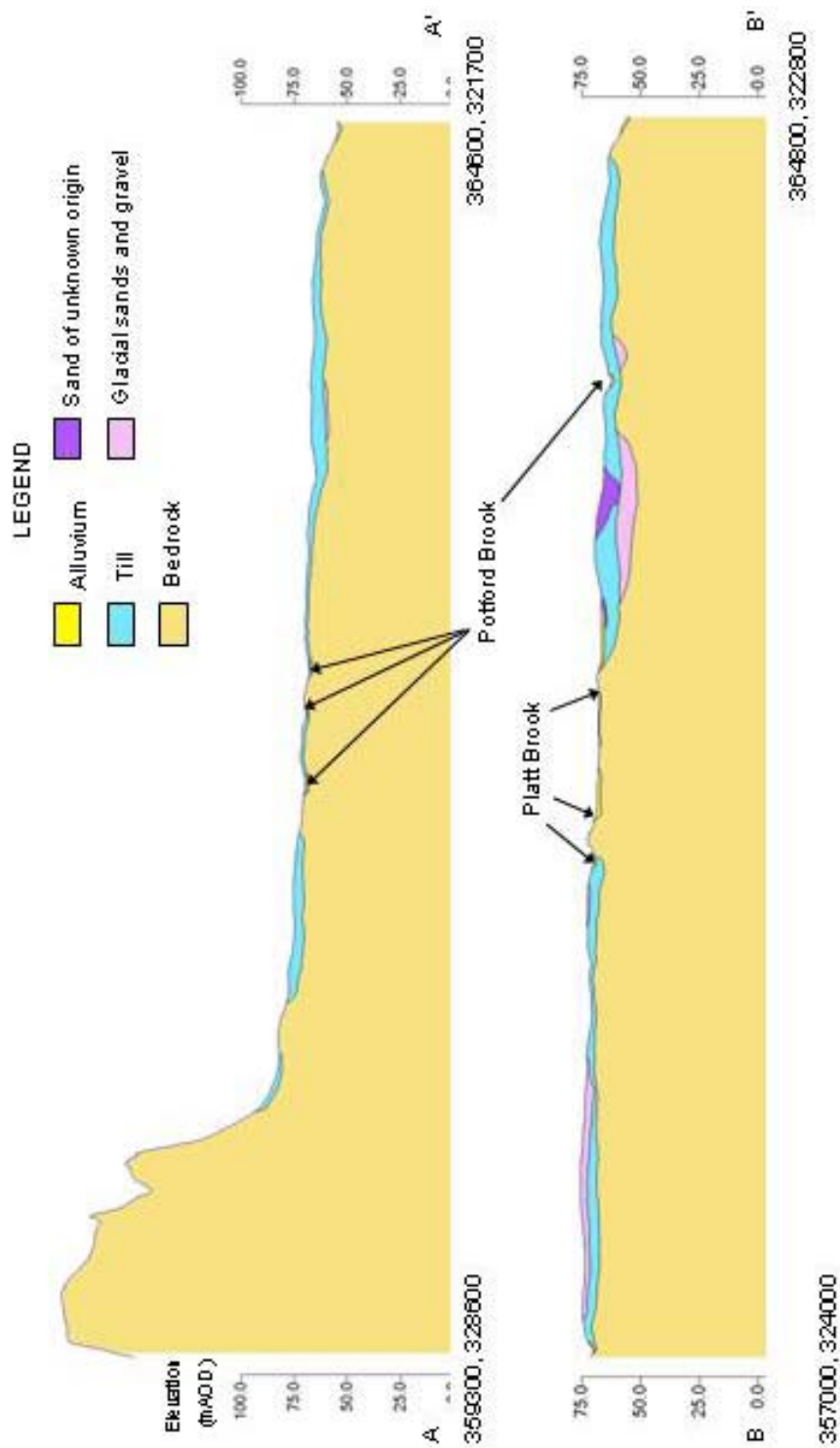


**Figure 2.8** Cross sections A-A' and B-B' as shown in Figure 2.5

The till deposits which dominate the drift cover in the catchment are predominantly thought to be lodgement tills laid down during ice advance. However there is some debate as to whether the deposit cropping out on the hill at High Hatton in the centre of the catchment (NGR SJ 605 250) is of the same age and type. It is possible that it may represent an older phase of till deposition or be flow till formed as ice flowed around this high point while depositing lodgement till across the rest of the catchment (Humpage 2005).

Several pebbles from soils in a till covered area of the Potford Brook catchment (around NGR SJ 638 228) were collected on a walk over survey. Among the specimens were examples of Chalk with flints and welded tuffs (ignimbrites). The presence of Chalk (assuming it is 'naturally' occurring) is consistent with the interpretation of Irish Sea Ice being responsible for glacial deposition in this area. The occurrence of welded tuffs may suggest the presence of Welsh Ice.

The cross sections shown in Figure 2.8 illustrate the likely relationships between the bedrock topography, the tills and the two phases of outwash material.

## **2.5 Meteorology**

### **2.5.1 Rainfall**

The distribution of raingauges in the Tern catchment is shown in Figure 2.2. The closest gauge to the Potford Brook area is that at Peplow Home Farm (M.O. Ref. 431312) just outside the catchment to the northeast. This gauge has a record from 1978 to present with two months of missing data in 7/99 and 3/01.

Double mass plots (cumulative rainfall for a gauge versus a reference gauge only counting days where rainfall is recorded at both gauges) were produced for the eight gauges

surrounding the Potford Brook catchment using the Peplow gauge as a reference. The plot for Peplow against Shawbury (M.O. Ref 433710) is shown as an example in Figure 2.9.

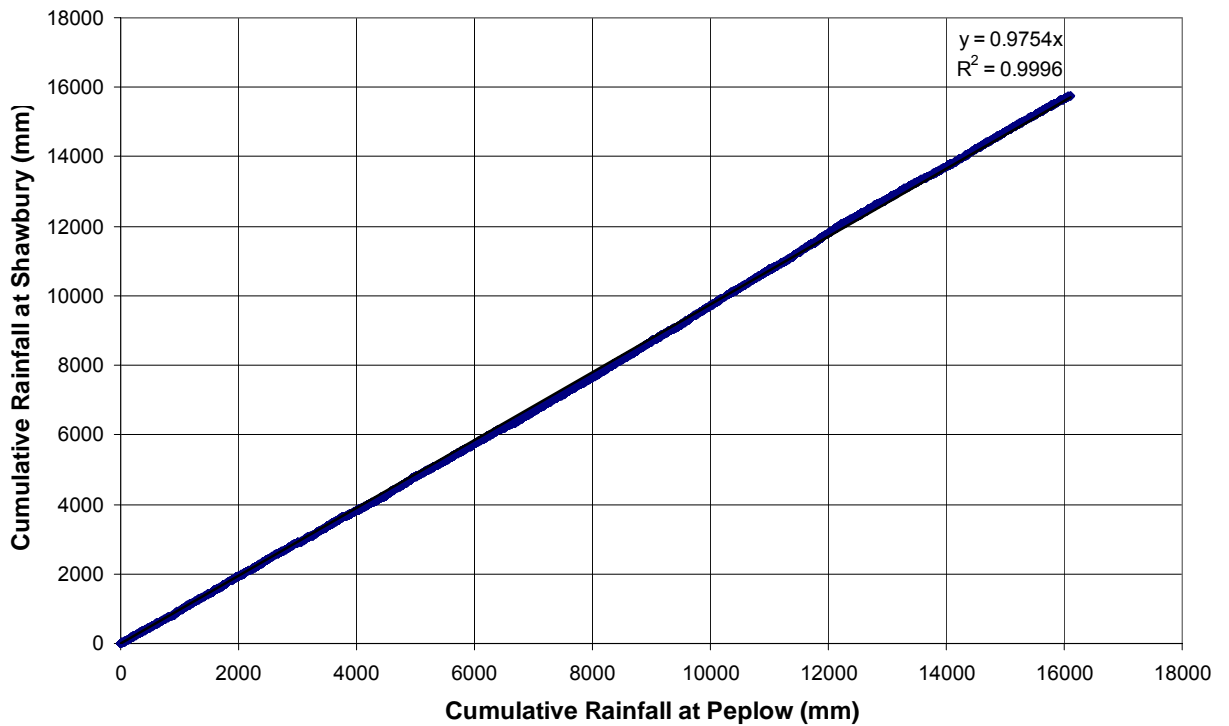


**Figure 2.9** Double mass plot for rainfall at Peplow (431312) and Shawbury (433710)

If a double mass plot deviated significantly from a straight line the rainfall record was checked manually for the suspect period. Errors in measurement at two gauges were identified using this method. In both cases errors were due to significant periods of zero rainfall recorded by a tipping bucket gauge (Prees 430989 and Market Drayton STW 430917) while other gauges in the area measured significant rainfall. These errors are likely to be due to the tipping mechanism of the raingauge becoming jammed for a time.

With these spurious data removed the percentage difference in gradients from unity of each double mass plot has been plotted against northing, easting and altitude for the gauge in question. The percentage difference represents the under or over catch of the gauge with

respect to that rainfall measured at Peplow. It was found that while there is little correlation between the percentage under or overcatch with easting, there was a moderate correlation with altitude ( $R^2 = 0.63$ ) and a very strong correlation with northing ( $R^2 = 0.96$ ).

If rainfall in the area is assumed to be distributed according to the derived relationship with northings alone, the rainfall measured at Peplow is representative of that for the Potford Brook catchment to within 0.25%. This is because almost exactly the same proportion of the area of the Potford Brook catchment lies to the north of the Peplow gauge as lies to the south of it.

The nearest high frequency LOCAR monitoring location is at Bowling Green (ref. T10, NGR SJ 625 255) which logs rainfall at 15 minute or hourly intervals with a tipping bucket recorder. These data have been aggregated into daily totals and compared with the Peplow record. The resulting double mass plot is shown in Figure 2.10 indicating that the Bowling Green gauge catches around 5% more rainfall than the Peplow raingauge. Given the difference in northing and altitude and using the relationships derived for the wider catchment we would expect the overcatch to be around 2 to 3 %. The remaining difference in catch may be explained by the differing raingauge design between the sites. It has been shown that a standard daily raingauge in its conventional setting (300 mm above ground surface) catches 6-8% less rain than a properly installed ground-level gauge (Rodda 1967). Controlled experiments in wind tunnels demonstrate how the standard gauge acts as an obstacle to wind flow resulting in turbulence, an increase of wind speed above the gauge orifice, and therefore an undercatch. The difference in catch will vary for any given location between individual storm events depending on wind speed and direction and rain drop size. Furthermore Rodda and Smith (1986) showed that a relationship exists between wind speed and difference in

catch between standard and ground level gauges. Using this relationship together with information on mean wind speeds and the type of terrain they produced a map of the likely distribution of undercatch for standard raingauges across the UK. For the Tern area an average undercatch of around 5% is likely for standard gauge compared with ground level gauges. This is corroborated by the undercatch of the standard gauge at Peplow in comparison to the ground level gauge at Bowling Green. Given that a 5% change in rainfall may mean a much larger change in groundwater recharge, this matter should be considered when carrying out recharge calculations.

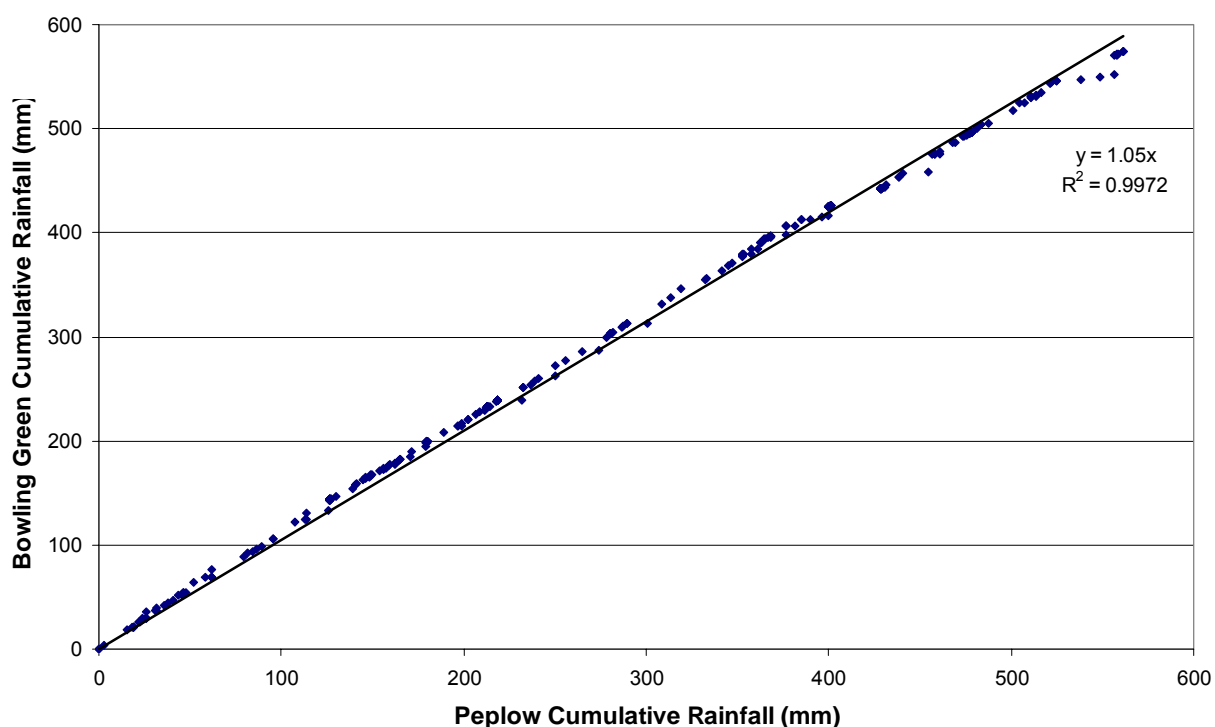


**Figure 2.10** Double mass plot for rainfall at Peplow (431312) and Bowling Green (T10)

### 2.5.2 Evapotranspiration

The nearest climate data available for the study catchment are for LOCAR sites at Bowling Green (ref. T10, NGR SJ 625 255) and Oakley Folly (ref. T17, NGR SJ 713 365). Unfortunately the automatic weather station (AWS) at Bowling Green which is actually

within the Potford Brook catchment was vandalised in 2004 and has not been reinstated. Nevertheless the existing data are useful for comparison against data from Oakley Folly which are the closest data available for modelling purposes. Oakley Folly lies approximately 11 km north and 9 km east of Bowling Green and is around 40 m higher in elevation.

Potential evapotranspiration (PEt) has been calculated for each site using the measured climatological variables and the FAO Penman Monteith equations (FAO 1998). A double mass plot of PEt for Bowling Green and Oakley Folly is shown in Figure 2.11 for the period of overlapping data (21 March to 2 September 2003). The comparison implies a reasonable consistency in the quality of the data and indicates that PEt is on average around 6% higher at Bowling Green.

A comparison has also been made between monthly aggregated PEt for Oakley Folly and the monthly MORECS (grass) figures for squares 114 and 124 for 2004. This is shown in Figure 2.12 indicating that although the pattern is similar, the MORECS values (annual total 614 mm/a) are significantly lower than those calculated for Oakley Folly (annual total 811 mm/a). Some difference would be expected due to differing parameters and time-step size in the calculation of PEt, and the averaging between widely spaced climate stations over an area of 3200 km<sup>2</sup>. However, the Meteorological Office is not able to explain why the discrepancy might be so large (Fullwood 2005).

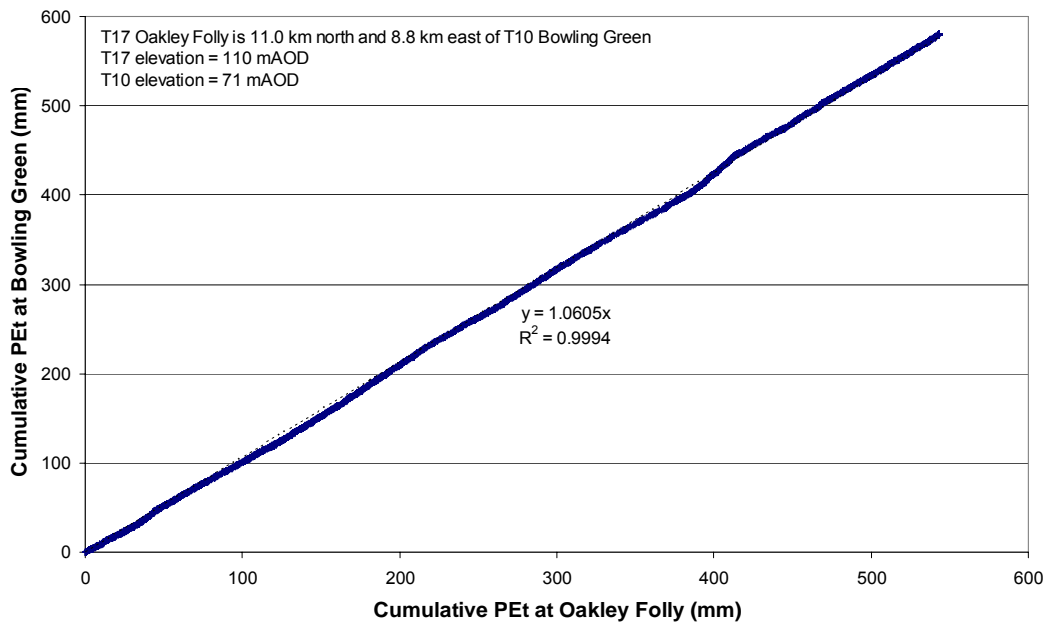


**Figure 2.11** Double mass plot for PET at Oakley Folly (T17) and Bowling Green (T10)

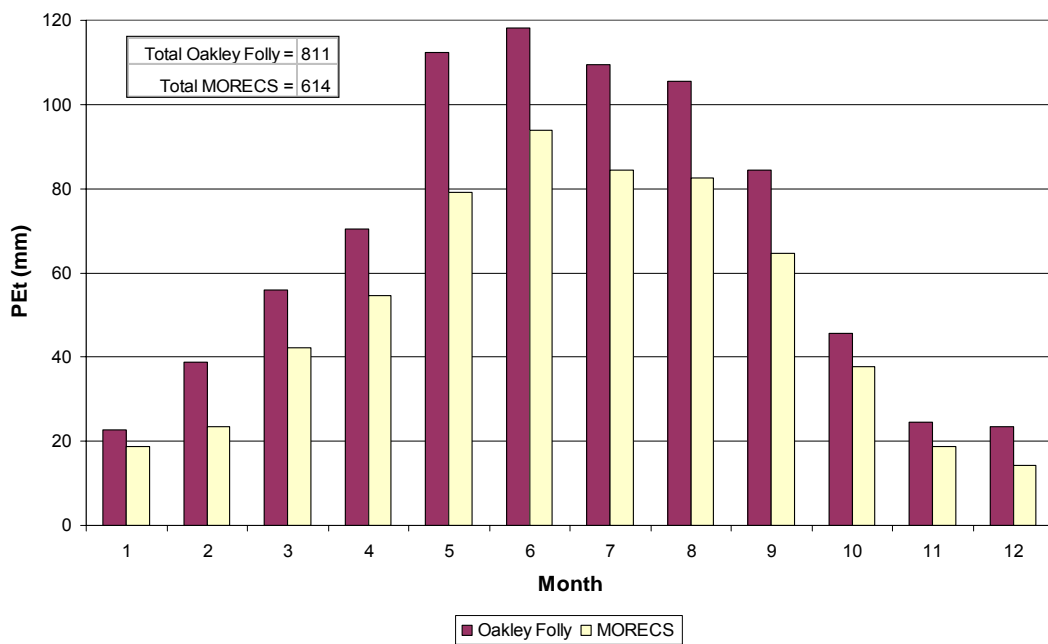


**Figure 2.12** Comparison of 2004 PET for Oakley Folly (T17) and MORECS (sq 114 and 124)

It is noted that the difference is potentially very significant and that such easily available datasets (e.g. MOSES the recent replacement of MORECS) should be critically assessed before being used for recharge calculations.

### 2.5.3 Long Term Average Rainfall and PET

Long term annual average (1970-1999) rainfall and MORECS potential evapotranspiration (grass) for the Potford Brook catchment are around 670 mm and 597 mm respectively. A plot of total annual rainfall and PET is shown in Figure 2.13. Significant dry periods occurred in 1975-6, 1989-1991 and 1995-1996 with significantly wetter years in 1979-82, 1992-1994 and 1998-2000.

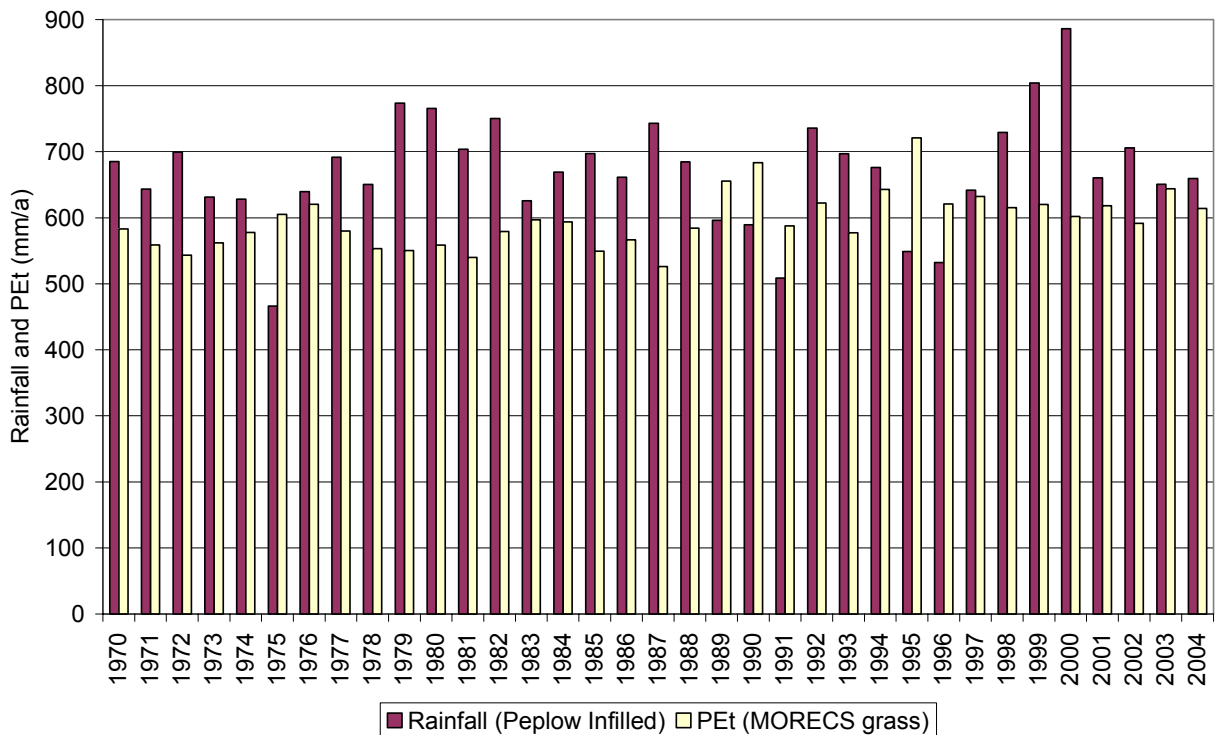


**Figure 2.13** Annual total PET (MORECS grass, sq 114 and 124) and Rainfall (Peplow 431312 infilled using Shawbury 422710 and the relationship defined in Figure 2.9)

## **2.6 Hydrogeology**

### **2.6.1 Hydrogeological Map**

A hydrogeological map of the area has been constructed and is presented in Figure 2.5. The map includes the locations of groundwater observation boreholes, raingauges, flow gauges and instrumented LOCAR sites for which data have been collected from the LOCAR data centre. The locations and magnitude of licensed surface water and groundwater abstractions have been added using data provided by the Environment Agency, Midlands Region. The underlying geology map is reproduced from the British Geological Survey Map Data (Sheet 138 Wem) at the original scale of 1:50 000. The rivers and surface water catchments are based on spatial data licensed from the Centre for Ecology and Hydrology, © CEH (including material based on Ordnance Survey 1:50 000 maps with the permission of the controller of Her Majesty's Stationary Office © Crown copyright). The groundwater level contours for January 1989 were constructed in the manner described below in Section 2.6.8.

### **2.6.2 The Permo-Triassic Sandstone Aquifer**

The Bridgnorth Sandstone which underlies most of the Potford Brook catchment is part of the regional Permo-Triassic sandstone aquifer. It is known to be a poorly cemented and lithologically relatively uniform fine to medium grained sandstone generally devoid of mudstone beds. Although fracturing may be important at a local scale in some areas, the main controls on aquifer transmissivity are likely to be thickness and, secondarily, the depth of weathering (SRA 1972). The Bridgnorth Sandstone is thought to have average values of horizontal and vertical hydraulic conductivity of around 2.5 and 0.25 m/d respectively with values of specific yield and specific storage of 0.14 and 0.00005 respectively (Soley *et al.* 1998). There is some evidence from pumping tests carried out in the area that the near-vertical Hodnet fault (shown on Figure 2.6) may be a significant low permeability feature although this is still open to debate (SRA 1976; Streetly and Shepley 2002).

### 2.6.3 Drift Properties

As described in Section 2.4.4, the catchment is covered in a range of drift materials dominated by glacial till and glaciofluvial deposits. The hydrogeological properties of such materials in Shropshire were the subject of a study forming part of the Hydrogeological Classification of Superficial Clays Programme run by the BGS and NRA (Wealthall *et al.* 1997). The study concentrated on two fieldsites at Forton Heath and Muckleton Moss the locations of which are shown in Figure 2.7.

The Forton Heath site is underlain by over-consolidated till weathered to a depth of around 7 m. It was concluded that the main controls on the hydrogeological properties of the till are the degree of over-consolidation and weathering in controlling the degree of fissuring. Laboratory values for hydraulic conductivity of the till ranged from  $1.0 \times 10^{-10}$  m/s to  $4.0 \times 10^{-10}$  m/s with one value of  $3.5 \times 10^{-9}$  m/s associated with a more weathered sample. Field values of hydraulic conductivity based on piezometer tests were found to decrease with depth and were in the range  $3.9 \times 10^{-10}$  m/s to  $1.16 \times 10^{-9}$  m/s. The dry bulk density of the till was found to be in the range 1659 to 1827 kg/m<sup>3</sup> with a moisture content range of 16.8 to 20.3%.

The Muckleton Moss site comprises mainly laminated glaciolacustrine silts and clays with glaciofluvial sands. It was concluded that the main controls on the hydrogeological properties of the deposits are the grain size and anisotropy of the sediments. Laboratory values for hydraulic conductivity of the glaciolacustrine clays ranged from  $6.0 \times 10^{-11}$  m/s to  $6.0 \times 10^{-10}$  m/s although it was not specified in the report whether these were the horizontal or vertical components. Field values of hydraulic conductivity based on piezometer tests were found to be much higher at  $1.0 \times 10^{-8}$  m/s to  $1.0 \times 10^{-7}$  m/s reflecting the horizontal permeability of the

sandier interbeds. The dry bulk density of the sediments was found to be in the range 1230 to 1472 kg/m<sup>3</sup> with a moisture content range of 16.1 to 45.0%.

## **2.6.4 Groundwater Recharge**

### **2.6.4.1 Introduction**

There have been several groundwater resource studies carried out in the Tern area since the 1970s which have included an estimation of areally averaged groundwater recharge. Other small scale studies have also been carried out deriving recharge estimates for specific locations. The influence of drift cover has been tackled in a variety of different ways and a summary of the studies pertinent to recharge through drift in the area is now given.

### **2.6.4.2 Regional scale studies**

In the Shropshire Groundwater Investigation Second Report (SRA 1974), effective precipitation (precipitation minus evapotranspiration) was estimated using a MORECS type calculation which was then multiplied by an infiltration factor according to the outcrop geology (0.2 for boulder clay and 0.8 for outcrop and glacial sand and gravel) to give an estimate of recharge to the sandstone aquifer. For example, the average recharge to the sandstone aquifer in the Peplow area on the eastern edge of the Potford Brook catchment (around NGR SJ 632 248) was estimated to be 195 mm/a for outcrop and glacial sand and gravel covered areas, and 49 mm/a for areas underlain by boulder clay.

In the recent East Shropshire Permo-Triassic Sandstone Groundwater Modelling Project carried out by the Environment Agency (Streetly and Shepley 2005), a lot of work was put into recharge estimation using the FAO methodology (FAO 1998; Hulme *et al.* 2001; Streetly *et al.* 2002). For the recharge model the Potford Brook catchment was split into 'conceptual recharge domains' based upon the superficial geology type defined by the 1:50 k drift map and data from existing borehole logs. Two domains were considered applicable for the

catchment these being ‘unsaturated sandstone aquifer’ and ‘sandstone aquifer with clay drift’. Potential recharge was calculated in a distributed manner and then the total recharge in each zone was aggregated and added to a drift store which discharged to the aquifer at a constant daily rate and generated interflow according to a linear decay constant.

Once the groundwater model had been developed and refined against groundwater levels and total river flows the ‘best model’ scenario required an average recharge of around 240 mm/a and 90 mm/a for outcrop/outwash sand covered areas and till covered areas respectively in the Potford Brook catchment between 1980 and 2000 (data used courtesy of Environment Agency, Midlands Region). Recharge was used as a calibration parameter. Significant amounts of ‘interflow’ conceptually representing lateral groundwater flow within the superficial deposits and within drains were also required to reproduce the characteristics of the surface water hydrographs. In order to close the water balance a percentage of rainfall above a minimum threshold was added as ‘bypass’ recharge since the soil moisture balance model used generated too little overall recharge.

#### **2.6.4.3 Small scale studies**

Soil moisture measurements using neutron probes have been taken at several sites in the Tern area as part of the Shropshire Groundwater Scheme (SGS) Investigation since the early 1970s. Three of these sites at Heath Farm (NGR SJ 6000 2430), Greenfields (NGR SJ 6138 2615) and Hodnet Heath (NGR SJ 6192 2624) are within the Potford Brook catchment and their locations are shown in Figure 2.5. The purpose of the monitoring was principally to assess the impact of the SGS abstractions on root zone soil moisture available to crops (STWA 1980a; STWA 1980b; STWA 1981) but several studies are of interest with respect to the influence of drift deposits on groundwater recharge.

One such study focused on the changes in soil moisture at different radial distances from boreholes being pump tested over a period of several weeks (Walley and Hedges 1979). Although the study was not directed at recharge assessment the results are nevertheless informative with regards to the influence of the drift deposits on the hydraulics of the system. It was found that significant effects on soil moisture due to pumping were seen at Heath House but there was no evidence of moisture loss at the Greenfields site. This difference was explained by the presence of low permeability till below the soil at the Greenfields site isolating the perched water table from the effects of pumping in the sandstone.

A separate study was carried out for the Hodnet Heath site concluding that there is negligible hydraulic connection between the perched water table within superficial sand deposits at the site and the sandstone aquifer beneath due to the presence of an intervening low permeability clay layer (Fletcher 1976).

As a result of agricultural concerns, the soil moisture monitoring network was expanded during the development of the first phase of the SGS in the early 1980s and two studies have used these data to study recharge processes with particular emphasis on the testing of soil moisture balance recharge estimation methods (Wheater and Sherratt 1983; Finch 1999). The studies show significant variability in recharge between different sites across the area highlighting the importance of soil heterogeneity. The problem of using site specific data to upscale to the catchment level is therefore raised as noted elsewhere (Streetly and Shepley 2002). Both studies focus on calculations of potential recharge rather than actual recharge to the sandstone (i.e. they don't account for the possibility of lateral flow at depths greater than the soil moisture data) so they are of limited use in discussion about the effects of drift. However it is noted that at sites underlain by boulder clay derived soils, soil water can be

drawn up from a significant depth (1.6 m) greater than that of the extent of the root zone (in this case grass roots to around 0.8 m) (Finch 1999).

A 1996 study, focussed directly at the problem of estimating groundwater recharge through glacial drift in Shropshire, presented analysis of data from a site at Bacon Hall (NGR SJ 6528 2371) (McDonald 1996). The site is situated 1500 m to the east of the Potford Brook catchment on the other side of the River Tern (Figure 2.7). At this location around 12 m of glacial till overlies the sandstone aquifer. The till appears to be a layered sequence of sand and clay horizons. A hydraulic gradient close to unity was measured between piezometers with screen midpoints at around 2.35 and 4.65 mbgl, the water table varying between 1 and 2 mbgl. The ZFP method was applied to soil moisture data measured by a neutron probe to a depth of 2.8 m and a value of 167 mm/a calculated for the monitored period of 1989 to 1990. Although the value of 167 mm may be a reasonable estimate of the recharge to the perched water table at this location, no attempt was made to account for lateral flow which seems likely in such a layered sequence, limiting the usefulness of this study.

#### **2.6.4.4 Runoff recharge**

Although not the subject of any previous work it is likely that runoff recharge is a significant process in the Potford Brook catchment. The term runoff recharge is here defined as infiltration of runoff some distance away from where the water reached the ground surface as precipitation. There are three instances in which I propose that this process may be significant:

- i. At the north end of the catchment Tarporley siltstones of relatively low permeability crop out on the hills to the west of the Hodnet Fault. The coincidence of steep slopes and low permeability substrata are likely to lead to the generation of significant

amounts of runoff during larger precipitation events. Any runoff flowing downslope would encounter a band of outcrop sandstone running around the foot of the escarpment. Hence focussed infiltration may take place in this location leading to recharge of the sandstone aquifer even in times of high soil moisture deficit.

- ii. Since the covering of glacial till is discontinuous across the catchment, runoff generated on low permeability soils may recharge the aquifer downslope as runoff occurs across the till margin into areas underlain by more permeable deposits.
- iii. Groundwater levels often fall below stream bed levels in the upper sections of the Potford Brook. Hence surface water runoff may infiltrate through the stream bed where the underlying alluvial drift deposits are sufficiently permeable. The potential significance of runoff recharge should not be underestimated as it has been shown elsewhere in the Midlands that such losses can be greater than 1 Ml/d/km (Cuthbert and Soley 2000). This study analysed the results of an augmentation experiment for a stream with a similar flow and geological context to the Potford Brook in which a known volume of water was pumped into the stream during a low flow period in the summer. A series of current gauging measurements were made at various points downstream at time intervals before, during and after the period of augmentation allowing the loss from the stream bed to be estimated.

The degree to which any of these processes actually occurs is open to debate and will only be discovered by carrying out further fieldwork and modelling.

#### **2.6.5 Groundwater – Surface water Interaction**

Few data are available on which to base an understanding of the interaction between the Potford and Platt Brooks with the underlying aquifer. River bed elevation data are incomplete

and flow accretion surveys have not been carried out historically. However, during a pumping test at Wood Mill Farm (near groundwater observation borehole 445 in Figure 2.5) it was noted that the effects of pumping were seen on the opposite side of the Platt Brook but not on the other side of the Potford Brook (SRA 1976). The inference from this observation is that in this area the Platt Brook may be hydraulically isolated from the aquifer due to low permeability drift but that the Potford Brook may be in hydraulic continuity acting as a 'recharge barrier' during the pumping test.

Owing to the lack of baseline data available, the accretion of the Potford Brook and Platt Brooks was investigated by conducting a set of spot flow measurements at strategic points up each water course during the summer of 2003. This fieldwork was carried out with an MSc student who has presented the method, data and a full discussion of the results in her MSc project report (Garrick 2003). Here it is simply noted that both brooks accreted strongly along most of their length at this time. The Potford Brook gained most strongly in its upper reaches, the Platt Brook in its lower. Furthermore, the accretion starts at the location of the intersection of aquifer groundwater levels with the stream bed elevation as would be expected.

As discussed above, at times of low groundwater level the Potford Brook may lose water to the aquifer due to infiltration through its base.

#### **2.6.6 Abstractions and Discharges**

The Potford Brook catchment contains several abstractions that are part of the Shropshire Groundwater Scheme (SGS). This is an Environment Agency scheme to augment flows in the River Tern and hence the River Severn for surface water abstraction further downstream during times of particular need.

The locations of all licensed abstractions and consented discharges located within the catchment, including the SGS, are shown in Figure 2.5. Time series of the best estimate of abstractions and discharges for the catchment are given in Figure 2.14 since records began (data courtesy of the Environment Agency, Midlands Region). To arrive at this best estimate, abstraction returns have been infilled using uptake factors and loss coefficients (Streetly *et al.* 2002). Where returns data was missing for a particular licence, the actual abstraction was assumed to be equal to the licensed abstraction multiplied by an uptake factor. The uptake factor was derived, where returns data were available, from the ratio of the volume actually abstracted to the licensed volume, for abstractions licensed for the same use. Loss coefficients were then applied based on compiled data for consumptive loss of groundwater abstractions for different uses.

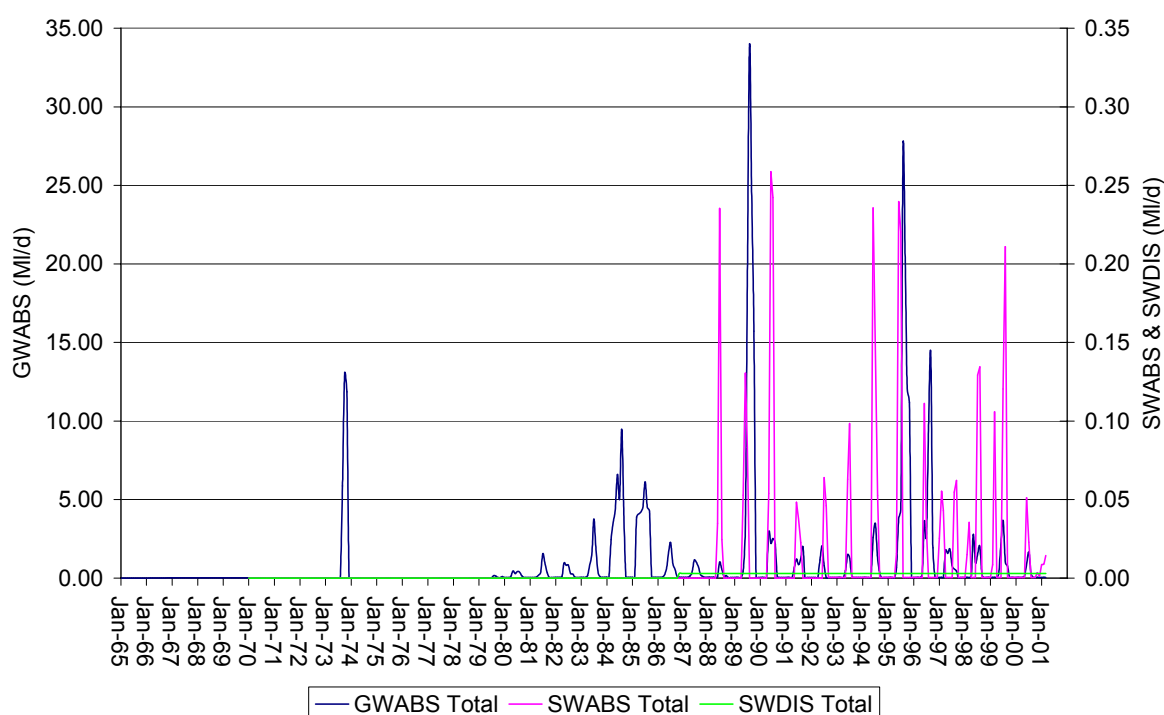


**Figure 2.14** Groundwater abstraction (GWABS), surface water abstraction (SWABS) and surface water discharge (SWDIS) in the Potford Brook catchment

The one surface water discharge of 3 m<sup>3</sup>/d at High Hatton (NGR SY 613 236) is minor in the context of the whole catchment. Surface water abstractions are likewise minor (average 0.025 Ml/d 1989-99) in comparison with the total catchment flows (average 11 Ml/d 1989-1999). Groundwater abstractions are however significant amounting to an average of 33 mm/a across the Potford Brook catchment over the period 1989 to 1999 inclusive. The most significant abstractions by far are associated with the SGS which pumped during 1989, 1995 and 1996 accounting for around 70% of the total groundwater abstraction between 1989 and 1999 inclusive. Other large abstractions in the catchment are generally for spray irrigation.

### **2.6.7 Groundwater Chemistry**

The groundwater chemistry of the area has been documented as part of the SGS investigations but also more recently by the BGS for the Tern catchment as a whole (BGS 2001). This report shows that the groundwaters of the Permo-Triassic sandstone are typically of calcium bicarbonate type whereas calcium sulphate and calcium chloride types predominate in groundwater from drift deposits. This difference may be due to dissolution of gypsum and halite derived from the Mercia Mudstone Group rocks incorporated during glaciation.

The hydrochemical data from the wider Tern area show that beneath areas of thin or sandy drift, groundwater in the sandstone is often higher in nitrate than in areas where thick or clayey drift overlies the aquifer. This can be explained by either the clayey/thicker drift reducing recharge and hence nitrate flux or causing reducing conditions leading to lower levels of nitrate (Streetly and Shepley 2002).

### **2.6.8 Groundwater Hydrographs**

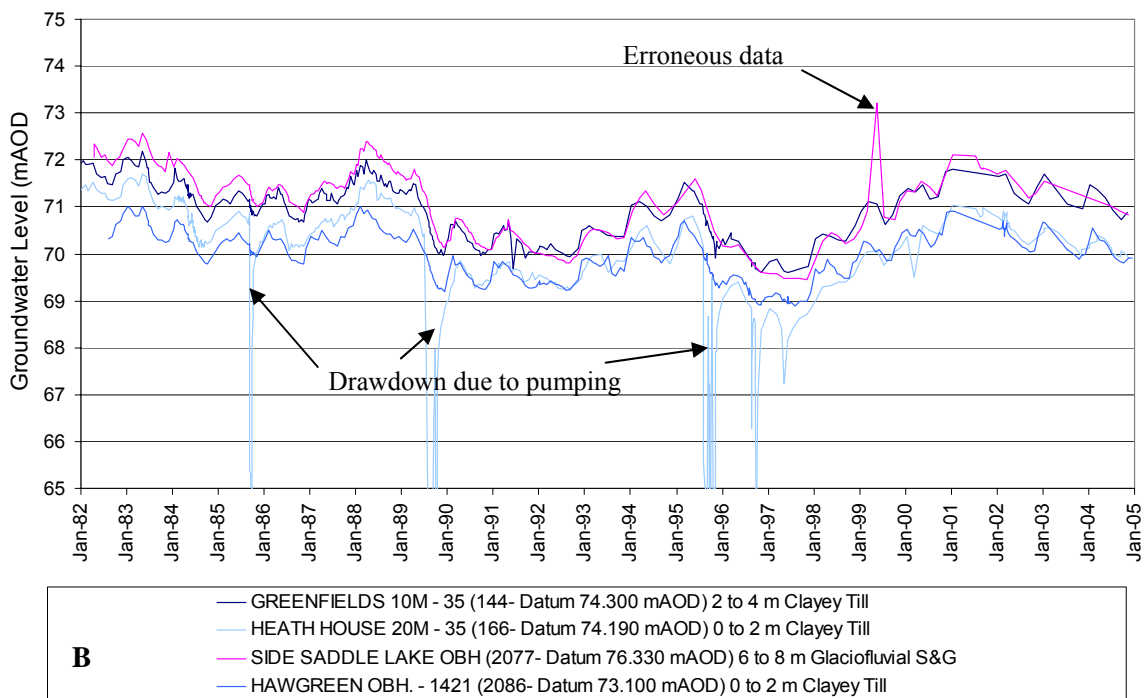
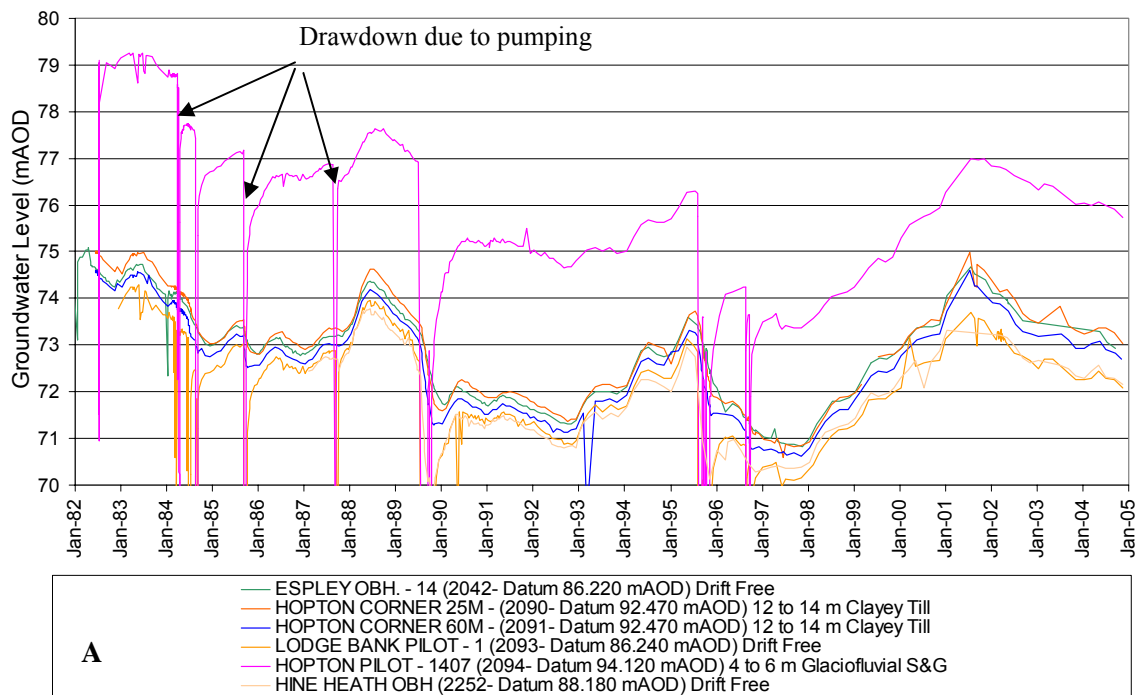
Groundwater levels are monitored in many boreholes across the area by the Environment Agency. Selected hydrographs monitoring water levels in the sandstone aquifer are shown in

Figure 2.15 for the period 1989 to 2004. The locations of the observation boreholes are shown in the hydrogeological map Figure 2.5.

Groundwater hydrographs show annual fluctuations of around 0.5 to 1.5 m. This annual response to recharge is superimposed on a background climatic response and the effects of drawdown due to nearby abstractions can also be clearly seen in some locations.

The background climatic response is greater in the upper parts of the catchment and smaller where groundwater levels are recorded in the lower parts of the catchment. For example the Wood Mill Farm hydrograph (Figure 2.15C) shows a range of variability of just 1 m between 1982 and 2005 compared with a variation of more than 4 m for Hopton Corner (Figure 2.15A). This suggests that the groundwater levels are in part controlled by river base levels of the River Tern and the lower reaches of the Potford and Platt Brooks, consistent with the pattern of baseflow accretion noted above (Section 2.6.5).

As noted by Streetly *et al* (2002) it is interesting that little or no recovery of groundwater levels is seen in the upper part of the catchment during the dry winters of 1988-89 and 1991-92 (e.g. Hopton Corner 25m - 2090) in contrast to a marked recovery in levels in the lower part of the catchment (e.g. Radmoor 29 – 330). This is illustrated in Figure 2.16. For these years the potential recharge was estimated to be approximately 100 mm in comparison to a long term average of 240 mm (data used courtesy of Environment Agency, Midlands Region).



**Figure 2.15 A to B** Groundwater hydrographs for the Permo-Triassic sandstone in the Potford Brook catchment (monthly data)

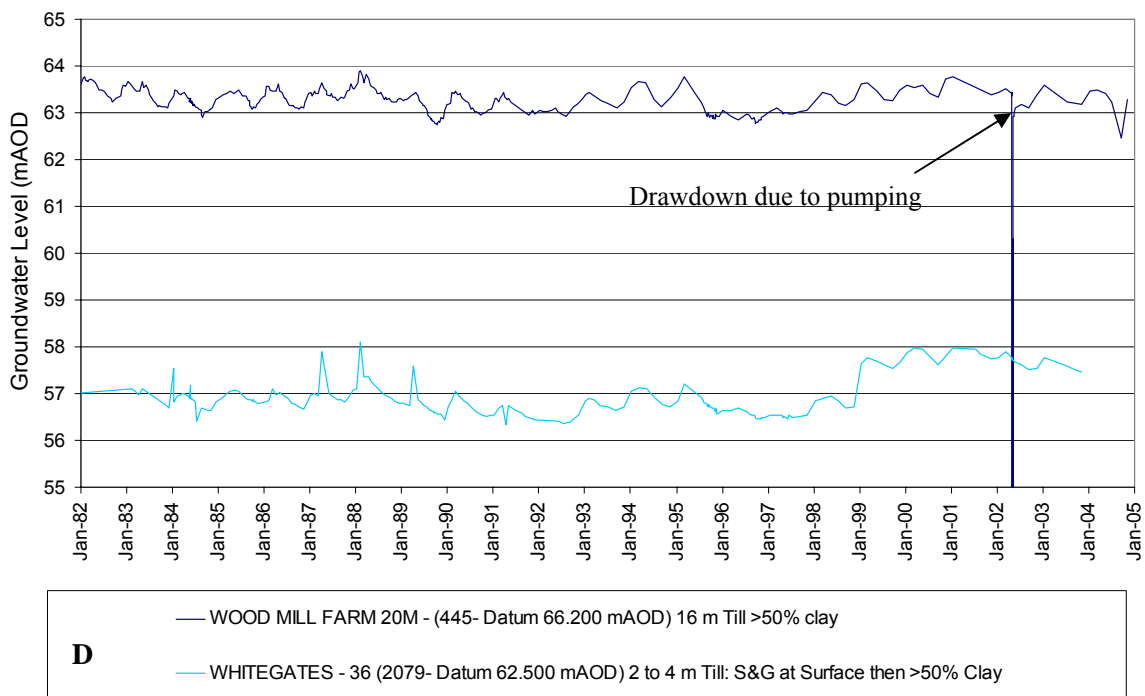
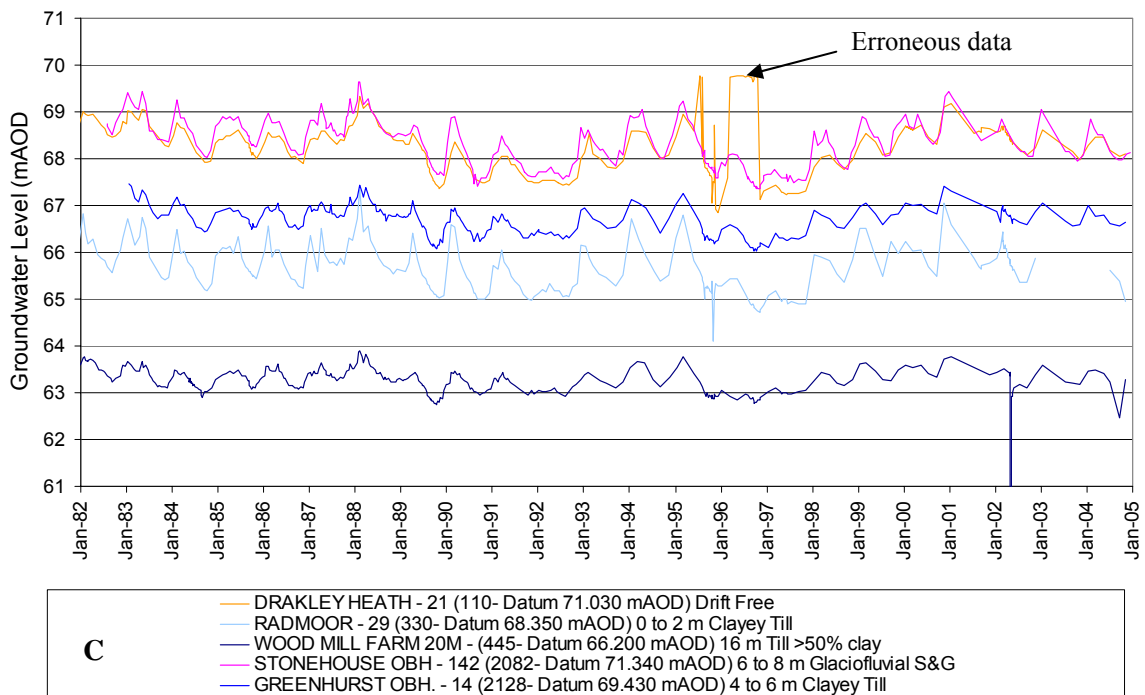


**Figure 2.15 C to D** Groundwater hydrographs for the Permo-Triassic sandstone in the Potford Brook catchment (monthly data)

It is possible that this effect could be due to runoff recharge occurring in the central parts of the catchment during these dry winters as hypothesised by Streetly *et al* (2002), causing recovery in groundwater levels lower down the catchment while a relatively small amount of recharge is occurring higher up the catchment. However, for the winter of 1988-89 the issue is complicated by the effects of pumping in the upper parts of the catchment which in itself may have led to the absence of a recovery in groundwater levels. In addition it was shown above in Section 2.6.4 that runoff recharge may not be limited to the central parts of the catchment but may also be expected to occur in the upper parts (due to runoff from the steep slopes above Hodnet infiltrating into outcrop sandstone at the foot of the escarpment).

Without more detailed investigation into the process of runoff-recharge and detailed modelling of the catchment this matter cannot be resolved.

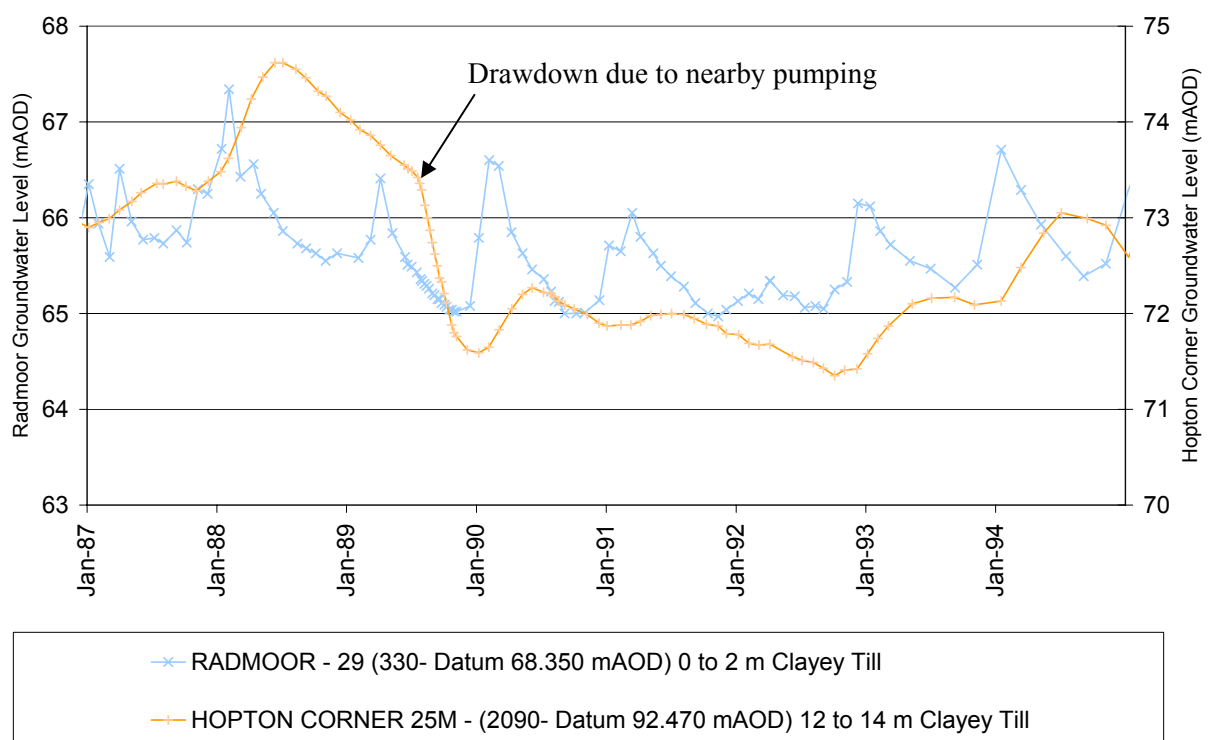


**Figure 2.16** Comparison of Radmoor and Hopton Corner hydrographs

The hydrogeological map in Figure 2.5 includes a set of groundwater contours (constructed by hand and then digitised) for the Permo-Triassic sandstone aquifer of the Potford Brook area for the situation in January 1989. Although the groundwater levels used are all monitored within the aquifer, a lack of available construction details for the observation wells leaves some uncertainty as to whether these groundwater levels are more akin to the water table or to some deeper piezometric level within the aquifer. Groundwater flow is predominantly from northwest to southeast. It seems likely based on these approximate contours that a significant amount of the groundwater recharge entering the aquifer within the Potford Brook surface water catchment flows eastwards to discharge to the River Tern without being intercepted by the Potford or Platt Brooks. However a degree of control is seen to be exerted by the brooks in their lower reaches where the groundwater contours are deflected implying some discharge to the surface water courses in these areas. It is noted that a certain amount of freedom is often available in drawing hand contours through relatively sparse data points. This can potentially lead to slightly different implied flow directions. However in this case, using all the available data, it was impossible to draw contours which show major discharge to the Potford and Platt Brooks.

## **2.7 Hydrology**

At Sandyford Bridge on the Potford Brook, river stage is measured by the Environment Agency using a Flat V weir. These readings are then converted to flows by means of a rating curve. The daily mean flow hydrograph for the Potford Brook at Sandyford Bridge is shown in Figure 2.17.

On the basis of available check gauging information the gauge is accurate at low and medium flows. However, the highest spot flow recorded on 15/11/93 is around 44 Ml/d, just 66% of

the value given by the flow gauge record for that day. Hence it is possible that at high flows the rating equation overestimates the actual flow in the brook.

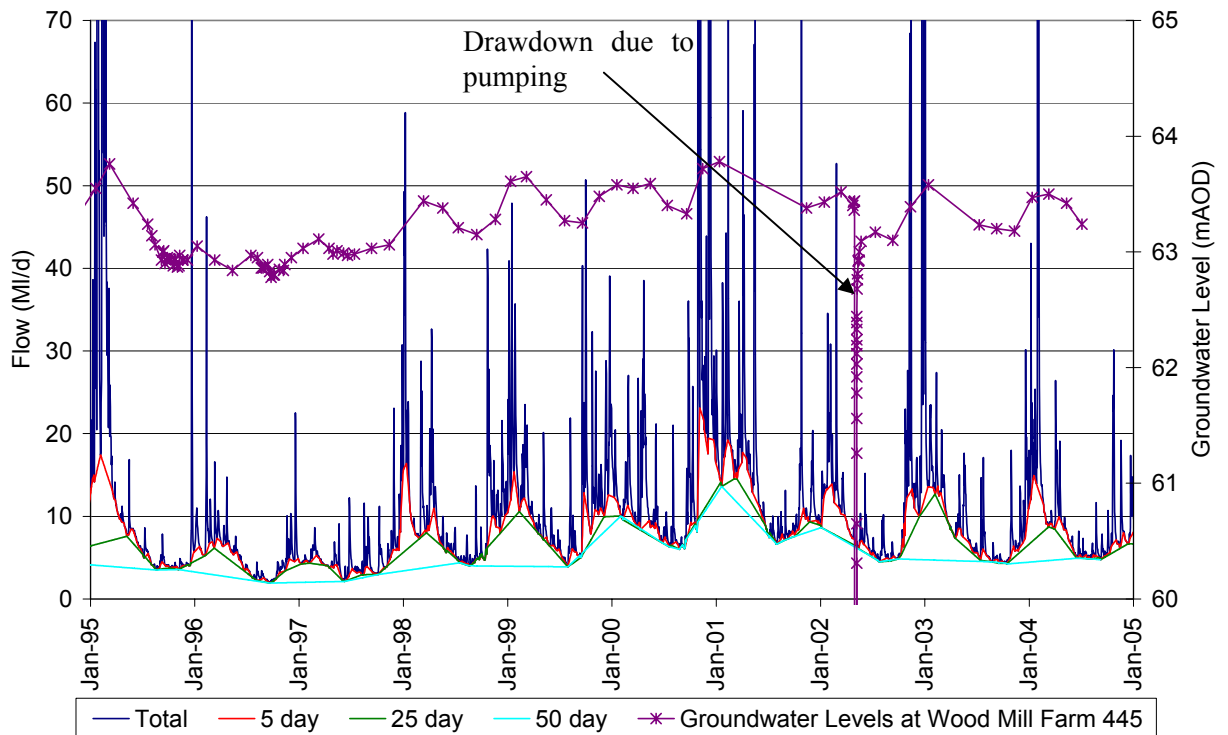


**Figure 2.17** Mean daily stream flow for the Potford Brook at Sandyford Bridge with baseflow separations and groundwater levels at Wood Mill Farm (445)

The hydrograph shows that there are a range of processes operating in the catchment giving responses to rainfall events at a variety of timescales:

- i. An almost immediate quickflow response representing a near surface ‘runoff’ component.
- ii. Intermediate timescale flows (several days to a few weeks) are evident. Such ‘interflow’ may represent drainage via field drains and groundwater discharge from superficial deposits.

- iii. A slowflow response representing the ‘baseflow’ input of groundwater discharge from the underlying sandstone aquifer.

A common approach in regional water resource studies is to deconvolute the hydrograph using a hydrograph separation approach such as the minimum turning point method (IoH 1989). It is however recognised that this method has no good physical basis and is simply a convenient way of quickly making a first separation. The separation into runoff, interflow and baseflow is thus arbitrary but is a useful way of splitting the total hydrograph to make some preliminary judgements about how the catchment hydrology is operating. Some VBA code was written in order to apply this method to the Sandyford Bridge hydrograph and implemented within an Excel spreadsheet. The code is given in Appendix 1. The method requires the user to input two parameter values. These are NDMIN, the number of days for the calculation of flow minima, and TPFAC, used to determine whether each identified minima is a turning point. The mean daily flow data series is split into blocks of NDMIN days and the minimum flow value ( $Q_n$ ) for each block is determined. Each minimum is then checked against the adjacent minima and is considered to be a baseflow turning point if  $Q_{n-1} > TPFAC * Q_n$  and  $Q_{n+1} > TPFAC * Q_n$ . The daily value of baseflow is then determined by linear interpolation between the baseflow turning points. If this calculated value exceeds the actual total flow then the baseflow is set equal to the actual flow.

Separations for NDMIN values of 5 and 25 and 50 days and a TPFAC value of 0.9 are shown in Figure 2.17. Also shown is the groundwater hydrograph for Wood Mill Farm (445) located near the confluence of the Platt and Potford Brooks in an area where the brooks are accreting. The 25 day separation broadly reflects the nature of this groundwater hydrograph and therefore may be a reasonable approximation to a baseflow contribution. This follows

from the assumption that baseflow will be proportional to the head difference between the brook and the aquifer. Everything between the total flow and the 5 day separation is for now considered to be runoff and everything in between the 5 and 25 day separations will for now be termed interflow.

Using this separation then as an indicative starting point, the runoff, interflow and baseflow contributions to the total gauged flow of 11.0 MI/d (178 mm/a) amount to 4.2 MI/d (68 mm/a), 1.4 MI/d (22 mm/a) and 5.4 MI/d (88 mm/a) for the period 1989 to 1999 inclusive.

A 25 day minimum turning point baseflow separation was used by the Environment Agency during the first stages of the East Shropshire Groundwater Model (Streetly *et al.* 2002). However, on completing the groundwater model it was apparent that the modelled baseflow contribution from the aquifer to the brooks was much smaller and less variable than anticipated (Streetly 2005). This was explained by showing that the variability of the hydraulic gradients over time which drive groundwater flow to the brooks is relatively small. Hence the actual baseflow may be a relatively constant value compared with the 25 day separation which is much more variable. If this is the case then the amount of interflow recorded at the gauge increases significantly. Furthermore if this water is generated by discharges from drift and drainage systems then the influence of the superficial flow system is very significant on the overall flow functioning of the Potford Brook catchment.

However, it is noted that the Environment Agency model used a horizontal grid of 250 m (Streetly and Young 2004), a resolution too coarse to realistically model the surface water-groundwater exchange, and that the modelled near stream groundwater levels at Wood Mill Farm were 1 to 1.5 m lower than observed values (Streetly and Young 2004). Hence, the relatively constant baseflow generated by the model may represent a failure of the model to

adequately simulate the interaction between the aquifer and the brooks. More detailed groundwater modelling of the catchment is needed to resolve this issue.

## **2.8 Summary**

The Potford Brook catchment is a lowland catchment of gently undulating terrain underlain predominantly by a Permo-Triassic sandstone aquifer. In the far north of the area steeper slopes are encountered underlain by rocks of the Mercia Mudstone group bounded by the regionally continuous Hodnet fault.

As mapped at 1:50 k scale, around 70% of the catchment is underlain by drift deposits comprising a variable covering of glacial till, glaciofluvial deposits and valley alluvium. Soils generally reflect the nature of the underlying superficial geology.

Analyses presented in this Chapter have shown that historic rainfall data, and the rainfall and climate data produced by the recent LOCAR installations, are of good quality. However, potentially significant differences in data between standard and ground level raingauges and between MORECS and FAO Penman-Monteith PEt calculations have been highlighted.

Evidence from existing literature about the catchment suggests that low permeability till and glaciolacustrine clays can in places restrict the downward movement of water to the underlying sandstone causing perched water tables in some areas. The surface water hydrograph suggests that there is a significant component of quickflow presumably generated in part by runoff from soils associated with low permeability drift materials. The distribution of nitrates in the sandstone of the wider Tern area may suggest reduced recharge in areas underlain by clayey/thicker drift.

Groundwater recharge to the sandstone may be on average greater than 240 mm/a in outcrop areas. Recent work shows that a soil moisture balance approach alone does not generate enough water to close the water budget for the area within a regional groundwater model and bypass recharge is needed (Streetly and Shepley 2005). In areas covered by low permeability drift, groundwater recharge to the sandstone may be significantly lower at 50 to 90 mm/a. However there is significant uncertainty in this estimation and in the distribution of recharge across the catchment. It is hypothesised that runoff recharge may contribute a significant amount of recharge to the sandstone.

The largest licensed groundwater abstractions in the catchment are from Environment Agency Shropshire Groundwater Scheme (SGS) boreholes used to augment flow in the River Tern in dry periods.

There is a reasonable degree of hydraulic connection between the Potford and Platt Brooks and the sandstone aquifer and the brooks receive enough baseflow to maintain flows throughout the year. However, intermediate timescale flows are a significant part of the total hydrograph. The mechanisms by which these flows are generated are largely unknown but may be due in part to drainage via field drains and groundwater discharge from superficial deposits.

## **2.9 Conclusion**

The major components of the hydrologic functioning of the Potford Brook catchment have been described in this chapter. Compared with many other catchments in the UK data availability and quality are very good, largely as a result of the presence of the SGS and more recently the LOCAR monitoring installations. Thus approaches to quantifying recharge such as that taken recently by the Environment Agency, which make good use of available data

(Streetly and Shepley 2005), are as accurate as is presently possible for a regional water resources study.

However, given all this, major uncertainty still remains at the scale of the subcatchment in regard to the distribution and magnitude of recharge in areas of variable drift lithology and thickness and the generation of intermediate timescale stream flows. In part this is due to uncertainty as to the detail of the thickness, extent and geometrical relationships between different drift units in the catchment. The best available data are given by the existing 1:50 k drift geology map, although this has no information about geological layering, and widely spaced geological logs. In addition the hydraulic processes involved in recharge at the site and local scale are not well understood and hence upscaled parameters for confident modelling of recharge at the catchment scale are not available.

The next chapter, in the context of the information described in this chapter, attempts to reduce some of the uncertainty for understanding recharge through drift at the local scale.

## **3 LOCAL SCALE INVESTIGATIONS**

### **3.1 Aim**

As presented in Chapter 2, the distribution and properties of the drift geology in the Potford Brook catchment are known only from 1:50 k mapping and borehole logs of variable quality from widely spaced locations. A more accurate knowledge of drift distribution and geometry within the catchment is vital as a first step to a better understanding of its affects on aquifer recharge.

A field programme was therefore needed to explore the geometry of the major drift units within the catchment and their spatial relationship to each other at the local scale (10s m to km). In order to understand ways in which the drift structure may control aquifer recharge some knowledge of the hydraulic properties of the drift would also be needed in order to infer hydraulic behaviour from structural models. Hence a requirement of the field programme was to include sampling of the drift materials in order to allow laboratory hydraulic and textural analyses to be carried out.

This chapter presents the methodology and results of local scale field investigations with the aim of defining local scale hydraulic processes controlling recharge through drift.

### **3.2 Experimental Design and Methodology**

#### **3.2.1 Introduction**

In order to define the most significant structural features in the drift and to allow sampling of the materials encountered, a programme of augering, drilling and geophysical surveying was designed.

A range of locations were targeted on the basis of the mapped drift geology and existing borehole logs. Once land access had been agreed, walk over surveys and some investigative

hand augering were then carried out to test the drift map and confirm the choice of survey locations. It was decided that the following 4 areas (locations shown in Figure 3.5) would be investigated to cover the three main types of glacial drift encountered in the area (till, glacial outwash and glaciolacustrine deposits):

1. The expanse of till around Wood Farm (NGR SJ 621 229)
2. The finger of glacial outwash material near Hazles Farm (NGR SJ 596 235)
3. The thick lens of outwash material beneath Whitegates farm (NGR SJ 633 229)
4. The mixture of glacial outwash, glaciolacustrine clay and till near Hollycroft farm (NGR SJ 640 230)

It was decided that geophysical surveying would be carried out in these areas and a limited number of boreholes would be augered/drilled and logged to test the geophysical interpretation and provide samples of the different lithologies for further analysis.

The methods of surveying, sampling and laboratory analysis are now described in turn.

### **3.2.2 Geophysical Surveys**

#### **3.2.2.1 Method selection**

Existing borehole logs indicate that the drift in the catchment is generally less than 20 m thick. Hence the range of geophysical techniques that were most applicable for better defining the drift architecture were ground penetrating radar (GPR), electromagnetic approaches or electrical resistivity tomography (ERT). The best choice seemed to be ERT for several reasons. Firstly, along with GPR, ERT gives the potential for a readily interpretable, fully 2-dimensional image of the subsurface to be derived in comparison to the electromagnetic methods. Secondly it was considered that the strong contrast of electrical

properties between the different types of drift in the catchment (e.g. sand versus clay) would potentially yield better results than those derived from variations in acoustic response required by the GPR method. Furthermore equipment and expertise on this method were readily available within the Earth Sciences Department at the University of Birmingham.

Although the ERT method is relatively time consuming it was thought that a reasonable spatial coverage could be made over part of the catchment within the first field season allowing time for some invasive investigations to also be carried out to ground truth the results and to provide samples for laboratory analysis.

### **3.2.2.2 Basic ERT principles and procedures**

The ERT technique is well documented (e.g. Griffiths and Barker (1993)) and so only a summary of the method will be described here.

A Wenner configuration of electrodes was used throughout this project in which four electrodes are inserted into the ground in a straight line with equal spacing between adjacent electrodes ( $a$ ). A known current ( $I$ ) is then passed through the outer two electrodes and the potential difference ( $\Delta V$ ) is measured between the inner two electrodes. This enables the apparent resistivity ( $\rho_a$ ) of the ground to be calculated using the equation:

$$\rho_a = \frac{2\pi a \Delta V}{I} \quad (3.1)$$

For an ERT survey a series of Wenner measurements at a fixed spacing ( $a$ ) is made along a traverse line with the spacing between adjacent measurements being equal to  $a$ . A series of subsequent traverses is then carried out along the same line with the spacing of the electrodes doubling each time but the spacing between adjacent measurements staying equal to  $a$ . The

choice of  $a$  is determined by the desired spatial resolution of the survey, the spacing of the final traverse dependent on the desired total depth of investigation.

The set of apparent resistivities calculated from the measured resistances can then be inverted into a 2D resistivity model of the subsurface.

### **3.2.2.3 Equipment and controlling parameter values**

The ERT carried out for this project used a set of equipment comprising 50 electrodes to which 2 multicore cables, each with 25 moulded electrode takeouts at equal predetermined intervals of 1, 2 or 5 m, were attached. The cables were connected to a switching module and resistance meter (Campus Tigre), and then to a laptop computer powered by an external battery. The set-up of a parameter file allows the user to choose which readings will be taken and to define the current magnitude and on/off times as well as the number of readings (cycles) taken for each electrode combination. The software TIGIMG2.EXE (Campus International Products Ltd. Automatic Control Software Version 2.04) loaded on to the laptop reads the parameter file, controls the switching module and logs the resistance measurements into an output data file.

In order to survey a line longer than a 50 electrode spread, a roll along technique was employed whereby after the initial survey was complete, 20 electrodes were then moved from one end to the other in the desired direction and the cables moved along by the same amount and reconnected. A parameter file was created to take the appropriate tranche of readings without repeating readings taken from the previous survey. Using a total of 50 electrodes and rolling along by 20 electrodes each time, a laterally continuous ten 'level' survey can be carried out i.e. up to a maximum spacing of  $10a$ .

The number of measurements taken per electrode combination, referred to as cycles, can be controlled using the parameter file. Having more than one cycle allows an estimate of the error to be made by comparing the resistance values for each cycle. However although errors can be reduced by using more cycles this also increases the time taken for the survey. It was found for the ground conditions encountered in the project area that 4 cycles provided a good compromise between minimising errors and being time efficient.

Generally, larger currents are required for larger electrode spacings. For the ground conditions encountered in the project area it was found that 0.5 mA for a 0.5 m spacing to 10 mA for the configurations with the widest spacings of 32 m worked well. Current time on was set to 1 s and time off to 0.5 s for all surveys conducted for this project.

A photograph of the ERT equipment is shown in Figure 3.1.

#### **3.2.2.4 Locating surveys**

The location of each survey line was measured with reference to field boundaries and fixed landmarks using a tape measure and compass. Sometimes this would mean measuring the distance of the start and end points from known locations and then following a bearing between these points. More often survey lines were chosen to follow known field boundaries at a set distance. These locations were entered into ArcView GIS using Ordnance Survey (O/S) Landline data.

Areas close and parallel to roads or overhead power cables were avoided in order to minimise interference from other electrical signals or man-made disturbances of the subsurface.

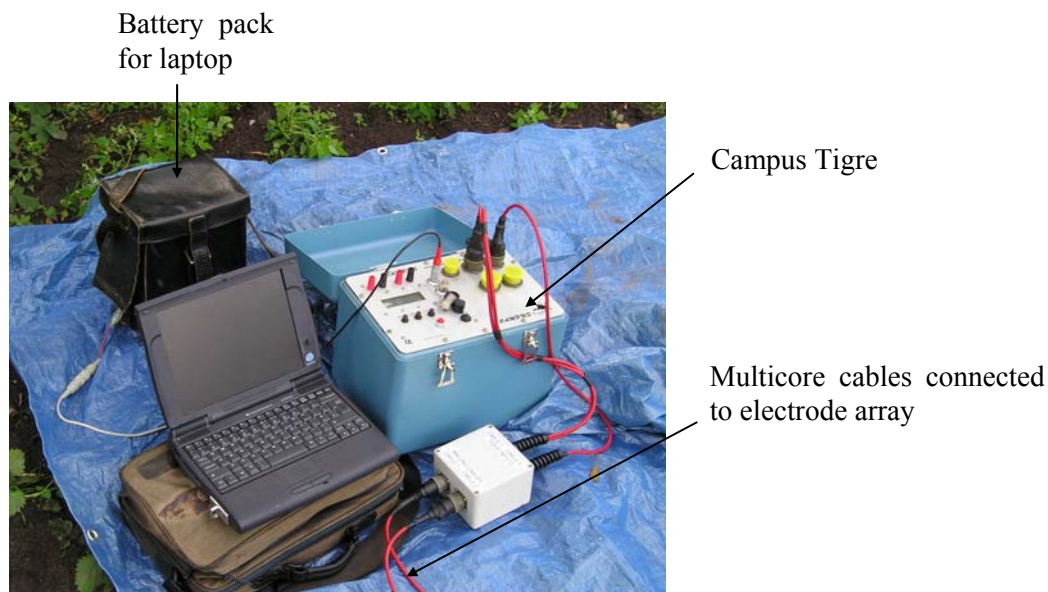


**Figure 3.1** Photograph of the ERT equipment

### 3.2.2.5 Survey procedure

The equipment was set up by first laying out the cables in a straight line in a given location. Electrodes were then pushed 10 to 15 cm into the ground at the intervals prescribed by the takeouts on the cables. The cables would be attached to the ERT equipment via a junction box and the appropriate parameter file loaded onto the laptop. The contact resistances between the electrodes and the ground would then be checked. If these were greater than  $2000 \Omega$  the electrode of concern would be replanted to ensure a better contact. Once the contact resistances were within the required range the survey was then started with a 1% acceptability criterion for the repeatability of resistance reading over the 4 cycles. Where the error was greater than this the reading would automatically be re-taken 5 times to try and achieve a lower error. The time taken by the TIGRE for each reading is around 12 s for 4 cycles.

Once the survey had finished, the data would be checked manually taking note of any readings with errors greater than 1%. These readings would then be re-run until a

satisfactorily low error was achieved or it became clear that an error this low was unachievable.

### **3.2.2.6 Inversion methods**

Inversion of the measured resistances was carried out in a 3 stage process:

Firstly, observed resistances were converted to apparent resistivity values (based on Equation 3.1) and re-ordered into a format suitable for input to the inversion software RES2DINV version 3.54, which incorporates the work of Loke and Barker (1995; 1996a; 1996b). The program CONCAT64.EXE was used for this procedure which was written and provided by Ron Barker of the University of Birmingham. For roll along surveys this program also concatenates consecutive data files along an ERT line into one file ready for inversion. Secondly, topographical data were then added to the inversion input file using a combination of DTM and O/S maps as appropriate. Thirdly, the data were inverted using RES2DINV. Since the inversion produced is non-unique, a range of parameters were tested and a parameter set that consistently gave reasonable results was chosen to be applied to all the surveys. Inversions were run using default parameters for a least-squares inversion, except where changes were made to the following options:

1. Topographic modelling. Where topography was included in the inversion process the method chosen was “distorted finite-element grid with damped distortion.” In this option, the subsurface nodes are shifted to a lesser extent compared with the surface nodes, i.e. the effect of the topography is "damped" with depth. The damping value was set to 0.5. This option is a reasonable choice given that the amplitude of the curvature of the topography is less than the depth of the deepest model layer.

2. Reduced effect of side blocks. In some cases during inversion a greater weight can be given to the side blocks compared to the interior blocks of the model and this can result in unusually a high or low resistivity value for the side blocks. Thus the option to reduce the effect of the side blocks was chosen and model blocks were set to equal widths.
3. Vertical to horizontal flatness filter ratio. This ratio was generally set to 0.3 to damp out geologically unrealistic vertical anomalies from the inverted images.

Inversions were iterated until an RMS error of less than 2% was achieved. This generally took around 5 to 10 iterations.

A series of inversions for data collected from Hazles Farm (survey line B on Figure 3.5) for a range of parameters is shown in Figure 3.2. It is noted that the interpretation of the broad geological structure is insensitive to these parameter changes.

### **3.2.3 Invasive Sampling**

#### **3.2.3.1 Introduction**

Invasive investigation of the upper 5 m of the drift within the project areas was initially carried out by means of a combination of augering by hand and by using a mechanical auger. The choice of these methods was governed by the equipment readily available within the Department of Earth Sciences at the University of Birmingham. Samples were taken as disturbed bag samples and undisturbed drive samples. In addition to using the in-house equipment, resources were available to fund several cored holes using a Sonic drilling rig at the two fieldsites used for site scale hydraulic characterisation (from hereon referred to as Site 1 and Site 2 and dealt with in detail in Chapters 4 to 6). Each method is described

separately in turn although the methods were used in combination for many of the auger holes.

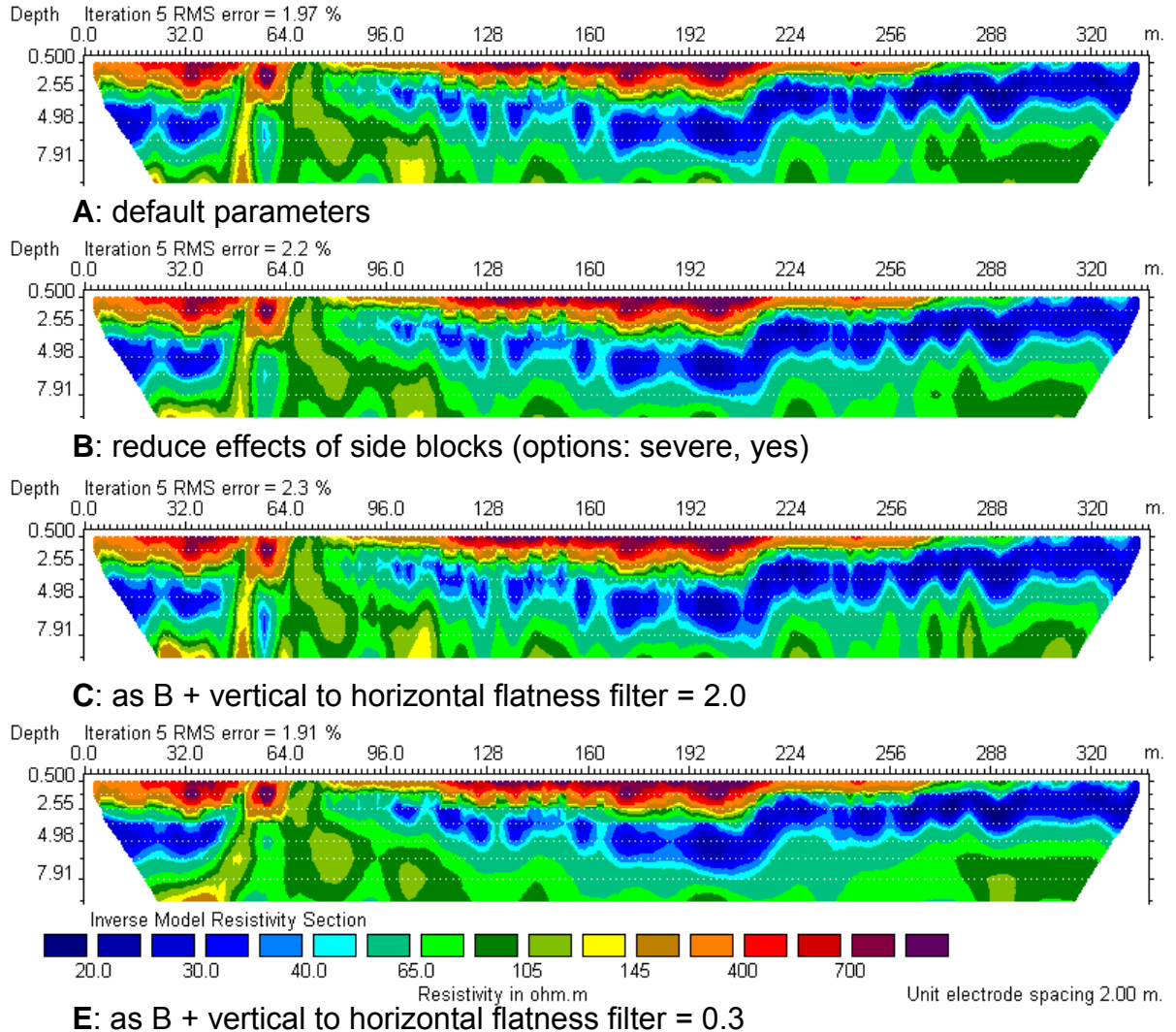


**Figure 3.2** Sensitivity of ERT inversion to parameter variation

### 3.2.3.2 Locating drill holes

The location of each auger hole was measured with reference to field boundaries and fixed landmarks using a tape measure and compass. These locations were then converted to grid references using O/S Landline data within ArcView GIS software.

### **3.2.3.3 Auger methods and drive sampling**

A bucket auger was used to make 65 mm diameter holes up to 2.5 m below ground level (mbgl). Each full bucket was emptied and inspected enabling an approximate geological log to be produced.

Since stiff clays were often encountered it was not possible to hand auger to depths much greater than around 2.5 mbgl. In addition, when large pebbles were encountered it was often impossible to make further progress with the hand auger. For reaching greater depths or for breaking past pebbly obstructions a mechanical Minute-Man auger was used. It is a rotary auger driven by a petrol engine. The drill strings are 65 mm diameter and 3 ft in length. In theory it is possible to reach depths of 10 to 15 m with this rig. However, due to the age of the engine it was not safe to drill much below 4 mbgl while ensuring that retracting the drill string was still possible. Only an approximate geological log could be produced based on cuttings brought up the hole due to the mixing that occurred up and down the drill string while drilling. With both augering methods significant smearing of the hole walls is unavoidable especially when damp clays are encountered.

Within the auger holes a 45 mm external diameter steel mechanical drive sampler was used to take 150 mm length, 35 mm diameter undisturbed samples housed in a plastic tube. A cutting shoe screws onto the main body of the sampler holding the plastic tube in place. Above the void into which the sample is taken there is a hole through which air can escape. This hole is covered by a rubber ring to stop it being blocked up as the sampler is moved up and down the auger hole and to prevent air entering the sampler as it is withdrawn. The sampler was adapted to screw onto a series of 30 mm steel rods linked by grub screws. A steel hitting block was then fitted onto the top link rod.

While augering, samples were taken at set depth intervals or more frequently if a change of lithology was encountered. Augering equipment was then removed from the hole and cleared to one side to make room for the drive sampling equipment.

While every effort was made to ensure that as much loose material was removed from the hole as possible before sampling commenced, there was often some material remaining. In order to remove this debris, the drive sampler was pushed firmly into the base of the hole and then pulled back up and emptied. This was found to be an effective way of clearing debris from the base of the hole. With a little experience it was found that it was possible to “feel” with the sampler whether any loose material remained at the bottom of the hole.

Once the hole was sufficiently clean, the drive sampler, cleaned and loaded with a fresh plastic tube and attached to the appropriate number of link rods, was then lowered carefully into the auger hole. A piece of tape was attached 150 mm above some datum on the string of link rods and the hitting block screwed onto the uppermost link rod. A large slide-hammer was then used to drive the sampler into the base of the hole until the marker tape was flush with the datum.

It was often impossible to retrieve the sampler by hand. If this was the case the hitting block was removed and a jack fitted over the end of the string of link rods. The jack works by a series of ball bearings which grip the link rods stopping them from slipping back down the hole but allowing the link rods to move freely upwards out of the hole. The sampler could then be unscrewed and the sample removed for storage/transit to the laboratory.

The sample would be carefully retrieved and end caps fitted to the end of the sample tube and sealed with waterproof tape. The sample tube was marked using a permanent marker with the sample bottom depth, orientation (“way up”) and sample number.

Photographs of the Minute-Man and the drive-sampler are shown in Figure 3.3.

#### 3.2.3.4 Sonic drilling

At Site 1 and Site 2 several holes were continuously cored at 74 mm ID using a sonic drilling rig. The sonic drilling equipment employed by our contractors Drillcorp uses very high frequency mechanical oscillations to diffuse deep vibrations through the drill string to the bit. The vibrations cause the soil particles that come into immediate contact with the drilling tools to be effectively fluidised allowing rapid penetration without the need for a flushing medium.

This method of drilling was chosen in preference to conventional techniques in order to produce high quality core with minimal site disturbance. Furthermore, due to the rapid penetration possible in unconsolidated materials the method was deemed to be cost effective for the range of drift materials we expected to encounter. A photograph of the sonic drill rig is shown in Figure 3.4.



A



B

**Figure 3.3** Photographs of the Minute-Man auger (A) and drive-sampler (B)



**Figure 3.4** Photograph of the sonic drilling rig at Site 1

### **3.2.4 Laboratory Analysis of Hydraulic Properties**

#### **3.2.4.1 Introduction**

The methods of laboratory analysis described in this section were chosen in order to allow a relatively quick hydraulic characterisation of the deposits at the core scale. Thus, it is acknowledged that aspects of the analysis (such as the lack of repeat testing) fall short of what might be required for a state of the art investigation into the material properties.

#### **3.2.4.2 Borehole logging and sampling**

The cores taken with the sonic rig were logged to BS5930 with the help of staff from the BGS. Samples of approximately 100 g were taken at approximately 10 cm intervals or at abrupt changes in lithology, weighed ( $M_w$ ), dried in an oven at 100 °C for 24 hours and re-weighed ( $M_d$ ). A gravimetric moisture content by mass ( $G_m$ ) was then calculated as follows for each sample:

$$G_m = \frac{(M_w - M_d) \times 100\%}{M_d} \quad (3.2)$$

### 3.2.4.3 Falling head permeameter tests

Falling head permeameter experiments requires 'foreign' water to come into contact with the samples. In order to minimise any chemical reactions between the samples and water used for these experiments a synthetic groundwater was needed which matched as closely as possible the chemistry of the sample porewaters. As part of the LOCAR programme, a suite of pore water chemistry analyses has been carried out for materials from 6 depths in a cored borehole (T06) within the study area (Wood Farm NGR SY 622 230). The drift materials from which pore water was extracted are clayey tills from the same till sheet as those from which the samples for this study have been taken. The analysis with the best ionic balance was chosen as the desired hydrochemistry for the synthetic groundwater to be used for the laboratory experiments.

In order to make up the synthetic groundwater, concentrations of salts as given in Table 3.1 were added to de-ionised water to match the concentration of major anions as closely as possible, taking into account the waters of crystallisation.

Salt	Mass Added Per Litre De-ionised Water (g)
MgSO <sub>4</sub> .7H <sub>2</sub> O	0.3990
CaCl <sub>2</sub> .2H <sub>2</sub> O	0.3605
NaCO <sub>3</sub>	0.1913
K <sub>2</sub> SO <sub>4</sub>	0.0067g

**Table 3.1** Synthetic groundwater recipe

The resulting groundwater had a TDS of 670 mg/l compared to a theoretical TDS of 665 mg/l and a major ion breakdown as shown in Table 3.2. The pH of the synthetic groundwater was around 8.5 compared to the pH of the target porewater of 8.3.

Ion	Concentration (mg/l)
Mg <sup>2+</sup>	39
Ca <sup>2+</sup>	98
K <sup>+</sup>	3
Na <sup>+</sup>	53
SO <sub>4</sub> <sup>2-</sup>	160
Cl <sup>-</sup>	174
“CO <sub>3</sub> <sup>2-</sup> ”	138

**Table 3.2** Ionic concentration of synthetic groundwater as calculated from the recipe in Table 3.1

The core produced by sonic drilling was subsampled using 35 mm plastic tubing pressed into the side or up the middle of the core. Undisturbed samples taken with the drive sampler were used directly. The plugs of undisturbed material in each case were then removed from the plastic tube and trimmed at either end. The mass, length and average diameter was measured in order for an approximate volume and density to be calculated before the samples were wrapped in PTFE. A heat shrink sleeve was applied leaving material at the sample base exposed and a section of sleeve above the top of the sample that formed a tube of narrower diameter to which a rubber bung was fitted. A piece of stocking was doubled up and attached with a small cable tie around the open base of the sample to discourage disaggregation of the end of the sample when saturated.

The samples were placed the right way up (open end downwards) into a beaker of synthetic groundwater with the level of the water just below the top of the plastic sleeve. The mass of the samples was taken at regular intervals until it was no longer increasing and water was beginning to seep from the top of the sample. It was assumed at this point that the sample was saturated.

The samples were then attached to a falling head apparatus filled with synthetic groundwater ensuring no air bubbles were trapped in the sample or permeameter tubes. An initial head of around 2 m was used and the head over time was regularly recorded. The time interval between measurements depended on the rate of decline in the head but in most cases enabled at least 5 readings to be taken before the head reduced to less than 0.5 m. For samples with relatively low permeability this took up to 1 month.

The apparatus used enables the permeability of up to 20 samples to be measured at one time. However, one control standpipe was filled with water to around 2 m and left closed at the lower end over the time period in which permeability measurements were being made. The head in this tube was regularly monitored in order to assess the loss of water by evaporation from the top of the tube and the decrease in head due to degassing.

The results were then entered into a spreadsheet and plotted as a graph of log head against time. The data should plot in a straight line and the gradient can be used to calculate the permeability using the following equation (Freeze and Cherry 1979):

$$K = \frac{aL \ln\left(\frac{H_0}{H_t}\right)}{At} \quad (3.3)$$

Where

$a$  = cross sectional area of standpipe

$A$  = cross sectional area of sample

$L$  = length of sample

$H_0$  = initial head in standpipe

$H_t$  = head in standpipe at time  $t$  corrected against the control standpipe

$t$  = time from the beginning of the experiment

Plotting  $\ln(H_0/H_t)$  against  $t$  and calculating the gradient ( $g$ )  $K$  can be calculated as:

$$K = \frac{aLg}{A} \quad (3.4)$$

#### 3.2.4.4 Constant head permeameter tests

Constant head permeameter tests were carried out on a limited number of samples of unconsolidated glacial outwash using the method described in Bloomfield (1994). Samples of core were subsampled into shortened 60 ml plastic syringes of known mass. The length ( $L$ ) and diameter was measured and the cross sectional area ( $A$ ) calculated. A rubber bung and outlet was attached to the open end of the syringe barrel and attached to the permeameter apparatus. The sample was then saturated and removed from the apparatus to be re-weighed to allow the saturated mass ( $M_s$ ) of the sample to be calculated. The sample was then re-attached to the constant head apparatus and the time ( $t$ ) recorded for a known volume ( $V$ ) of around 100 ml to pass through the sample. The head difference between the constant head and the flow outlet was measured ( $\Delta H$ ) and the hydraulic conductivity was then calculated using Darcy's Law:

$$K = \frac{VL}{At\Delta H} \quad (3.5)$$

#### 3.2.4.5 Grainsize analysis

A selection of samples was subjected to manual grainsize analysis using sieves of phi size increments from 63 microns to 4 mm. Each sample was first wet sieved through a 63 micron sieve to establish the proportion by mass of fines (silt and clay) according to the methodology of Gale and Hoare (1991). The retained proportion was then dried and subjected to a standard sieve analysis to establish the proportion by mass for each phi increment.

A selection of finer grained samples was also subjected to an automated particle size analysis using Mastersizer 2000 made by Malvern Instruments. This allows a small mass of sample

mixed in a dispersant (water) to be analysed using laser diffraction to generate a particle size distribution of particles from 0.02 microns to 2 mm. To test consistency in the results each sample was split into 3 approximately 0.5 g subsamples. For each analysis the subsample was mixed in 100 ml of water and passed through a 2 mm sieve. The background diffraction of the water passing through the instrument was first measured before the sample suspension was added and particle size measurements made. The background readings were then automatically subtracted to generate the particle size distribution of the sample.

#### **3.2.4.6 X-ray diffraction**

Just one sample of till was sent to the Natural History Museum of London for a standard x-ray diffraction analysis to determine the phase proportions of the minerals in the sample. Results were obtained by least-squares fitting of diffraction patterns with close-matching standard phase patterns with uncertainties estimated to be in the region of  $\pm 3\%$  for the weight % values reported.

#### **3.2.4.7 Thin sections**

Thin sections of two samples of till and one of glaciolacustrine clay were made in vertical and horizontal orientations in order to study the micro-scale texture, structure and lithology. A number of digital photomicrographs were taken of each sample at a variety of scales.

#### **3.2.4.8 Bulk density and porosity calculations**

Once samples had been removed from falling head or constant head permeameter apparatus they were oven dried at 100 °C for 24 hours and their mass was measured ( $M_d$ ). The approximate volume of each sample at in situ moisture ( $V_w$ ) and dry moisture ( $V_d$ ) contents was calculated on the basis of average sample length and diameter. From these data the dry bulk density was calculated ( $D_d$ ) by the following equation:

$$D_d = \frac{M_d}{V_d} \quad (3.6)$$

Knowing  $D_d$  the approximate volumetric moisture content ( $\theta$ ) of each sample could then be calculated knowing its gravimetric moisture content by mass ( $G_m$ ) and the density of water ( $D_w$ ) by the following equation:

$$\theta = \frac{(G_m D_d)}{D_w} \quad (3.7)$$

### 3.3 Results

#### 3.3.1 ERT Surveys

Approximately 5 km of ERT roll-along surveys were carried out, mostly using a minimum electrode spacing of 2 m. The locations of the survey lines are given in Figure 3.5 and shown in relation to the augerhole locations and Sites 1 and 2 in Figures 3.6 to 3.8. Model resistivity inversions are shown in Figure 3.9 A to M along with superimposed lithological logs of auger/drill holes.

A frequency distribution of the resistivity value to which resistivity depth soundings tend at depth was constructed by re-interpreting National Resistivity Depth Sounding Database (archived by Ron Barker at the University of Birmingham) data for 256 surveys in the Potford Brook area as shown in Figure 3.10. This represents the likely distribution of the saturated resistivity of the underlying Permo-Triassic aquifer. This indicates that values in the range 60 to 145 ohm-m are to be expected with the greatest frequency of occurrence at around 90 ohm-m.

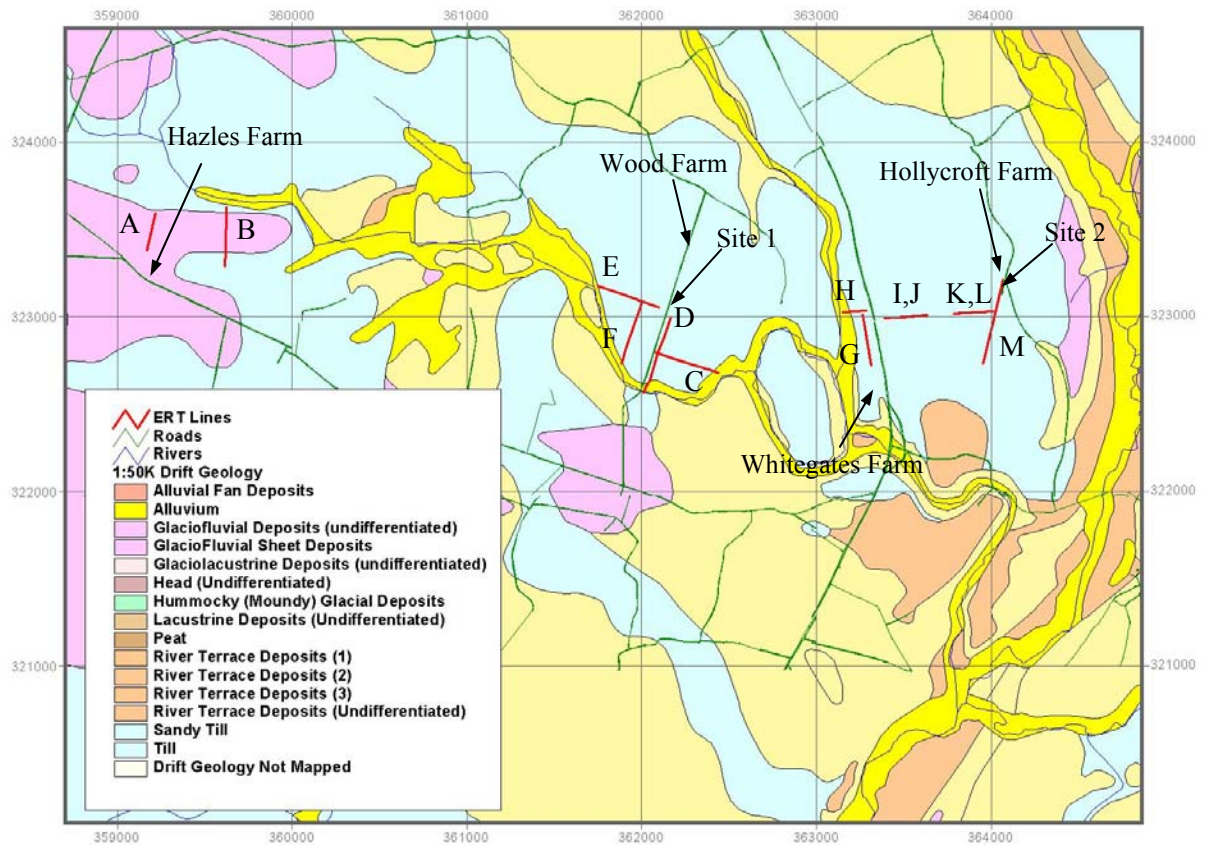


**Figure 3.5** Locations of ERT survey lines A to M

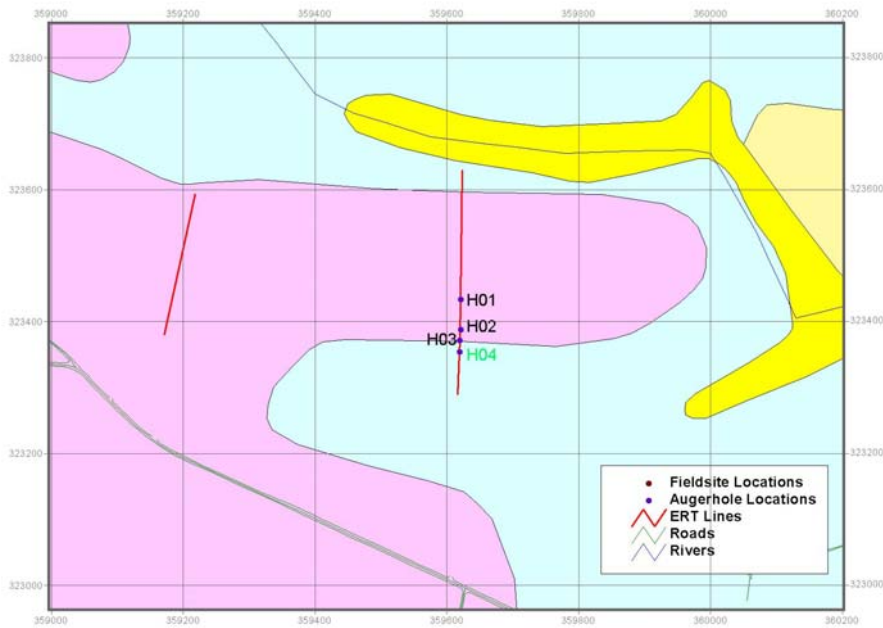


**Figure 3.6** Locations of augerholes around Hazles Farm (geology as for Figure 3.5)

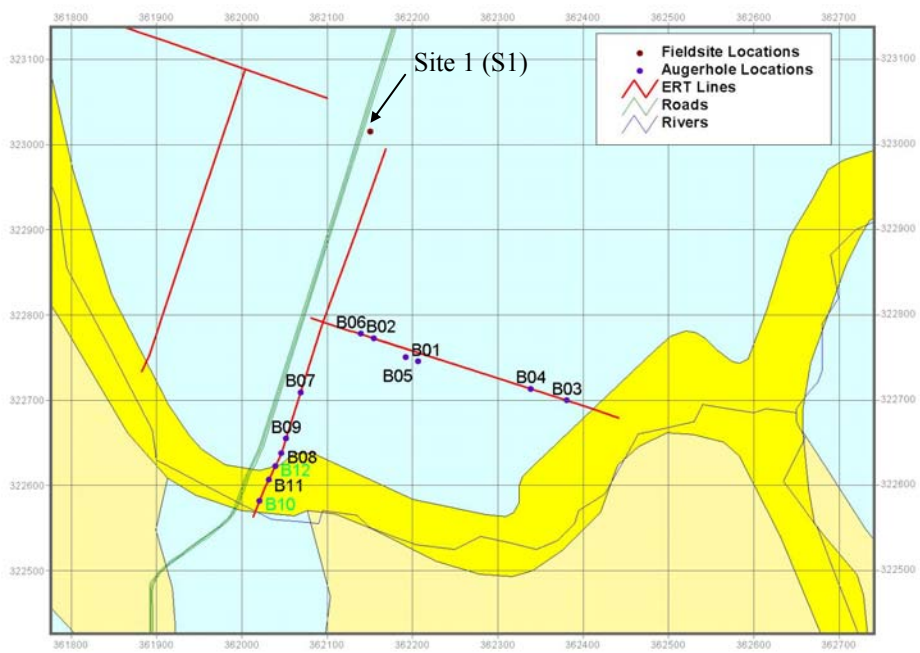


**Figure 3.7** Locations of augerholes around Wood Farm and Site 1 (geology as for Figure 3.5)

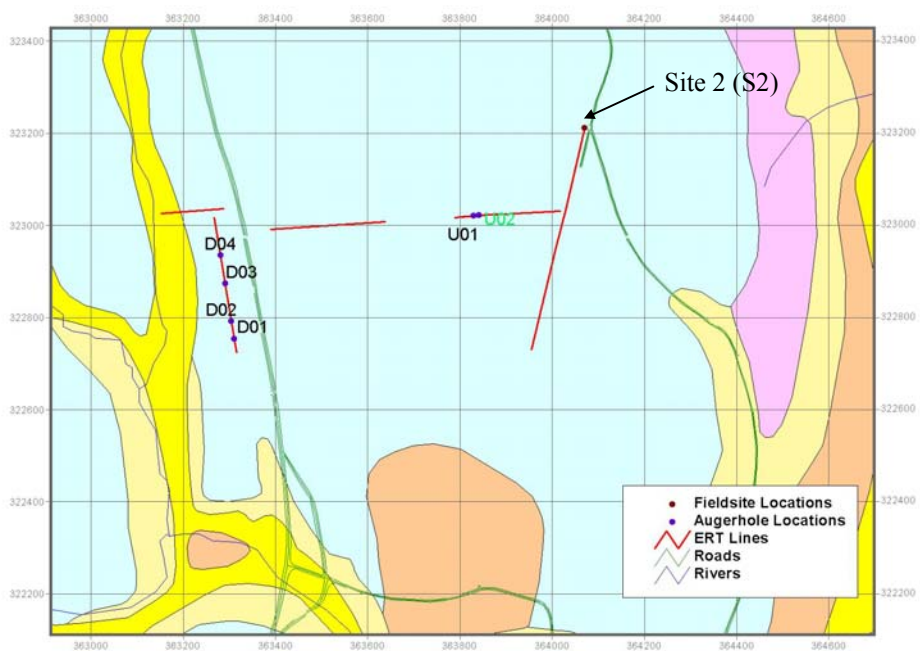


**Figure 3.8** Locations of augerholes around Whitegates Farm and Site 2 (geology as for Figure 3.5)

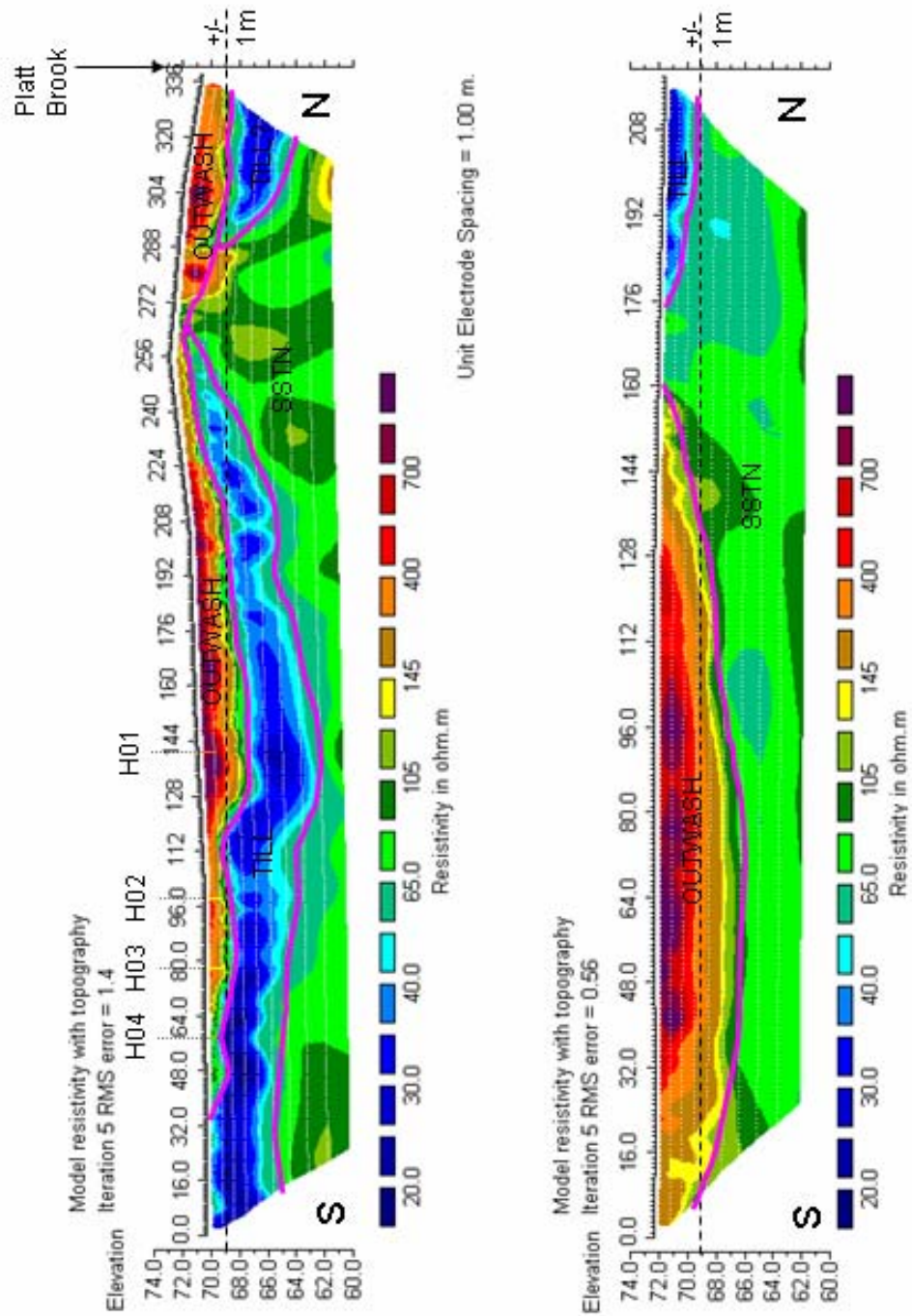


**Figure 3.9 A to B** Interpreted ERT inversions with locations of augerholes

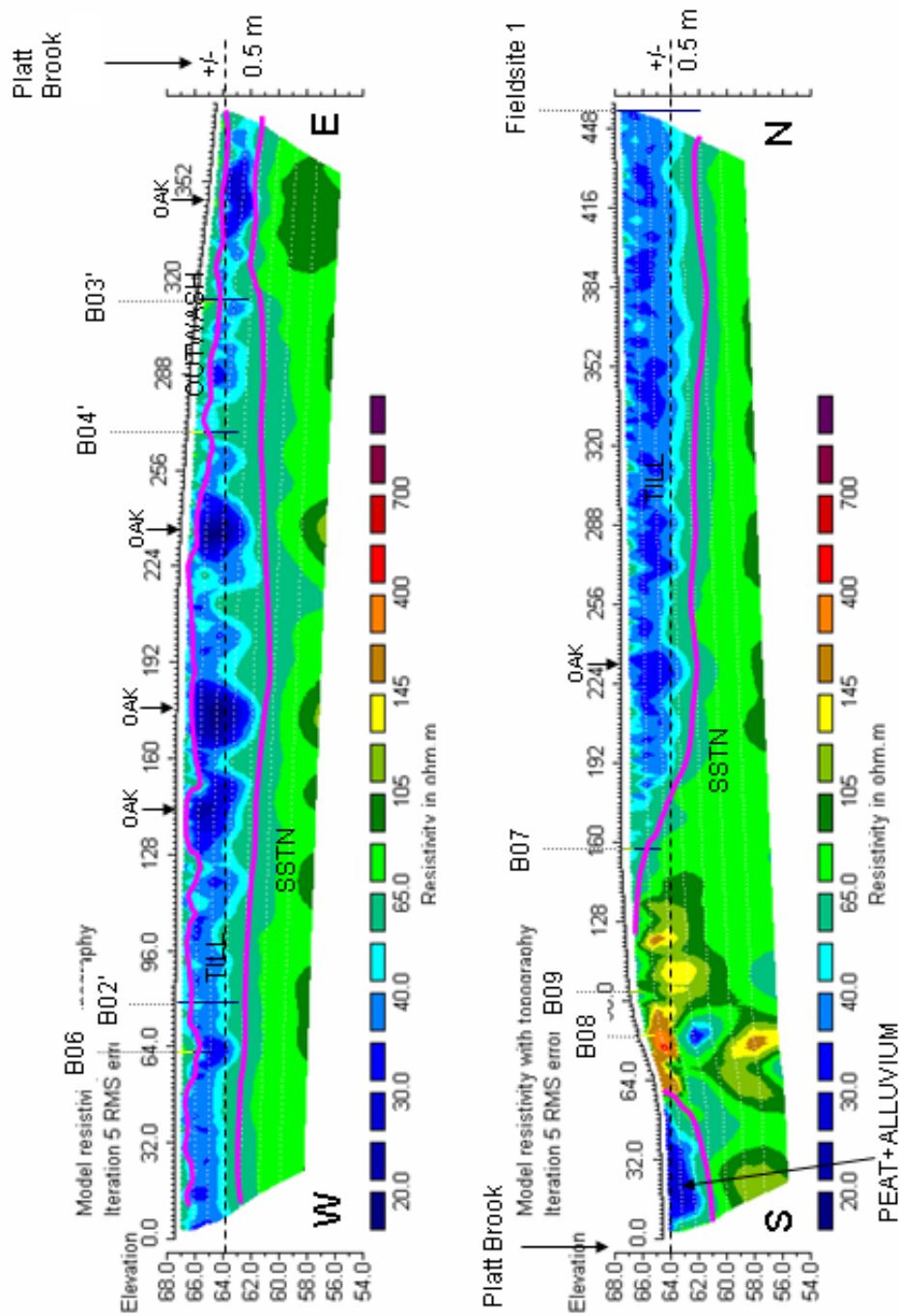


Figure 3.9 C to D Interpreted ERT inversions with locations of augerholes

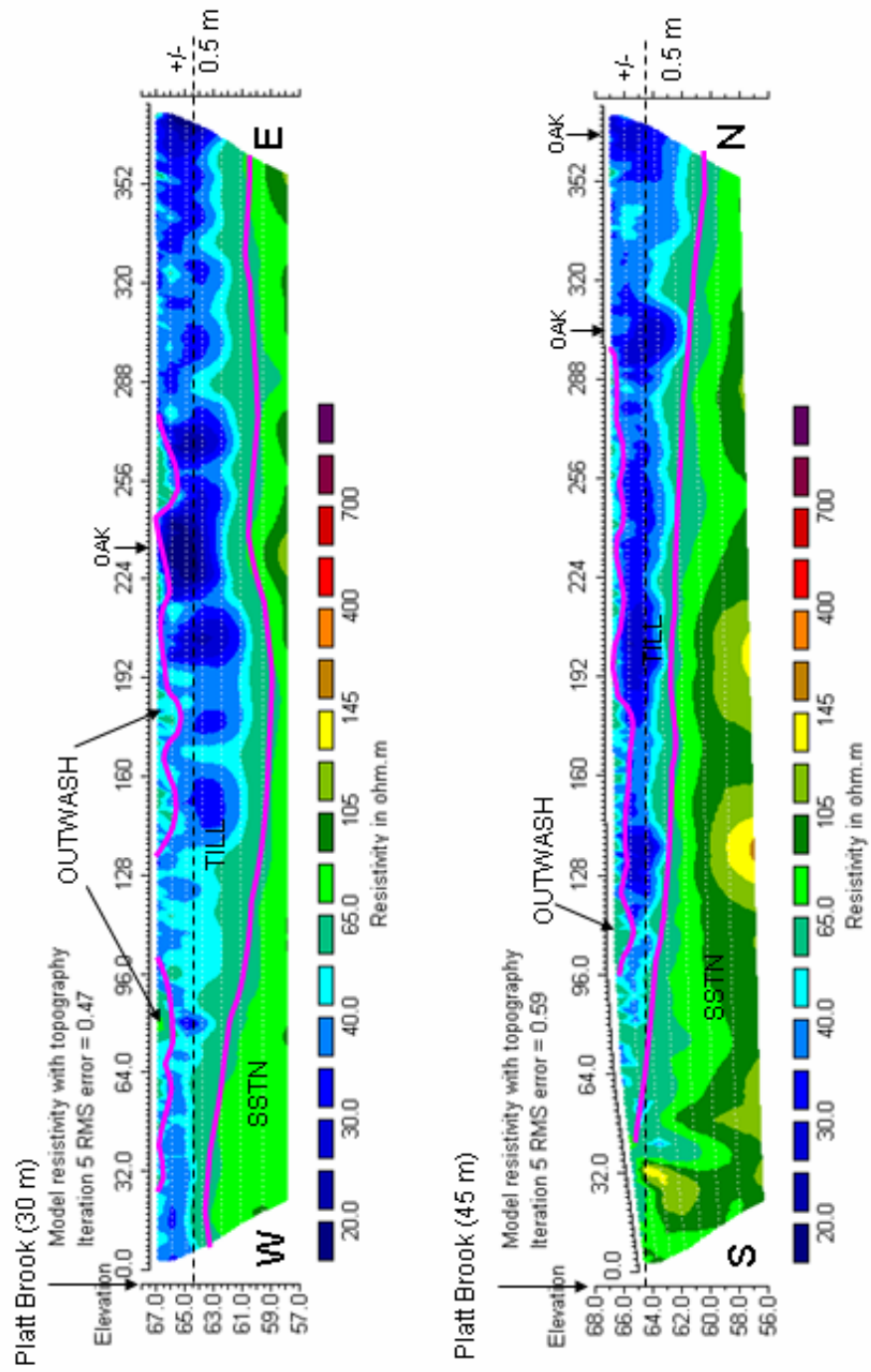


Figure 3.9 E to F Interpreted ERT inversions with locations of augerholes

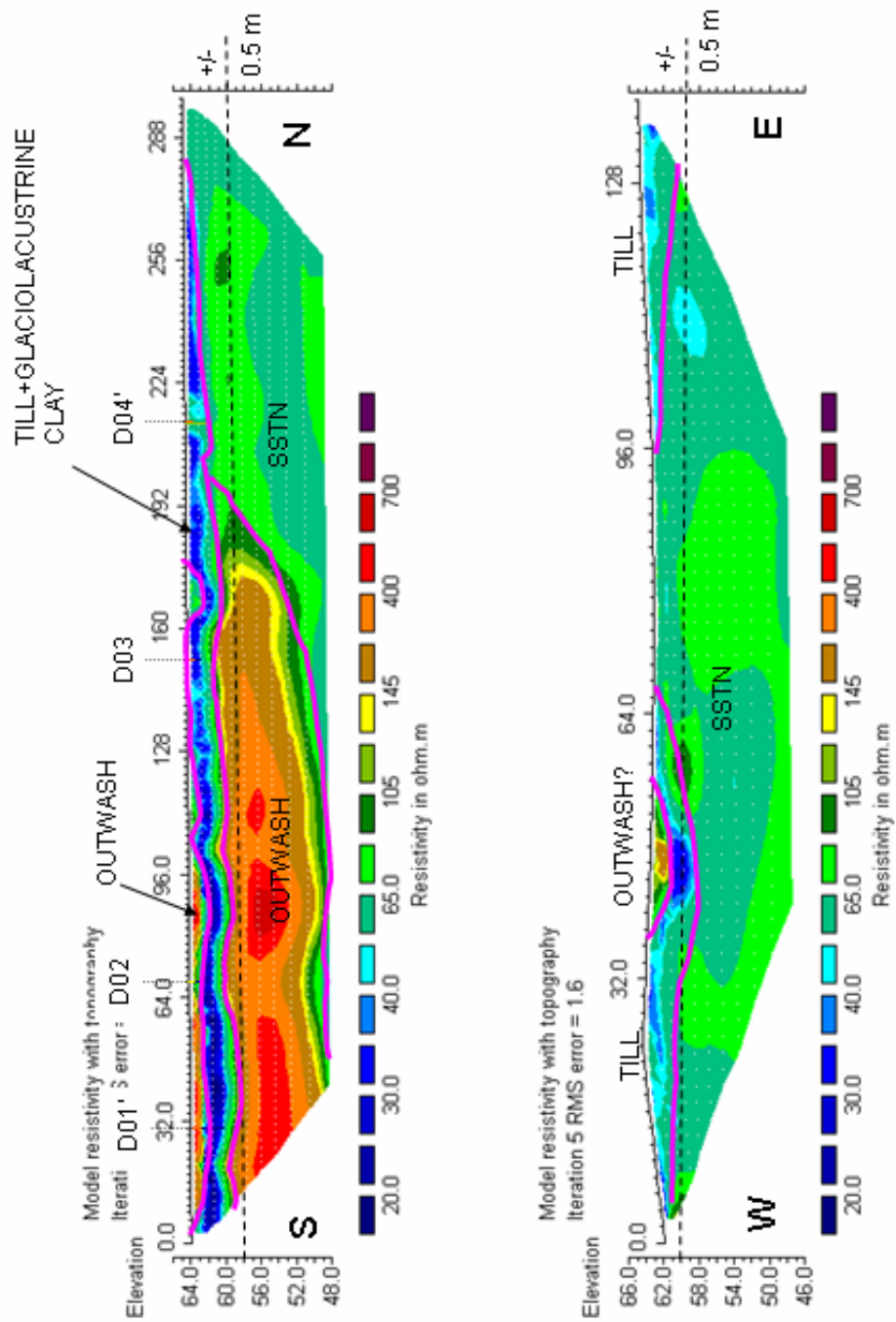


Figure 3.9 G to H Interpreted ERT inversions with locations of augerholes

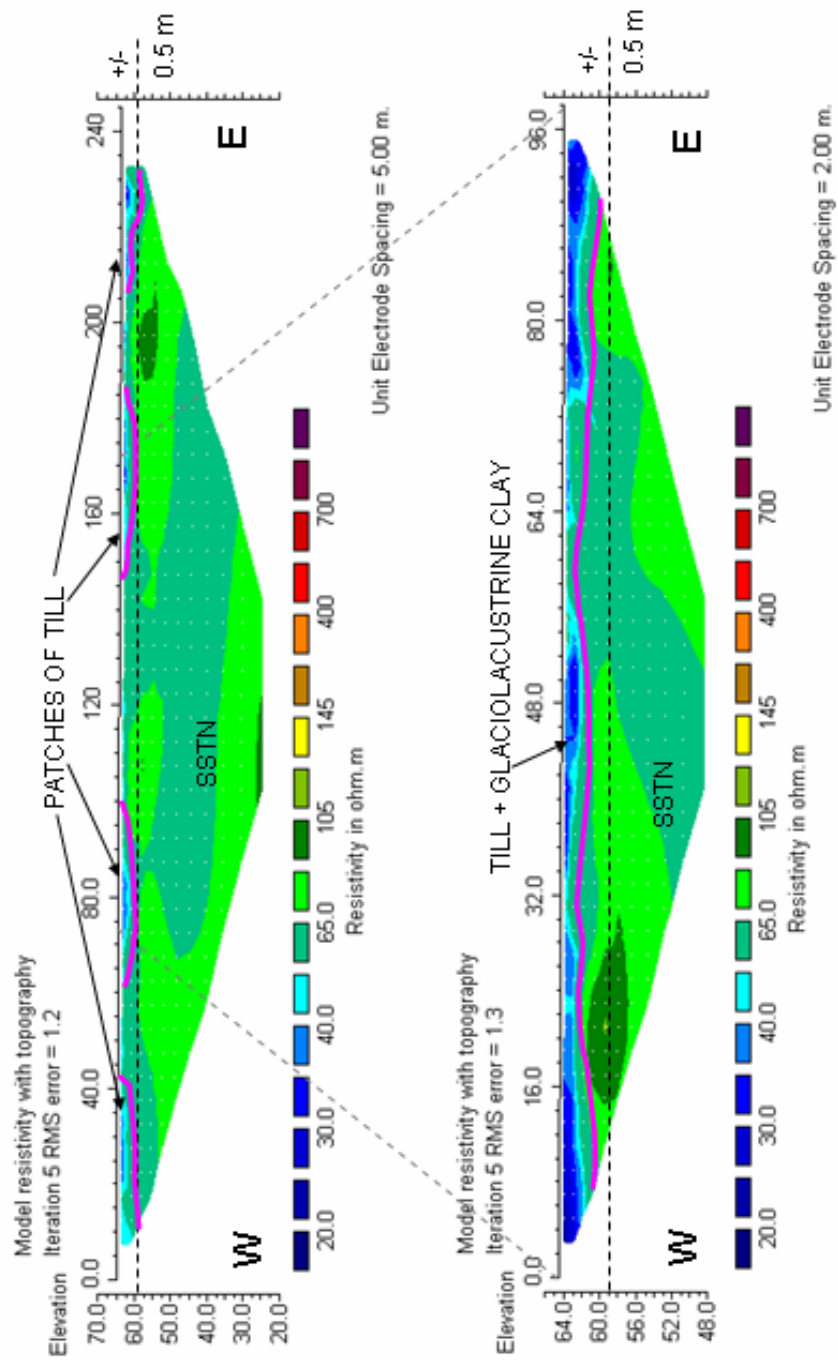


Figure 3.9 I to J Interpreted ERT inversions with locations of augerholes

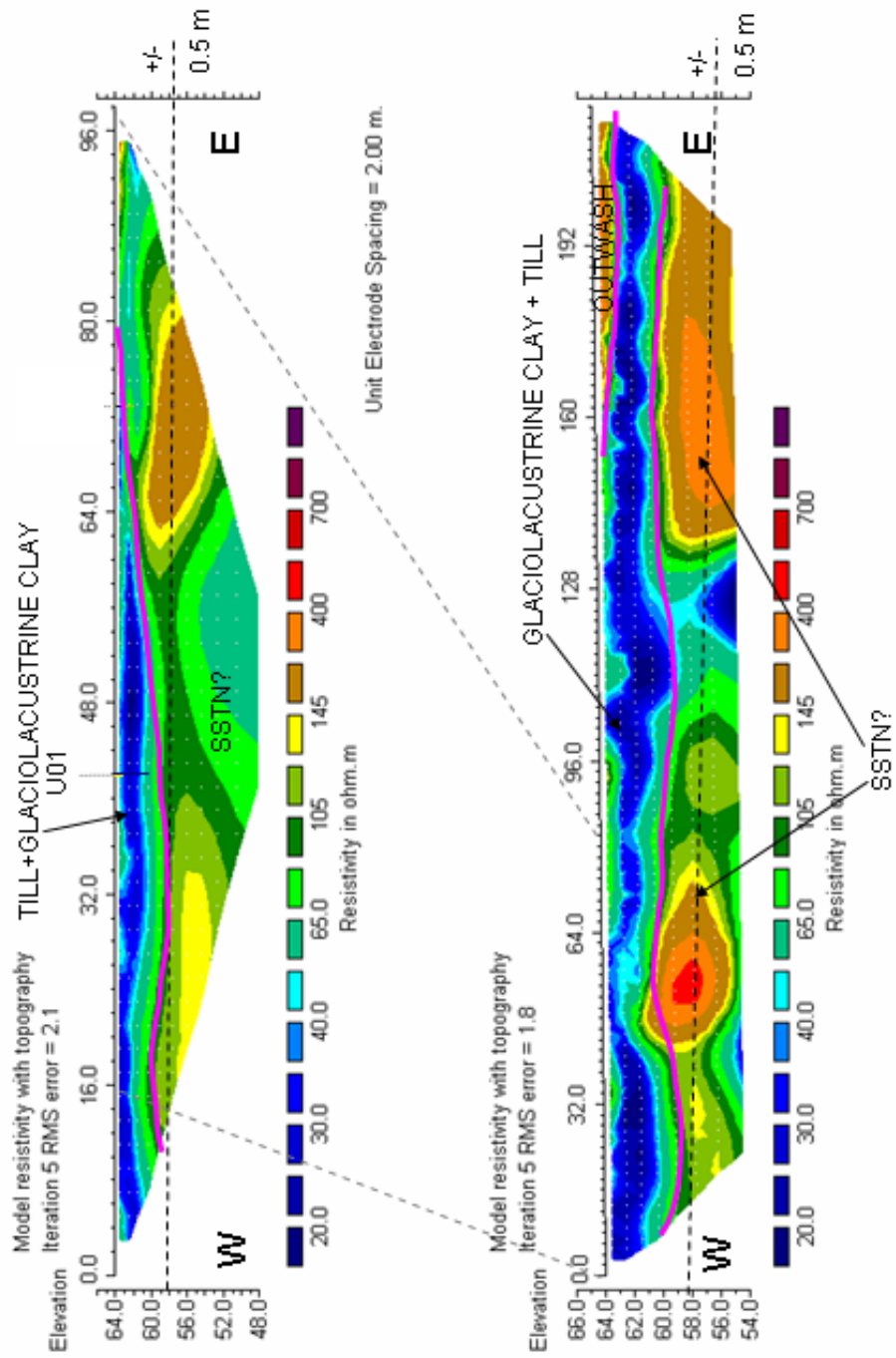


Figure 3.9 K to L Interpreted ERT inversions with locations of augerholes

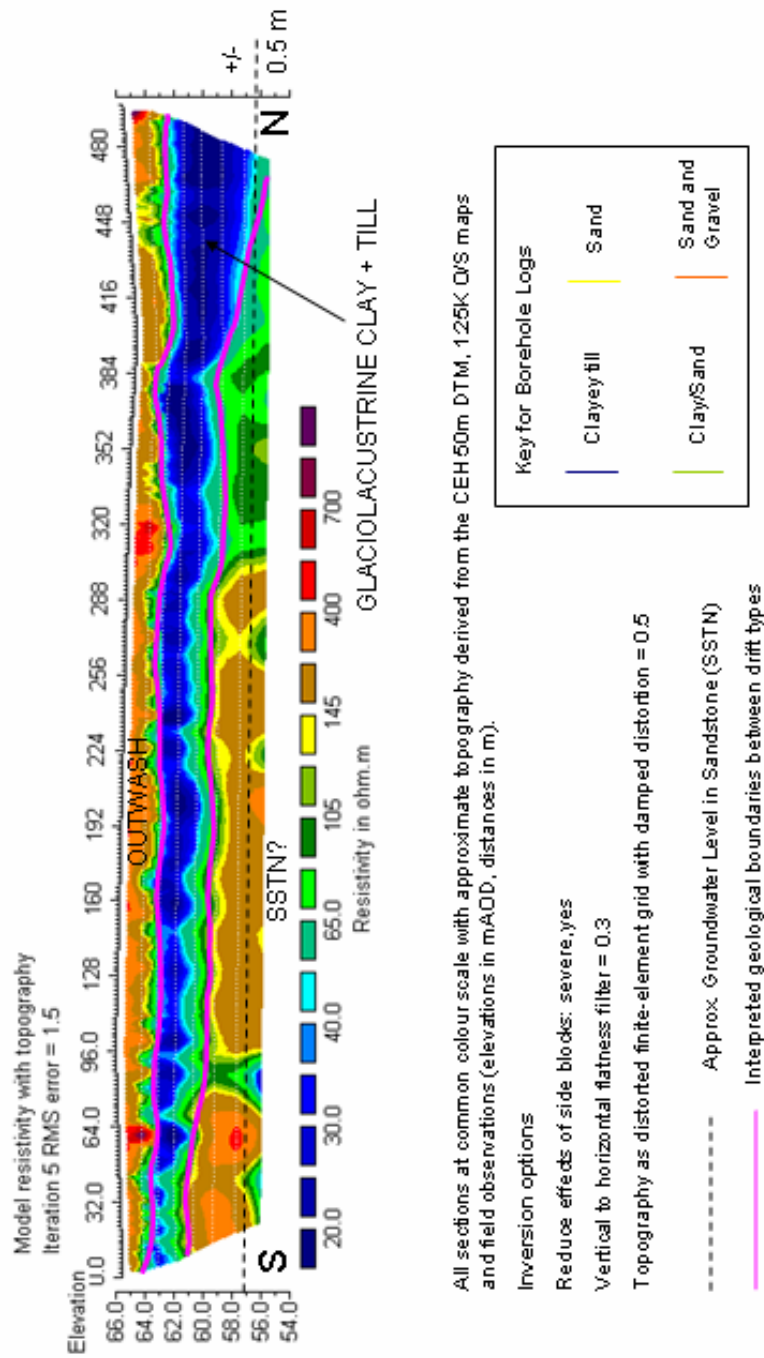
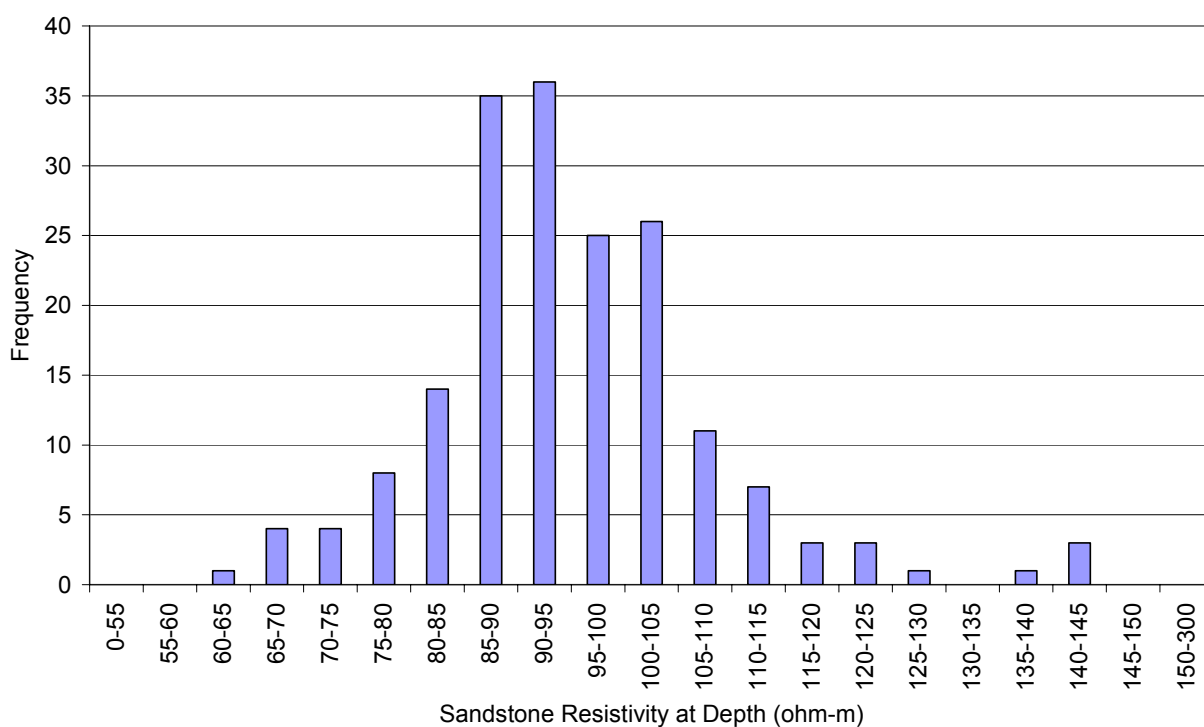


Figure 3.9 M Interpreted ERT inversions with locations of augerholes



**Figure 3.10** Frequency distribution of Permo-Triassic sandstone resistivity at depth based on re-interpreted soundings from the National Resistivity Depth Sounding Database

Till and glaciolacustrine clays are known to have resistivities in the range 20 to 40 ohm-m (Russell and Barker 2004). Values for coarser textured glacial outwash material were expected to range very widely from around 100 to 1000 ohm-m. The resistivity of each deposit will of course vary with saturation, pore water conductivity and temperature as well as with lithology (Rein *et al.* 2004). Thus we should expect a more confident interpretation to be possible when distinguishing a clay from a coarse sand unit than we might, for example, when interpreting a change from a wet coarse sand to a drier fine sand which may have similar bulk resistivity values. In addition a limitation is to be expected in the resolution of possible interpretation due to the averaging out that is implicit in the method and the inversion procedure. Thus the expectation was to be able to delineate the structure of the drift units at

the 10 to 100 m scale, accepting that smaller scale variations will be missed by using ERT with a 2 m minimum electrode spacing.

By using the range of values expected for each drift type it was possible to interpret the inverted sections and define the likely geometry of the different drift units. These structural interpretations are shown superimposed on the resistivity inversions in Figure 3.9. Based on the comparison between the auger holes and the interpreted ERT inversions it was generally found that the ERT method (using a 2 m minimum electrode spacing) allowed a confident definition of the boundary between major drift units to within approximately 0.5 m vertically and 5 m horizontally. However where the deposits were thinly layered, lithological differentiation was impossible due to the spatial averaging involved. In areas with no borehole control there is also some uncertainty as to the possible geological interpretation. The limitations of the method can be illustrated by two examples.

Firstly, considering the northern extremity of the survey shown in Figure 3.9 M, the ERT implies that a high resistivity layer around 2.5 m thick overlies a low resistivity layer continuing to around 9 mbgl. When we look at the logs for the boreholes drilled at this location (Site 2) we see that there is a layer of outwash material of around 2.5 m thickness at the surface but that the apparently electrically homogeneous low resistivity layer beneath is in fact made up of a layered clay-sand-till sequence (Figure 3.11).

Secondly the material at depth in the surveys shown in Figure 3.9 K to M is at times in the range expected for the Permo-Triassic aquifer but in many instances the resistivity is higher than expected. However, the deposit is not obviously channelised and therefore does not easily lead to an interpretation of the material being an older phase of glacial outwash such as that seen in Figure 3.9 G. The higher resistivities may be caused by partial saturation and/or

variable weathering of the sandstone such as that encountered in augerhole B08 in Figure 3.9 D. Without further borehole control it is difficult to say.

An interesting feature seen in Figure 3.9 C to F is the low resistivity associated with the locations of large oak trees within 10 m or so of the survey lines. This is likely to be caused by the presence of relatively soft and fine tree roots at this radial distance from the trees which are known to be electrically conductive (in contrast to the drier thicker woody roots found closer to the tree trunk and at shallow depths which have much higher resistivity) (Hagrey *et al.* 2004).

Given these expected limitations, the ERT surveys have enabled a range of geometrical relationships to be defined between different drift types. Furthermore the method is very good at picking out large units of low resistivity. Given that these deposits are likely to be of relatively low permeability and thus critical to determining recharge the method is potentially very useful in the hydrogeological context.

### **3.3.2 Augering and Sonic Drilling**

Locations of the auger holes are given in Figures 3.6 to 3.8 along with the locations of Sites 1 and 2. The locations of the boreholes within Sites 1 and 2 are shown in Figures 4.1 and 4.2. The range of materials encountered was very diverse including consolidated till, laminated glaciolacustrine deposits, glacial outwash sand and gravels and weathered Permo-Triassic sandstone. Summary logs for the 18 auger holes and 8 cored holes using the sonic drilling are given in Figure 3.11. Detailed logs of the core are also included in Appendix 2. Photographs of the continuous core taken from Sites 1 and 2 are given in Appendix 3.

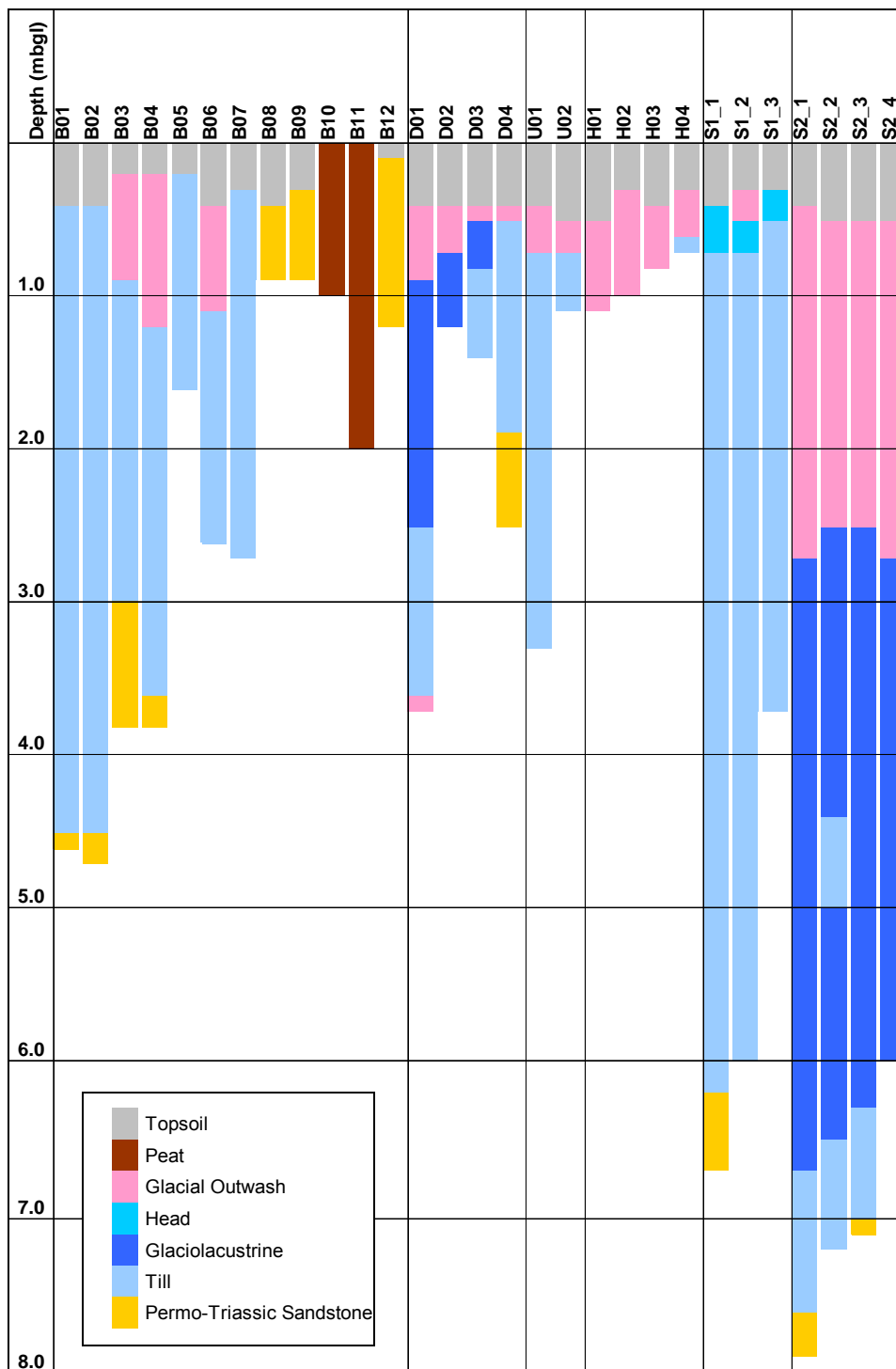


**Figure 3.11** Summary of borehole logs

Hand augered holes within the till reached a maximum depth of around 2.5 m due to the consolidated nature of the deposits. Within sandier materials greater depths were possible

although collapse of the holes was a problem especially where the deposits approached saturation. The drive sampling procedure produced relatively satisfactory undisturbed samples but was not very time efficient. The sonic drilling was very successful where the deposits were not too consolidated. The penetration rates were very high and core recovery averaged more than 90%. However when drilling through the consolidated lodgement till and weathered sandstone the rig struggled and the method was much less efficient. Overall the method was a success as in just 3 days 8 holes were drilled producing 50 m of continuous core and an additional 4 piezometer installations were completed using a 'lost point' method described in Section 4.3.2.

### **3.3.3 Summary of Laboratory Results**

A brief summary of the results of hydraulic conductivity and particle size distribution (PSD) analysis now follows in order to contrast the different types of drift deposit. However the details of the results are discussed for each drift unit in turn in the following Section 3.3.4.

A summary of results from the falling and constant head permeability experiments is shown in Figure 3.12.

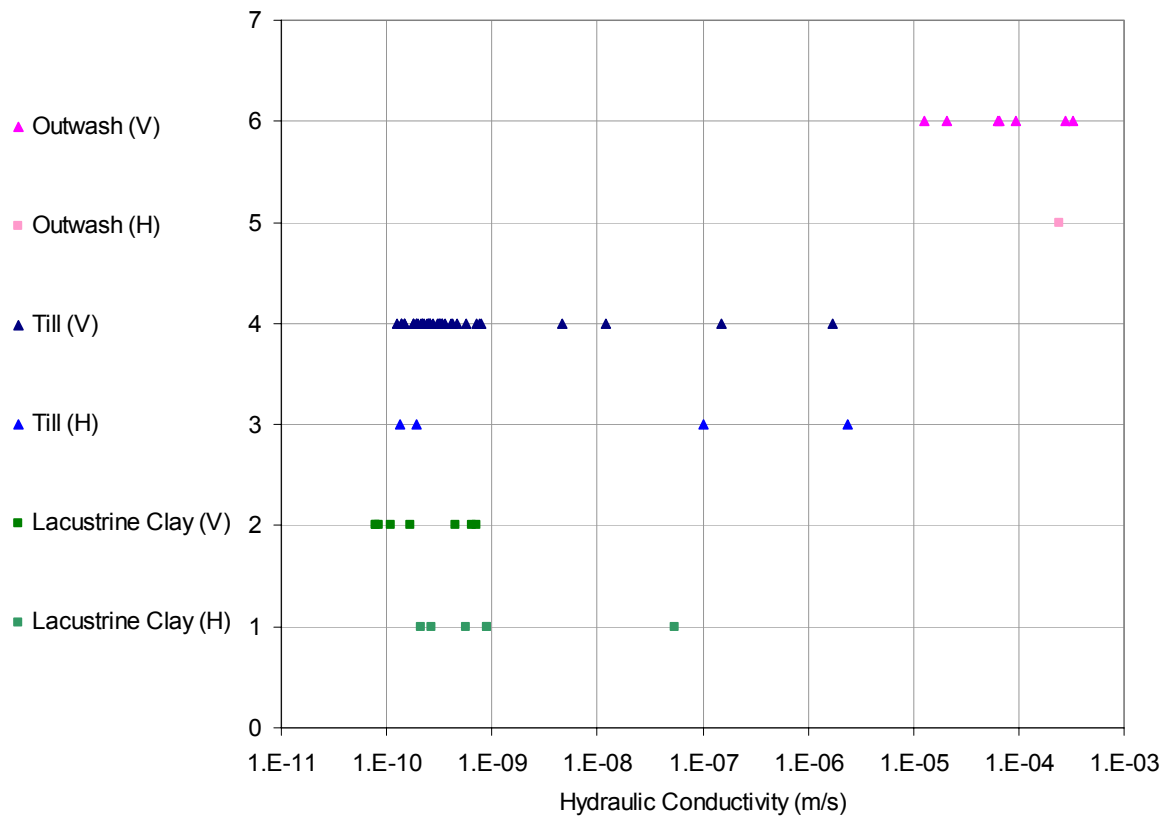


**Figure 3.12** Summary of permeameter tests for horizontal (H) and vertical (V) sample orientations

Only eight samples of glacial outwash were analysed successfully using constant head apparatus. Several samples failed due to the unconsolidated nature of the sediments and the ease with which artificial preferential flow pathways could be created while setting up the experiments. Fourteen glaciolacustrine and 43 till samples were run successfully using a falling head apparatus although several samples failed due to artificial flow pathways being created between the sample and the heat shrink material in which the sample was wrapped. Although disturbance of the samples was kept to a minimum, some alteration of their hydraulic properties is inevitable. It is thus considered that these tests give the hydraulic conductivity of the deposits accurate to 1 order of magnitude.

In total 168 samples were analysed using a standard sieve analysis to derive particle size distribution (PSD) data. A summary of the results is shown in Figure 3.13 as a ternary plot of fines (silt plus clay), sand and gravel proportions by mass.

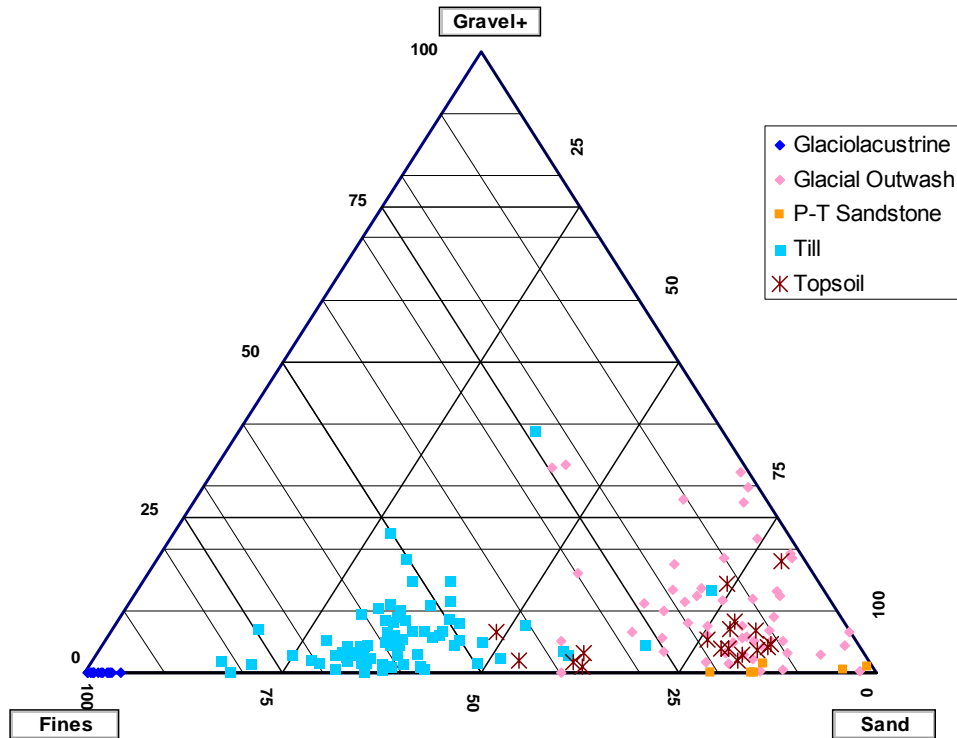


**Figure 3.13** Ternary diagram representing grain size distribution by proportion of fine (<63  $\mu\text{m}$ ), sand (63  $\mu\text{m}$  to 2 mm) and gravel+ (>2 mm) size particles for different drift types

Mass balance errors were generally less than 0.5%. Sample mass ranged between 50 to 200 g. This is an inadequately large sample size to be statistically representative of particle sizes greater than a few mm (Gale and Hoare 1991) and it is therefore acknowledged that significant error may have been introduced due to sampling bias.

### 3.3.4 Presentation and Discussion of Results for Main Drift Units

#### 3.3.4.1 Introduction

A summary of results for each of the three main types of drift deposit encountered (glacial outwash, till and glaciolacustrine deposits) is discussed in this section. A selected photograph

taken of the core and/or outcrop is given along with a field description of the material. The geometry of the depositional unit and its relation to other drift units based on the ERT results is described. In addition the results from permeameter experiments, PSD, XRD and thin section analysis, and bulk density and porosity calculations are also presented.

#### 3.3.4.2 Glacial outwash

Glacial outwash materials were found both below and above deposits of lodgement till. Since the till is thought to have been laid down during ice advance it is likely that the outwash material it overlies is a first phase of outwash deposited by meltwater streams issuing from the advancing glacier. Outwash material overlying the till is likely to be a second phase of glaciofluvial deposition laid down during ice retreat. The deposits range in lithology from fine silty sands through to much coarser gravely sands and in colour from reddish to greyish brown. The high degree of spatial variability encountered reflects complex facies distributions controlled by variations in lateral and distal proximity to the meltwater source through time (Anderson 1989). A photograph of some typical outwash material is shown in Figure 3.14.

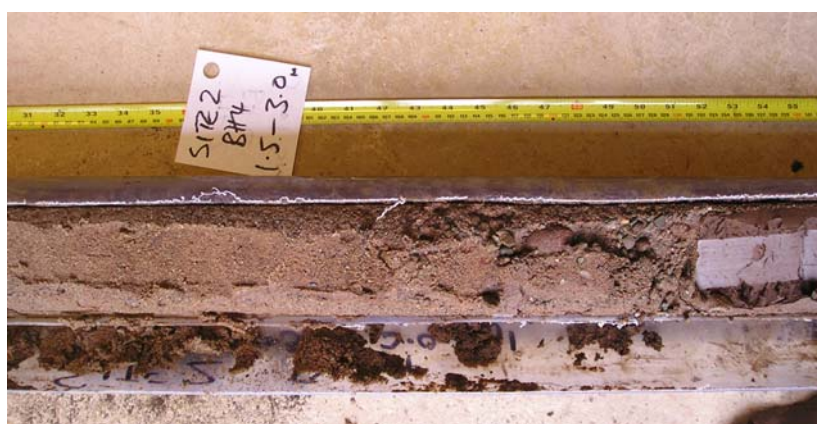


**Figure 3.14** Core from borehole S2\_4 showing the transition from gravely sand (glacial outwash) into the underlying glaciolacustrine clay

The first phase of outwash was only encountered at Whitegates Farm (as shown in Figure 3.9 G) and in this location is over 12 m thick and has a channelised form. It is likely that more of the area would have been covered by this first phase of outwash material but the material was subsequently removed by the scouring of the advancing ice sheet. Over much of the study area only a thin covering of the second phase of outwash material is present sitting in hollows on the irregular till surface masking the till surface topography (Figure 3.9 F and G). However, thicknesses in excess of 5 m are found in infilled channels as illustrated by Figure 3.9 A and B, either lying directly on the underlying sandstone aquifer or overlying till or glaciolacustrine deposits. An exposure of outwash material overlying the sandstone aquifer is shown in Figure 3.15.



**Figure 3.15** Exposure of glacial outwash material overlying Permo-Triassic sandstone at NGR SJ 582236

A very limited permeability analysis of 8 cored samples was carried out on gravely sand samples from Site 2 and the results have already been presented graphically in Figure 3.12.

Vertical hydraulic conductivity was found to range from  $1 \times 10^{-5}$  m/s to  $3 \times 10^{-4}$  m/s (1 to 28 m/d). One sample analysed for horizontal hydraulic conductivity gave a value of  $2.5 \times 10^{-4}$  m/s in comparison to the vertical hydraulic conductivity of  $6.2 \times 10^{-5}$  m/s for a sample of adjacent core material. These values of hydraulic conductivity are entirely consistent with literature values for sand and gravel mixes (e.g. 5 to 100 m/d in Kruseman and de Ridder (1990)). Furthermore, a simple calculation using Hazen's formula (Hazen 1911) based on the PSD data for these samples gives values of 20 to 60 m/d. Approximate values of porosity for these samples were calculated as 0.37 to 0.52 with bulk density ranging from 1200 to 1800 kg/m<sup>3</sup>. The latter value of porosity is unfeasibly high for a sandy deposit and unfortunately this is likely to imply that the material had become disturbed during drilling and/or sub-sampling.

It is anticipated that the hydraulic properties of outwash material across the catchment are likely to be highly variable reflecting the observed variations in texture and sorting. However, we can expect that for the most part glacial outwash materials will be highly permeable in comparison with till and glaciolacustrine deposits and possibly also an order of magnitude or two more permeable than the Permo-Triassic aquifer underlying the catchment.

#### **3.3.4.3 Till**

The till encountered in the field investigations was often highly overconsolidated and is interpreted as being laid down during ice advance by sub-glacial lodgement processes. In some areas it reaches thicknesses greater than 9 m sometimes overlying the first phase of outwash material but more often lying directly on top of weathered bedrock. In other areas it is thin, patchy and highly weathered (Figure 3.9 I to J). When exposed as the ice front retreated, the till is likely to have had an undulating surface of ridges, mounds and hollows, some of the hollows acting as conduits for meltwater or else becoming ephemeral lakes. It is

thought that the till in this area represents one main phase of ice advance. However one borehole at Site 2 (S2\_2) indicates a laminated sand and clay probably of glaciolacustrine origin which is both underlain and overlain by till deposits. This would suggest that at least one additional phase of ice advance occurred in this area.

Based on the evidence from the ERT surveys, the internal structure of the till is apparently relatively homogeneous on the scale of tens to hundreds of metres with no significant sand lenses or other discontinuities. Where the till crops out the transition from topsoil to relatively stiff till was often found to be quite sharp although a poorly laminated mottled pale brown sandy clay with occasional shears was also encountered between the soil and the till in several boreholes and is best interpreted as a solifluxion deposit.

An example of a till core sample is shown in Figure 3.16. Typically in the field it was described as a firm to very stiff reddish brown slightly gravelly slightly sandy clay with matrix supported clasts to 20 mm and, more rarely, 50 mm (using BS5930 terminology). The PSD data shown in Figure 3.13 indicate that the till often comprises 30 to 50% sand, 0 to 10% gravel with the remainder made up of silt and clay. PSD data for the <2 mm fraction of 12 till samples (36 subsamples) are shown in Figure 3.17 illustrating how the till is poorly sorted and generally unimodal. It was found that the proportion of clay size particles within the till ranged between 11 to 15% as a percentage of the fine fraction (silt and clay) for the small number of samples tested.



**Figure 3.16** Core from borehole S1\_1 showing head, lodgement till and a sandstone cobble

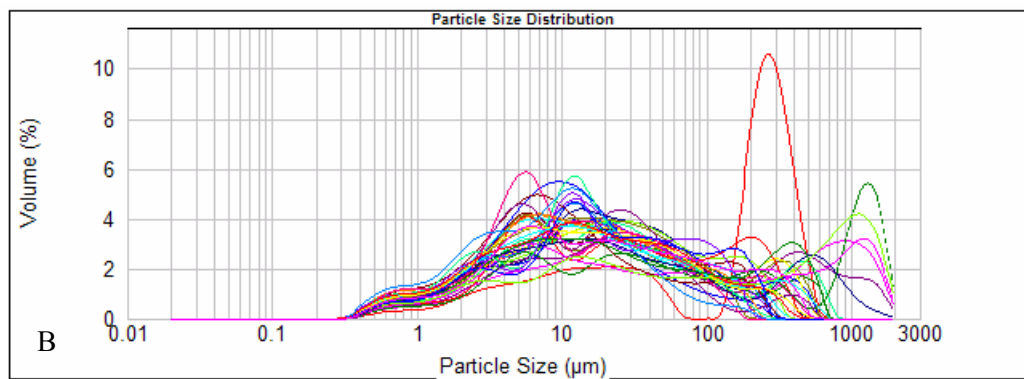


**Figure 3.17** PSD data for the <2 mm fraction of 12 till samples (3 subsamples were analysed for each till sample yielding 36 results as plotted)

Several thin sections were made up of till samples taken from cored boreholes. Two examples are shown in Figure 3.18 for the same sample in vertical and horizontal section. The samples are poorly sorted with angular to sub-rounded clasts dominated by quartz grains (feldspar and rock fragments are less common) set within a matrix of clay minerals. No preferential grainsize orientation or layering is evident.

The results of the XRD analysis for a sample of till from Wood Farm are shown in Table 3.3. These results are consistent with the thin section evidence with quartz and clay minerals making up over 80% of the rock mass with feldspars, mica and hematite representing the

remainder. The clay mineral assemblage is dominated by illite but also includes a significant proportion of the swelling clay montmorillonite. The absence of any sulphate or sulphide minerals is unexpected given the porewater chemistry of the till presented in Section 5.2.7. However it may be that these minerals were present in amounts below the detection limit of the XRD analysis.

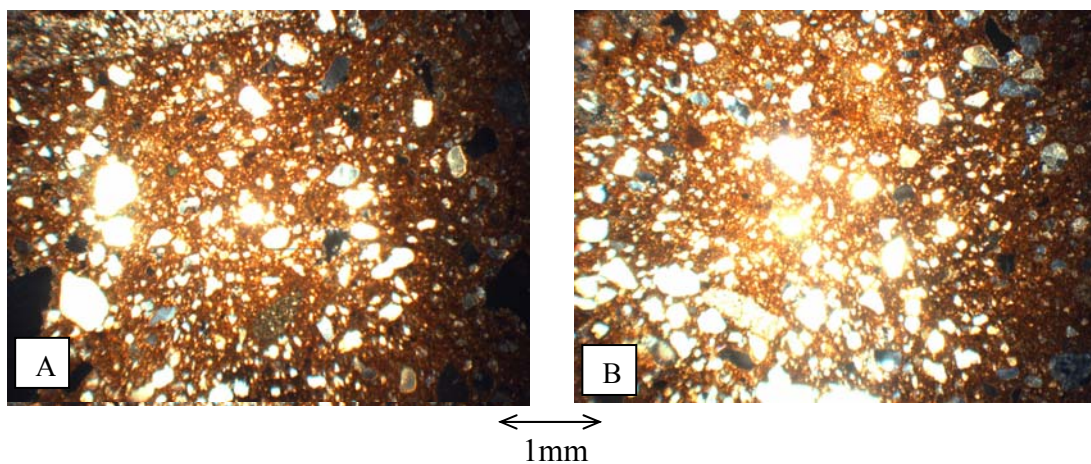


**Figure 3.18** Photomicrographs of vertical (A) and horizontal (B) thin sections from S1\_3 (crossed polars)

Phase	%
illite	26.6
kaolinite	7.3
montmorillonite	15.8
muscovite	8.2
quartz	32.3
albite	3.8
orthoclase	2.7
hematite	3.3

**Table 3.3** Phase proportions (values in weight %) determined by XRD analysis

A total of 43 till samples were tested using a falling head permeameter and the results have been presented graphically in Figure 3.12 in comparison to other drift types. Although only 4 samples were tested for horizontal hydraulic conductivity the values span the same range as those for the vertical component from  $1 \times 10^{-10}$  m/s to  $2 \times 10^{-6}$  m/s (4 mm/a to 0.2 m/d). However, most values plot in the range  $1 \times 10^{-10}$  m/s to  $1 \times 10^{-9}$  m/s with only 6 samples having significantly higher hydraulic conductivity. No apparent discontinuities were apparent from visual inspection to explain the increased permeability of the samples. Furthermore meaningful relationships between grainsize and hydraulic conductivity have not been found. This was investigated using simple correlations between proportions of certain grainsizes and hydraulic conductivity. An example is shown in Figure 3.19 which plots proportion of fines (clay plus silt) against hydraulic conductivity for the 43 till samples.

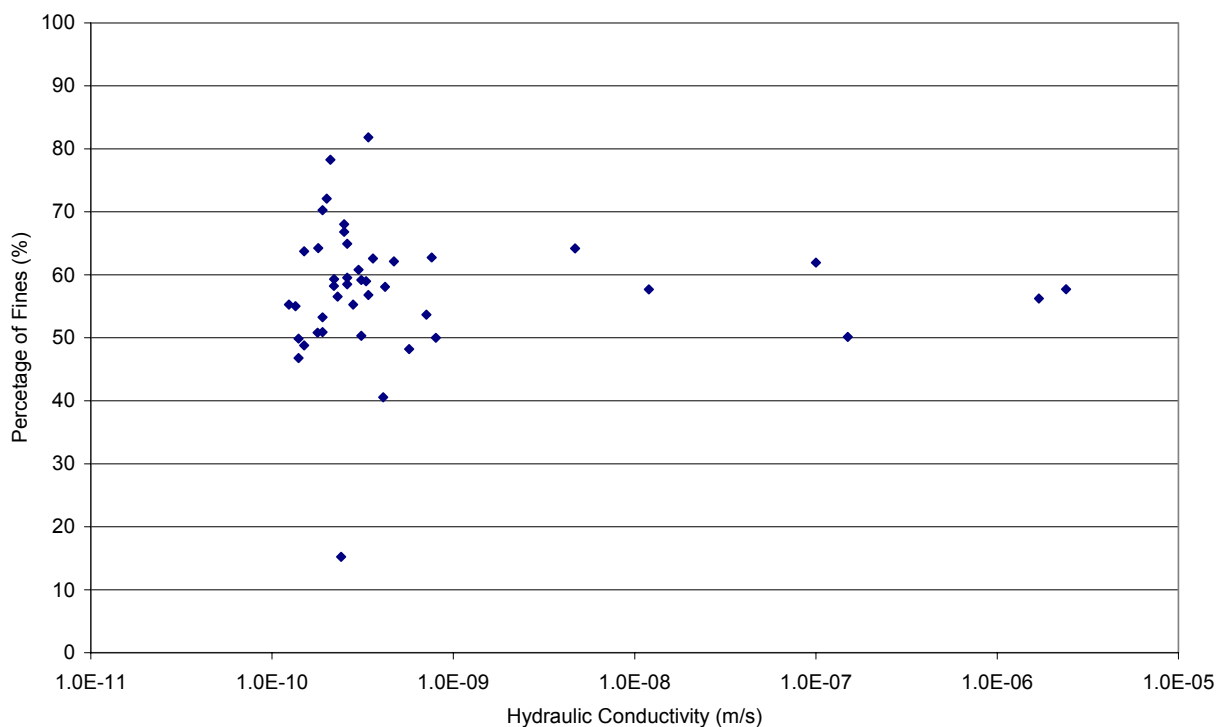


**Figure 3.19** Correlation between hydraulic conductivity and percentage of fines for 43 till samples

The lack of correlation between grain size and hydraulic conductivity is not surprising given the high proportion of silt and clay (generally 40 to 80 %) sized particles and the lack of sorting. Although the coarser material may account for a significant proportion of the total volume, since the till is so poorly sorted, the poresize distribution is dominated by the finer fractions with limited development of larger pore spaces. In fact, when isolated from other sand grains and surrounded by clay and silt particles a sand grain may actually be expected to reduce the permeability of the sample. At a larger scale if suitable measurements had been taken we might have expected to find a relationship between grain size and permeability if for example tills with certain grain size distributions are more prone to certain types of weathering and/or fracturing (Bonell 1976).

Most of the samples of till had approximate values of porosity in the range 0.23 to 0.32 with dry bulk density ranging from 1600 to 2100 kg/m<sup>3</sup>. Fracturing was not evident from any undisturbed samples or cores with the exception of one large semi vertical fracture found in borehole S1\_3 between 1.5 and 2.0 mbgl. A photograph of this feature is shown in Figure 3.20.

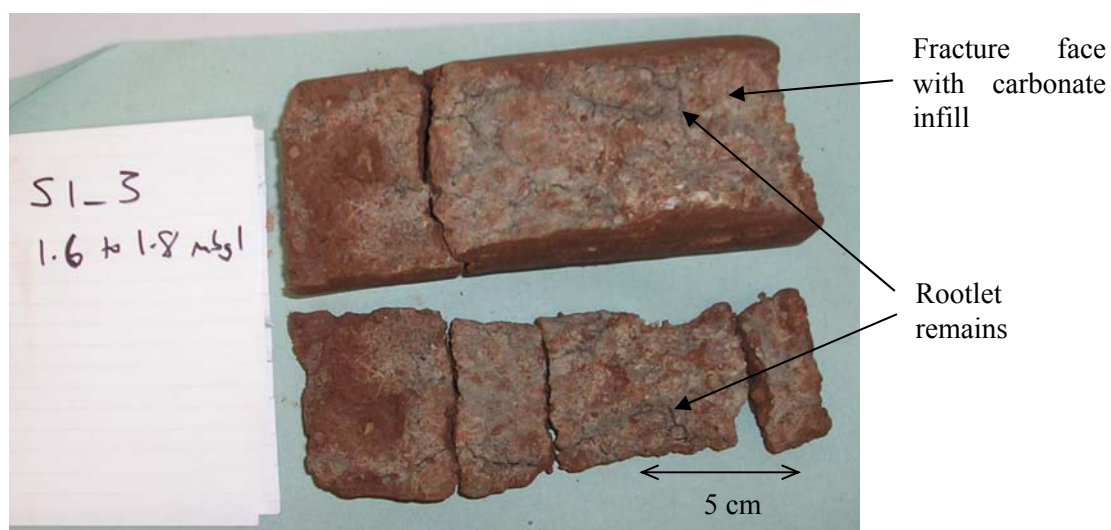


**Figure 3.20** Fracture in till within core from borehole S1\_3

The fracture seems to be planar and shows blue discolouration and the remains of organic matter. It is most likely a desiccation fracture that has been exploited by the root network of former surface vegetation. The root activity of large trees is likely to have affected the upper few metres of much of the catchment in the past before the clearance of trees for agriculture.

#### **3.3.4.4 Glaciolacustrine deposits**

Although the presence of glaciolacustrine deposits is reported in borehole logs from Muckleton Moss (NGR SJ 595 222) (Wealthall *et al.* 1997), this type of deposit is not mapped as cropping out within the catchment. However, glaciolacustrine clays are present in the drift profile more or less continuously between Whitegates Farm (NGR SJ 633 229) and Hollycroft Farm (NGR SJ 640 230). On the east bank of the Potford Brook at Whitegates Farm, 1 to 2 m of glaciolacustrine clay lies beneath the most recent glacial outwash material and overlies a thin layer of till as illustrated by the ERT section in Figure 3.9 G and borehole logs D01 to D04 in Figure 3.11. To the north of this section the glaciolacustrine deposits pinch out leaving till overlying sandstone. To the east, thin patches of glaciolacustrine clay and till crop out (Figure 3.9 I to L) until Hollycroft Farm is reached where the glaciolacustrine deposits thicken substantially to around 4 m and are covered once more by glacial outwash material (Figure 3.9 M and borehole logs S2\_1 to S2\_4). From Hollycroft Farm to the south the clay unit thins to 1 to 2 m thickness. Presumably laid down in small depressions in the underlying till and sandstone (permafrost may have restricted infiltration during the peri-glacial period following the retreat of the ice-sheet) the deposits are basal in form.

An example of a glaciolacustrine core sample is shown in Figure 3.21. Predominantly the glaciolacustrine deposits encountered in the field were soft to firm plastic brown to dark brown very thinly laminated clays with little or no coarser elements. However at Site 2 a layered sequence of well sorted silty fine sand and medium to coarse sand with occasional

granules was logged (S2\_2 and S2\_3) with slightly dipping bedding. These deposits most likely were formed in a pro-glacial deltaic environment.

PSD analysis showed the glaciolacustrine clay samples to be predominantly bi-modal and well sorted as shown in Figure 3.22 with modal frequencies presumably coinciding with the particle size dominating the laminations across which the sample was taken. The proportion of clay of the fine fraction varied between 10 and 20% in the 6 samples analysed.



**Figure 3.21** Laminations in glaciolacustrine clay within core from borehole S2\_4

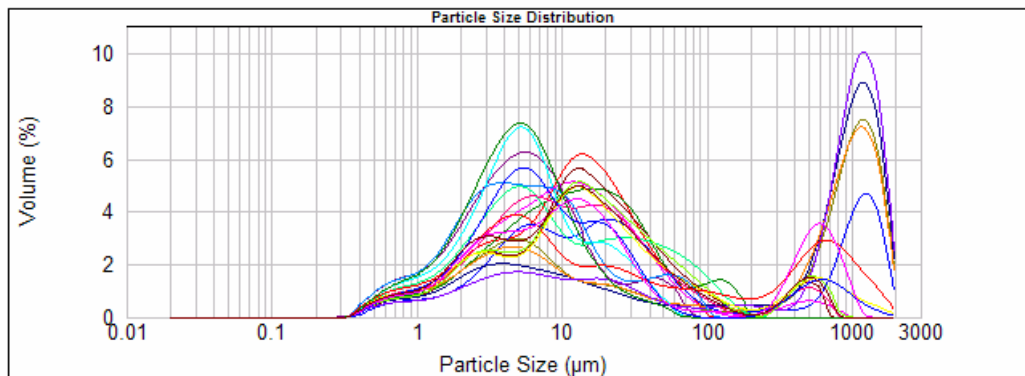


**Figure 3.22** PSD data for the <2 mm fraction of 6 glaciolacustrine clay samples (3 subsamples were analysed for each sample yielding 18 results as plotted)

Several thin sections were made up of glaciolacustrine clay samples taken from cored boreholes. A photomicrograph is shown in Figure 3.23 for a vertically oriented thin section. Laminations of variable thickness can be clearly seen within the sample largely comprising clay minerals with coarser laminations dominated by preferentially oriented quartz grains.

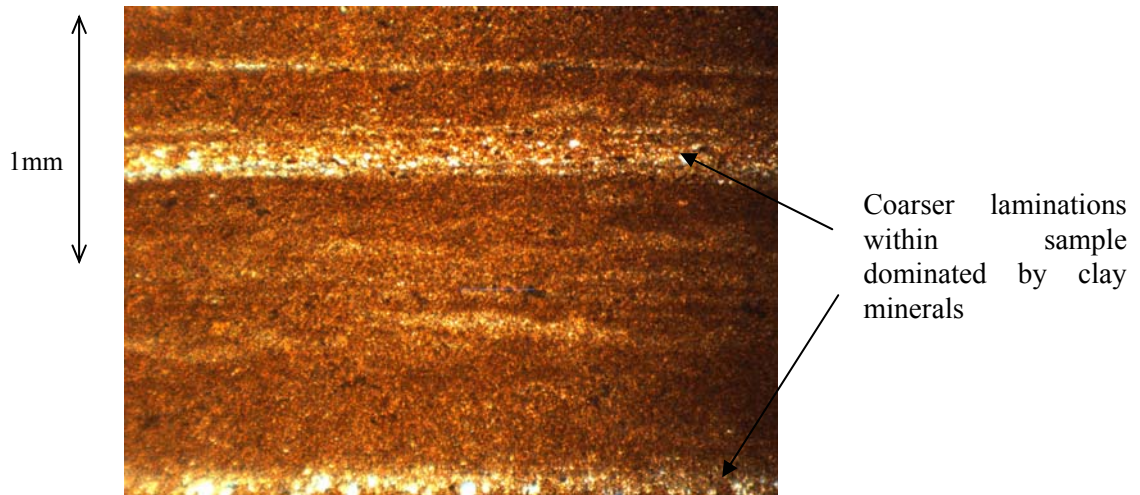


**Figure 3.23** Photomicrograph of a vertically oriented thin section from S2\_4 (crossed polars)

A total of 14 glaciolacustrine samples were tested using a falling head permeameter and the results have been presented graphically in Figure 3.12 in comparison to other drift types. Although only 6 samples were tested for horizontal hydraulic conductivity the values span a range of higher hydraulic conductivity values from  $2 \times 10^{-10}$  m/s to  $5 \times 10^{-8}$  m/s compared with values for the vertical component in the range  $8 \times 10^{-11}$  m/s to  $7 \times 10^{-10}$  m/s. This difference may be due to the laminated nature of the deposit. The laboratory samples were prone to shrinkage and cracking upon drying so it was not possible to derive accurate dry bulk density or approximate porosity values. However the saturated bulk density was found to range from 2400 to 3200 kg/m<sup>3</sup>.

### 3.4 Conceptual Recharge Models

Based on the more detailed knowledge of the drift distribution, geometry and hydraulic properties derived from the field investigations, a series of local scale conceptual recharge models for the catchment have been produced. These are shown schematically in Figure 3.24 and are now described in turn.

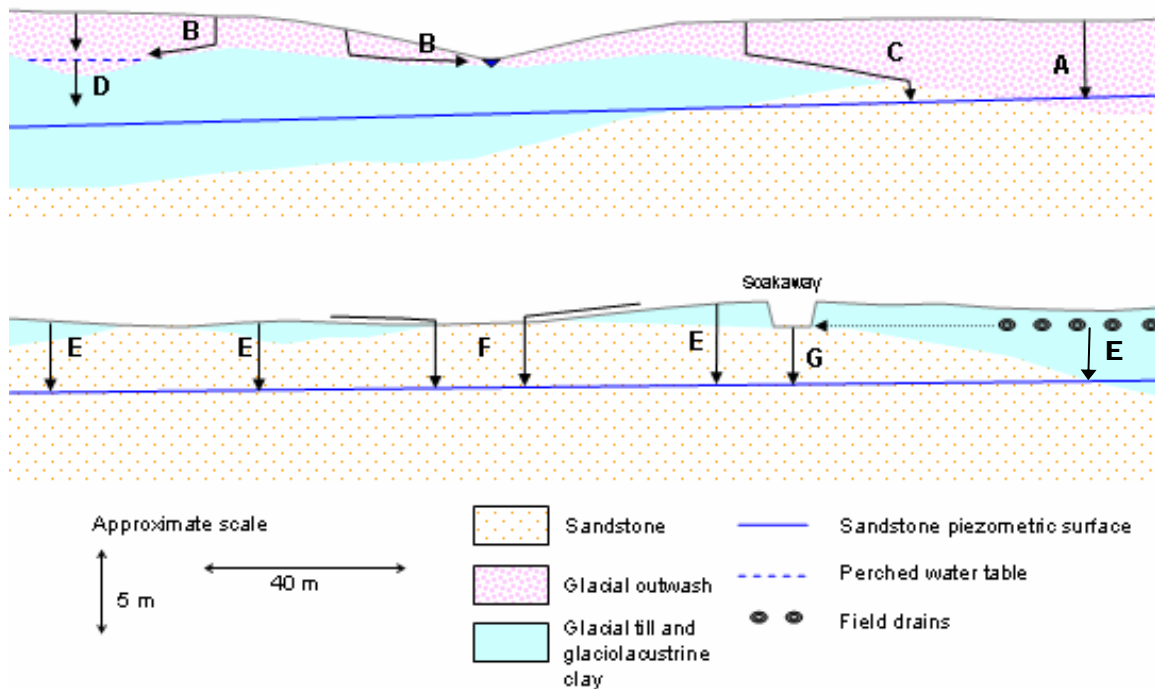


**Figure 3.24** Local scale conceptual recharge model schematics

**A** In some areas glacial outwash deposits directly overlie the sandstone aquifer and predominantly comprise sands and gravels. Such deposits are likely to have relatively high vertical hydraulic conductivities and provide little barrier to the downward movement of recharging water.

**B** In many locations low permeability layers, such as till, glaciolacustrine clays or finer grade outwash material, underlie more permeable glacial outwash deposits. Where such layers are

laterally persistent, lateral flow at the interface will occur resulting in discharge to drains, watercourses or seepage/riparian areas.

*C* Where low permeability layers are laterally discontinuous, water flowing laterally within the overlying layer may recharge the aquifer some distance away from where it infiltrated.

*D* Where the interface between the upper permeable layer and the underlying low permeability deposit is uneven, water may pond in hollows at the boundary providing a reservoir from which recharge can occur slowly through underlying deposits during much of the year.

*E* Where till directly overlies the aquifer (a thin covering of outwash or head may also be present) the recharge will depend on the bulk permeability of the deposits and the hydraulic gradient between the till water table and the aquifer piezometric surface. The bulk permeability is likely to vary with lithology and the depth/degree of fracturing. Where the till is thin and highly fissured, the bulk vertical hydraulic conductivity is likely to be much greater than that of the matrix allowing significant amounts of recharge to the underlying aquifer.

*F* In areas where the till is patchy and at the till margins, water running off clayey soils overlying the till may run on to more permeable deposits and recharge the aquifer in these locations.

*G* Agricultural land drains are present in many areas and in some cases discharge to soakaways cut through the till into the weathered top of the sandstone aquifer. Thus water can bypass the low permeability till below and recharge the aquifer directly via these drains.

### **3.5 Adequacy of Existing Drift Mapping**

#### **3.5.1 Introduction**

It was noted in Chapter 2 that the 1:50 k drift geology map does not provide information about geological layering and is therefore limited in its usefulness for understanding drift structure. An attempt was made to improve the understanding of the drift structure as part of a recent Environment Agency groundwater modelling investigation (Bridge *et al.* 2002). Information from existing borehole logs was collated and analysed alongside the 1:50 k drift geology map to produce a hydrogeological drift domain map based solely on lithology and ignoring the morphology of the deposits and their genetic origin. Some simplification was necessary during this exercise as the domains were to be used for a regional groundwater model and so detail at a length scale below 250 m was not included. Part of this map has been reproduced in Figure 3.25 and overlain with the locations of the ERT survey lines, data from which were presented earlier in this chapter. A description of the domains is given in Table 3.4.

For the area covered by the ERT lines, areas shown as till and glaciofluvial deposits on the 1:50 k drift geology map correspond directly with domains 1 and 2 respectively. The only exception is at the south end of ERT survey line G which is mapped as till but has been allocated to domain 4.

#### **3.5.2 Comparison of Existing Mapping and Research Results**

The following discussion compares the results of ERT surveys (shown in Figure 3.9) and invasive investigations, with the existing 1:50 k drift map and the hydrogeological domain map shown in Figure 3.25. Comparisons from each of the four investigation areas defined in Section 3.2.1 are described in turn:

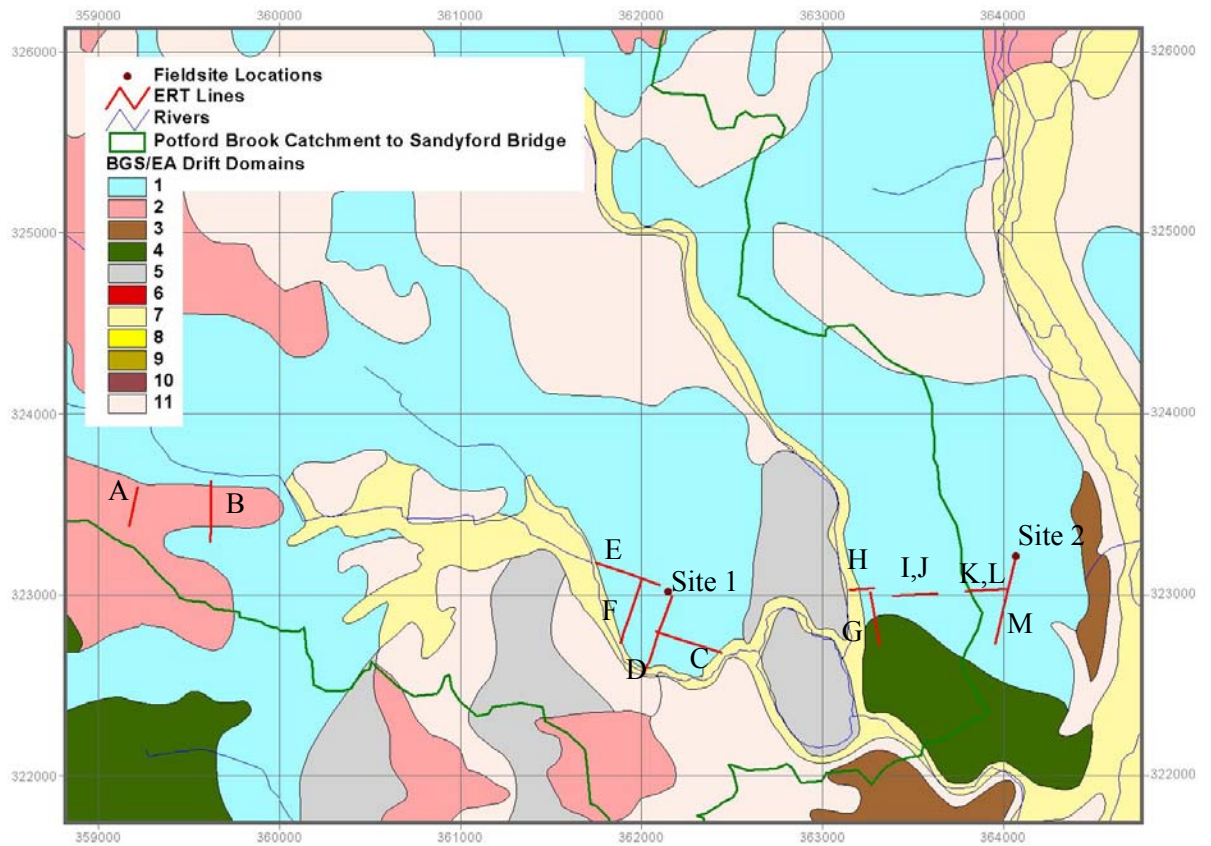


**Figure 3.25** Hydrogeological drift domain map. Reproduced from Bridge *et al.* (2002).

Domain	Description
1	Clay at surface and 100% clay to rockhead
2	Sand and gravel at surface and 100% sand and gravel to rockhead
3	Sand and gravel at surface and >50% sand and gravel to rockhead
4	Sand and gravel at surface and >50% clay to rockhead
5	Clay at surface and >50% clay to rockhead
6	Clay at surface and >50% sand and gravel to rockhead
7	Undifferentiated fluvial deposits on bedrock
8	Undifferentiated fluvial deposits on other drift
9	Peat on bedrock
10	Peat on other drift
11	Bedrock at surface

**Table 3.4** Description of hydrogeological drift domains

1. Wood Farm. ERT survey lines C to F are in areas mapped as till and within domain 1. This is reasonably consistent with the results of the ERT and augering/drilling although the presence of thin glacial outwash deposits was also found overlying the till over much of this area.
2. Hazles Farm. ERT survey lines A and B both lie across areas mapped at the surface as glaciofluvial deposits consistent with the results presented in this Chapter. Furthermore the mapped boundaries between the till and the glaciofluvial material are also consistent with the results from the ERT surveys. However, the domain map implies that sand and gravel are present to rockhead along ERT survey line B but an intervening clayey till layer was found in this location.
3. Whitegates Farm. ERT survey line H shows a patchy covering of till and glaciofluvial material in contrast to the continuous till implied by the drift geology map. Line G is mapped as till and the domain map shows a transition from domain 1 in the northern half to domain 4 in the southern half. This is consistent with the ERT results for the northern half. The transition to domain 4 for the southern half of the survey line is consistent with the implication from the ERT that outwash material overlies till. However the ERT results suggest that the material underlying the till is a thick glacial outwash deposit rather than bedrock as implied by the domain map.
4. Hollycroft Farm. The locations of ERT survey lines I to M are mapped as till and classified as domain 1. However, the ERT and augering/drilling results suggest that this area has a complex covering of patchy till and glaciolacustrine deposits to the west and thicker glaciofluvial and glaciolacustrine material overlying till to the east.

Hence this is the area where most disagreement is found between the existing drift mapping and domain maps and the findings presented in this chapter.

### **3.6 Conclusions and Way Ahead**

By a focussed and detailed local investigation of the geology of parts of the Potford Brook catchment, the typical geometry of the main drift units have been defined at a resolution of tens to hundreds of metres. Hydraulic properties have also been derived although it is noted that the focus has predominantly been on core scale measurements. Only a limited description of the larger scale features, which may be hydraulically important, has been given. A number of local scale conceptual recharge models has been proposed. It has been shown that when supplemented with a degree of borehole control the ERT method is very effective for building a more complete picture of the drift geometry.

On the basis of existing drift mapping at a scale of 1:50 k it has been shown that it is not possible to identify many of the local scale features of the drift structure which may be important in controlling recharge. More complex mapping taking account of existing borehole log information such as the hydrogeological domain approach carried out for the East Shropshire Permo-Triassic Sandstone Groundwater Modelling Project (Bridge *et al.* 2002) also misses key features at the local scale.

Given the progress made in defining the recharge processes operating at the local scale within the catchment, the next step is to further understand the detailed hydraulics at the site scale in order to move from qualitative conceptual models towards quantitative recharge estimation for each situation. Only once this has been achieved can robust upscaling calculations be carried out in order to move back up the scales to allow more confident modelling at the

regional level (something that is not within the scope of this thesis). The following questions are of particular importance:

- Can the core scale permeability measurements presented in this chapter be used directly for modelling hydraulic behaviour at the site scale, or are there also site scale structural/lithological features which control recharge?
- Is it possible to realistically model recharge through the drift using conventional soil moisture balance models coupled with saturated groundwater flow models or is an explicit representation of the unsaturated zone processes necessary?

The following three chapters of the thesis therefore seek to develop the understanding of the site scale hydraulic processes for two detailed fieldsites within contrasting drift environments in order to answer these questions.

## **4 SITE SCALE INVESTIGATIONS 1: SITE INSTRUMENTATION AND MONITORING**

### **4.1 Aim**

Catchment scale and local scale investigations presented in the previous chapters have enabled a good understanding of the main structural features of the drift to be developed. Furthermore, inferences have been made about how these features may control subsurface flows leading to aquifer recharge. In order to understand the hydraulic processes governing recharge, investigations at a smaller scale were needed. For this reason two sites in contrasting geological environments were chosen for detailed site scale investigation.

This chapter introduces the two fieldsites and describes and explains the choice of the experimental design in terms of instrumentation and investigative methods. The results of the investigation and monitoring are presented for each fieldsite in turn in the subsequent Chapters 5 and 6.

### **4.2 Site Selection**

It was desirable to pick fieldsites which would allow a detailed investigation of all three of the dominant drift types in the catchment i.e. till, glaciolacustrine deposits and glacial outwash. Fortunately, given the geological constraints, two sites were found for which landowner permission was granted for drilling and regular access, and which had easy access from the road.

Site 1 is located near Wood Farm (NGR SJ 6215 2302) and is underlain predominantly by till overlying the sandstone at around 6 mbgl. The site lies in the corner of a field used for grazing horses.

Site 2 is located adjacent to Hollycroft Farm (NGR SJ 6408 2321) and has a more complex geology of layered glacial outwash, glaciolacustrine deposits and till overlying the sandstone at around 7 mbgl. This site was under winter wheat at the time of developing the site (June 2004) but was cleared by hand at harvest time to let grass (and other wild vegetation) become established.

The location of each site in the context of the wider area was shown previously in Figure 3.5.

### **4.3 Instrumentation**

#### **4.3.1 Introduction**

It was decided that each site would be equipped with very similar instrumentation to allow direct comparisons to be made. A good understanding of the geology of each site was clearly important and this was achieved by sonic coring, logging and sampling as outlined in Chapter 3.

In order to develop an understanding of the site hydraulics it was necessary to be able to monitor tension and soil moisture in the unsaturated zone and pressure heads in the saturated zone. It was intended that the recorded variations in pressure and moisture content would, when integrated with climatic data and with the aid of suitable models, help to identify the hydraulic processes operating in the near surface.

It was also necessary to have a way of quantifying the spatial heterogeneity of the hydraulic responses in order to be able to define the transferability of point measurements. Permanent ERT arrays were installed for this reason. It was intended that temporal moisture content changes could be inferred from the observed variations of subsurface resistivity with time.

In addition to the insitu monitoring capability, a certain amount of hydraulic and tracer experimentation on the site was considered to be necessary. It was anticipated that hydraulic

tests on the piezometers would show whether the hydraulic conductivity at this larger scale is consistent with core-scale measurements made in the laboratory. It was hoped that the use of applied and environmental tracers would enable groundwater velocities through the drift to be inferred. The goal was to produce a conceptual understanding of the hydraulic functioning of each site by combining the results from a wide range of approaches that may not have been possible by applying one method in isolation.

The rest of this section describes the monitoring equipment installed at each site. Plans of Site 1 and Site 2 showing the monitoring and experimentation locations are given in Figure 4.1 and Figure 4.2 respectively. Each installation and ERT array was surveyed relative to a site datum using a dumpy level and tape measure to a precision of 1 mm vertically and 1 cm horizontally. All location numbers are prefixed by S1 for Site 1 and S2 for Site 2.

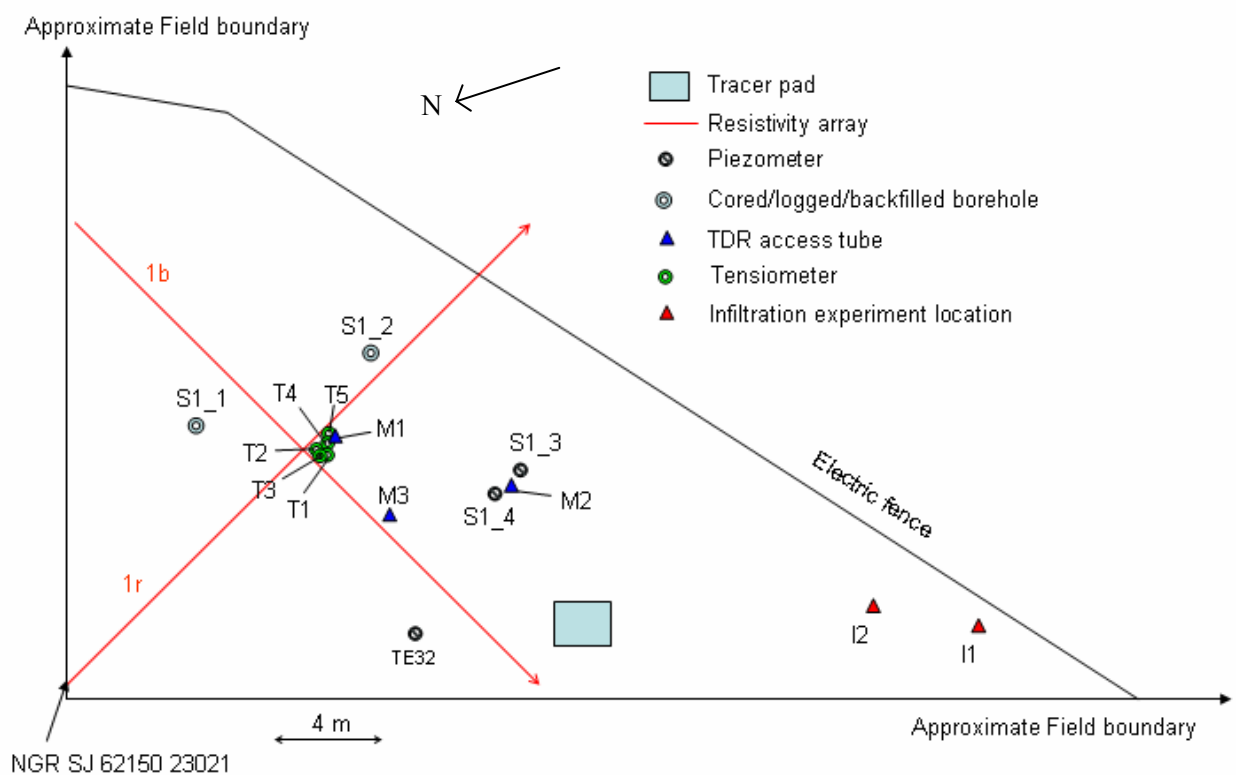


**Figure 4.1** Site 1 location plan

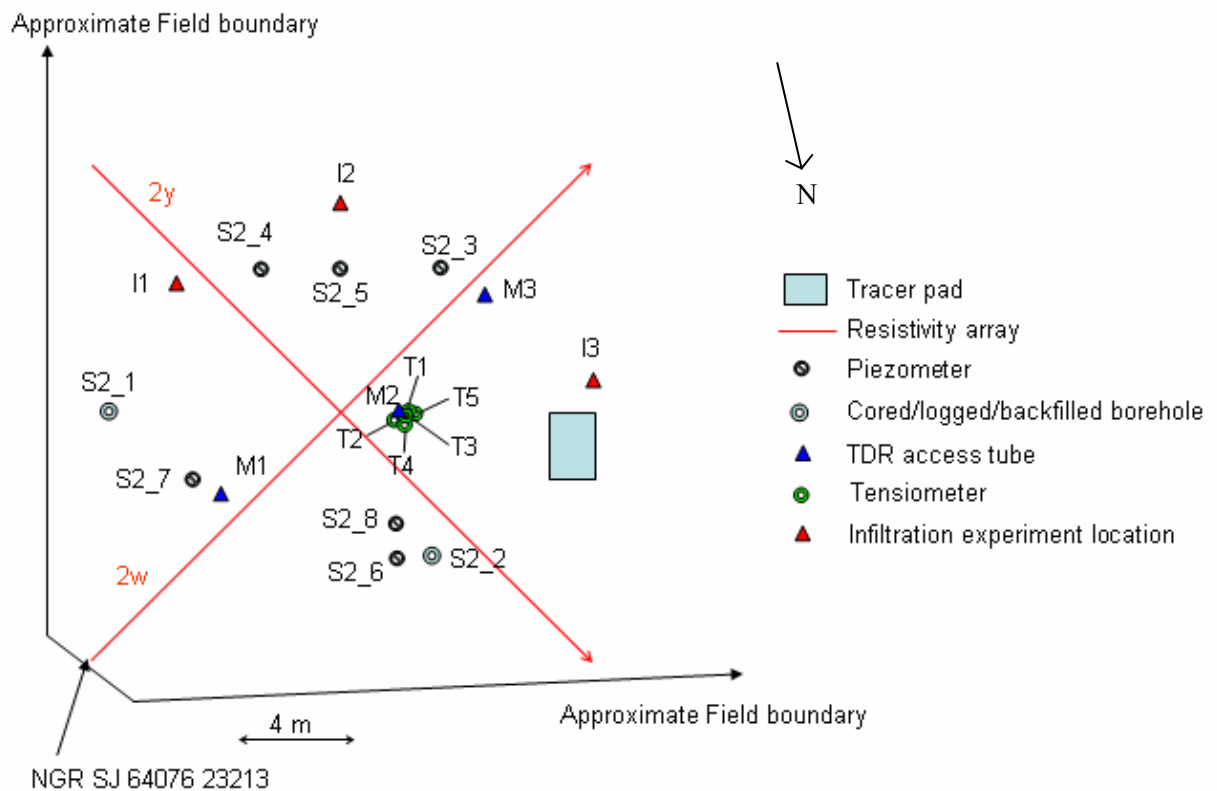


**Figure 4.2** Site 2 location plan

### 4.3.2 Piezometers

#### 4.3.2.1 Construction

Piezometers were installed in June 2004 either within 90 mm cored boreholes or using the ‘lost point’ method of drilling with the sonic rig. For the latter the drill string is loaded with a disposable tip (lost point) and then driven in with sonic vibrations to the desired depth. The installation is then carried out within the drill rods before they are withdrawn leaving the lost point and piezometer installation in place.

In both cases the piezometer design was identical with a monitoring section comprising a pre-fabricated sand filter and filter gauze around 25 mm ID plastic casing with 0.3 mm slots. The screen sections used were between 20 and 40 cm in length dependent on the targeted monitoring horizon. A seal section was screwed directly onto the monitoring section

comprised of a preformed bentonite collar 1 m long. A ‘sand catcher’ (swelling sponge material) was added above the bentonite section before sections of plain pipe were added to bring the installation to ground level. A photograph of the preformed materials is shown in Figure 4.3. The complete installation was lowered to the base of the hole in every case and a little water added to swell the sand catcher in order to stop any material passing the bentonite collar before it had had time to hydrate. Bentonite pellets were then added from the surface to fill the annular space between the level of the sand catcher and to within 30 cm of the ground surface. More water was then added so that in time the bentonite seal and pellets would seal off the monitoring section. Finally the top 30 cm was filled with a cement grout and a monitoring well cover was fitted at ground level.

The construction details of the piezometers installed at both sites is shown in Table 4.1.

#### **4.3.2.2 Pressure transducers**

Two piezometers at each site were fitted with pressure transducers in order to enable data to be logged automatically at regular intervals. The transducers used were differential and had a range of 0 to 15 psi (Radio Spares (RS) 296-692). Circuit boards were made up to regulate the input voltage to the transducer from a 12 V battery and amplify the output signal to be read by a voltmeter or datalogger. A vent tube was added onto the low pressure side of the transducer leaving the other nipple to measure the pressure in the piezometer. The straight line calibration relationship between pressure on the high pressure side of the transducer and the output voltage was recorded using a hand held manometer.

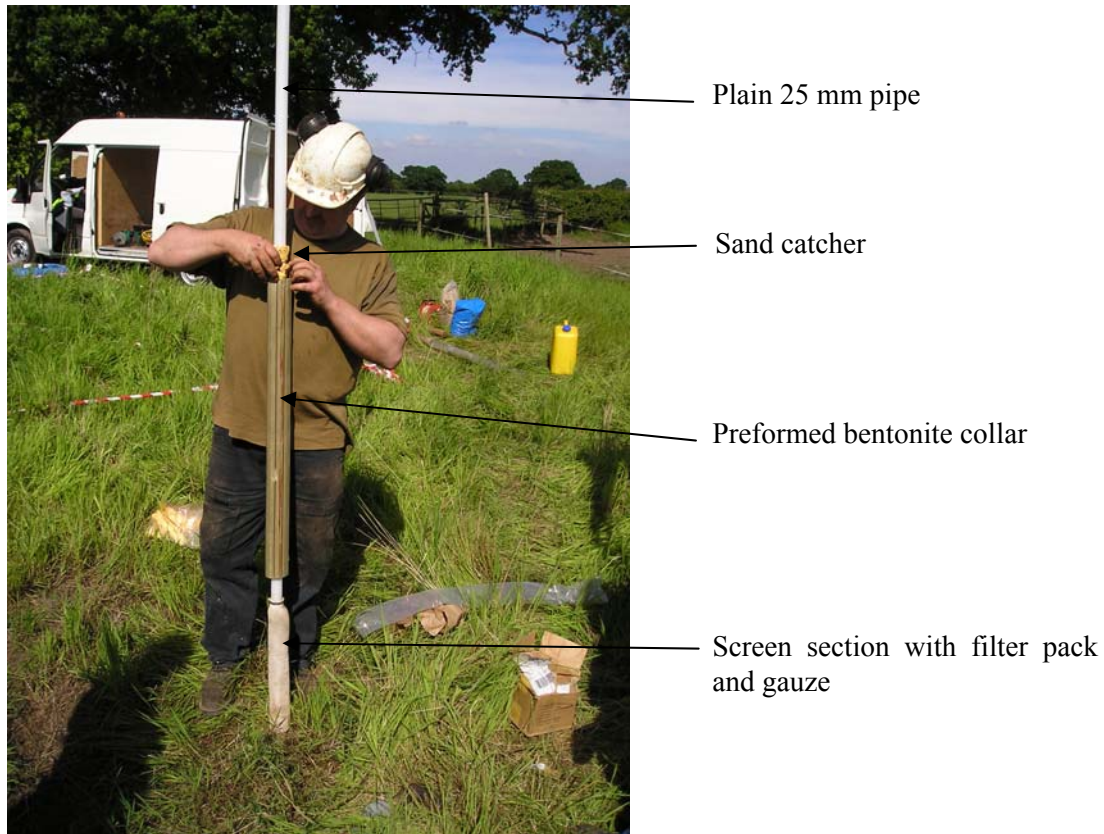


**Figure 4.3** Piezometer installation materials

The circuit board was then enclosed in heat shrink and sealed in potting compound to make it water tight, and lowered into the piezometer positioning the transducer nipple at a known depth below datum. The vent tube was brought to the surface to be open to atmospheric pressure. The electric cable was fitted with a three pin plug to allow easy interface with a voltmeter or datalogger. The output voltage was then recorded over time allowing the pressure at the transducer nipple to be calculated using the calibration relationship relative to atmospheric pressure. This value was then subtracted from the depth of the transducer below datum to arrive at the piezometric head in the piezometer. Water levels were recorded manually every few days from June to October 2004 and were then automatically logged from November 2004 to September 2005 at 5 or 10 minute intervals.

<b>Location Number</b>	<b>Total Depth (m)</b>	<b>Screen length (m)</b>	<b>Monitored interval</b>	<b>Pressure Transducer Installed?</b>	<b>Method of Installation</b>
<b>S1_3</b>	3.7	0.4	Till	Y	Cored borehole
<b>S1_4</b>	5.0	0.4	Till	Y	Cored borehole
<b>S2_3</b>	7.1	0.2	Till	N	Cored borehole
<b>S2_4</b>	6.0	0.4	Glaciolacustrine	N	Cored borehole
<b>S2_5</b>	2.7	0.5	Glacial Outwash	Y	Lost Point
<b>S2_6</b>	2.7	0.5	Glacial Outwash	Y	Lost Point
<b>S2_7</b>	2.7	0.5	Glacial Outwash	N	Lost Point
<b>S2_8</b>	5.1	0.4	Glaciolacustrine	N	Lost Point

**Table 4.1** Piezometer construction details

### **4.3.3 Tensiometers**

#### **4.3.3.1 Design**

Although other methods for measuring matric potential are available (e.g. heat dissipation sensors and thermocouple psychrometers) it was decided to use tensiometers due to their established reputation as a robust instrument and their nominal cost. Tensiometers were designed and built specifically for this project incorporating the use of pressure transducers to allow the option of datalogging.

The tensiometer design comprised a 21 mm OD unglazed porous ceramic cup with a bubbling pressure of 1.5 bar (manufactured by SDEC (France) and distributed by van Walt (UK)) and a pore size of around 2  $\mu\text{m}$ , glued (with ABS cement) to a length of 20 mm OD, 17 mm ID

Durapipe ABS. At the top end of the pipe an ABS socket union was added with the upper section of the union filled with a solid section of ABS glued in place with ABS cement. Into this top section of the socket union four small holes were drilled. Luer valve fittings were glued into two of the holes using Araldite © glue. A circuit board was then constructed in the manner described in Section 4.3.2.2 but with the vent pipe attached to the high pressure side of the differential transducer. Again each transducer was calibrated using a hand held manometer. The sealed circuit board was then inserted into the ABS tube and the vent tube and electric cables passed through the two remaining holes in the top of the socket union. The remaining gaps around the cable and vent tube were sealed with Araldite © glue and the socket union screwed in place. A three pin plug was added to the electric cable to allow easy connection to a voltmeter or datalogger.

This tensiometer design overcomes many of the problems associated with tensiometers in the past such as changes in pressure due to a needle/septum arrangement and the need for manual reading (Marthaler 1983; Digges La Touche 1998).

Additionally a type-K thermocouple (RS 363-0294) was fixed with tape to the outside of the tensiometer tube just above the level of the top of the ceramic cup in order to monitor soil temperature.

#### **4.3.3.2 Installation**

To install the tensiometers a 20 mm screw auger was used to auger to the desired depth. The complete tensiometer was then gently pushed into the slightly undersized hole to ensure a snug fit between the ceramic cup and the soil. Since the OD of the piezometer tube matched the size of the augered hole it was hoped that preferential flow pathways down the outside of the tensiometer could be excluded by the natural settling of the soil around the tube over time.

The tensiometer was filled with de-aired water using a 60 ml syringe attached to one of the luer valves until water was squirting out of the other luer valve. At this point the two luer valves were closed before the syringe was removed.

The short length of tensiometer protruding from the ground surface (<30 cm) was covered by a white PVC cover. An installed tensiometer at Site 2 is shown in Figure 4.4 without its PVC cover. The installations were carried out in August 2004. The total depth of the ceramic cup of each tensiometer is given in Table 4.2.

<b>Tensiometer</b>	<b>Depth of base of ceramic cup (cmbgl)</b>
S1_1	29
S1_2	57
S1_3	88
S1_4	124
S1_5	140
S2_1	33
S2_2	73
S2_3	88
S2_4	132
S2_5	159

**Table 4.2** Tensiometer installation depths

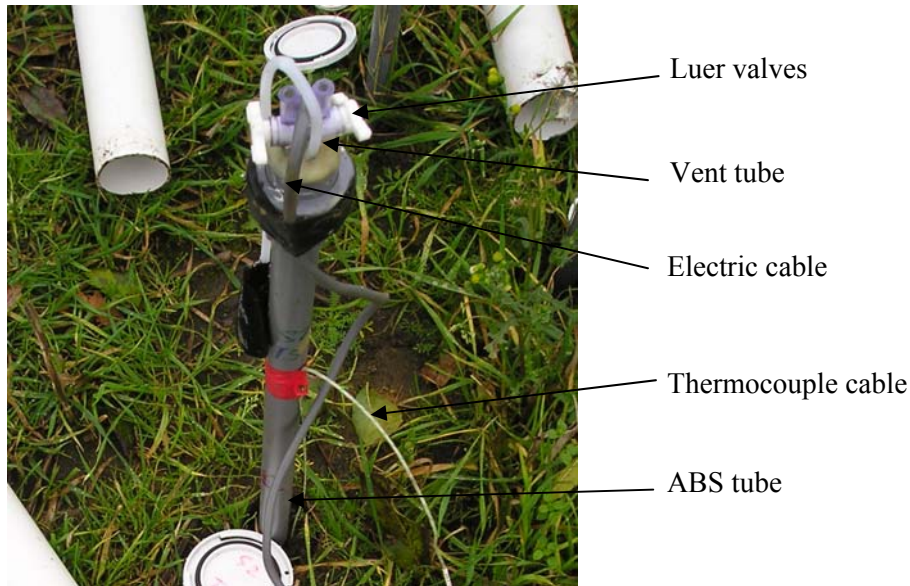


**Figure 4.4** Photograph showing a tensiometer installation at Site 2

#### 4.3.4 Data Loggers

At Site 1 two four-channel HOBO U12 dataloggers (manufactured by Onset Computer Corporation, Part No. U12-006) were used to monitor four tensiometers and two piezometers at 5 minute intervals. At Site 2 an older 16 channel ELE International MM900 Battery Powered Data Logging System was used to record data from 5 tensiometers, 2 piezometers and 5 thermocouples. In order to log the thermocouple temperatures accurately a cold junction temperature was monitored using a platinum resistance device attached directly to the first logger channel. Measurements were taken every minute and an average logged every 5 or 10 minutes.

Owing to the potential for noise in pressure transducer readings produced by variations in solar radiation (Cain *et al.* 2004) all the cables running from the monitoring devices to the loggers were buried 10 cm beneath the ground. The loggers were placed in water tight boxes and put in heavy duty bin liners to avoid drawing the attention of any passing vandals.

The tensiometers were recorded manually every few days from August to October 2004 and were then automatically logged from November 2004 to September 2005 at 5 or 10 minute intervals.

### **4.3.5 Soil Moisture Measurement**

#### **4.3.5.1 Choice of method**

There are many ways to measure soil moisture in the field. A helpful review is given by Schugge *et al.* (1980) while a more recent comparison of techniques is given by Walker *et al.* (2004). Destructive gravimetric sampling is the most reliable approach but is no good for measuring changes over time in exactly the same location. The most established method for taking repeated measurements in the same location is the neutron probe. However the health, safety and security issues regarding the storage, transportation and use of radioactive sources has become highly problematic recently, rendering the method impractical for this project.

The next best choice is one of the range of electromagnetic approaches which depend upon the effect of moisture on the electrical properties of soil. The method chosen is a type of time domain reflectometry (TDR) called TRIME TDR (manufactured by IMKO in Germany) which measures the dielectric constant of the soil at a frequency of between 600 to 1200 GHz by recording the travel time of an electromagnetic wave sent through the soil. This frequency range is chosen so that the imaginary (in the sense of a complex number description) part of the dielectric constant, that part which is variable with factors other than moisture content such as temperature and electric conductivity, is at a minimum. This allows the real part of the dielectric constant to dominate to allow more accurate estimations of soil moisture content to be achieved. Theoretically therefore TRIME TDR gives more accuracy than other electrical techniques such as capacitance probes or microwave, near-infrared and resistance methods.

Another benefit of the TRIME TDR approach is that a ‘down tube’ probe is available for measurement within a plastic tube installed vertically into the ground in a similar way to a neutron probe access tube. This avoids the disturbance of the soil needed to install standard TDR rod probes below the soil surface. The probe and tube are shown in Figure 4.5. The probe is cylindrical with 4 wave guides, two on opposing sides. A 2.5 metre length cable connects the probe to a hand held meter with a digital readout. The effective penetration depth of the probe is about 15 cm with the highest sensitivity in the vicinity of the access tube and decreases exponentially away with distance. The measuring volume is elliptical and thus 3 measurements are recommended at each depth interval, with the probe in a different orientation each time, to achieve a mean moisture content. The orientation of the probe is controlled using a metal rod which attaches to the top of the probe and is extended in 1 m sections as the probe is lowered down the access tube.

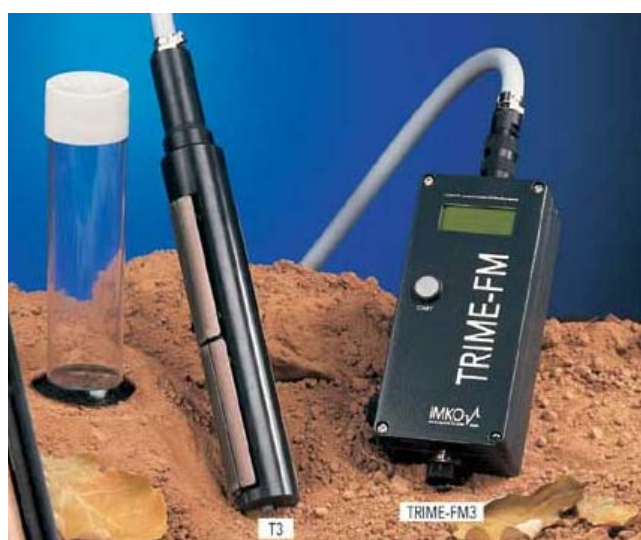


**Figure 4.5** TRIME TDR T3 probe and access tube

The probe is factory calibrated against dry and water saturated glass beads to compensate for the cable length and tolerances of the probe mechanics. A universal polynomial calibration is

then applied to relate the measured dielectric constant to the moisture content of common mineral soils. This calibration function is empirically determined and covers a wide range of soils. Although the equipment is still a relative newcomer, independent comparison between the TRIME TDR and other soil moisture measurement techniques indicates that the equipment is robust and reliable but has a tendency to overestimate moisture contents (Evet *et al.* 2002; Laurent 2002). As more researchers use this tool the empirical dataset for calibration will increase, potentially leading to a greater degree of accuracy in the method. It was considered the best alternative to a neutron probe for the current project.

#### **4.3.5.2 TDR tube installation**

Three TDR access tubes were installed at each fieldsite. The depth to which each tube was installed is shown in Table 4.3. This depended on the position of the water table and the difficulty of the installation.

A hole was augered by hand with a 40 mm OD Edelman auger to the desired depth with samples taken every 10 cm to be taken to the laboratory for gravimetric moisture content determination. A 44 mm OD access tube made of very strong and light Tecanat plastic was then pushed into the slightly undersized hole to ensure a snug fit to try and minimise the risk of creating preferential flow pathways down the outside of the tube wall. It is believed that this was successful for all three tubes installed at Site 2 but for only one of the tubes at Site 1 (S1\_M1). It is thought that difficulties at Site 1 were caused by till pebbles within the side of the augerhole obstructing the downward progress of the tube and pushing the tube away from the augerhole wall creating small cavities. This is discussed further in Chapter 5 with reference to the results obtained from the installations.

The tubes were installed during the summer (August 2004) at times of low water table. However, a screw expandable rubber bung was lowered slowly into each tube and sealed off at its base to stop the tube filling with water should the water table rise within this range over the winter period.

The top of each tube was cut off at 20 cm above ground level (agl) and fitted with a cap to stop rain from entering the tube.

<b>Location Number</b>	<b>TDR Tube Total Depth (cmbgl)</b>
S1_M1	174
S1_M2	97
S1_M3	180
S2_M1	172
S2_M2	157
S2_M3	142

**Table 4.3** TDR tube depths

#### **4.3.5.3 Monitoring procedure and consistency**

At each location 3 TDR moisture content values were taken at 10 cm depth intervals, at orientations separated by 120° to enable an average reading to be calculated. The 3 orientations were marked on the top of the TDR access tube so that each set of readings could be taken using consistent orientations of the probe. Readings were taken at an average frequency of 2 weeks at 1 to 3 week intervals for 12 months beginning in August 2004.

The repeatability of the measurements was checked by repeating readings at the same depth location and orientation 10 times for 5 combinations of depth/orientation. The variability

between readings at the same depth/orientation was found to be very small and equal to the resolution of the digital readout of the meter at 0.1% moisture content by volume.

However, comparing the three different orientations, the moisture content was often found to vary significantly. This difference was larger in drier conditions. At Site 1 the typical standard deviation across the three readings was less than 2% at the higher moisture content range but could be as high as 9% under drier conditions. For Site 2 the range was from less than 1% in wet conditions to around 4% at drier times. The data from the different orientations clearly have a potential use in understanding preferential wetting and drying patterns and the detailed heterogeneity of soil moisture changes that could not be measured with, for instance, the neutron probe method.

#### **4.3.6 ERT Arrays**

##### **4.3.6.1 Choice of method**

The tensiometers and TDR access tubes allow hydraulic responses to be monitored at a point in space. However it was also desirable to have a way of quantifying the spatial variability of moisture content changes across each site. It was therefore decided that permanent ERT arrays would be installed to enable the resistivity of the subsurface to be monitored at different times since changes in soil/rock resistivity are, in part, controlled by changes in moisture content.

The potential use of time lapse ERT for such a hydrological application was first recognised by Daily *et al.* (1992) and has been the subject of much research since (Binley *et al.* 2002; Fox 2003; Michot *et al.* 2003; Hagrey *et al.* 2004). It is noted that the success of applying the method in a quantitative manner is limited by the accuracy to which the relationships between soil/rock resistivity and the variables of soil moisture content, temperature and pore water

salinity can be defined. However, useful qualitative information can be gained without accurate knowledge of these relationships.

#### **4.3.6.2 Equipment**

At each site, two 50 electrode resistivity arrays were installed in orthogonal directions with a common midpoint and a minimum electrode spacing of 0.5 m. The arrangement is shown for each site in Figures 4.1 and 4.2. The electrodes have dimensions 100x10x3 mm and are individually wired to two 32 pin plug sockets located at the array midpoints. To install the array the soil was split with a spade to between 5 and 10 cm depth and the cables laid within the channel created. The electrodes were tapped into the ground at measured 0.5 m intervals and then the soil was pressed back over the cables and electrodes. A made up array is shown in Figure 4.6 A and is being installed in Figure 4.6 B.

The arrays have been monitored at a frequency of between 1 and 3 weeks for a 12 month period beginning in July 04 using the Campus Tigre in the manner described in Section 3.2.2.

#### **4.3.6.3 Forward modelling**

In order to interpret the time lapse ERT data effectively it is necessary to calculate the difference in resistivity between inversions for different points in time. These changes can then be related to changes in moisture content, if changes due to other natural time dependent variations such as temperature and pore water salinity can be accounted for (Rein *et al.* 2004).

The simplest approach is to carry out the inversions without taking other variables such as temperature into account but then to correct for the differences in the resulting data. To check the adequacy of this approach and to gauge the magnitude of the potential errors involved a simple forward model has been constructed. The model consists of two layers and is similar

to the situation encountered at Site 2. In the model a simple relationship between moisture content and resistivity has been assumed based on Archie (1942) as follows:

$$\rho_t = a\rho_w\phi^{-m}S_w^{-n} \quad (4.1)$$

where

$\rho_t$  = bulk resistivity at saturation  $S_w$

$\rho_w$  = pore water resistivity

$\phi$  = porosity

$a, m, n$  = empirical constants

$S_w$  = saturation as a fraction of  $\phi$  (i.e. 0 when completely dry, 1 when completely saturated)

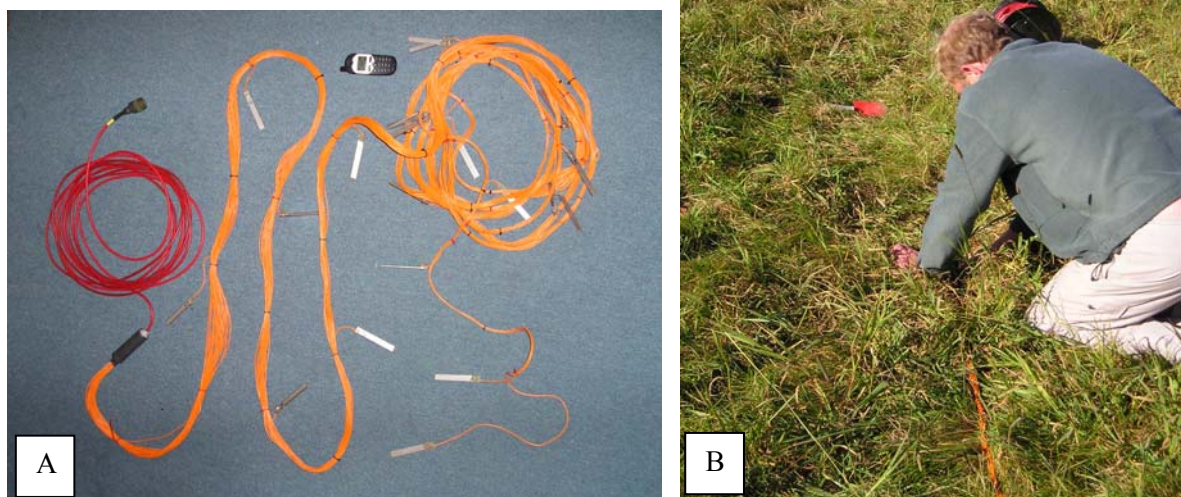


**Figure 4.6** Permanent ERT array (A) being installed (B)

It was decided to model the effect of temperature on resistivity but to leave out the effects of changing pore water salinity in order to make the interpretation of the results as transparent as possible. The following relationship was assumed between temperature and resistivity (Michot *et al.* 2003):

$$\rho_w = \frac{\rho_w^{ref}}{1 + \alpha(T - T^{ref})} \quad (4.2)$$

where

$\rho_w^{ref}$  = pore water resistivity at reference temperature

$T^{ref}$  = reference temperature

$T$  = temperature

$\alpha$  = temperature co-efficient of resistivity

In order to model the propagation of seasonal temperature effects an analytical solution to the 1-D diffusion equation has been used for the case of a sinusoidally varying upper boundary condition (Carslaw and Jaeger 1959):

$$T(z,t) = T_a + A_0 \exp\left[-\left(\frac{\pi}{\tau\kappa}\right)^{\frac{1}{2}} z\right] \sin\left[\frac{2\pi t}{\tau} - \left(\frac{\pi}{\tau\kappa}\right)^{\frac{1}{2}} z\right] \quad (4.3)$$

where

$T(z,t)$  = temperature at time  $t$  and depth  $z$  below ground level

$A_0$  = amplitude of boundary wave at  $z = 0$

$\tau$  = period of boundary wave

$\kappa$  = thermal diffusivity

A model was constructed using RES2DMOD ver 3.0 (Loke 2002), a forward modelling program which calculates the apparent resistivity pseudosection for a user defined subsurface model. The program uses a finite-difference or finite element method and requires the user to divide the subsurface into a number of blocks using a rectangular mesh. Each block is assigned a resistivity value and the forward model is run to generate a grid of apparent resistivity values.

The upper layer of the model is 2.5 m thick and represents unconsolidated sand. Parameters were as defined in Table 4.4. The lower layer from 2.5 to 4 mbgl representing clay has identical parameters except  $\rho_w^{ref}$  which was set to 20 ohm-m. Model blocks were 0.1 m thick at the surface increasing to 0.5 m at depth. The model was 24.5 m wide with block widths of 0.125 m.

The baseline model (model a) was assumed saturated from the base up to 1.2 mbgl. Moisture contents above this point were set to decrease until the top of the model is reached. The temperature profile of the baseline run was set to coincide with the peak of the boundary sinusoidal wave i.e. 20°C at the surface representing mid summer conditions.

The bulk resistivity was calculated for each model block for the baseline parameters within an Excel spreadsheet. These resistivity values were forward modelled using RES2DMOD to generate an array of apparent resistivity values. These apparent resistivities were then inverted using RES2DINV (Loke 2004) to generate a resistivity model. The process was repeated for 3 further models representing later times for a simulated rising water table and

increasing of the moisture contents in the unsaturated zone. The moisture content profiles for each model input are shown in Figure 4.7. These models were run for  $t$  of 60 (model b), 120 (model c) and 182.5 (model d) days from the baseline (model a) ending in a mid-winter condition. Input and output files for the forward model are given in Appendix 4.

Parameter	Value	Unit
$a$	0.2	-
$\phi$	0.3	-
$m$	1.5	-
$n$	2	-
$\rho_w^{ref}$	200	ohm-m
$T^{ref}$	10	°C
$\alpha$	0.02	°C <sup>-1</sup>
$\tau$	365	d
$\kappa$	0.05184	m <sup>2</sup> /d
$T_a$	10	°C
$A_o$	10	°C

**Table 4.4** Model parameters for layer 1

A comparison of the resulting inverted model outputs at the horizontal midpoint of the model with the input to the forward models is shown in Figure 4.8. The resulting inversions are significantly different from the inputs to the forward models. In particular the sharp transition between the upper and lower layer at 2.5 mbgl is smoothed out to a great extent and an artificial zone of increased resistivity has been created at 1 to 1.5 mbgl. The resistivity of the lower layer has also been overestimated by a factor of nearly two.

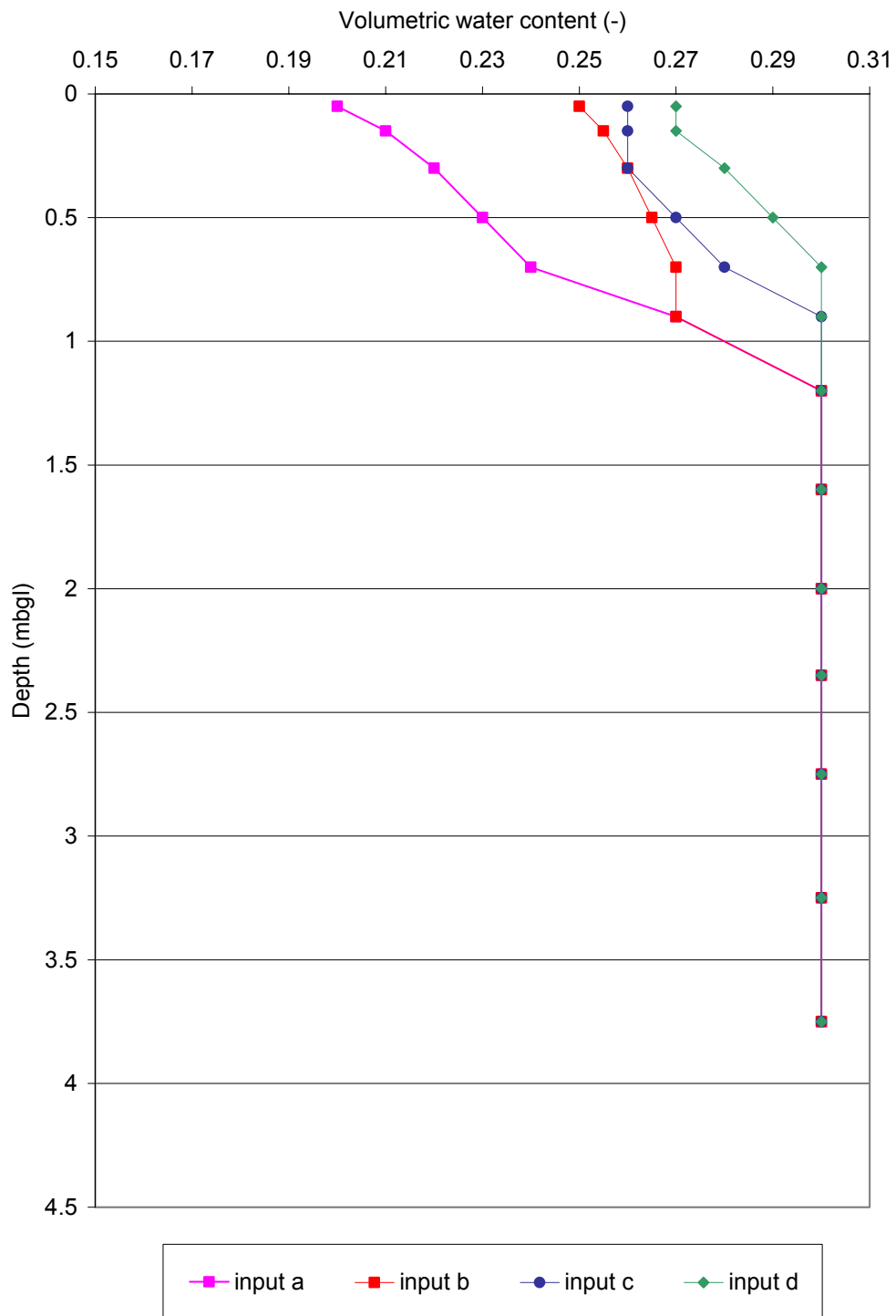


**Figure 4.7** Volumetric water profiles used as forward model inputs

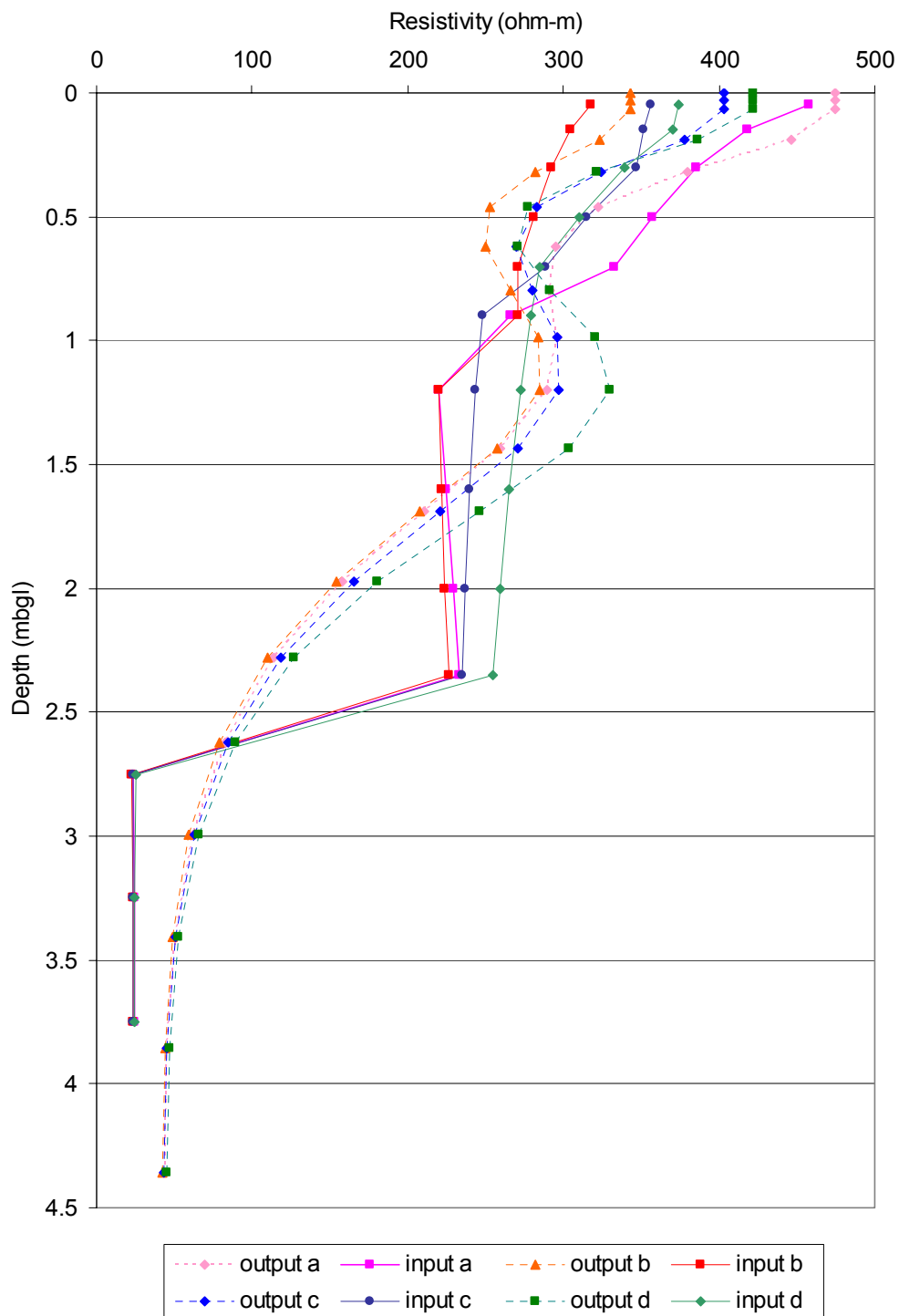


**Figure 4.8** Comparison of forward model inputs and inverted outputs

To check that this result was not peculiar to the inversion parameters chosen, a number of other inversions were run using a variety of options but all gave a very similar result to that

presented. These results indicate the lack of accuracy that may result from the ERT method for a situation with a sharp lithological change.

Changes in the input and output resistivity of the model blocks between models b to d and the baseline were then calculated. The results are shown in Figure 4.9 and indicate that below around 1 mbgl the comparison is very good. Above this level in the unsaturated zone the differences are much larger.

The model output was then analysed further to derive the differences in predicted moisture content from the baseline using the parameters and equations used for the inputs to the forward model. The results are compared with the changes in moisture content in the input data in Figure 4.10 for the case of no temperature correction. As time progresses from models b to d the comparison gets worse and worse as would be expected due to the increase in the temperature contrast over time.

When the temperature correction is made to the inverted resistivity values, the comparisons improve significantly as shown in Figure 4.11. The errors in the predicted moisture content changes are strongly correlated with the errors in the inversions as a comparison of Figure 4.9 and Figure 4.11 shows. This implies that the additional error involved by the method of post inversion temperature correction is minimal given the other errors introduced through the inversion process. Hence it is felt that this justifies the use of this type of correction when applied to the field data from the fieldsites.

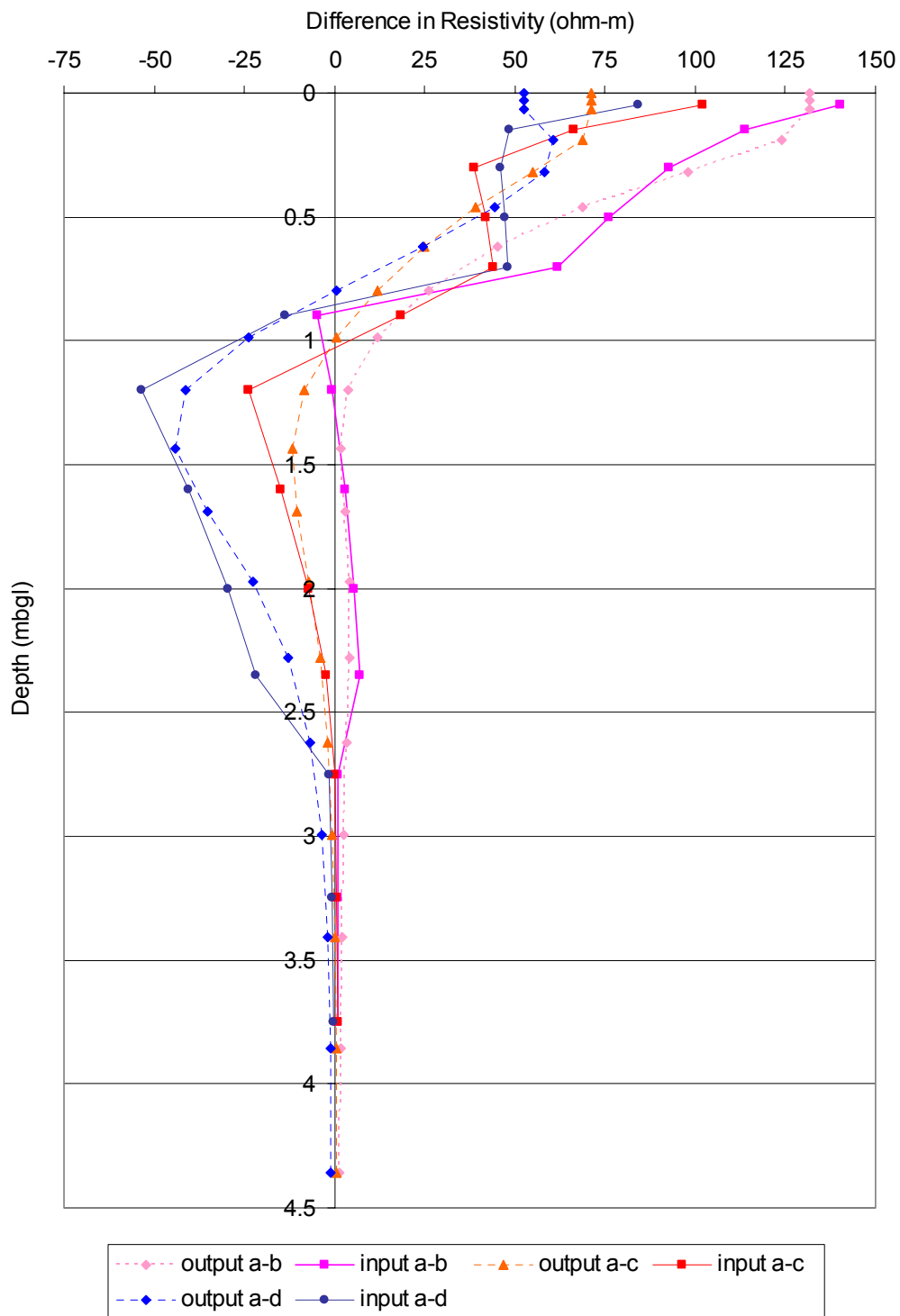


**Figure 4.9** Comparison of changes in forward model inputs and inverted outputs to the baseline model (a)

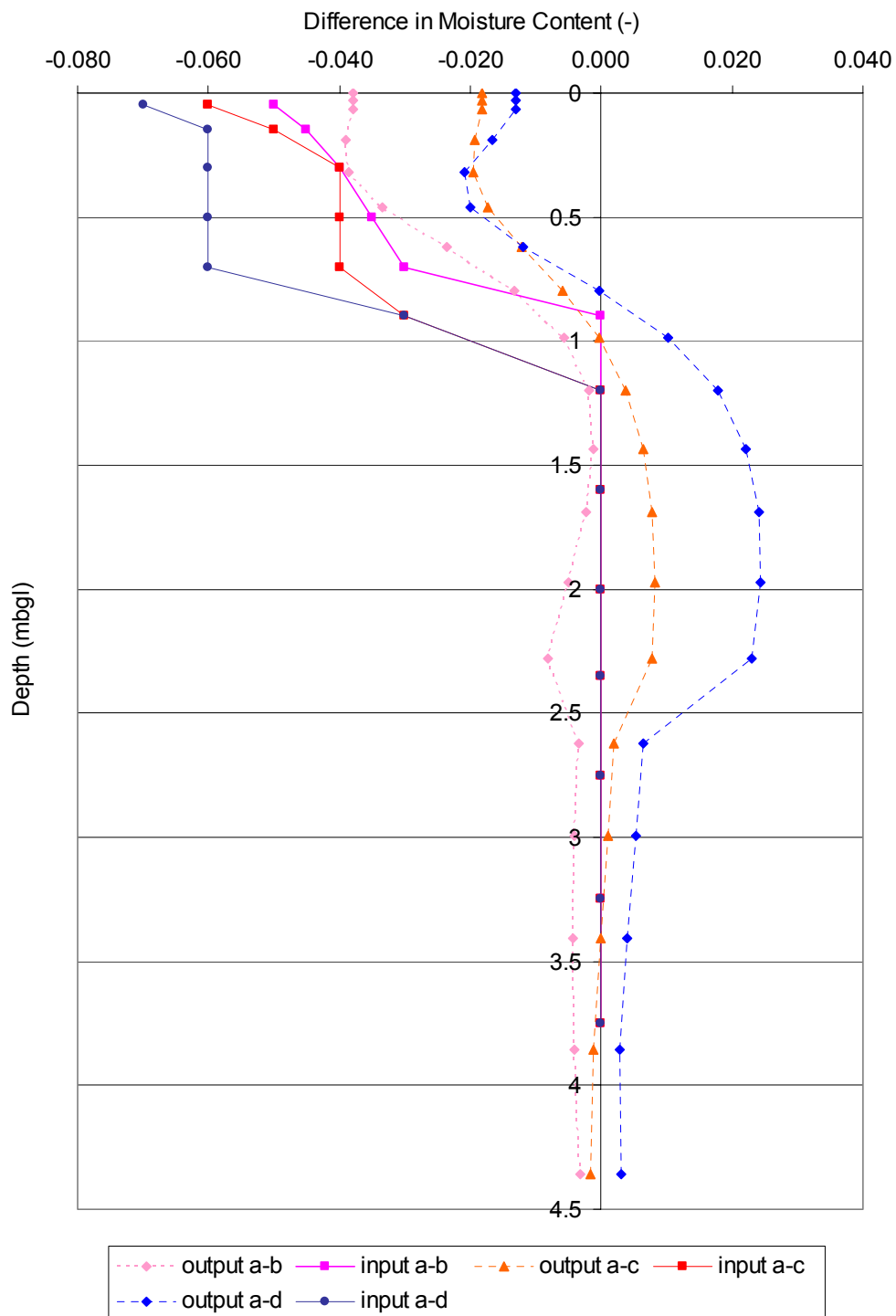


**Figure 4.10** Comparison of changes in predicted moisture contents between forward model inputs and inverted outputs and the baseline model (a) with no temperature correction applied

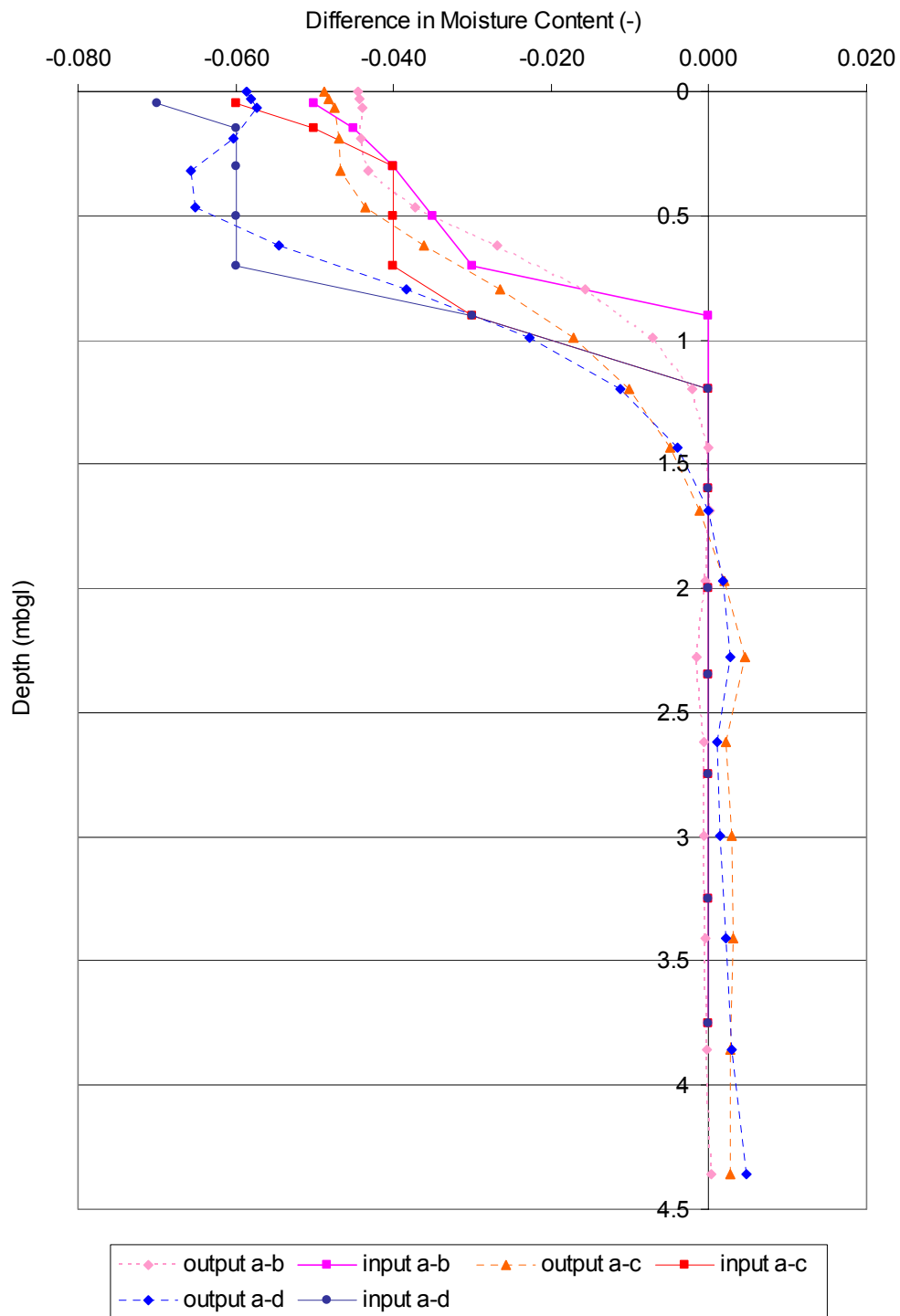


**Figure 4.11** Comparison of changes in predicted moisture contents between forward model inputs and inverted outputs and the baseline model (a) with a temperature correction applied

#### **4.3.6.4 Data processing**

The time series of ERT data generated for each array was inverted using RES2DINV and the inverted data were exported as a Surfer grid file. All inversions were carried out using default settings, model refinement and topographic modelling using a distorted finite element grid with a damped distortion factor of 0.5. The vertical to horizontal flatness filter was set to 0.3 and 0.6 for Site 1 and Site 2 respectively. The effects of the side blocks were reduced at Site 1 to smooth out unrealistically abrupt changes in resistivity near the edges of the model.

The difference between the resistivity model for each survey and a baseline survey in summer 2004 (21/7/04 for Site 1 23/7/04 for Site 2) was calculated using Surfer grid functions and plotted with a common colour scale. This was automated using VBA scripts within Surfer Scripter, the code for which is given in Appendix 5.

### **4.4 Experimentation**

#### **4.4.1 Introduction**

In addition to the monitoring of pressures, moisture contents, temperatures and resistivity three types of test were carried out at each site to further elucidate their hydraulic functioning. These were tracer tests, infiltration tests and piezometer tests and are now described in turn.

#### **4.4.2 Applied Tracer Experiments**

##### **4.4.2.1 Choice of tracers**

Many tracer types have been used in the past for helping to determine groundwater flow velocities and pathways. The main categories of chemical tracers are salts, radioisotopes and fluorescent dyes (Freeze and Cherry 1979). Of these it was concluded that fluorescent dye would be the most appropriate type of tracer since the interaction of applied salt may affect the permeability of the deposits being studied, and radioisotopes require comparatively expensive analysis and have associated permission issues.

A seminal work on fluorescent dye tracers was published by Smart and Laidlaw (1977) who evaluated several dyes for water tracing. Since then many other authors have published information regarding the use and properties of a range of fluorescent dyes (Omoti and Wild 1979; Trudgill 1987; Kasnavia *et al.* 1999; Harden *et al.* 2003). It was decided that two different types of tracer would be used for comparison which fluoresce at wavelengths different enough to be able to tell them apart.

Amino G acid and fluorescein were chosen and have the following properties. Sodium Fluorescein ( $C_{20}H_{10}Na_2$ ) is a highly soluble fluorescent dye which is bright yellow to the eye and has a maximum emission of 513 nm at an excitation of 491 nm (Harden *et al.* 2003). It is popular in groundwater tracing studies since it is inexpensive, easily detectable, non-toxic, and stable over time although it is sensitive to photochemical decay and adsorption, particularly on organic material (Smart and Laidlaw 1977). Amino G acid (7-amino 1,3 naphthalene disulphonic acid) is a blue fluorescent dye and has a maximum emission of 445 nm at an excitation of 355 nm (Smart and Laidlaw 1977). It has similar benefits to fluorescein and is less absorptive than many other fluorescent dyes (Trudgill 1987) although it also suffers from being sensitive to photochemical decay (Smart and Laidlaw 1977). Fluorescein and amino G acid plot in different places on the excitation-emission matrix (EEM) so that their intensity peaks do not overlap sufficiently to cause confusion for independent detection.

#### **4.4.2.2 Method of application**

A request to carry out both tests was sent to the Environment Agency taking due account of the recommendations contained in the Environment Agency R&D Technical Report W160 “Groundwater Tracer Tests”, and permission was granted.

The upper few cm of topsoil were excavated over an area of 3.5 m<sup>2</sup> and 4.0 m<sup>2</sup> at Sites 1 and 2 respectively. The locations of the tracer experiments are shown in Figures 4.1 and 4.2. Thin half-demy sheets (0.26 m<sup>2</sup>) of blotting paper soaked in a 14 g/l solution of each tracer was laid out in the excavation and covered as quickly as possible with gravel to ground surface as soon as each sheet was laid. It was hoped that this method of application would lead to an even distribution of tracer and reduce the loss of tracer by evaporation and photochemical decay. Both tracer experiments were installed on 4/10/04. The resulting mass of tracer applied was around 4.7 g/m<sup>2</sup>. A photograph of the tracer experiment being set up is shown in Figure 4.12.



**Figure 4.12** Setting up the tracer experiment at Site 1

#### **4.4.2.3 Invasive sampling**

On 20/1/2005, approximately 3 ½ months after the tracer application, samples were taken from Site 1 by the following method. The tracer patch was divided up into 16 segments and each sampling location was placed within a segment chosen at random (the patches of applied tracer were made large enough so that sampling could continue into the summer to build up a

picture of the changing distributions of tracer with time but due to time constraints in the end only three samples were taken from each site).

A small patch of gravel was removed and a 50 mm OD (1 mm wall) stainless steel tube was inserted 10 cm into the underlying soil. A 25 mm OD (1 mm wall) stainless steel tube was driven inside the first tube and removed. The soil sample was extracted from the end of the tube, bagged, and placed in a dark box. A 40 mm diameter dutch auger was then used to clear the remaining soil out of the larger tube before this tube was knocked another 10 cm into the soil. The smaller tube and auger were cleaned to prevent cross contamination of samples and the process was continued until a depth of 50 cm. At this point it was realised that the sampling method was compressing the soil materials to such a great extent that there was significant uncertainty as to the exact depth that each sample was coming from. Thereafter the smaller diameter tube was abandoned and samples were carefully taken with the auger instead, continuing to use the larger diameter steel tube as a casing. This first sample hole was designated S1\_H2, the first hole (S1\_H1) having been abandoned as some stray gravel had hampered the downward progress of the larger steel tube. Two further sample holes were made at Site 1 on 7/2/05 (S1\_H3 and S1\_H4). Samples were taken from Site 2 by the same method on 20/1/2005 (S2\_H1) and a further two sample holes made on 1/2/05 (S2\_H2 and S2\_H3).

#### **4.4.2.4 Sample analysis**

In order to measure the concentration of tracer within the pore water of each sample a methodology was developed using a Cary Eclipse Luminescence Spectrophotometer.

Standard dilution series of each tracer were made up in the range 0.00001 to 0.1 g/l. The spectrophotometer was used in 'Simple Reads' mode with the appropriate excitation and

emission wavelength set to measure either the fluorescein or amino G acid peak intensity. Excitation and emission slit widths were set to 5 nm, with open excitation and emission filters and using an average measurement time of 0.1 s. Each tracer dilution was then transferred by pipette into a clean cuvette and the emission intensity measured for a range of 6 photomultiplier tube (PMT) voltages from 400 to 1000 V. Increasing the PMT voltage increases the sensitivity of the readings taken. Each reading was taken 10 times and an average taken. The variation between readings was small and always less than 0.5% of the average reading. Cuvettes were thoroughly cleaned in dilute acid and distilled water between each sample reading and disposable pipettes were used to ensure no cross contamination between samples.

It was found that for PMT voltages higher than 600 V for fluorescein and 725 V for amino G acid the emission intensity for most dilutions was out of range. Graphs of emission intensity versus sample concentration for different PMT voltages were plotted for the lower voltages and straight lines resulted in all cases except for fluorescein at 400 V. This case plotted as a curve with the intensity of emission increasing at a decreasing rate with increasing tracer concentration. This is due to re-adsorption effects within the higher concentrations which were within range at this voltage. The remaining straight line plots were therefore used to derive linear relationships between tracer concentrations and spectrophotometer emission intensity for different PMT voltages. These calibrations are shown in Figure 4.13 and Figure 4.14.

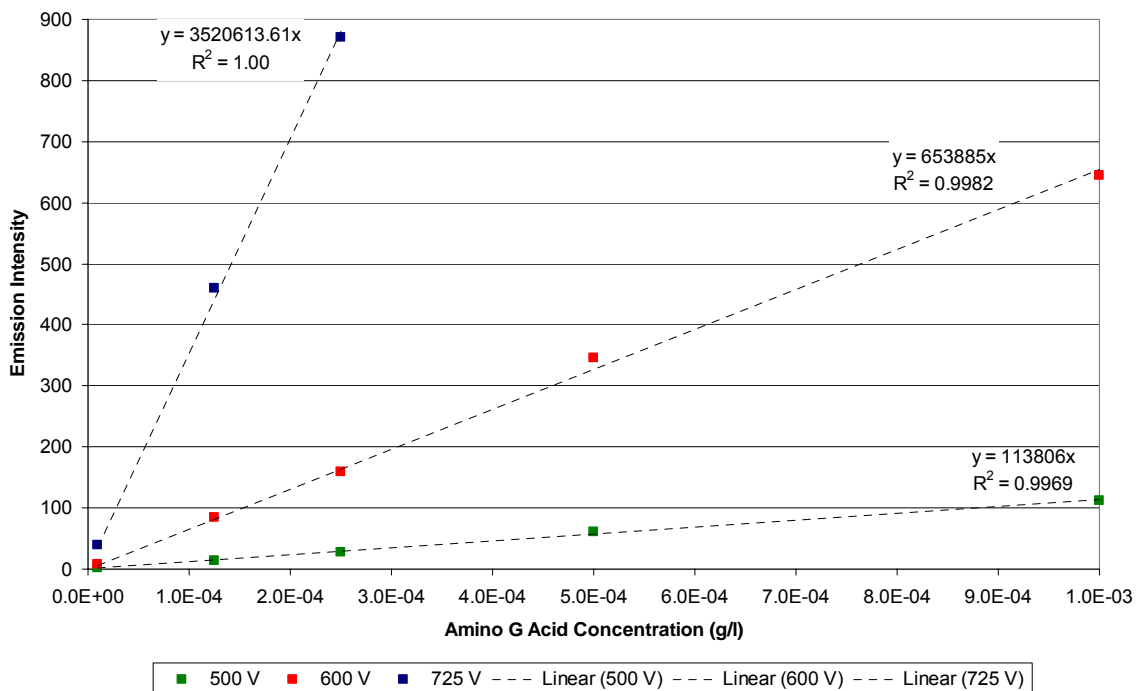


**Figure 4.13** Spectrophotometer calibrations for amino G acid

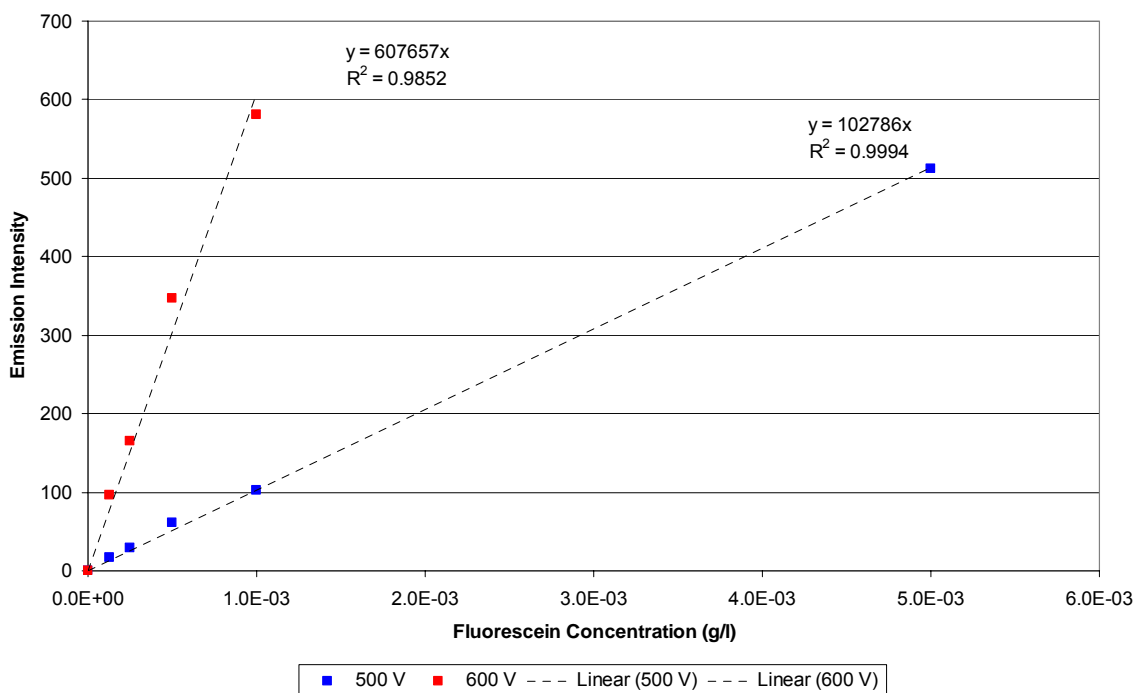


**Figure 4.14** Spectrophotometer calibrations for fluorescein

Sediment sample sizes of the order of 100 to 150 g were added to a known volume of deionised water (150 to 200 cm<sup>3</sup>) and whisked mechanically until all aggregates were broken down and a paste was formed. Before any settling occurred a 60 ml centrifuge tube of known mass was filled with the paste and then spun for 15 minutes at 20 000 rpm. Care was taken to avoid cross contamination of samples and a sample blank of deionised water was taken periodically to check the cleanliness of the equipment being used. A small volume (around 2 cm<sup>3</sup>) of diluted pore water was transferred by pipette from the top of the centrifuge tube into a cuvette. The emission intensity of the sample was measured at the calibration voltages for the peak emission and excitation wavelengths for fluorescein and amino G acid respectively. Ten readings were taken and averaged with a small associated error of less than 0.5%. The subsample was then added to the rest of the sample that had been made into a paste and dried in an oven at 100°C for 24 hours. The dilution factor ( $D$ ) of each sample was then calculated from the dry sample mass ( $M_D$ ), the insitu sample mass ( $M_I$ ), the mass of water added ( $M_A$ ) by the following equation:

$$D = \frac{(M_I - M_D)}{(M_I - M_D + M_A)} \quad (4.4)$$

The concentration of each tracer in each sample was finally calculated by using the calibration relationships and dividing by the dilution factor.

Since more than one calibration voltage was used for each tracer an average value was calculated along with an associated error defined as the difference of the reading from the average reading. This error, as a percentage of the average reading, was as high as 20% in some cases and although the test results range over 5 orders of magnitude this error should be taken into account when making interpretations.

Due to limited time available for the laboratory work, no tests on sorption of the tracers were able to be carried out.

#### **4.4.2.5 Background fluorescence**

An excitation-emission matrix (EEM) for a sample from Site 2 is shown in Figure 4.15. The fluorescent centres of fluorescein and amino G acid can be picked out but there also appear to be significant amounts of background fluorescence particularly in the region of the amino G acid peak. Problems caused by background fluorescence are widely reported in the literature (Smart and Laidlaw 1977) and for agricultural land on which the fieldsites are located the most significant source of background fluorescence is likely to be dissolved organic matter. The effect in the area of the fluorescein peak is likely to be small for such organic material but fulvic-like and humic-like organic acid can fluoresce in a similar location on the EEM as amino G acid (Baker and Lamont-Black 2001; Baker 2002). For this reason some investigation into the background fluorescence around the amino G acid peak was carried out.

Diluted porewater, from a limited number of samples of core uncontaminated with tracer taken from soil and glacial outwash materials at Site 2, was extracted and analysed. The analysis was carried out in an identical manner to that described above for samples taken from the tracer experiment but only using a PMT voltage of 725 V.

For the 7 samples of glacial outwash the resulting range of apparent amino G acid concentration was 0.0002 to 0.002 g/l and 0.003 g/l for 1 sample of topsoil analysed. This amount of background fluorescence is clearly very significant when trying to identify the presence of amino G acid at low concentrations and must be taken into account when interpreting the tracer test results.

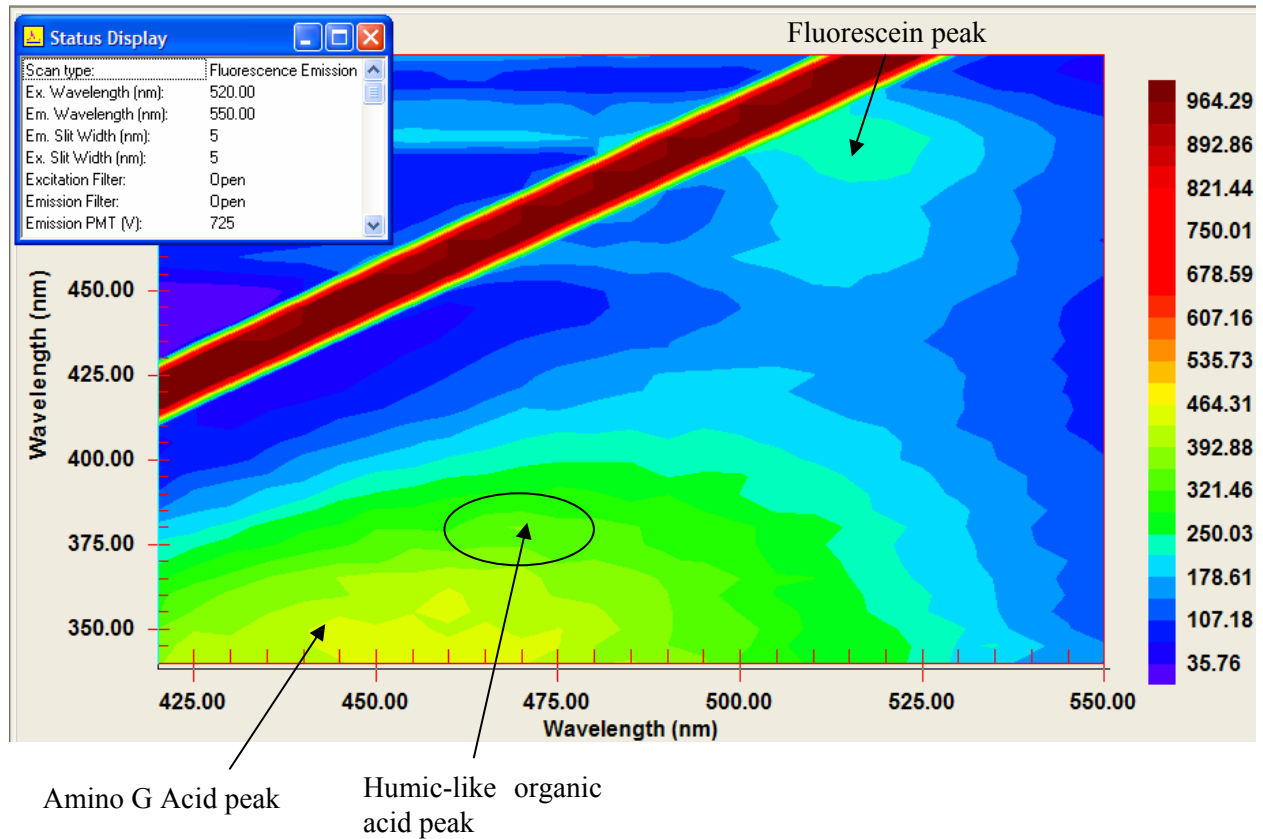


**Figure 4.15** EEM at PMT voltage of 725 for soil sample (20 to 30 cmbgl) in S2H1

#### 4.4.3 Environmental Tracer Measurement

##### 4.4.3.1 Tritium analysis

Natural background atmospheric concentrations of tritium ( $^3\text{H}$ ), the radioisotope of hydrogen with a half-life of 12.38 years, are estimated to be less than 20 tritium units (TU). However, between approximately 1952 and 1963 atmospheric concentrations were raised to over 1000 TU in some parts of the world as a result of thermonuclear testing. Tritium levels have declined since this time but present day levels remain above the natural background (Schwarz and Zhang 2003). As a result, the presence of tritium concentrations above the natural background indicates the presence of post-1952 water. More quantitative estimates of the age of groundwater using tritium concentrations are complicated by uncertainties in the precise input concentration of tritium in rainwater at a particular location, and the fact that tritium

decays with a short half-life. The limitations of using tritium alone can be addressed by also measuring  $^3\text{He}$  as summarised by Hiscock (2005).

In order to measure tritium concentrations for the purpose of potentially dating porewater within the till and glaciolacustrine deposits, core samples were sent to RDC Lockinge for tritium analysis. Unfortunately,  $^3\text{He}$  analysis cannot be performed on porewater samples which, as described above, limits the usefulness of the tritium dating method.

Porewater was extracted by vacuum distillation. The porewater was subjected to electrolytic enrichment followed by conversion of the water to hydrogen. This was combined with ethene to form ethane and counting of the ethane gas was then carried out in a gas proportional counter. The errors quoted with the data presented in Chapters 5 and 6 cover water extraction, processing and measurement of the tritium and reflect precision rather than accuracy. The accuracy is gauged against a blank taken from palaeowater from the Lower Greensand shown with a resulting tritium activity well below 1 TU.

#### **4.4.3.2 Chlorofluorocarbon (CFC) analysis**

Atmospheric concentrations of CFCs have been rising since the 1940s as a result of their use as propellants in aerosol cans and refrigerants. Since the atmospheric concentrations of different CFCs over time are known, CFCs can be used as a groundwater dating tool assuming that the concentration in the recharging water is in equilibrium with the atmospheric gas phase according to Henry's Law (Schwarz and Zhang 2003). There are, however, limitations of the method since CFC concentrations in anaerobic environments may be reduced through microbial degradation (Goode *et al.* 1997).

Samples of water were taken from borehole TE32, screened within the Permo-Triassic sandstone at Site 1, using a peristaltic pump. The borehole was purged before sampling by

pumping several boreholes volumes of water and CFC samples were collected unfiltered without atmospheric contact in glass bottles contained within metal cans by the displacement method of Oster *et al.* (1996). This method ensures that the sample is protected from possible atmospheric contamination by a jacket of the same water.

CFC analysis was performed using a method based on that of Bullister and Weiss (1988) involving pre-concentration cryogenic trapping followed by gas chromatographic analysis using an electron capture detector. The measurement precision is of the order of 5%.

#### **4.4.4 Infiltrometer Tests**

Double ring infiltrometer experiments were carried out at 2 locations at Site 1 and at 3 locations at Site 2 as shown in Figures 4.1 and 4.2 in order to estimate the saturated hydraulic conductivity of the soil.

The double ring infiltrometer used consists of two 50 cm high steel rings with diameters of 30 and 60 cm. The vegetation was carefully cropped at the site of each test and any thatch removed from the soil surface. The rings were driven carefully into the ground to a depth of around 15 cm, with the second ring placed around the first. Every effort was made to avoid creating preferential flow pathways under the edge of the rings. A measuring tape was attached to the wall of the inner ring, and both rings were filled simultaneously to the same depth of water. A piece of towelling was laid on the soil surface in the inner ring whilst pouring was undertaken to prevent any disturbance of the soil surface and was carefully removed before the start of the timed period. The depth of water in the inner ring was then measured over time to the nearest mm. The test was finished when the water depth decreased to around 5 cm due to the presence of the cropped vegetation and unevenness of the soil surface.

In theory, water infiltrating from the outer ring will act as a buffer forcing flow from the inner ring to remain vertical. The results obtained should therefore predominantly reflect the vertical rather than the horizontal component of hydraulic conductivity. For a uniform soil the infiltration rate should decrease exponentially and tend to a constant rate equal to the saturated hydraulic conductivity as the driving hydraulic gradient approaches unity (Tindall and Kunkel 1999).

#### **4.4.5 Piezometer Hydraulic Tests**

In order to measure the saturated hydraulic conductivity of the drift units at a scale larger than that of the small samples tested in the laboratory permeameters, falling head tests were carried out in piezometers installed at the fieldsites. This method was chosen over rising head tests since several of the boreholes at Site 2 were dry.

The initial water level in the piezometer relative to a datum was measured ( $H$ ). A volume of water was added and the water level in the piezometer ( $h$ ) was then monitored over time ( $t$ ) until the water level had declined to its original level. Owing to the low permeability of some of the deposits, some of the tests took a significant amount of time to recover. Hence, repeat tests were not carried out because as much 'natural' data from the piezometers as possible was required for developing an understanding of the sites.

The method of analysis applied to all the tests was that of Hvorslev (1951) described in Freeze and Cherry (1979). The analysis assumes a homogeneous, isotropic, infinite medium in which both soil and water are incompressible. The rate of inflow (or outflow) ( $q$ ) at the piezometer tip at any time is assumed to be proportional to the hydraulic conductivity ( $K$ ) of the soil and to the unrecovered head difference ( $H-h$ ). If  $h_0$  is the head at time equals zero, by

this analysis a plot of  $\ln \left[ \frac{(H-h)}{(H-h_0)} \right]$  versus  $t$  should be a straight line. The value of  $t$  when

$\ln\left[\frac{(H-h)}{(H-h_0)}\right] = -1$  is defined as the basic time lag ( $T_0$ ). For a piezometer intake of length  $L$

and radius  $R$ , with  $\frac{L}{R} > 8$ , the resulting expression for  $K$  is:

$$K = \frac{r^2 \ln\left(\frac{L}{R}\right)}{2LT_0} \quad (4.5)$$

Tests were carried out at the piezometers installed at the two fieldsites and analysed by the Hvorslev method. The assumptions made in the analysis are unrealistic for the conditions we have encountered at the fieldsites. It is noted that more complex analyses are available to overcome, for instance, anisotropy. However, using the simple form of analysis, hydraulic conductivity estimation to within an order of magnitude is likely to be achieved, an adequate accuracy for the purpose of this thesis.

#### **4.5 Summary**

Two fieldsites have been chosen for detailed investigation into the hydraulic behaviour of recharge through drift at the site scale. This chapter has described the instrumentation installed and monitoring and experimentation carried out at both sites. The choice of site locations and equipment as well as measurement and analysis techniques have been justified with reference to other approaches described in the relevant literature. Sources of error and uncertainty have been identified and quantified to a reasonable extent. The following two chapters follow on by describing the results for each fieldsite and defining conceptual and numerical models for the hydraulic behaviour based on the results obtained.

# **5 SITE SCALE INVESTIGATIONS 2: SITE 1 RESULTS AND MODELS**

## **5.1 Aim**

This chapter presents the results of the monitoring and investigation carried out at Site 1 using the equipment, techniques and analysis methods described in Chapter 4. Based on these results, a conceptual model of the site hydraulic processes is proposed. Results from numerical models undertaken to test the conceptual model and to quantify the magnitude and timing of likely recharge fluxes are then described and conclusions drawn.

## **5.2 Results**

### **5.2.1 Geology**

The geology is known from 4 cored boreholes drilled using the Sonic rig (S1\_1 to S1\_4) and one LOCAR borehole drilled using a percussion rig (TE32), from shallow augering undertaken for installation of tensiometers and TDR access tubes, and indirectly from ERT surveys.

Topsoil is encountered from the surface to between 0.3 to 0.4 mbgl comprising loose soft dark brown variably sandy clayey silt with rootlets and organic material. Below the topsoil reddish brown poorly laminated silty sandy clay interpreted as a head deposit is present in several of the boreholes at the site down to a maximum depth of 0.7 mbgl. In one location (S1\_2) a 0.15 m thick layer of fine sand was found between the topsoil and the head deposit. These deposits overlie a layer of till to a depth of around 6.3 mbgl which overlies Permo-Triassic sandstone. The characteristics of the till have been described in some detail in Section 3.3.4.3.

A schematic cross section is shown in Figure 5.1 to indicate the likely geometry of the different lithologies. Also shown are the monitoring locations of TDR access tubes (M1 to M3), piezometer screen intervals (S1\_3, S1\_4 and TE32) and tensiometers (T1 to T5). The depth of each installation is accurate but since the horizontal position is only approximately projected onto a north-south line across the site the figure is schematic. Each installation is, however, shown correctly in relation to its geological context.

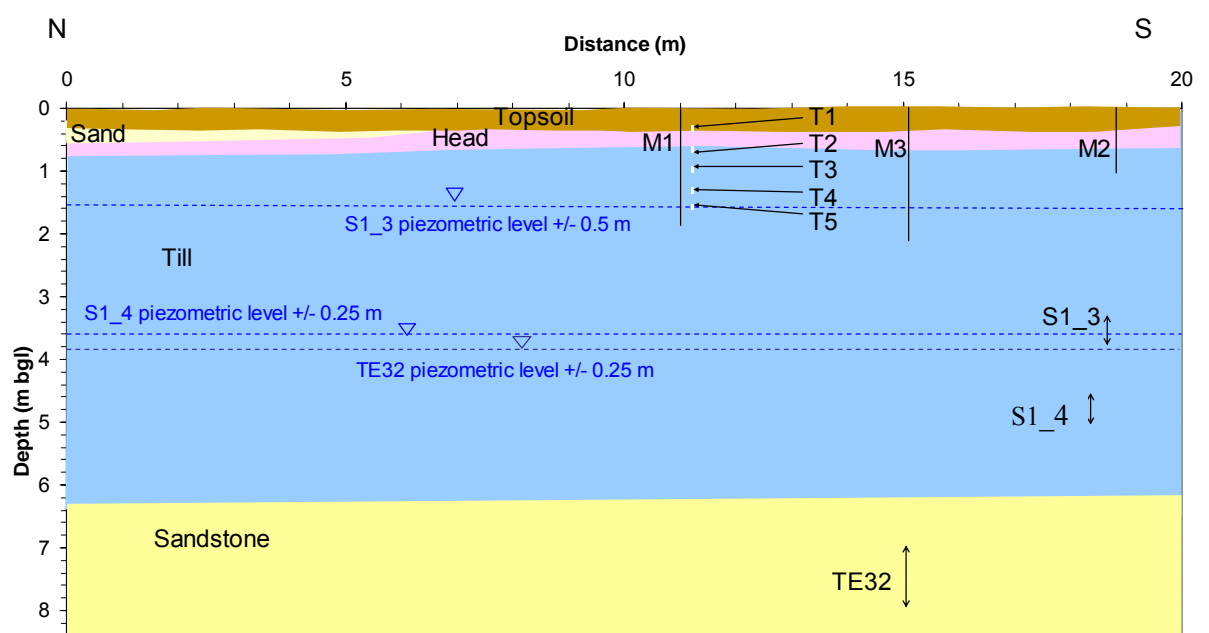


**Figure 5.1** Schematic geological cross section of Site 1 (M = TDR access tube, T = tensiometer)

### 5.2.2 Pressures

Pressures have been recorded at two piezometers (S1\_3 and S1\_4) and 5 tensiometers (T1 to T5) within the till as described in Chapter 4. Data from the LOCAR Data Centre for borehole TE32 monitoring water levels in the Permo-Triassic sandstone have also been collated. The depths of the monitoring intervals relative to ground level are shown in Figure 5.1.

The pressure heads recorded have been added to an elevation head with reference to a site datum to produce a total head. The site datum chosen was the cover of LOCAR borehole TE32 which is near ground level. Time series of average daily total heads are shown in Figure 5.2 for the whole monitored period in cm above site datum (cmasd). Spurious data from malfunctioning tensiometers have been removed. Manual readings are plotted as points and logger data presented as continuous lines.

Time series of groundwater levels in piezometers S1\_3, S1\_4 and TE32 are shown in Figure 5.3 for the entire monitored period and in Figure 5.4 for the period 1/11/04 to 1/3/05 alongside scaled atmospheric pressures. Time series of pressure heads recorded at the tensiometers T1, T3 and T5 are shown in Figure 5.5 for the period 7/12/04 to 11/01/05 at 5 minute intervals. Figure 5.6 shows daily average values of tensiometer pressure head for the whole monitored period.

The piezometer transducer/data logger equipment gave results in excellent agreement with manual dips taken sporadically through the monitored period as shown in Figure 5.2. Tensiometers T2 and T4 unfortunately malfunctioned within 1 month of installation due to electronic failure. The exact cause of the problem has not yet been discovered. The other tensiometers generally performed well although pressure effects due to freezing of the water column occurred at times correlated with sub-zero ground temperatures. Examples of this are shown in Figure 5.5 around 21/12/05 and 27/12/05. A daily cycle of variable magnitude is also seen in the data. This is likely to be a pressure response to the heating and cooling of the water column due to diurnal temperature variations.

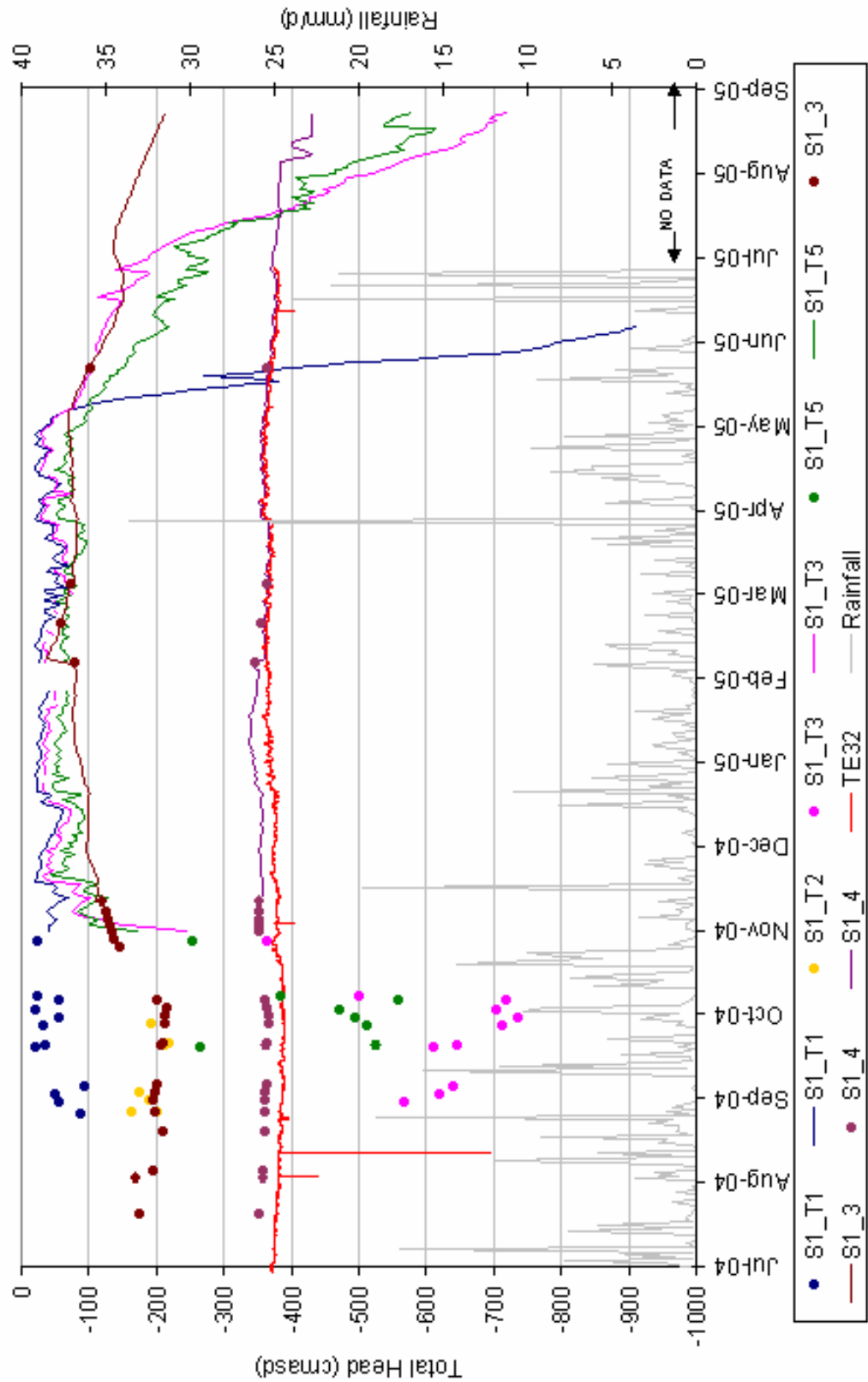


**Figure 5.2** Time series of total pressure heads recorded at Site 1 piezometers and tensiometers in cm above site datum (cmsd)

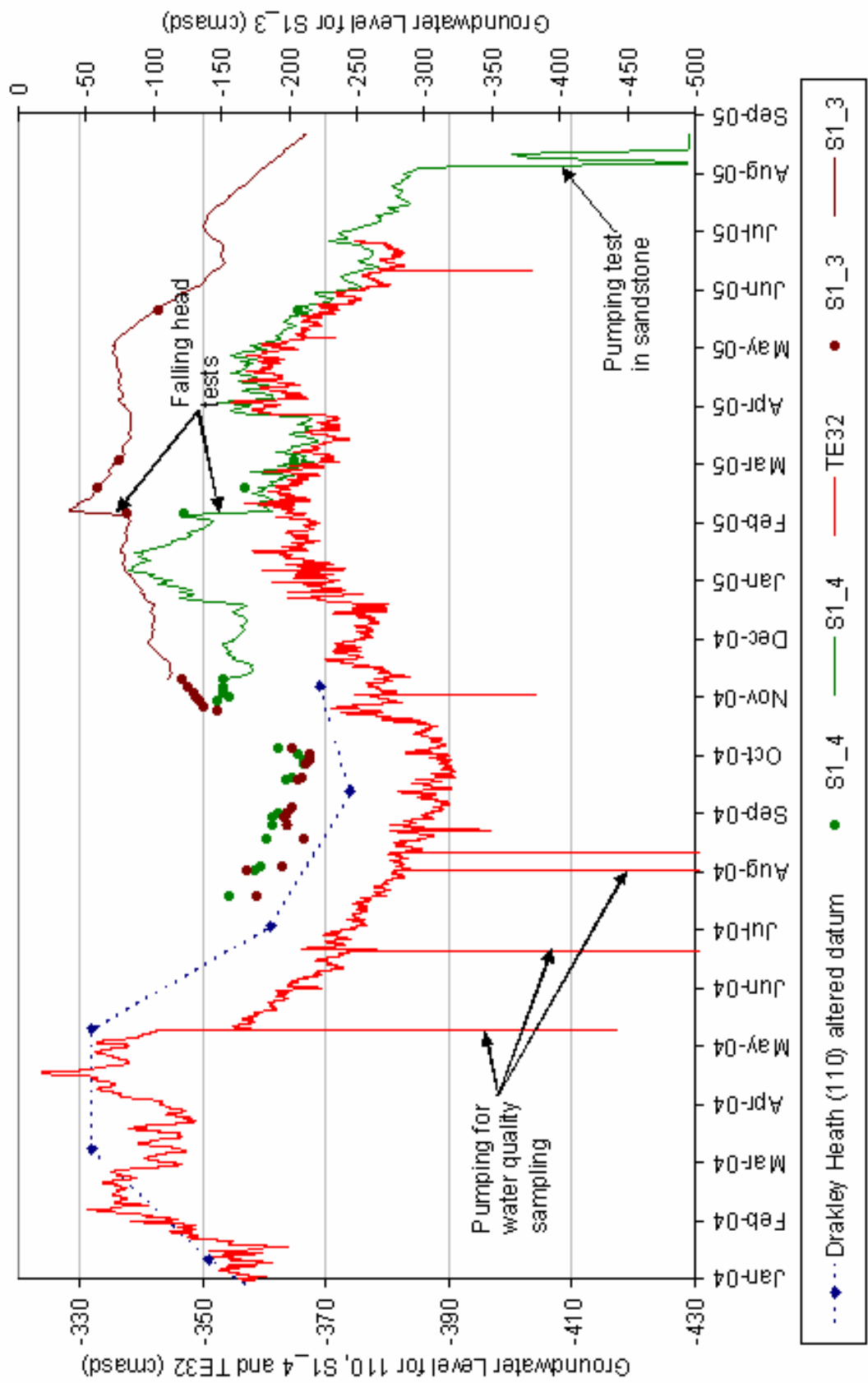


**Figure 5.3** Time series of groundwater levels recorded at Site 1 piezometers

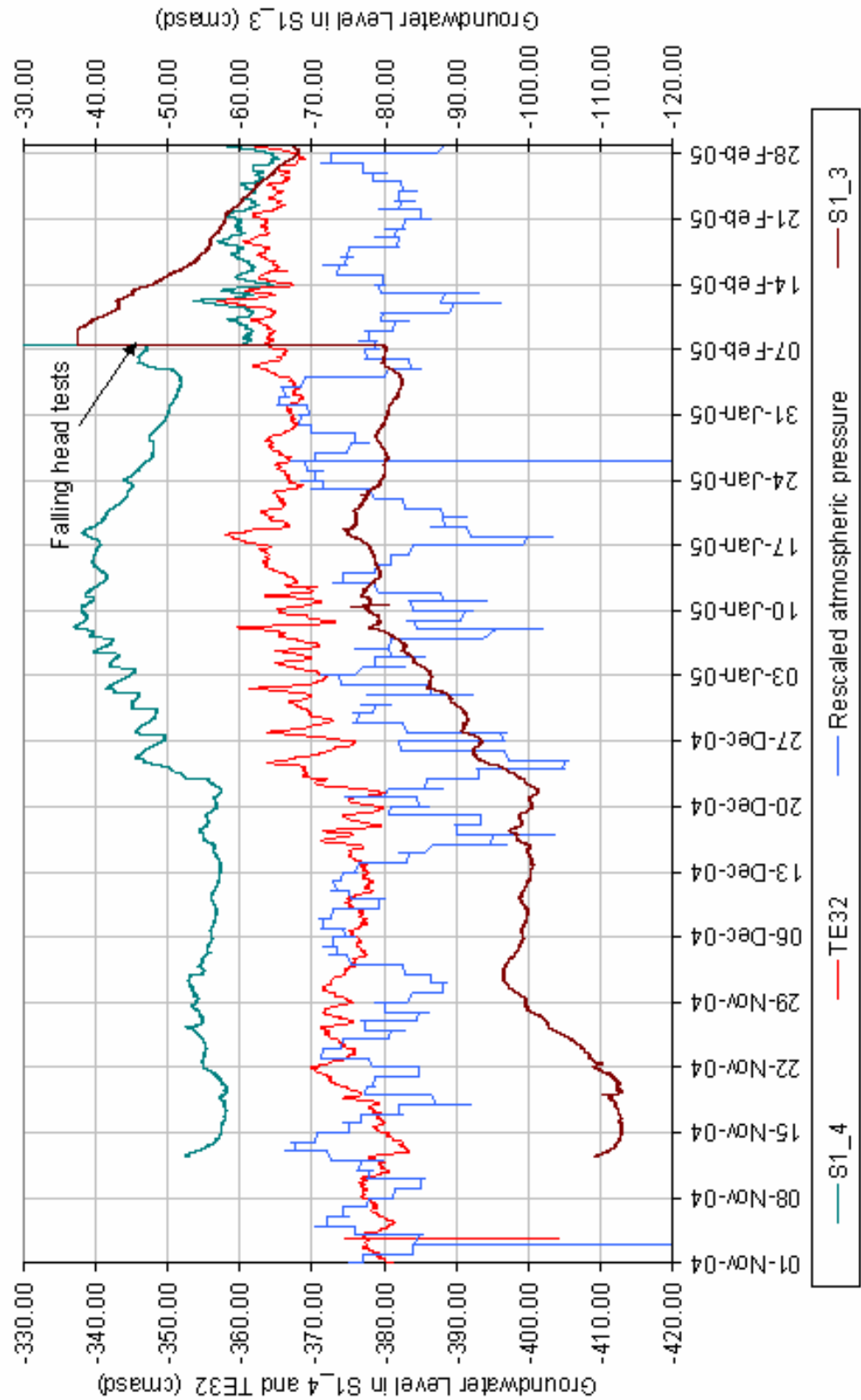


**Figure 5.4** Time series of groundwater levels recorded at Site 1 piezometers from 1/11/04 to 11/3/05 alongside rescaled atmospheric pressure

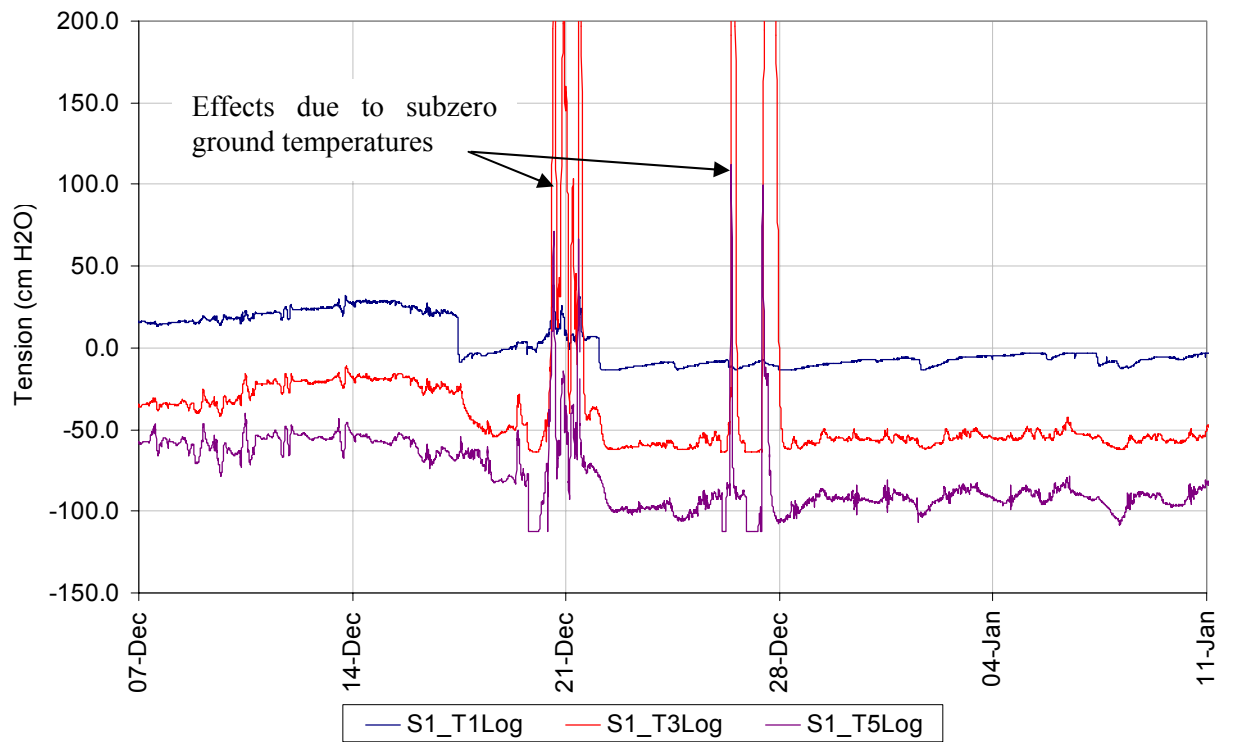


**Figure 5.5** Soil tension recorded at Site 1 tensiometers at 5 minute intervals between 7/12/04 to 11/01/05

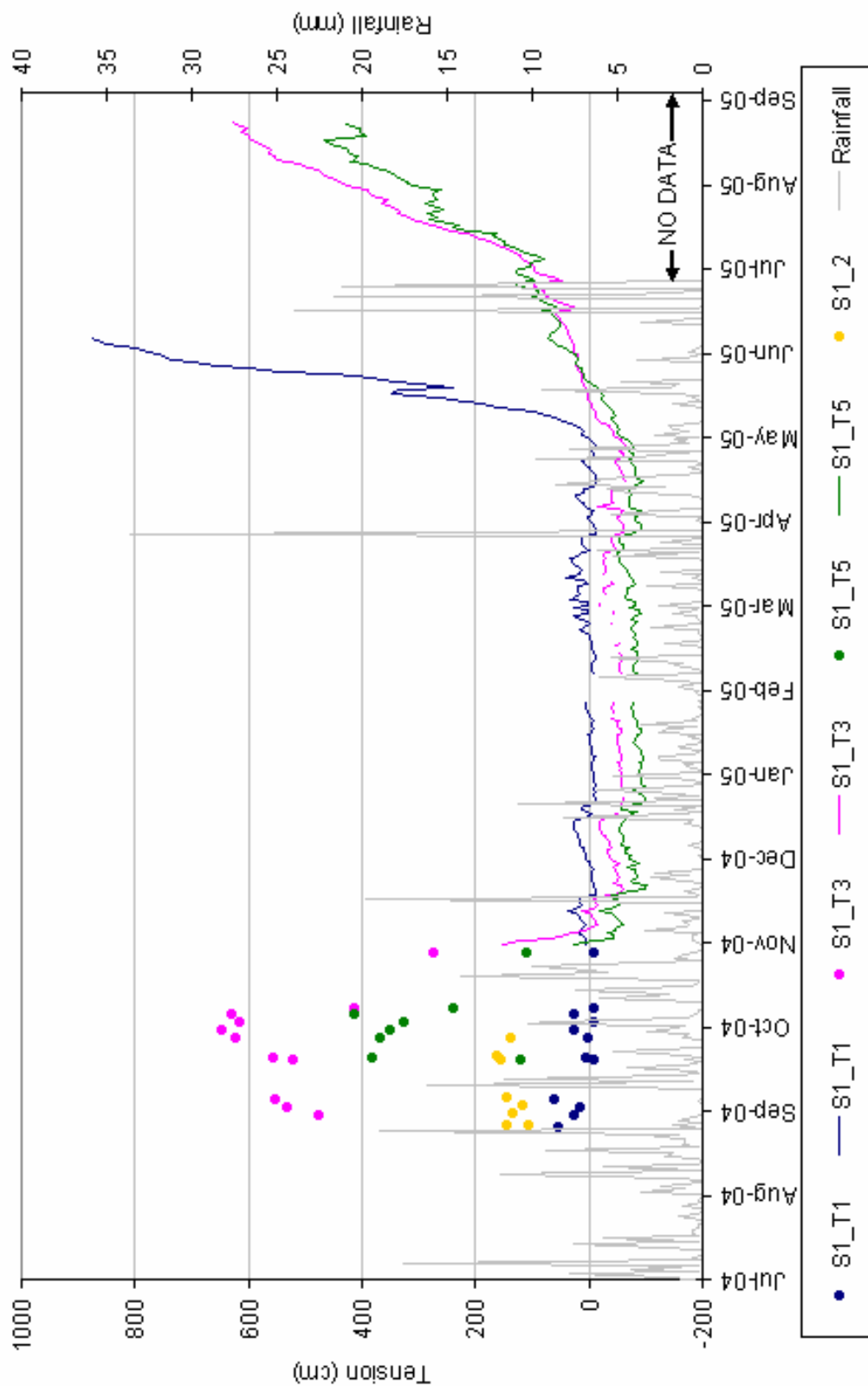


**Figure 5.6** Time series of average daily pressure heads recorded at Site 1 tensiometers

The detailed groundwater level data shown in Figure 5.4 indicate short timescale variations in pressure head which correlate strongly with changes in atmospheric pressure. Such an inverse relationship between increases in atmospheric pressure and decreases in water level, and vice versa, is to be expected for piezometers screened within confined formations (Jacob 1940; Todd 1959). Although the atmospheric data resolution is poor it is possible to see that the atmospheric changes are in phase with pressure changes recorded by piezometer TE32. In contrast a slight lag of approximately 1 to 1.5 days is seen between the change in atmospheric pressure and the corresponding change in hydraulic pressure response recorded at S1\_4 and S1\_3 respectively. This time lag in the piezometers screened within the till is an expression of the low permeability of the formation and is in the range expected for a head perturbation of a few cm based on the theory of Hvorslev presented in Section 4.4.5. The barometric efficiency of the till piezometers is in the range 0.1 to 0.2 and for TE32 is approximately 0.4 consistent with a relatively compressible formation. It is noted that after the falling head test had been carried out on S1\_4 the responses in this piezometer became indistinguishable from those recorded in TE32 as shown in Figure 5.4. In addition the head difference recorded by these two piezometers also fell significantly. These observations imply that the falling head test caused an increase in the hydraulic connectivity between the two monitored intervals. This is discussed further below in Section 5.2.9.

The small timescale and relatively small magnitude variations in water level due to barometric effects are superimposed on a larger seasonal trend as can be seen in Figures 5.2 and 5.3. Groundwater levels for all three piezometers are at a minimum during September and begin to recover during October. Water levels in S1\_4 and TE32 have a maximum in January with a subsidiary peak in April in contrast to S1\_3 in which a plateau of high water levels persists between January and May before summer recession begins. The magnitude of the seasonal

fluctuations in water level varies greatly between the piezometers with S1\_4 and TE32 having a variation of just 0.4 m in comparison to 1.4 m for S1\_3. The greater seasonal fluctuations seen in S1\_3 are likely to be due to a relatively low specific yield of the till. This pressure response is thus attenuated with depth as would be expected for till with moderate specific storage and low permeability. Figure 5.3 shows the groundwater levels recorded within the Permo-Triassic sandstone at Drakley Heath (Location 110 in Figure 2.5) adjusted to a different datum for comparison against TE32. This indicates that the fluctuation within the sandstone below the till at Site 1 is very similar to seasonal variations in an area of outcrop sandstone at Drakley Heath. This is unsurprising given that Site 1 is only 500 to 1000 m from areas of sandstone outcrop and pressure responses through the sandstone confined by till will only take a few days to propagate to the site using realistic values of transmissivity and storage coefficient. This was approximately calculated using the analogous equation for flow of that given for temperature in Equation 4.3 which simulates the propagation of a sinusoidally varying head boundary condition through an infinite homogeneous medium. Thus it is likely that the water level changes seen in TE32 reflect an aggregated response of the sandstone aquifer across the catchment in addition to any direct effects of recharge through the till at this location.

There is a persistent downward hydraulic gradient throughout the year between the water table and the groundwater level in the Permo-Triassic sandstone of approximately 0.4 during the summer and nearly 0.5 during the winter. There is some uncertainty as to the exact position of the summer water table but it can be inferred from the data from S1\_T5 and S1\_3 to be at approximately 1.7 m. As noted above, water levels in S1\_4 closely follow those in TE32 suggesting a good degree of hydraulic connection between the two piezometers. The absence of a significant time lag between these piezometers separated by more than 1 m of till

suggests that the till bulk hydraulic conductivity is significantly greater than that of the till matrix in this location.

The tensiometer data indicate that during the winter period between early November and early May a downward hydraulic gradient was present throughout the upper 1.4 m of the profile. During this time the pressure head at each tensiometer was always positive with the exception of periods of several days at a time when tensions of up to 30 cm were recorded in S1\_T1. A variable hydraulic gradient of around 0.2 to 0.6 was present between S1\_T1 and S1\_T3 and S1\_T3 and S1\_T5. Following large rainfall events S1\_T1 took as much as 1 day to respond with initial pressure increases at S1\_T3 and S1\_T5 at around 1.5 and 2 days respectively. After the initial response the pressure increase was relatively sudden for S1\_T1 becoming more and more gradual for S1\_T3 and S1\_T5. In contrast to the saturated pressure responses of the tensiometers to recharge the hydrograph for S1\_3 is very smooth. Although some attenuation of the recharge signal will occur due to the specific storage of the till (which may be in the range of  $1 \times 10^{-4} \text{ m}^{-1}$  (Keller *et al.* 1989)) the smoothing is likely to be due mainly to the piezometer construction and is consistent with the results of the falling head test carried out on this piezometer described below.

During May 2005, as evapotranspiration rates begin to become more significant, the tension in the topsoil zone as recorded by S1\_T1 increases very quickly and is out of range at 8.8 m by mid June. Tensions in S1\_T3 and S1\_T5 also began to increase during this time but at a slower rate reaching a maximum of 600 and 400 cm respectively by mid-August. The point at which transition is made to an upward hydraulic gradient between S1\_T1 and S1\_T3 coincides with the start of the summer recession in piezometer S1\_3.

During the late summer in 2004 an upward hydraulic gradient was in place between S1\_3 and S1\_T5 and between S1\_T5 and S1\_T3. However summer rainfall had been sufficient to keep the topsoil relatively moist and a downward gradient was present between S1\_T1 and S1\_T3. By late September pressure heads in S1\_T3, S1\_T5 and S1\_3 increased quickly until a downward hydraulic gradient persisted throughout the profile by mid November. The recovery in water level in S1\_3 occurred while tensions of several hundred cm were present over much of the upper 1.4 m of the profile. Given the low matrix permeability of the till in saturated conditions it seems unlikely that significant amounts of moisture could be flowing to depth through the till matrix while these tensions existed in the upper profile. The wetting of the profile between the topsoil down to a depth of 1.4 mbgl (S1\_T5) in one month is also problematic if vertical matrix flow is invoked as the flow mechanism. Furthermore, the pressure increase in S1\_3 occurs earlier (taking into account the piezometer lag) and is steeper than that observed in TE32 suggesting that the recovery higher up in the profile cannot simply be due to a rise in the piezometric level of the sandstone.

These assertions need to be tested by modelling. However, the observations strongly suggest the presence of preferential pathways enabling the relatively rapid wetting of the profile.

### **5.2.3 Moisture Content**

#### **5.2.3.1 TDR**

As described in Chapter 4 three TDR access tubes have been installed and monitored at Site 1. During tube installation samples were taken at 10 cm intervals and gravimetric moisture contents calculated using Equation 3.2. Moisture contents by mass were converted to approximate moisture content by volume using Equation 3.7 assuming bulk densities ranging from 1500 kg/m<sup>3</sup> for the topsoil through to 1900 kg/m<sup>3</sup> for the till based on measured values for similar materials taken from cored boreholes at the site. A set of additional gravimetric

samples were taken during the winter from an auger hole located 1 m from S1\_M1. This auger hole was then backfilled with bentonite.

Comparisons between the TDR measurements taken on the days of augering and the corresponding gravimetric values are shown in Figure 5.7. The pattern of the moisture content profiles is reasonably comparable with the exception of the top two samples for the 7/2/05 profile. However it is apparent that the TDR values are consistently higher under wet conditions and lower under dry conditions than the gravimetric samples by as much as 20% by volume. It is noted that lithological variations were found between the two holes taken for gravimetric analysis which is likely to explain the discrepant apparent drying of the profile at 70 cmbgl between 3/9/04 and 7/2/05. However the errors observed are so large that they cannot be accommodated by error in the gravimetric measurement. It is therefore concluded that the TDR may reliably indicate changes in moisture content at Site 1 but that the absolute values should be treated with caution.

The gravimetric moisture content profiles for 3/9/04 and 7/2/05 give an indication of the range of absolute moisture content variation between dry summer and wet winter conditions. It suggests that significant drying of the till of 3 to 8 % by volume occurs to a depth of at least 1.5 mbgl. The low moisture content at 3/9/04 is associated with tensions of several hundred cm as observed by tensiometers S1\_T3 and S1\_T5. The tensiometer data indicate that the profile is saturated at the moisture contents seen on 7/2/05. This suggests that the till has a porosity of approximately 0.3 consistent with the laboratory results presented in Section 3.3.4.3.

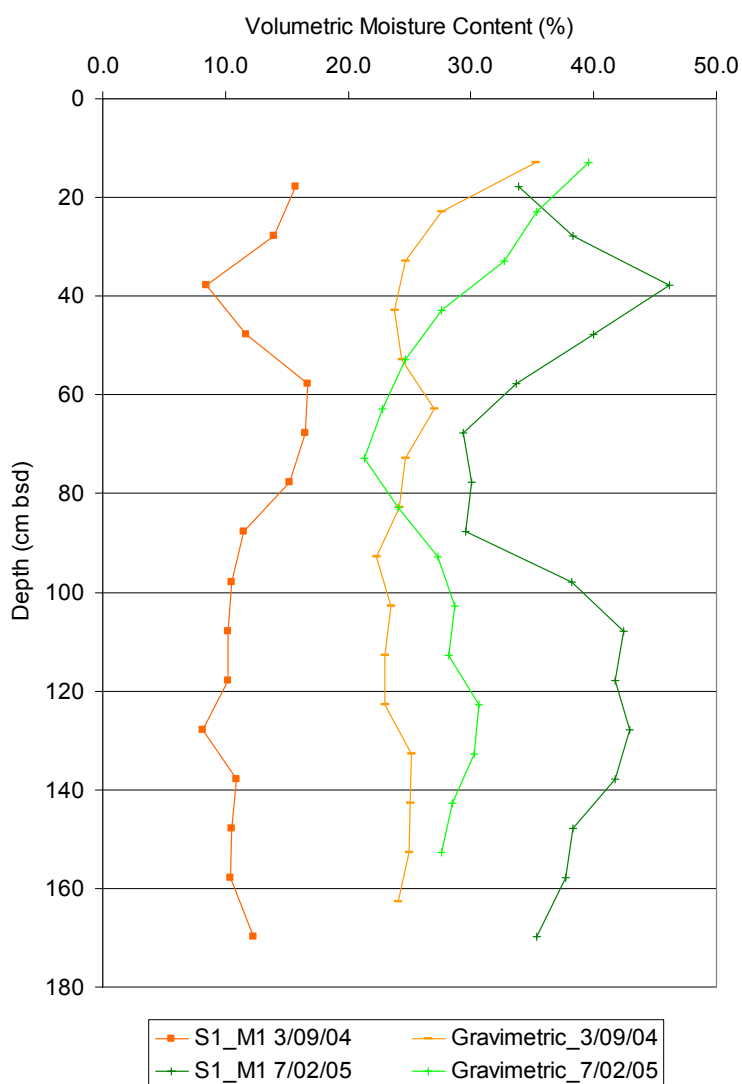


**Figure 5.7** Comparison of TDR and gravimetric moisture contents at Site 1

The first three sets of data for monitoring locations S1\_M2 and S1\_M3 are shown in Figure 5.8. It quickly became apparent that these two TDR tubes were failing to give reliable moisture data due to the creation of preferential flow pathways down the side of the tubes during installation. After the first heavy rainfall since installation the apparent moisture contents rose markedly in a manner inconsistent with the tensiometer data and data from S1\_M1. The first three sets of data for these monitoring locations are shown in Figure 5.8.

Furthermore the tecanat tubing remained loose within the auger holes implying a poor seal with the formation. The data were disregarded and the sampling tubes abandoned.

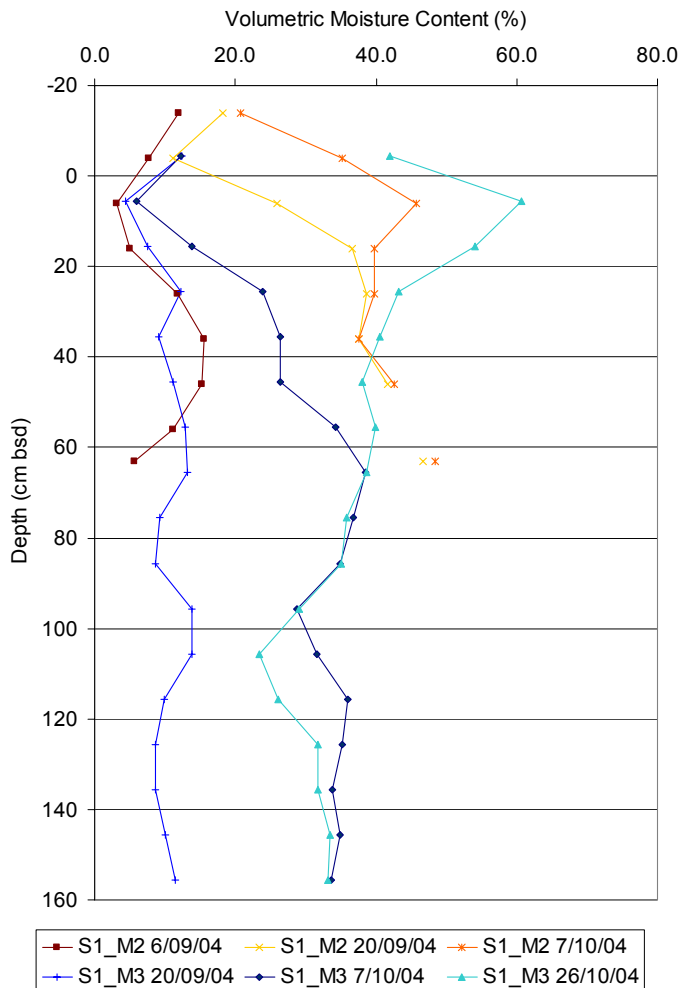


**Figure 5.8** TDR data for S1\_M2 and S1\_M3

Fortunately the data for S1\_M1 located next to the tensiometers seems of reasonable quality with more gradual and realistic changes in moisture content being observed. The tecanat tube could not be turned by hand within its auger hole suggesting a snug fit with the formation. A selected set of approximately monthly moisture content data for the S1\_M1 TDR access tube are shown in Figure 5.9 to illustrate the typical variations seen throughout the year of monitoring.

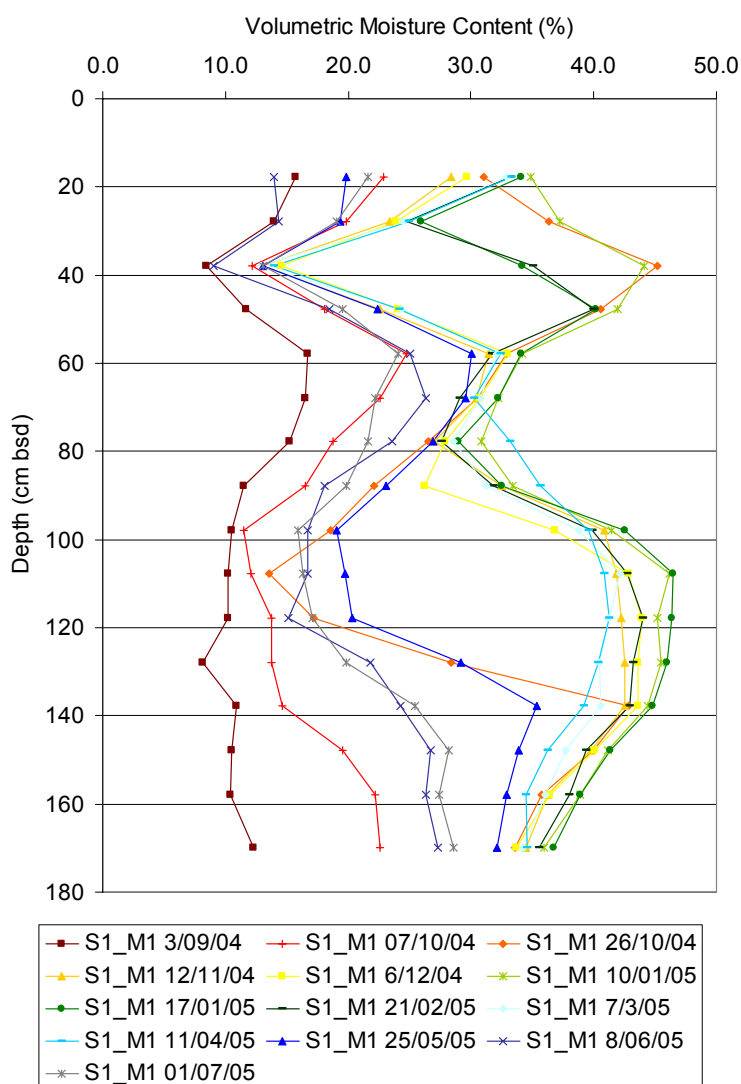


**Figure 5.9** TDR data for S1\_M1

Elevations are shown in cm below site datum (cmbd) to enable direct comparison of water table elevations with the pressure results described above. Variations in the upper 40 cmbd broadly correspond with changes in tension observed in S1\_T1. Highest moisture contents (e.g. 26/10/04, 10/01/05) are seen at times of positive pressure head (implying saturation) with lower moisture contents correlating to times of negative pressure head (tension). Moisture contents in this topsoil zone are more temporally variable than anywhere else in the profile with deeper levels showing a simpler pattern of wetting through the autumn and drying

through the spring. This is consistent with the tensiometer data whereby the deeper tensiometers (S1\_T3 and S1\_T5) remain in a saturated condition between November and May whereas unsaturated conditions come and go at the location of the shallowest tensiometer S1\_T1.

Significant variation was found between the readings taken at the three orientations at each monitored depth. The standard deviation in the readings is plotted against the average moisture content for all the data collected at S1\_M1. The resulting plot is shown in Figure 5.10 showing that deviations of less than three percent are found at higher moisture contents but that a much higher variation in readings is found during drier conditions. This suggests that the wetting and drying of the profile occurs in a non-uniform manner.

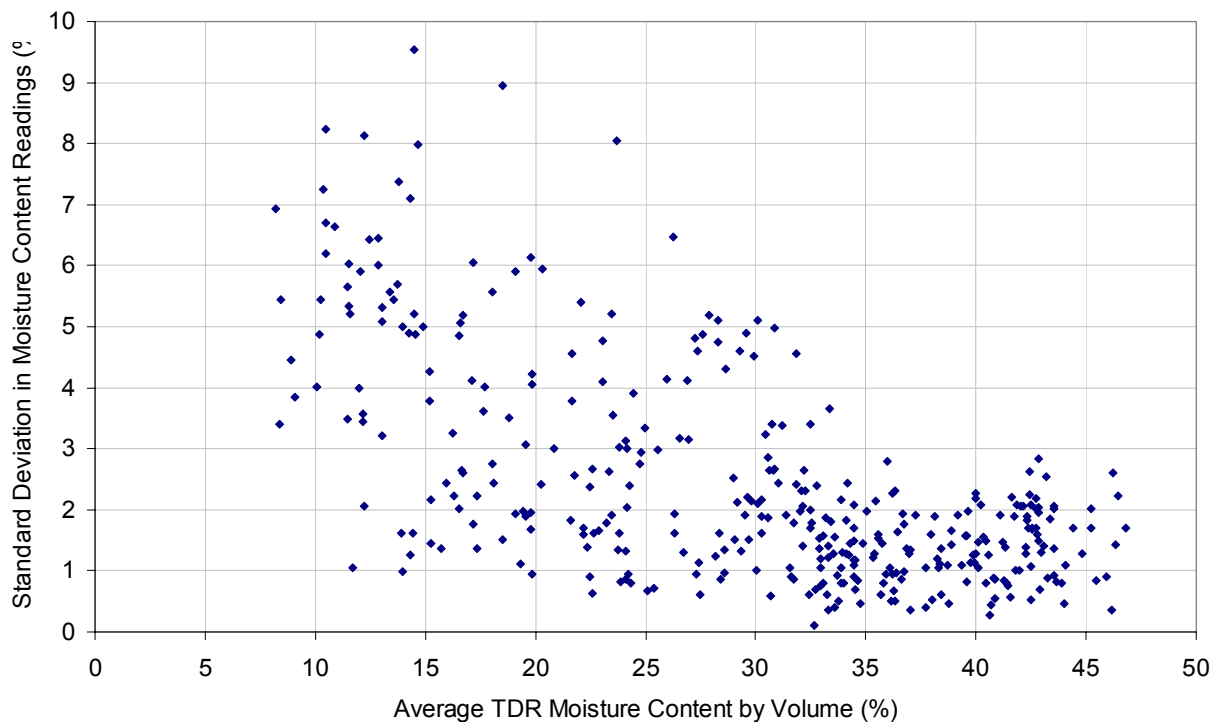


**Figure 5.10** Relationship between average TDR moisture content and standard deviation in the three moisture content readings taken at each depth at different orientations at S1\_M1

### **5.2.3.2 Gravimetric moisture contents from core samples**

At deeper levels the moisture content distribution has been investigated using gravimetric determination from core samples (drilled on 2/6/04) using the methodology described in Section 3.2.4. The results of moisture loss (% by mass) are shown in Figure 5.11. An unquantified error associated with moisture loss during drilling and more particularly during core storage over a period of 10 days is inevitable but was minimised as far as possible. Thus the conclusions from these results are only semi-quantitative. The moisture content profiles of core from the two different boreholes are very similar. The moisture content decreases with depth through the top metre of the profile from around 15% by mass to around 11% by mass. It then gradually increases to around 13% by mass by the time the base of the till is reached at just over 6 mbgl. These moisture levels suggest that the till is close to or at saturation over most of its depth.

### **5.2.4 Infiltrometer Tests**

The results of the two double ring infiltrometer tests carried out at Site 1 are shown in Figure 5.12. The results of both tests plot approximately in the form of an exponential curve with infiltration rate decreasing at a decreasing rate over time. However Test 2 reaches a steady state in less than 30 min whereas in Test 1 the infiltration rate was still decreasing after 2.5 hours. The differences are likely to be due to the degree of compaction the soil has encountered due to agricultural activity as well as any changes in the geology of the upper 0.5 m of the profile at each location. The results suggest that under ponded conditions infiltration rates as high as 0.25 cm/min (3.6 m/d) are possible and that the saturated hydraulic conductivity of the soil may be in the range 0.005 to 0.02 cm/min (0.07 to 0.3 m/d).

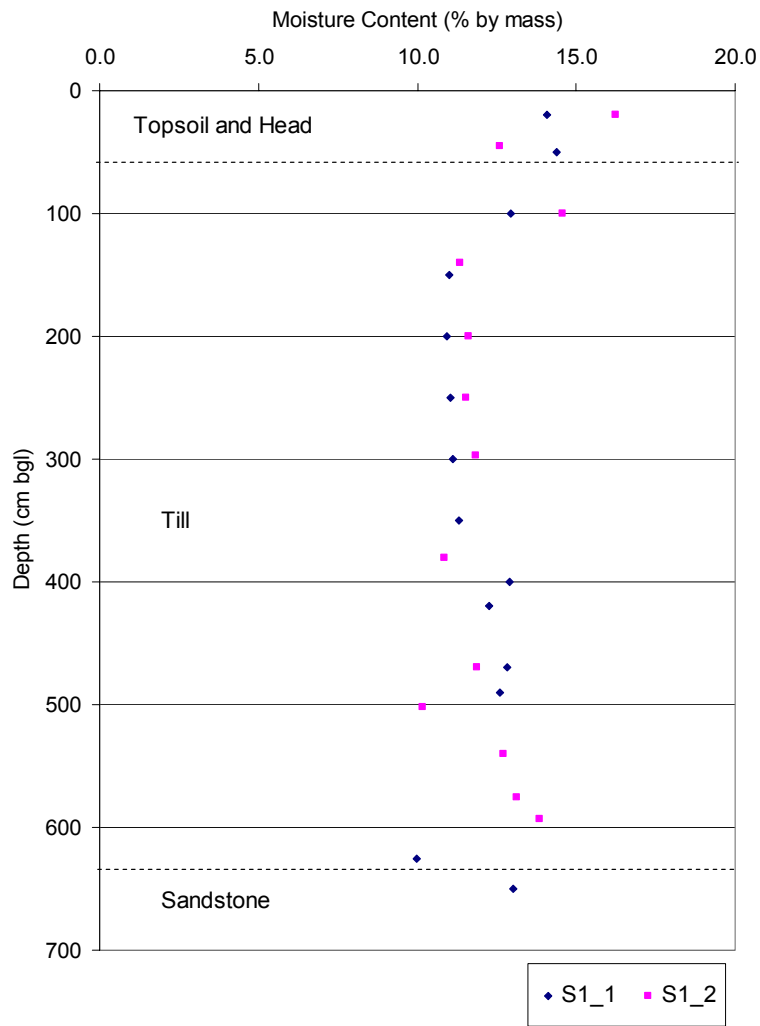


**Figure 5.11** Gravimetric moisture content profile for S1\_1 and S1\_2

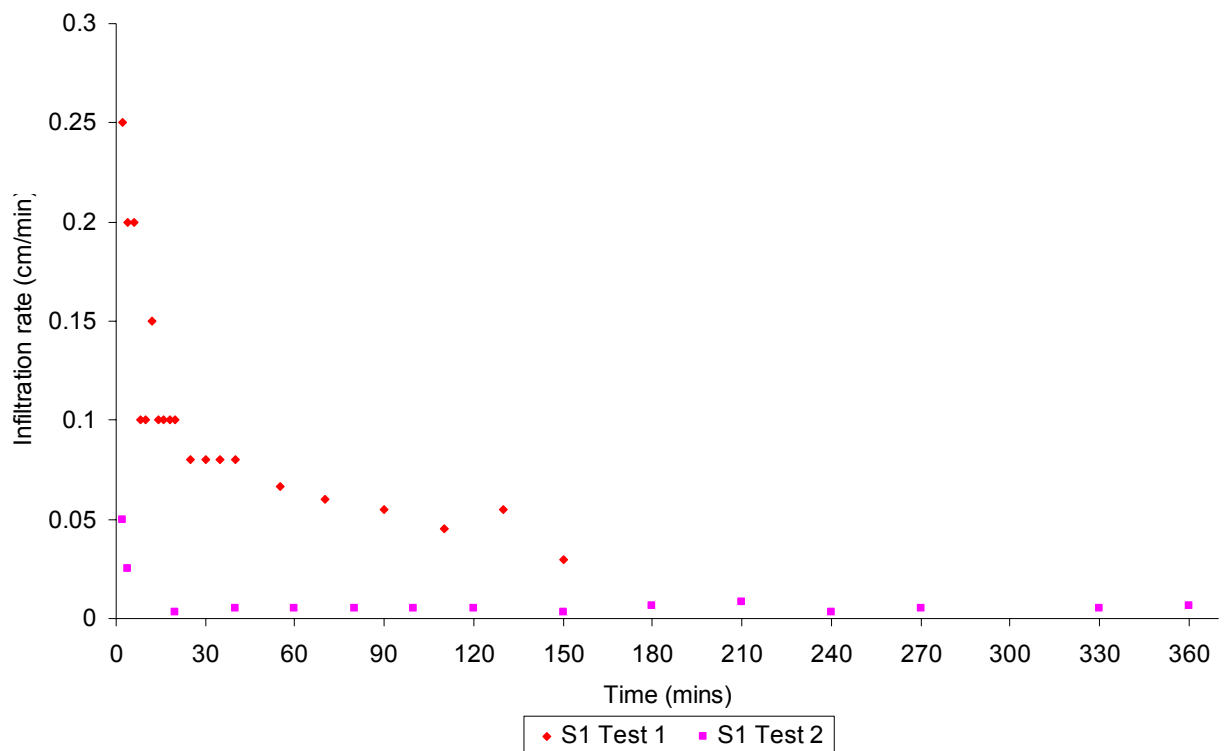


**Figure 5.12** Infiltrimeter tests results for Site 1

### 5.2.5 Piezometer Tests

Piezometer tests were carried out on both piezometers screened within the till at Site 1. The results are plotted in Figures 5.13 and 5.14. Both tests gave good straight line plots with an estimated hydraulic conductivity of  $3 \times 10^{-10}$  m/s and  $2 \times 10^{-7}$  m/s for S1\_3 and S1\_4 respectively. The result for S1\_3 is very close to the median value of till hydraulic conductivity measured in the laboratory presented in Section 3.3.4.3. The result for the test on S1\_4 is three orders of magnitude greater than that for S1\_3 but lies within the range of outlying values measured in the laboratory.

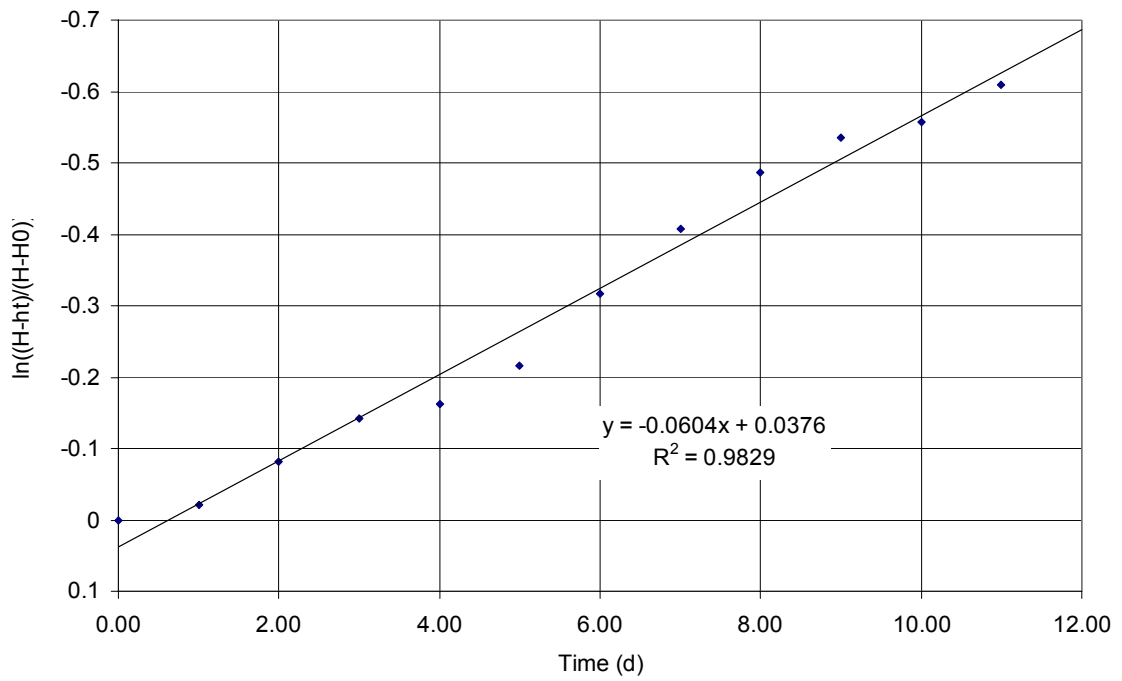


**Figure 5.13** Piezometer falling head test results for S1\_3

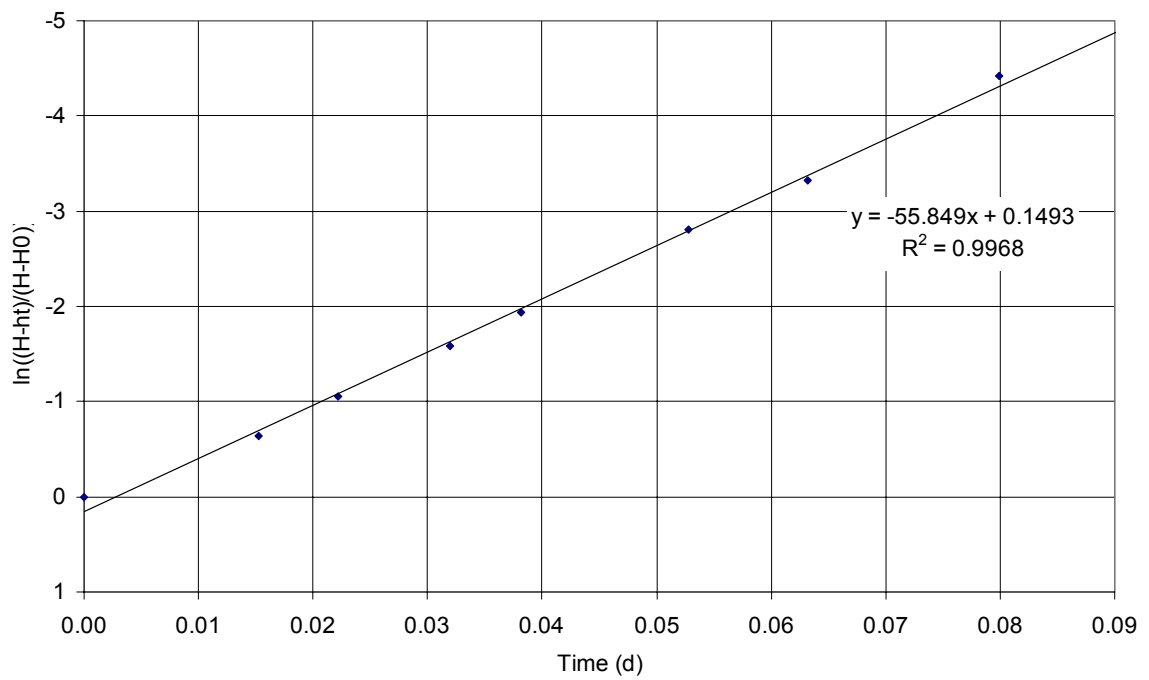


**Figure 5.14** Piezometer falling head test results for S1\_4

### 5.2.6 Tracer Test

The results of tracer concentrations with depth are shown in Figure 5.15. The results show relatively low concentrations of amino G acid throughout the profile with a change in concentration with depth of between 1 and 2 orders of magnitude and a recovered mass of 13, 36 and 8% of the interpolated recovery (calculated from the applied mass per unit area) for auger holes S1H2, S1H3 and S1H4 respectively. The results for amino G acid are thus perhaps less useful than those for fluorescein which show a greater variation and a larger retained mass. The large differences in the results may point to loss of amino G acid due to photochemical decay or non-reversible chemical reactions with the soil. The fluorescein profiles vary across 4 orders of magnitude and have a recovered mass of 129, 501 and 84% of the interpolated recovery for auger holes S1H2, S1H3 and S1H4 respectively. The profiles show an overall decrease of concentration with depth but with slightly elevated concentrations at 50, 80 and 95 cmbgl in the different sampling locations. It is noted that a large proportion of the retained mass is within the upper 10 cm of the profile implying that a significant proportion of the applied tracer has been retained at/near the surface layer to which it was applied. As described in Section 4.4.2.5 the background fluorescence of natural organic material is unlikely to produce a fluorescein-like signature. Thus, the results may suggest preferential redistribution of the tracer along pathways intersected by the auger holes. The presence of tracer at 0.95 mbgl after just 4 months indicates flow velocities far greater than would be expected due to flow through the low permeability till matrix.

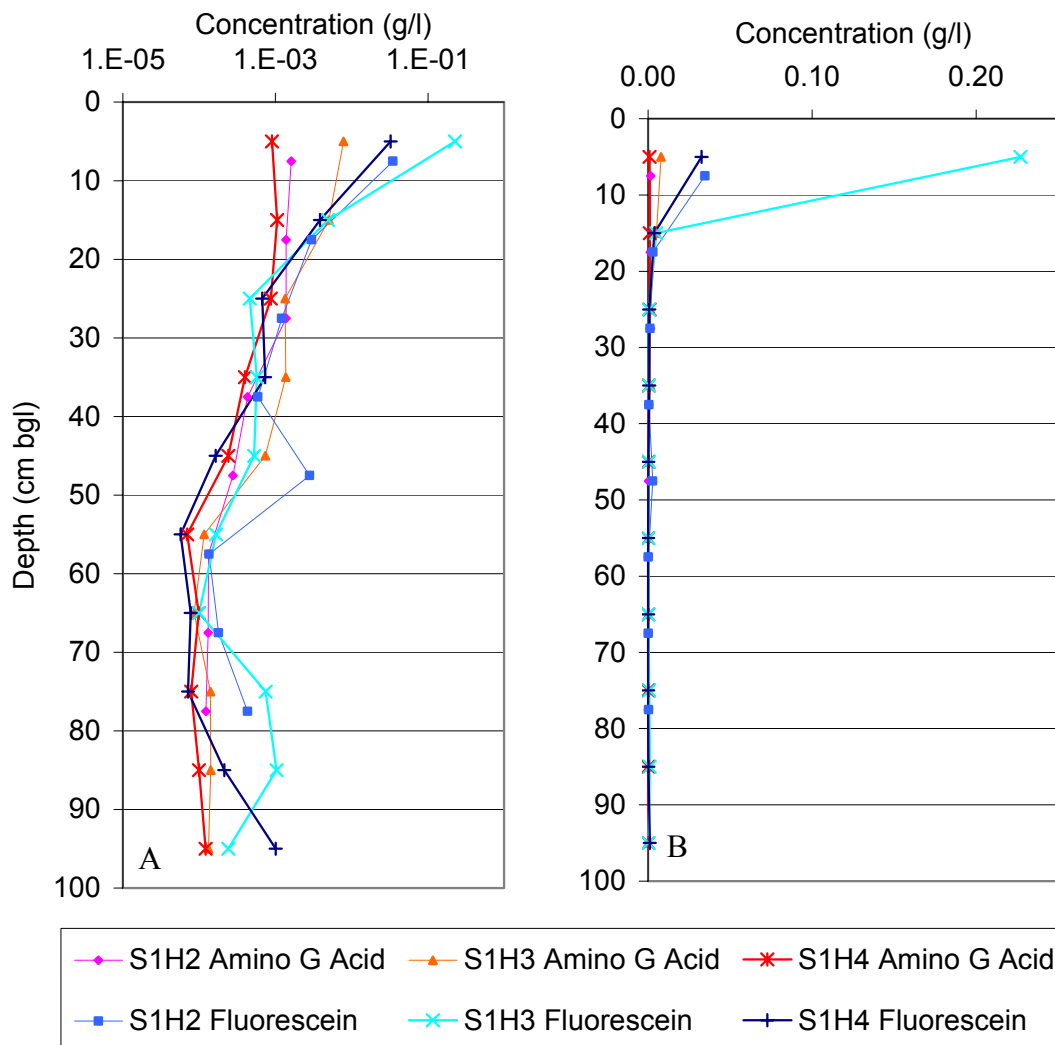


**Figure 5.15** Tracer distributions at Site 1 after 108 days (S1\_H2) and 126 days (S1\_H3 and H4) since tracer application with log (A) and linear (B) scales

## 5.2.7 Hydrochemistry

### 5.2.7.1 Porewater analysis from TE32

When the hole was drilled for the installation of the LOCAR piezometer TE32, U100 samples were taken from which porewater was extracted and analysed. The results of the hydrochemical analysis have been collected from the LOCAR data centre and form the basis of the discussion in this section. Analyses including major, minor and trace constituents are available for six porewater samples from the till and one sample of water from the completed

piezometer (TE32) screened within the sandstone between 7 and 8 mbgl. The ionic balance error ranged from 1 to 5%. A plot of the concentration of major ions, pH and total oxidised nitrogen (TON) versus depth is shown in Figure 5.16. The concentration of  $\text{NO}_3$  has only been reported by LOCAR for the upper 4 samples (a reason was not given with the data received). However, comparing  $\text{NO}_3$  with TON it is clear that  $\text{NO}_3$  dominates the TON concentration for these samples. Since other sources of N are low throughout the profile, and TON is reported for the whole profile, TON can be taken as a reasonable proxy for  $\text{NO}_3$  in this case.

The samples fall into three broad groups correlating with the geological context. The discussion of the hydrochemistry has been restricted to information pertinent to understanding the hydraulics of the system:

- i. The two shallow samples taken from the soil zone are characterised by lower pH, lower concentrations of Ca, Mg, Na, Cl,  $\text{SO}_4$ ,  $\text{HCO}_3$  and  $\text{NO}_3$ , and higher concentrations of Fe, P and  $\text{NH}_4\text{-N}$ . This suggests that the soil has been leached lowering the levels of soluble salts and carbonates. The low nitrate levels are conspicuous for an agricultural setting even given the fact that this field had been under pasture for the three years prior to drilling. This, along with the fact that  $\text{NH}_4\text{-N}$  is slightly elevated in the shallowest sample, may suggest that nitrate reduction has been occurring. However it is possible that the  $\text{NH}_4\text{-N}$  may come from a direct source rather than being derived insitu. The elevated concentration of Fe points to reducing conditions which in turn is consistent with the occurrence of nitrate reduction. It is uncertain what the source of the elevated P is but it is likely to be related to (agricultural) organic inputs.

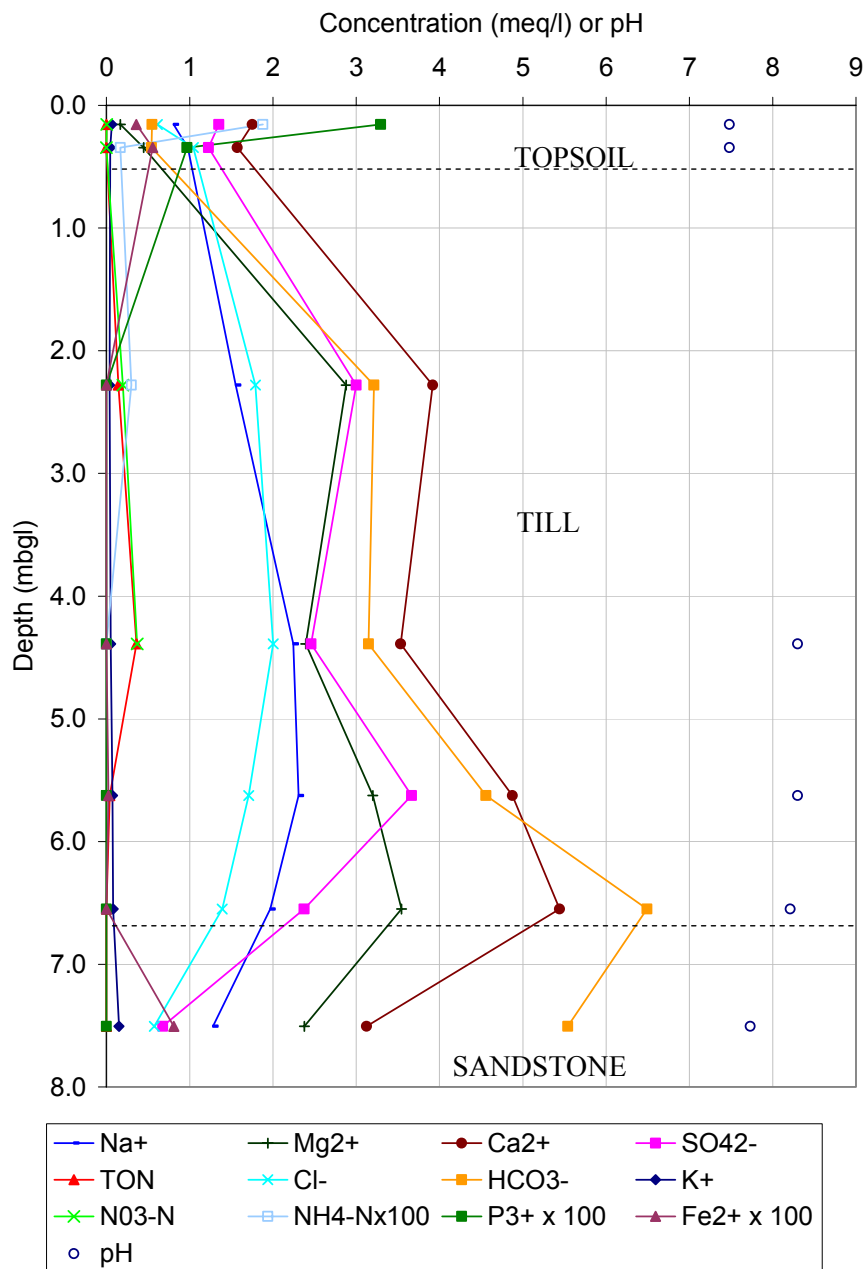


**Figure 5.16** Major ion, pH and TON profile for TE32

- ii. The second group of samples all lie within the till and are characterised by higher pH, higher concentrations of Ca, Mg, Na, Cl, SO<sub>4</sub>, HCO<sub>3</sub> and NO<sub>3</sub>, and lower concentrations of Fe and P. The positive correlation between elevated Ca and SO<sub>4</sub> has been reported for other tills in Shropshire and may be associated with gypsum (Wealthall *et al.* 1997) possibly due to incorporated Mercia Mudstone material within

the till matrix. However it is possible that the apparent correlation of Ca and SO<sub>4</sub> may be due to a combination of pyrite oxidation and carbonate dissolution. Furthermore, the formation SO<sub>4</sub> by oxidation of pyrite during porewater extraction cannot be discounted as no information is available on the sample extraction method employed. Elevated Cl may be due to dissolution of halite derived from the Mercia Mudstone. The NO<sub>3</sub> concentrations are at least one order of magnitude higher than would be expected for an unfertilised field but since the landuse was arable until three years prior to drilling the presence of a nitrate front within the profile is to be expected. Assuming that significantly elevated nitrate is of a modern agricultural origin, the fact that it is found at a depth of 4.4 m suggests a flow rate much greater than predicted using hydraulic properties measured on core-scale samples in the laboratory. Under a unit hydraulic gradient assuming a porosity of 0.3 and a vertical hydraulic conductivity of  $1 \times 10^{-10}$  m/s the travel time for a distance of 4 m is around 400 yr. This suggests that a mechanism exists for preferential flow through the till and that the laboratory derived value of hydraulic conductivity may not be applicable at the site scale. The lower levels of P may be due to sorption down the profile.

- iii. The third group consists of just one sample derived from the Permo-Triassic sandstone and is characterised by lower pH, lower concentrations of Ca, Mg, Na, Cl, SO<sub>4</sub> and NO<sub>3</sub>, and higher concentrations of Fe. Given the observed drop in concentrations in Cl and SO<sub>4</sub>, if elevated levels of Cl and SO<sub>4</sub> in the till samples are due to the geochemistry of the till itself rather than an external source, it is unlikely that the water in the top of the sandstone is solely derived from vertical matrix flow through the till. This leads to two possible conclusions which are not mutually exclusive. Firstly, flow through the till may be predominantly through preferential pathways and

have groundwater chemistry that is distinct from the till matrix porewater sampled during drilling. Secondly the groundwater flow through the till may be so low that water sampled by the piezometer screened 1.5 m below the base of the till is dominated by groundwater flowing from unconfined recharge areas several hundred metres up groundwater gradient.

### 5.2.7.2 CFC analysis

The CFC results for two samples taken from TE32 on 3/8/04 are shown in Table 5.1. The results are expressed in three ways:

- i. As absolute concentrations of CFC-12 and CFC-11 (pmol/L)
- ii. As a fraction of modern water (Frac Mod). This is the fraction of 2004 rainwater that would need to be mixed with distilled water to give the measured concentration of CFC.
- iii. As a recharge year (Rech Yr). Assuming no mixing has occurred between waters of different ages this is the year for which atmospheric concentrations of CFC match the measured concentration.

Sample	CFC-12	CFC-11	CFC-12	CFC-11	CFC-12	CFC-11
	pmol/L	pmol/L	Frac Mod	Frac Mod	Rech Yr	Rech Yr
TE32 (1)	0.32	0.31	0.11	0.06	1964	1962
TE32 (2)	0.33	0.36	0.11	0.07	1964	1962

**Table 5.1** CFC results for TE32 at Site 1

The results are relatively consistent both across samples and between CFC-11 and CFC-12. They suggest that all the water found at this location is less than 40 years old or that the sample is a mix of water both younger and older than 40 years old. As discussed in Section 4.4.3.2, CFCs may be subject to degradation under anaerobic conditions (Goode *et al.* 1997). Such conditions may persist in at least the upper part of the till as described in Section 5.2.7.1. This effect would act to make the groundwater appear older and as a result 40 years may be an overestimate for the maximum age of the groundwater sampled from TE32.

Given a regional hydraulic gradient in the sandstone of around 0.004 (based on contours presented in Figure 2.5), a kinematic porosity of 0.2 and a bulk hydraulic conductivity of 2.5 m/d (see Section 2.6.2), the groundwater velocity in the sandstone is around 0.05 m/d. Based on the published 1:50 k drift map, outcrop sandstone is reached around 1.3 km up hydraulic gradient from the site. At this groundwater velocity water recharging the outcrop sandstone would take around 70 years to reach Site 1. Unless the hydraulic properties of the sandstone are significantly different to the assumed values, the calculation suggests that a component of younger water is present in the samples taken from TE32 which must have recharged the sandstone through the overlying till. This then suggests a travel time of less than 40 years for recharge through the till to reach the sandstone. This equates to a minimum bulk permeability of approximately  $1 \times 10^{-9}$  m/s based on a porosity of 0.3 and assuming vertical flow under a unit hydraulic gradient. Since the median vertical hydraulic conductivity of the till matrix is 1 order of magnitude lower than this, these rough calculations are consistent with the hypothesis that preferential flow pathways are present within the till. However, the uncertainty in the parameters used is considerable and this evidence alone is not sufficient to reject alternative explanations. For instance, a more permeable till may exist up

hydraulic gradient from the site closer than the nearest sandstone outcrop, but was not encountered during the investigations described in Chapter 3.

### **5.2.7.3 Tritium analysis**

Two samples of core from S1\_2 taken from 5.3 to 5.6 mbgl and 5.6 to 5.9 mbgl were sent for tritium analysis and were found to have tritium activities of  $9.5 \pm 0.5$  and  $9.0 \pm 0.5$  T.U. respectively. These are tritium activities similar to that found in present day rainfall. Since such levels of tritium have only been present in the atmosphere since the 1960s the results again suggest that, using the same logic as described above, preferential flow pathways are likely to exist enabling water to move through the till at rates greater than would be predicted on the basis of the matrix permeability. The measured values could represent very recent recharge that has quickly reached this depth in the profile. However since tritium has a half life of around 12.3 years it could represent older water originally with a higher tritium activity. If preferential flow pathways do exist then it could be part of a diffusional front some distance away from such a feature. Without further data from other depths and lateral locations it is impossible to say which of these hypotheses is correct.

### **5.2.8 ERT**

Inverted ERT images for approximately monthly intervals from July 2004 to June 2005 are shown in Figure 5.17 for survey line 1R for which the most complete record is available. Difference plots between the inversion for each time interval and the inversion for 21/07/04 are shown in Figure 5.18 (i.e. resistivity on a particular date minus resistivity on 21/07/04). Plots for survey line 1B are included in Appendix 6 but have not been shown here as they show very similar features to line 1R.

A relatively high resistivity layer of variable thickness is present at the surface of the profile. It persists throughout the year and during the wettest times has a resistivity of around

60 to 70 ohm-m consistent with the lithology of the topsoil and head deposits observed in borehole cores. This layer is underlain by a lower resistivity material in the range 20 to 30 ohm-m to a depth of around 3.5 mbgl. This is consistent with the resistivity of moist to saturated till (Russell and Barker 2004). The inversions imply that the resistivity of the till increases in the lower 1 m of the model up to as much as 60 ohm-m. There is no lithological evidence for this from borehole core material and it is therefore likely that this effect is an artefact of the inversion process.

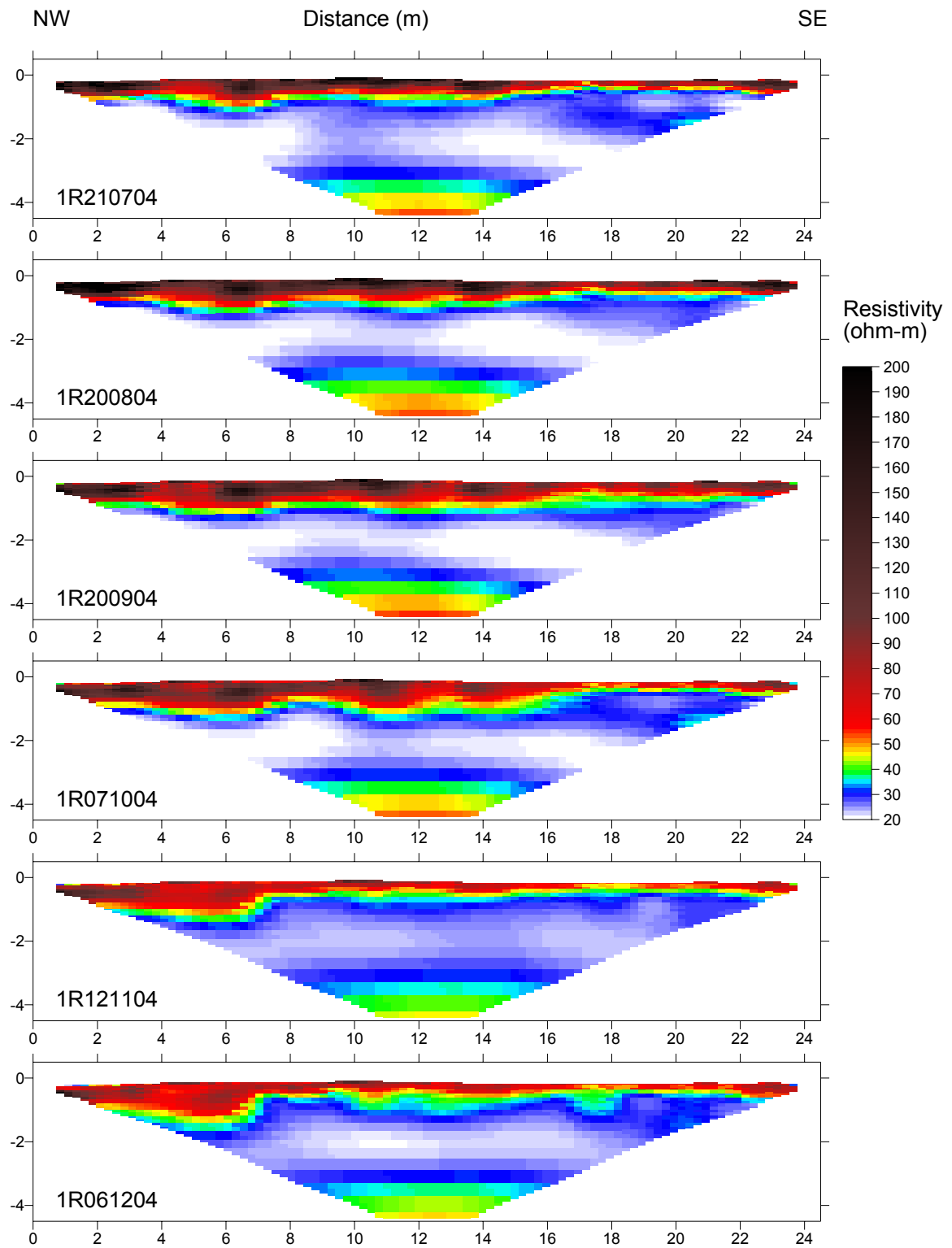


**Figure 5.17a** ERT inversions for Site 1 survey line 1R

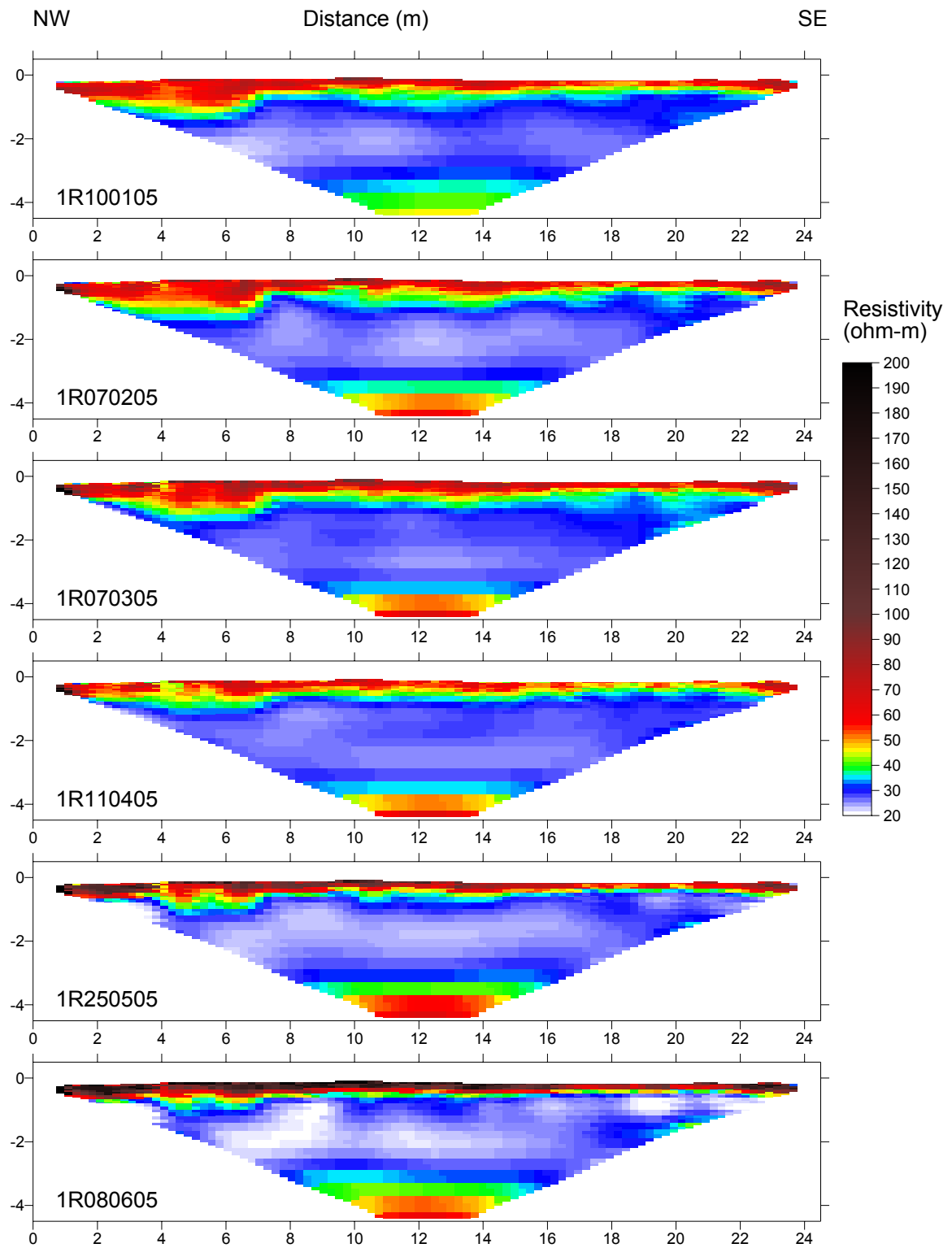


**Figure 5.17b** ERT inversions for Site 1 survey line 1R

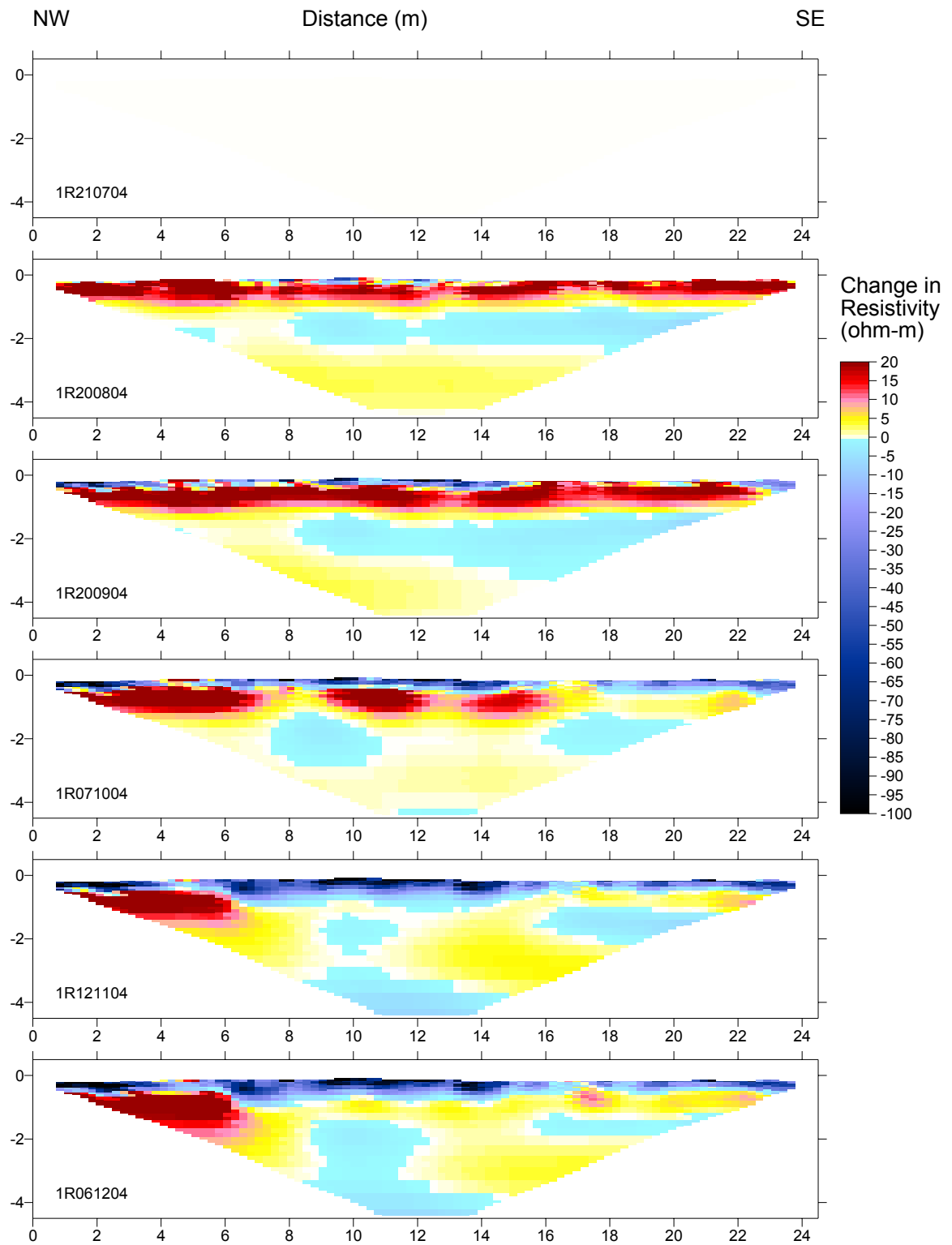


**Figure 5.18a** ERT difference from 21/07/04 for Site 1 survey line 1R (i.e. resistivity on a particular date minus resistivity on 21/07/04)

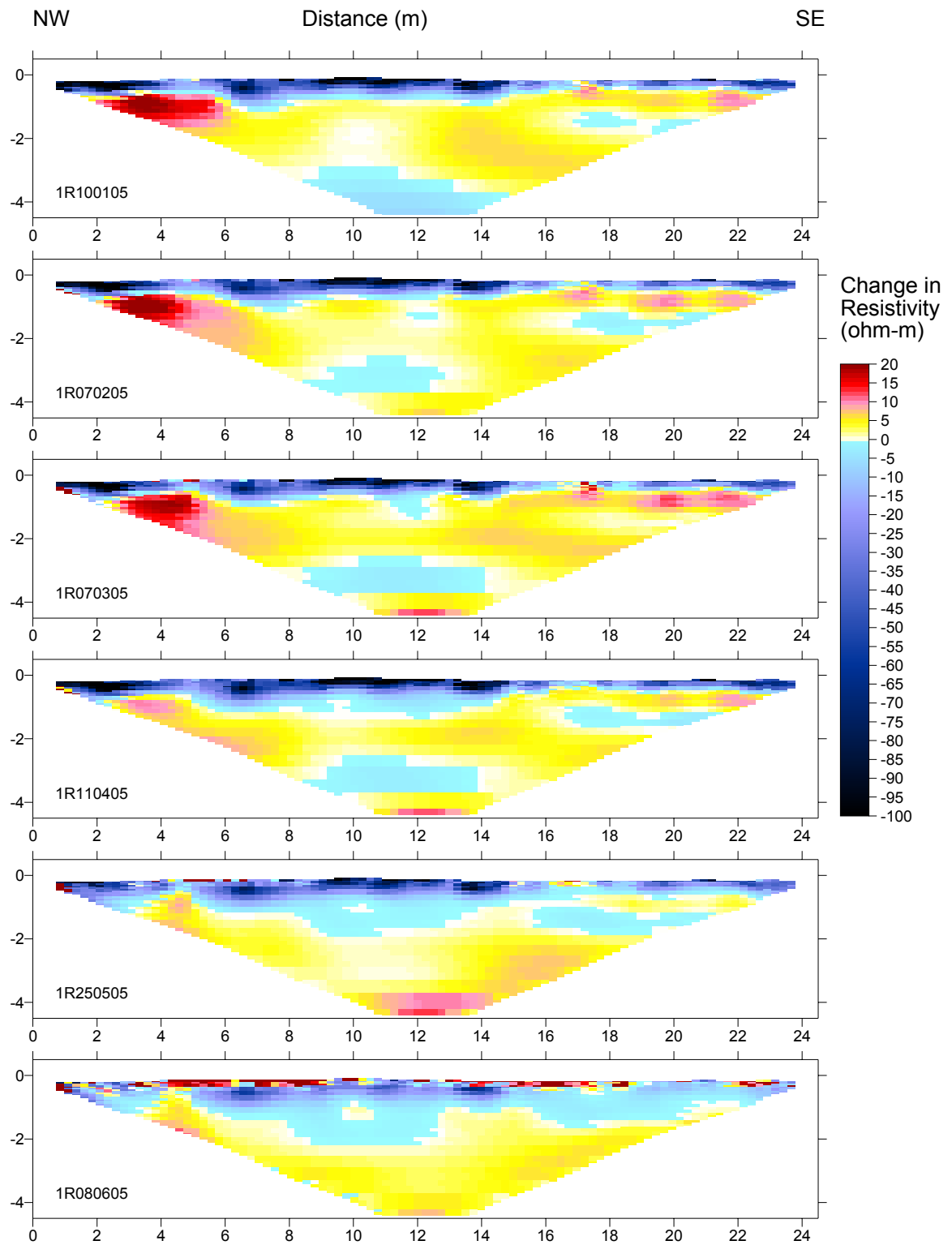


**Figure 5.18b** ERT difference from 21/07/04 for Site 1 survey line 1R (i.e. resistivity on a particular date minus resistivity on 21/07/04)

Based on recent research at the University of Birmingham carried out concurrently with the research for this thesis, a relationship between moisture content and resistivity at a constant temperature has been experimentally defined for a sample of till augered from a field adjacent to Site 1. The results are shown in Figure 5.19 copied with permission from Russell and Barker (2005).

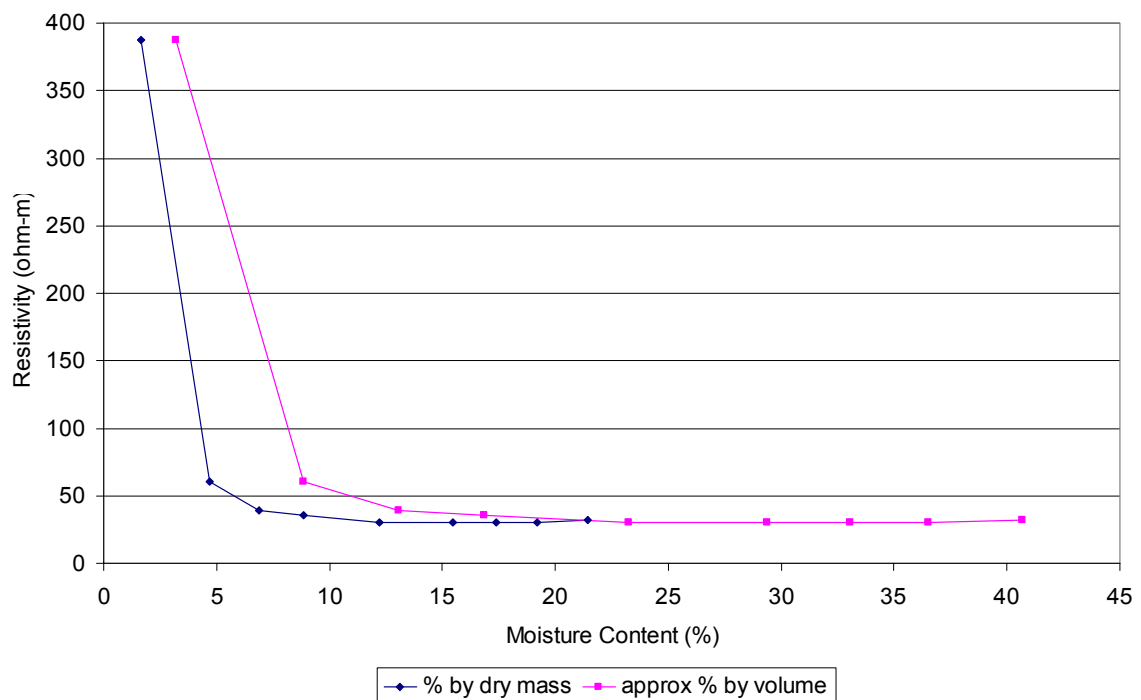


**Figure 5.19** Relationship between moisture content and resistivity for a sample of till taken from an adjacent field to Site 1 (from Russell and Barker (2005))

The moisture content by dry mass has been plotted alongside an approximate moisture content by volume based on a till dry bulk density of 1900 kg/m<sup>3</sup>. The results suggest that no significant change in resistivity occurs in the till sample until moisture contents fall to very low values below around 10% by volume. Moisture contents this low are unlikely to be observed in the field under natural conditions except perhaps in the shallow root zone, although the required tension in this range of moisture content is likely to be above the wilting

point of many plants (Feddes *et al.* 1978; Khanzode *et al.* 2002). It may therefore be impossible to use the ERT method to assess subtle soil moisture changes within the till. However, larger moisture content changes in the topsoil and upper part of the till due to evapotranspiration and infiltration may be reflected in resistivity changes to some extent.

Russell and Barker (2005) also defined the relationship between temperature and resistivity over the range 7 to 28°C for a sample of till from the field adjacent to Site 1 held at a constant moisture content. They found that the temperature increase in resistivity was linear over the measured range and of the order of 1.6 ohm-m per 1°C decrease in temperature. Shallow soil temperatures measured by the thermocouple attached to tensiometer S1\_T1 (thermocouple tip at 23 cmbgl) are shown in Figure 5.20.

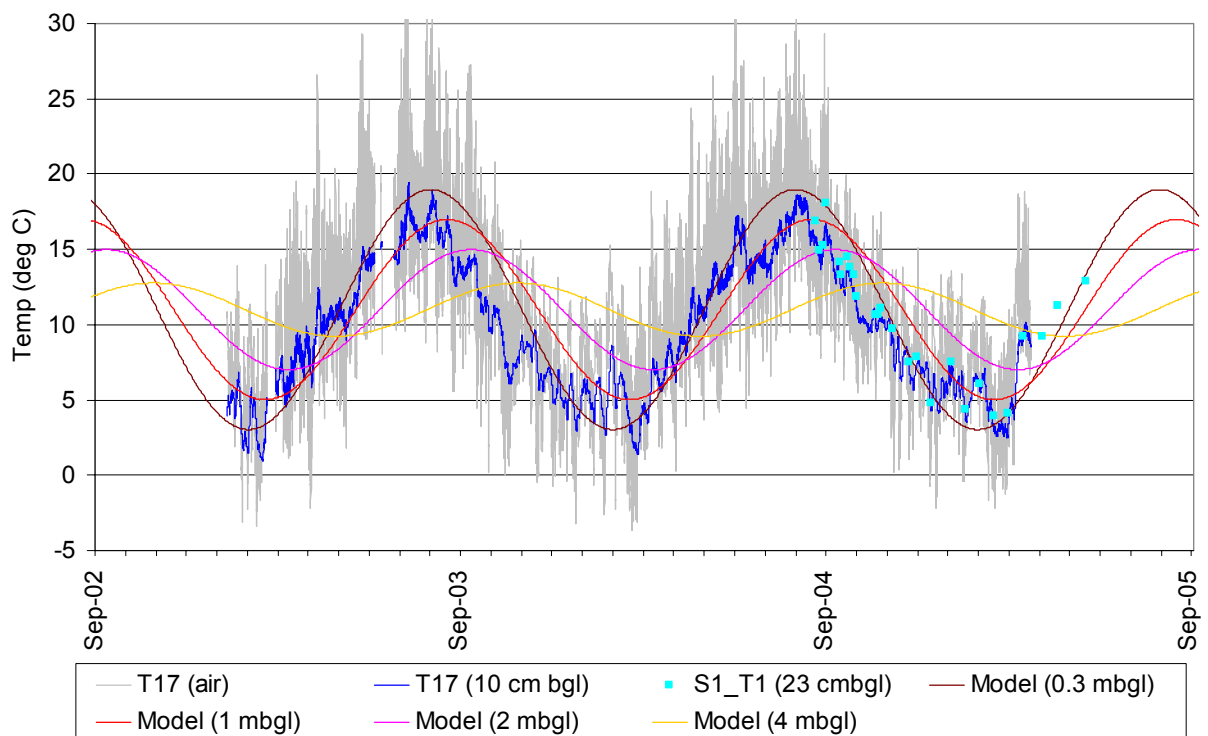


**Figure 5.20** Observed and modelled air and ground temperatures at Site 1 and T17 Oakley Folly

Also shown are soil temperatures monitored at LOCAR installation T17 at Oakley Folly approximately 16 km northwest of Site 1. It is clear that the high resolution shallow ground temperature data from T17 are strongly correlated to data from the S1\_T1 thermocouple. Hence the T17 record for which there is 2 complete years of data can be used to extrapolate backwards the likely soil temperatures at Site 1. Ignoring shorter timescale variations Equation 4.3 has been used to approximate the seasonal trend of ground temperatures using the values  $\kappa = 0.05 \text{ m}^2/\text{d}$ ,  $\tau = 365 \text{ d}$ ,  $T_a = 11^\circ\text{C}$  and  $A_0 = 9^\circ\text{C}$ . The results at depths of 0.3, 1, 2 and 4 mbgl are shown in Figure 5.20. The fit with the S1\_T1 temperature data is reasonable and the expected decrease in amplitude and increase in time lag at greater depths is apparent.

From Figures 5.17 and 5.18 it is notable that during the drier times of year between June and September the resistivity of the upper part of the profile increases significantly to over 200 ohm-m and steadily thickens from around 0.5 m to 1.0 m. Based on Figure 5.20 progressive temperature increase is to be expected in the upper 1 m during this time which would act to decrease the resistivity. Hence it is likely that the resistivity increases observed imply progressive drying of the topsoil and the upper part of the till profile during the summer months. This indicates that the relationship between moisture content and till resistivity shown in Figure 5.19 is not applicable for the shallow weathered/soily till zone which appears to show variation in resistivity over a larger range of moisture contents.

During the autumn and winter the resistivity of the upper layer gradually reduces. Again this is against the trend of increasing resistivity due to progressive decrease in ground temperature and is therefore likely to be as a result of increasing moisture content. It is interesting to note that it takes significantly longer for resistivities in the most north-westerly 6 m of the survey

to increase between 0.5 and 1.0 mbgl than for the rest of the line. This may be due to the interception of rainfall due to over-hanging vegetation in this part of the site, increased drying due to roots of the nearby hedgerow and the compaction of this area which is frequently driven across by agricultural machinery for access to the rest of the field. These factors may reduce the amount of infiltration in this location giving the effect seen in the resistivity profiles.

At around 2 m depth there is a broad increase in resistivity of 5 to 10 ohm-m between September and March which then decreases again into the summer. The till is saturated throughout the year at this depth so any changes in resistivity cannot be attributed to changes in moisture content. The modelled change in ground temperature between September and March is around 7.5 °C as shown in Figure 5.20. Coupled with the results of Russell and Barker (2005), the expected change in resistivity for this temperature change is around 12 ohm-m, a little higher than the observed changes. This may simply be due to heterogeneity in the till or may possibly suggest that the relationship between temperature and till resistivity is scale dependent and that the laboratory values are not applicable at the site scale. However it may be that artefacts created during the process of resistivity inversion (as shown in Section 4.3.6.3) are masking the true temperature effects at depth.

In summary, the ERT results have indicated a pattern of drying and wetting of the upper 0.5 to 1 m broadly consistent with the timing of moisture content and suction changes observed by TDR and tensiometer data. Some spatial variability across the site has also been observed associated with compacted soil and proximity to the vegetated field boundary. Variations in the saturated deeper profile are broadly consistent with predicted temperature effects.

### 5.2.9 Test Pit

Many of the data sets so far presented for Site 1 suggest the possibility that flow through the till may be enhanced by the presence of more permeable pathways allowing preferential flow to bypass regions of the till matrix. This result is consistent with the literature described in Chapter 1. For this reason it was decided that a test pit should be dug to look for the presence of possible preferential features.

To avoid incurring high costs and complicated health and safety issues, and to be able to create a practical excavation within the confines of the land to which access had been granted, it was decided that the dimensions of the pit should not exceed approximately 2x2x2 m. A 1.5 tonne digger was hired to dig the pit and a slightly undersized timber frame was built to sit inside it to provide support in case of collapse. A wooden cover was made to leave over the pit to prevent any danger to people or animals while the pit was unmanned.

Once completed on 13/7/05, three sides of the pit were worked by hand with a spade and trowel to remove the smeared surface created by the digger. Since it was vertical features that were primarily expected to be found, material was removed using the tools with a horizontal motion in order to avoid creating artificial vertical features. Since the digger was working at the limit of its reach the fourth side became very uneven and thus required too much work by hand to create a workable surface.

Once prepared, a 3 x 3 60 cm grid was constructed on each of the three surfaces (to the north, south and west of the pit) using string and small wooden stakes. Then each face was photographed digitally and the main features were sketched on a scale drawing. Sketches of the three faces are shown in Figures 5.21 to 5.23. Significant features 1 to 6 are indicated and corresponding photographs of each feature are shown in Figures 5.24 to 5.28.

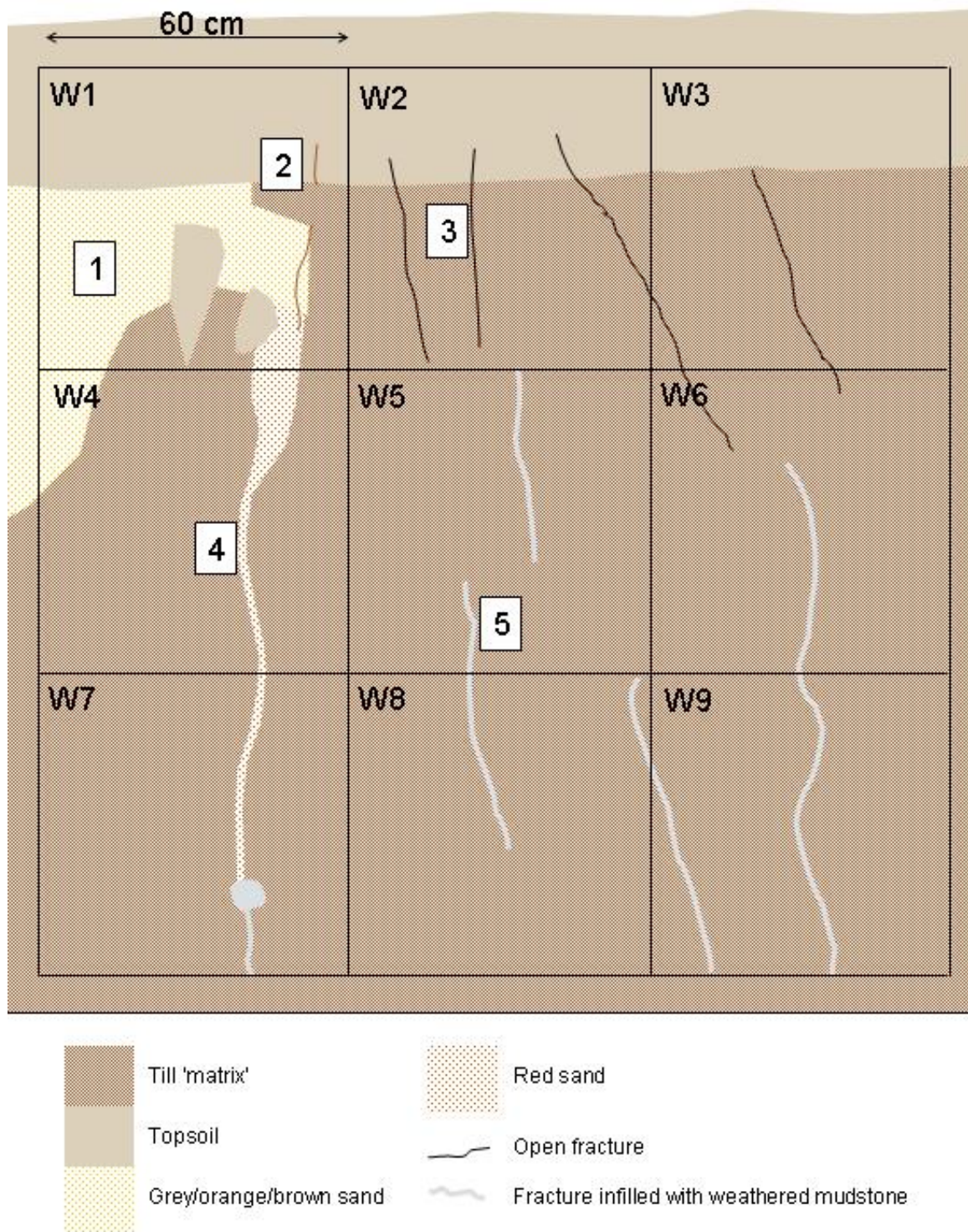


**Figure 5.21** Sketch of west face of test pit (vertical scale = horizontal scale)

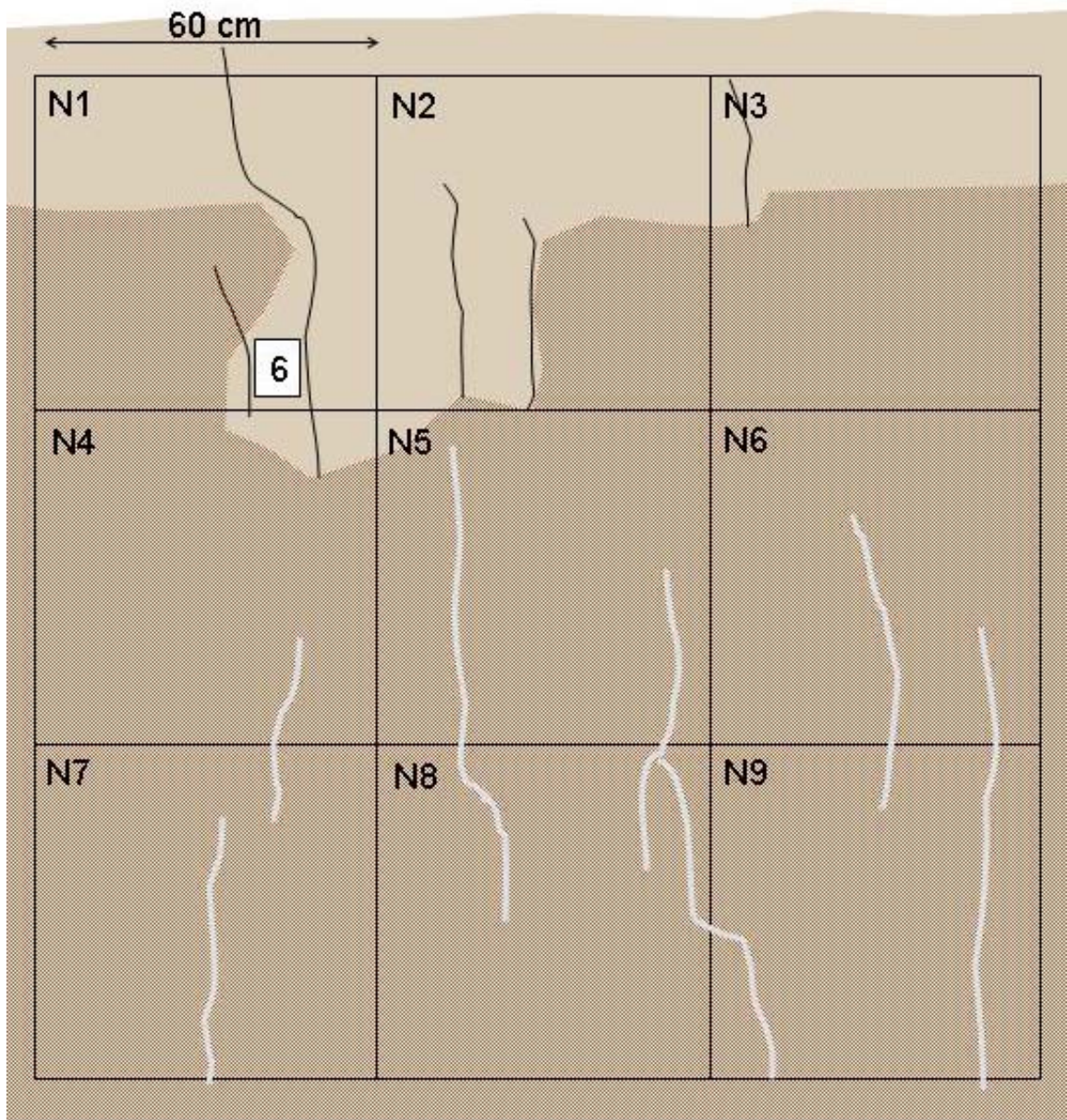


**Figure 5.22** Sketch of north face of test pit (key as for Figure 5.21, vertical scale = horizontal scale)

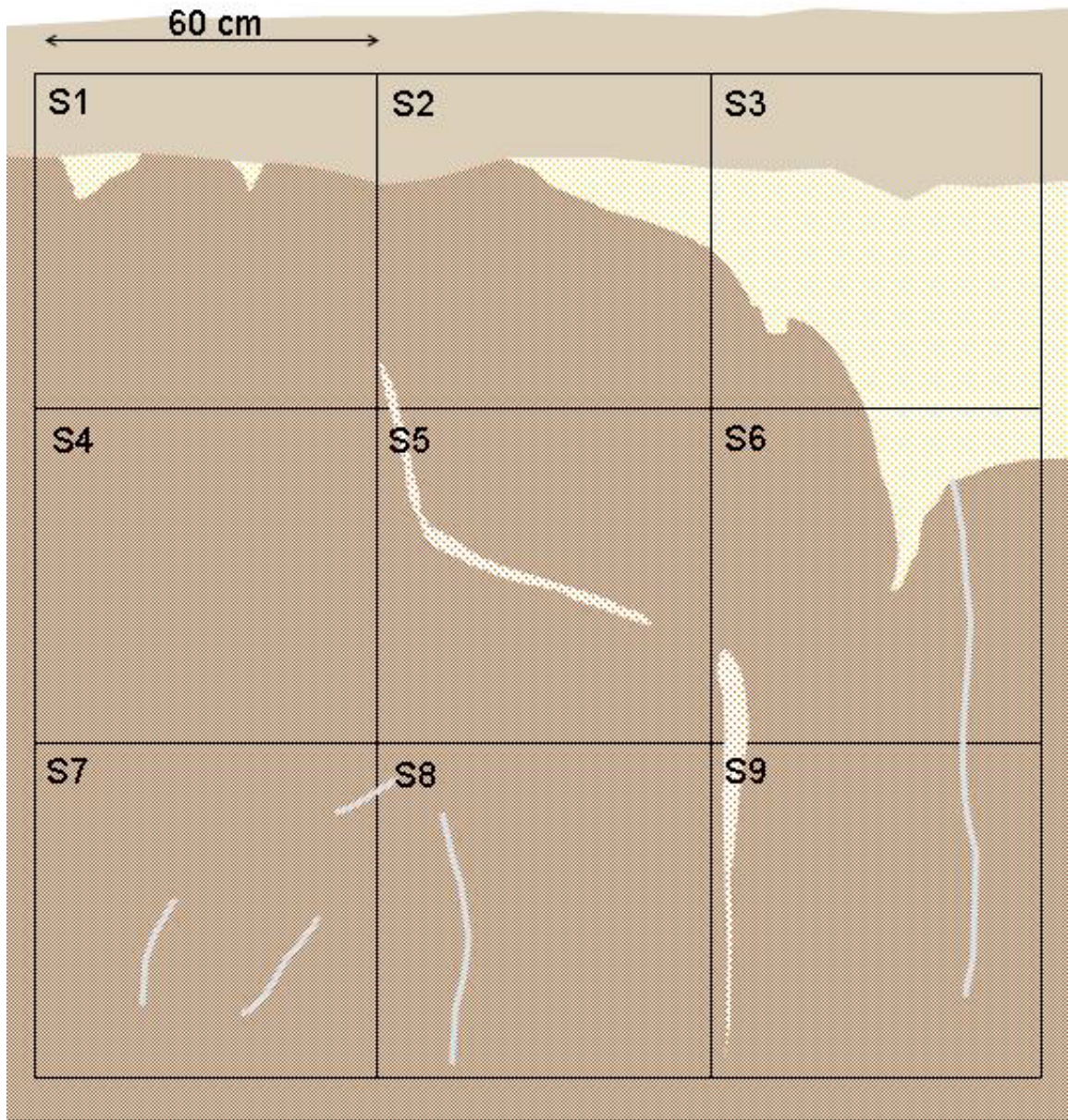


**Figure 5.23** Sketch of south face of test pit (key as for Figure 5.21, vertical scale = horizontal scale)

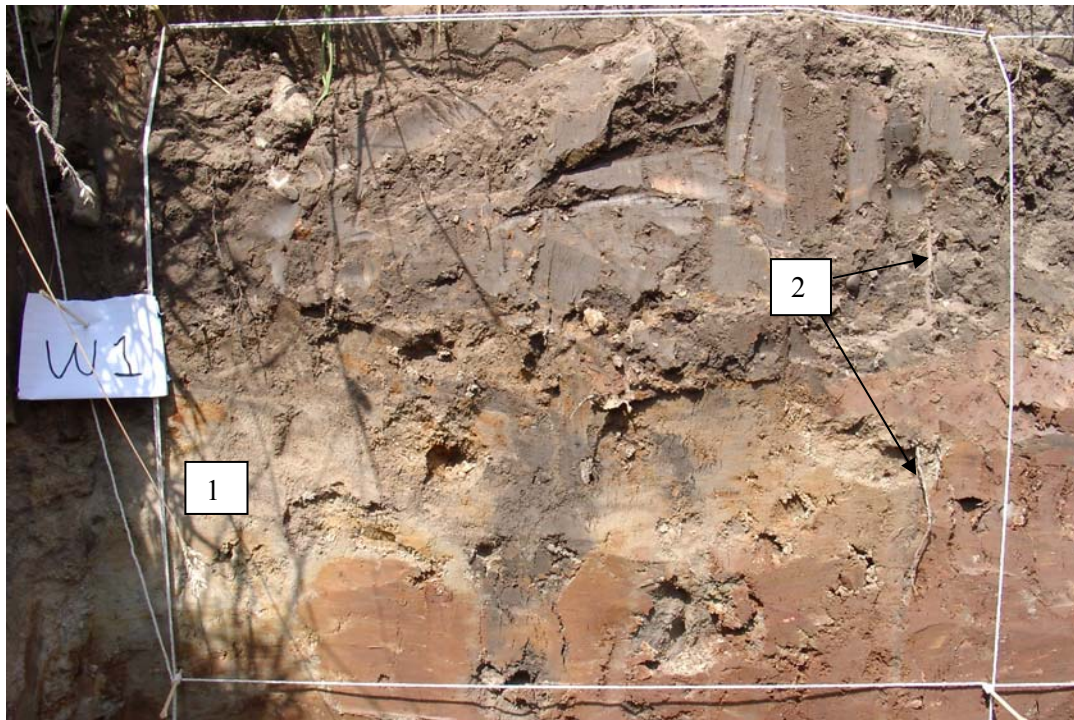


**Figure 5.24** Photograph of features 1 and 2 shown in Figure 5.21

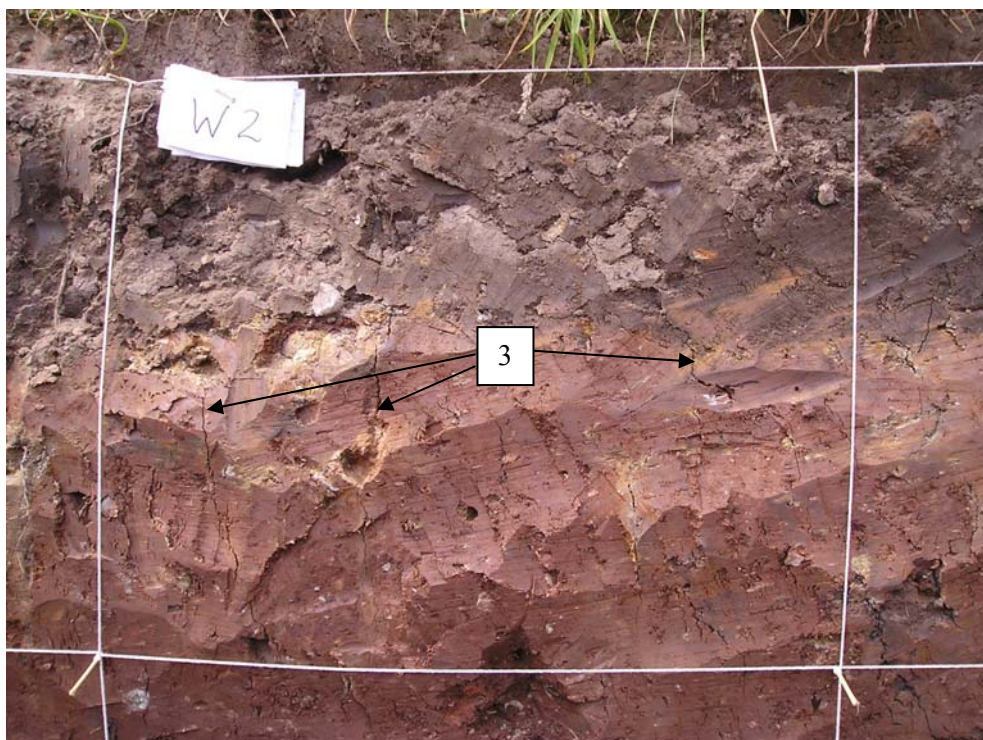


**Figure 5.25** Photograph of feature 3 shown in Figure 5.21

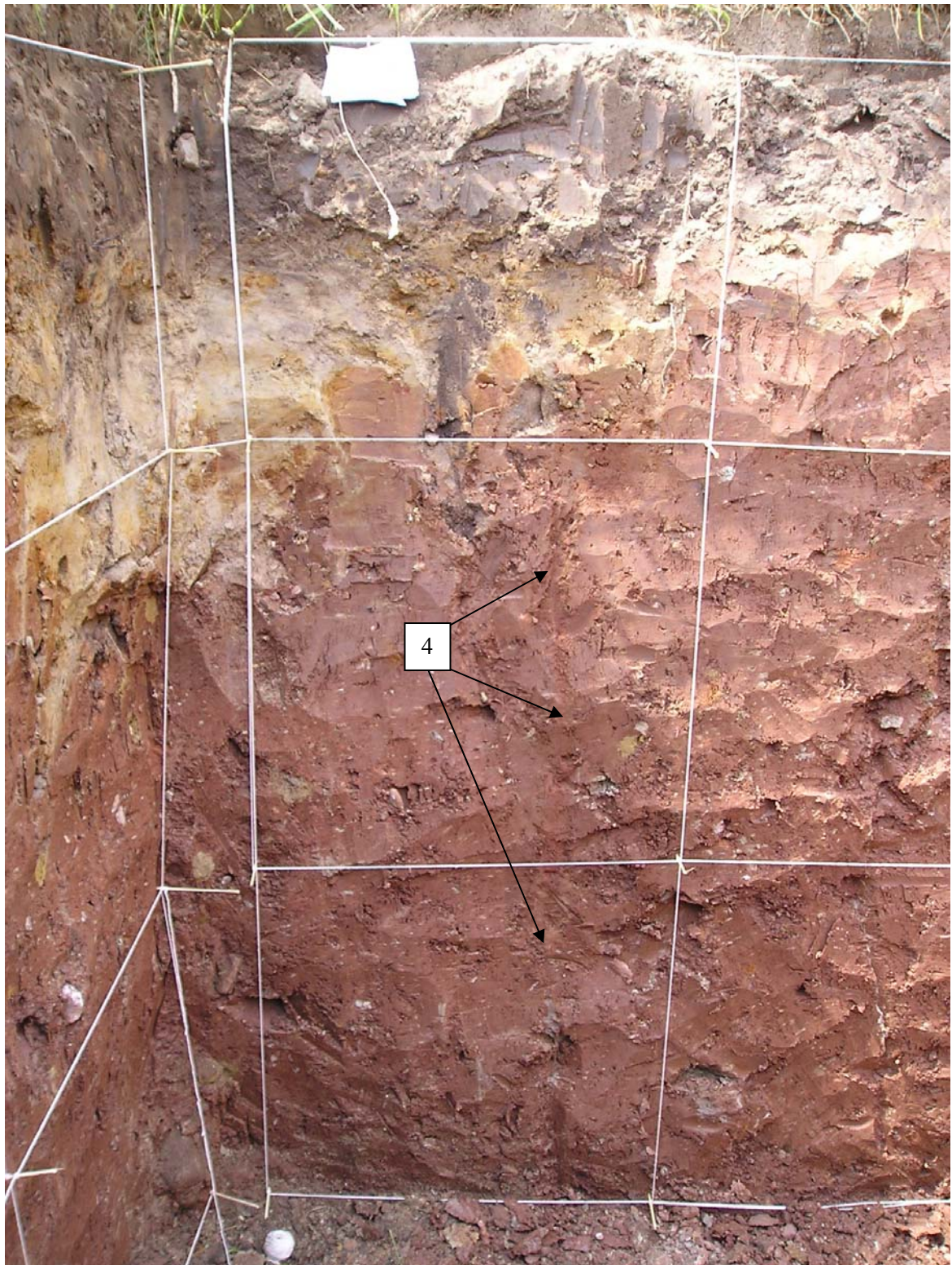


**Figure 5.26** Photograph of feature 4 shown in Figure 5.21



**Figure 5.27** Photograph of feature 5 shown in Figure 5.21

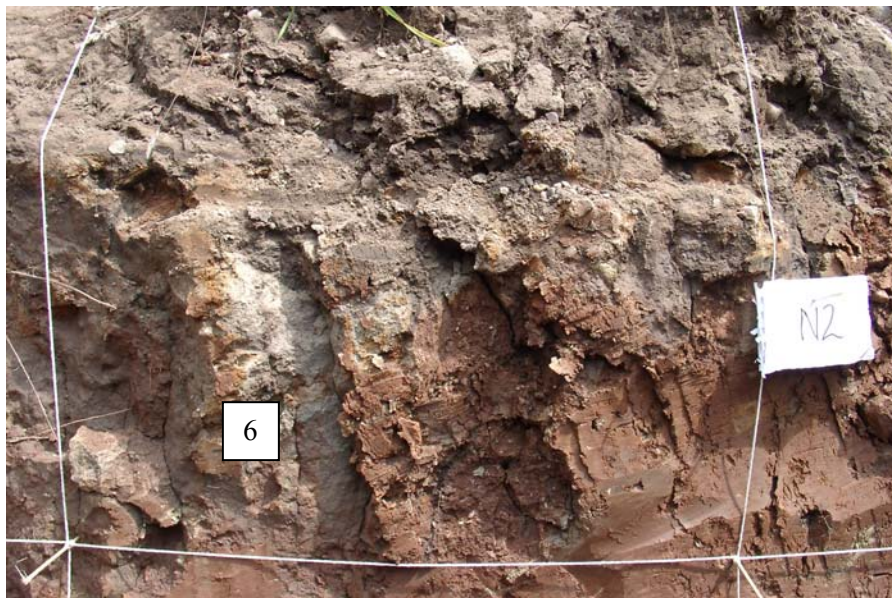


**Figure 5.28** Photograph of feature 6 shown in Figure 5.22

A layer of topsoil was present to a depth of 30 to 40 cmbgl with a very sharp transition to the underlying till. Present plant roots (such as shown in Feature 2) were observed to around

1 mbgl. In most places clayey till was present below the topsoil and near vertical open fractures were seen at a spacing of 10 to 20 cm to a depth of around 70 cmbgl (Feature 3). In the upper part of the north face lumps of till had fallen away from the face revealing fracture faces (Feature 6). These faces were often coated with topsoil indicating the downward movement of material into the fractures from above.

In the corner of the west and south faces a large weathered boulder of sandstone had been incorporated into the till just underlying the topsoil layer (Feature 1). This comprised fine to medium grained sand varying in colour from grey to orange brown indicating different states of weathering. At the boundary between the sand and the finer grained clayey till beneath, a thin rim of rust coloured material was sometimes present in the till. This is likely to be iron oxide formed by the diffusion of iron (in solution) into the clay matrix of the till.

In 3 locations on the south and west faces, fractures up to 2 cm wide were present to around 1.7 mbgl and infilled with red sandy material (Feature 4). The source of the infill appeared to be the weathered sandstone clast incorporated into the till higher in the profile. Below 60 cm depth, near vertical fractures approximately 1 to 2 mm wide infilled with very fine grained light grey material were common in all the faces of the test pit (Feature 5). These fractures had an average spacing of around 30 cm to approximately 1.4 mbgl and those persisting to at least 2 mbgl had a spacing of approximately 60 cm. The material filling these fractures was, in the field, indistinguishable from weathered calcareous (there was a vigorous reaction on application of dilute HCl) mudstone which is the most dominant clast found in the till within the test pit. This suggests that the fractures have at one time been hydraulically active transporting this material through the fractures from above. This explanatory mechanism for the infilling is consistent with the observation that the type of fracture infill is closely

associated with the types of clasts that the fractures intersect. For instance, consider the sand filled fracture shown as Feature 4 in Figures 5.21 and 5.26. This fracture extends from a large weathered sandstone clast situated higher in the profile and then intersects a soft mudstone clast at around 1.6 mbgl. The fracture then continues vertically downwards from this clast but is infilled not with sand but with material indistinguishable (to the eye) from the mudstone clast. Other mechanisms for infilling of the fractures with carbonate are possible, such as carbonate precipitation due to CO<sub>2</sub> degassing, or the mixing of waters of different chemistry at the fracture/matrix interface causing carbonate oversaturation. However, the spatial relationships between infill and clast lithology strongly suggest a mechanism of fracture infilling due to the downward transport of weathered material.

These features are of the kind observed in the core from S1\_3 described in Section 3.3.4.3. Decaying root material was present within fractures to as deep as 1.9 mbgl.

The base of the pit was excavated on its north side to enable the 3 dimensional pattern of fracturing to be observed. A perspective drawing of the fractures in this location is shown in Figure 5.29 with a photograph for comparison shown in Figure 5.30. It is apparent that the fractures form a network around columnar blocks of till. The pattern of decreasing intensity of fracturing with depth is consistent with the fractures being formed in response to stress changes at the ground surface. Such stress may have been caused by desiccation in response to long dry periods in the past perhaps combined with lower regional groundwater levels or due to freeze thaw cycles (Grisak *et al.* 1976; McKay and Fredericia 1995; Klint and Gravesen 1999).

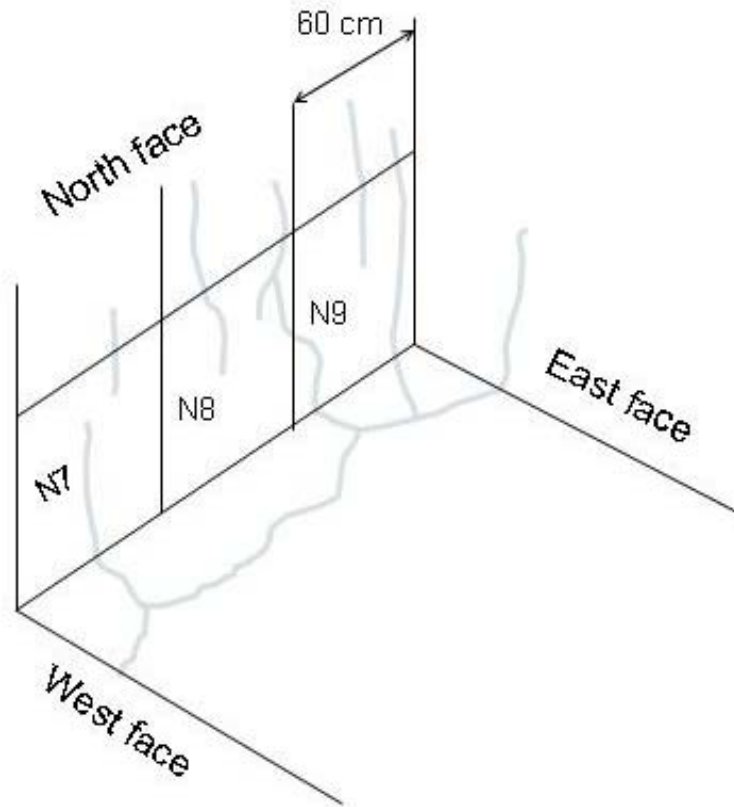


**Figure 5.29** Perspective sketch of fractures in north face and base of test pit

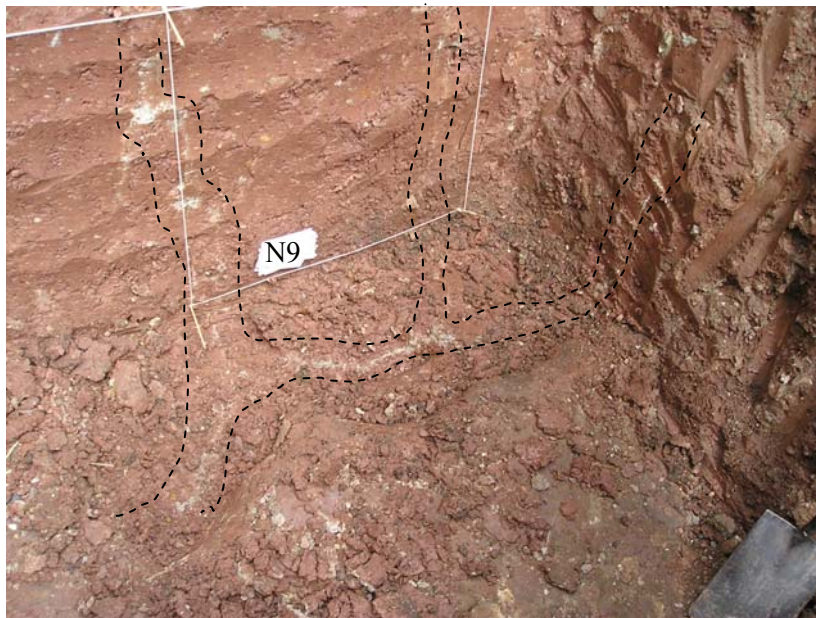


**Figure 5.30** Photograph showing the connectivity of fractures in north face and base of test pit

McKay and Fredericia (1995) suggest that fractures started due to desiccation in the upper part of a clay could extend downwards well below the depth of the water table. This assertion

is based on a linear elastic fracture formation model which simulates the formation of vertical fractures in clay (Mase *et al.* 1990). It may be possible therefore that desiccation fractures penetrate the entire 6 m deep till unit at this site. However, based on the observed doubling of fracture spacing with a corresponding doubling of depth, by 6 mbgl the spacing of the fractures is likely to be in the region of 1 to 2 m. It is also possible that deeper fractures exist caused by some other mechanism such as stress relief due to the removal of ice loading, although we have no direct evidence for this at the site.

A schematic cross section of the fracture distribution with depth is shown in Figure 5.31 and sketched in 3-dimensions in Figure 5.32.

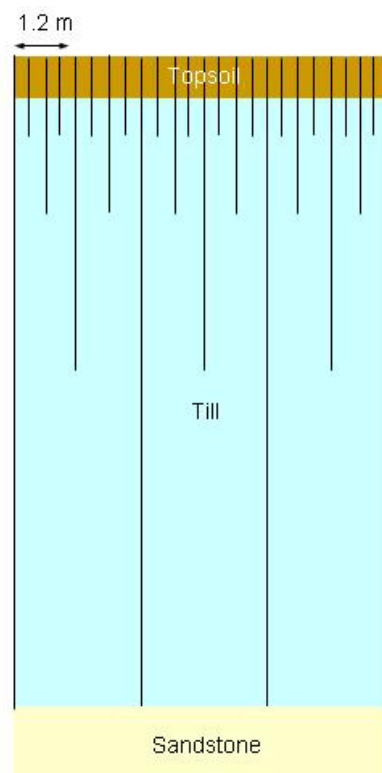


**Figure 5.31** Schematic cross section of fracture distribution with depth (vertical scale = horizontal scale)

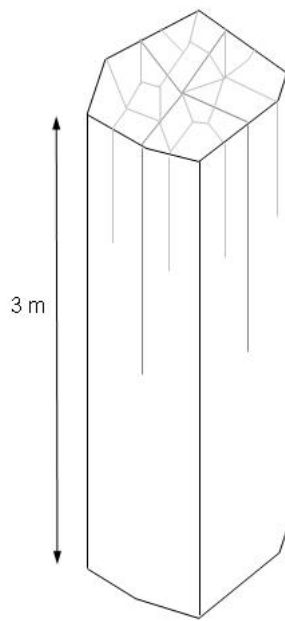


**Figure 5.32** Sketch of fracture distribution in 3-dimensions

If the fractures have been formed by desiccation or freeze-thaw processes then the infill of material derived from clasts within the till matrix is evidence of historic flow within these features. However since the fractures are now predominantly infilled with fine-grained material it is not clear how permeable they remain to the present day. During the excavation of the base of the pit it was noticed that several areas became particularly damp with time. It is noted that the groundwater level recorded by piezometer S1\_3 was above the base of the pit at the time of excavation at around 1.4 mbgl. When a fracture in the base of the pit on its north side was freshly excavated seepage was evident from the fracture as shown in Figure 5.33. With further investigation it was apparent that seepage from the fractures was discontinuous and localised in certain areas. This is strong evidence for the hydraulic significance of these fractures in the present day. However, flow within the fracture network appears to be channelised and as such is likely to be a highly unpredictable process.

It was noted in Section 5.2.2 that the occurrence of the piezometer test carried out on S1\_4 seemed to increase the hydraulic connectivity between this piezometer and the underlying

sandstone. Since rain water, that is likely to have been of relatively low pH, was used for this test this may have been due to enhancement of the permeability of a connecting fracture by dissolution of the carbonate infill.



**Figure 5.33** Photograph showing seepage from fracture in base of test pit

### **5.3 Conceptual Model of Hydraulic Processes**

The data and analysis presented so far in this chapter enable a picture of the hydraulic processes contributing to recharge at the site to be pieced together.

Infiltration into the shallow soil zone is likely to keep pace with all but the heaviest rainfall events. Owing to the uneven ground surface some temporary ponding does occur after heavy rainfall in several places across the site and may take a few days to evaporate or infiltrate. Unless the till profile has become completely saturated, the generation of significant amounts of runoff at the site is unlikely due to the flat topography, the moderate infiltration capacity of the soil and the storage provided by the uneven ground surface. Preferential infiltration

through closely spaced desiccation cracks is likely to be the primary mechanism during dry periods but the amount of water reaching the water table will depend on how much water is taken up by the matrix during such fracture flow. As the soil profile becomes wetter these features may control flow to a lesser extent as the soil swells and the cracks close up. During the summer months, transpirative demand for grass growth leads to tensions of several hundred cm to be built up over the upper 1.3 m of the profile. This drying occurs progressively from the top of the profile downwards and coincides with a recession in piezometric pressure deeper in the till. It is likely that this recession is due to a combination of evaporative demand from above, slow vertical drainage to the sandstone below and the falling piezometric level in the underlying sandstone aquifer. Pressure increases in the deeper till imply that recharge to the till water table can occur during the summer period in response to persistent heavy rainfall. It is hypothesised that this response is made possible by fracture flow through the till unsaturated zone. The relatively large variation in pressures in the saturated zone of the till is consistent with a low specific yield for the till.

During late summer the wetting of the profile begins with the initial re-saturation of the topsoil and underlying sandy horizons. From this moderately permeable wet upper layer it is hypothesised that water flows through partially saturated fractures in the till enabling relatively rapid recharge to the water table with a much slower wetting of the till matrix blocks. As time progresses greater equilibrium between the till fractures and matrix is achieved as the entire till profile becomes saturated. Numerical models are needed to test the reasonableness of this hypothesis.

It is thought that limited lateral flow occurs through the till since the relatively flat topography limits the build up of significant lateral head gradients and field observations suggest that

flow to field boundary ditches is minimal. Thus water infiltrating into the till is either drawn back to the atmosphere by evapotranspiration or flows vertically to recharge the underlying sandstone. However it is noted that these observations were made over a relatively dry year and it may be that runoff and lateral flow to the field ditches occurs to a greater extent in wetter years. Modelling is needed to quantify the likely flux reaching the underlying sandstone aquifer but the field evidence suggests that the bulk hydraulic conductivity of the till may be significantly greater than that of the till matrix.

## **5.4 Numerical Models**

### **5.4.1 Introduction**

The aim of the numerical modelling presented in this section is twofold:

- i. To simulate the hydraulic behaviour of variably saturated fractured till and in particular to show how recovery of groundwater levels in the deeper till could occur while significant tensions are present higher in the profile.
- ii. To quantify the likely magnitude and timing of the recharge flux to the Permo-Triassic sandstone through the till.

A variably saturated fractured medium can be modelled in a variety of ways. The most popular approaches are 1-D mechanistic models (Simunek *et al.* 2003) although the assumptions involved in mechanistic modelling of preferential flow may be difficult to justify (Beven 1991). The simplest approaches are equilibrium flow models combining the Richards equation with modified equations for the hydraulic properties (Durner 1994). Single porosity models have also been described for capturing the non-equilibrium nature of preferential flow (Ross and Smettem 2000). However, the most common approach is to split the soil up into two or more pore spaces (e.g. fracture and matrix) viewing the system as overlapped

interacting continua (Liu *et al.* 2003). A mass transfer function is then used to govern flow between these pore systems based, for example, on the water content or head difference between the regions (Gerke and van Genuchten 1993b; Gerke and van Genuchten 1996; Kohne *et al.* 2004). Dual-permeability models allow advective flow in two pore spaces (Gerke and van Genuchten 1993a) whereas dual-porosity models assume one of the pore spaces is immobile (Philip 1967).

However, the weakness of these approaches is the need, in some way, to average the response of the matrix and its interaction with the fracture system. Since the till matrix is of very low permeability a large hydraulic disequilibrium may be expected between the matrix and fracture regions in the unsaturated zone. For this reason it was decided to model the system using an explicit representation of the fracture and matrix geometry thus avoiding the problems of averaging. Fracture network models have been applied to variably saturated conditions in the literature (Liu *et al.* 2002) although it has been noted that constraining the parameters which most strongly control fracture flow under these conditions is nearly impossible from field data (Pruess 1999). For the purpose here of exploring hydraulic concepts the approach of using the variably saturated code FAT3D-UNSAT in 2-dimensions is deemed the most suitable.

FAT3D-UNSAT was developed by Professor Rae Mackay at the University of Birmingham (Hydrogeology Group, Department of Earth Sciences). The code assumes that one-dimensional water movement in a partially saturated rigid porous medium can be adequately described by a modified form of the Richards equation. The main assumptions of the approach are that the air phase plays an insignificant role in the liquid flow processes and that water flow due to thermal gradients can be neglected (Nielson *et al.* 1986). It implements the

soil-hydraulic functions of van Genuchten (1980) who used the statistical pore-size distribution of Mualem (1976) to obtain a predictive equation for the unsaturated hydraulic conductivity function in terms of soil water retention parameters. This approach has been used for the modelling for this thesis and inherently assumes that any hysteresis in the soil moisture characteristic curve can be neglected. A fuller description of the assumptions and equations used in FAT3D-UNSAT and details of the numerical implementation are given in Appendix 7.

Before detailed fracture flow modelling was embarked upon, a simple 1-D single porosity model was used to check that, as hypothesised above, the observed pressure increases in the saturated till while large tensions existed higher up the profile cannot be accounted for by matrix flow alone without the need for invoking preferential flow through fractures.

#### **5.4.2 1-D Single Porosity Model**

A 1-D model (run S1\_A in Appendix 8) was set-up to simulate a column of till situated between the base of the topsoil at 0.4 mbgl and a water table positioned at 1.4 mbgl. The vertical discretisation used was 50 x 2 cm cells with a cell width and breadth of 1 cm. The upper boundary was set up to simulate moist topsoil in late summer with a constant pressure head of zero for 60 days. To simulate the soil filling up in early autumn the pressure head was gradually increased to 30 cm by day 90 and then remained constant until the end of the run. The initial conditions used were approximately based on the observed pressure profile during September 2004 and vary linearly from a pressure head of zero at the top of the model (base of soil) up to a tension of 500 cm in the centre of the profile. The pressure heads then increase back to zero at the base of the model to the water table. The initial pressure distribution is shown in Figure 5.34. The lower boundary was left as the default no-flow condition.

A hydraulic conductivity of  $1.4 \times 10^{-10}$  m/s was used based on the laboratory results presented in Chapter 3. A specific storage of  $1 \times 10^{-6}$  cm<sup>-1</sup> was assumed based on literature values for till (Keller *et al.* 1989). The soil moisture characteristic curve was defined using van Genuchten parameters to be consistent with the gravimetric moisture contents and tensions measured on 3/9/04 and 7/2/05. This resulted in a steep characteristic curve which is shown in Figure 5.36 with the van Genuchten values. The retention curve is consistent with published values for other tills (Khazode *et al.* 2002). Time steps of 1 day were run for 1 year. The resulting mean absolute volumetric error on all cells was  $7.7 \times 10^{-5}$  cm<sup>3</sup> and the model took less than a minute to run. The resulting head profile after 1 year is shown alongside the initial heads in Figure 5.34. The results show that even after 1 whole year re-saturation has occurred in only the upper 15 cm of the profile and no increase in pressure is seen at the water table. These results suggest that preferential flow needs to be invoked to model the deeper pressure response seen at Site 1.

#### **5.4.3 2-D Fracture Block Model**

The 1-D model presented above was therefore extended to include fractures around a till block half-space of 15 cm (run S1\_B in Appendix 8). The purpose was not to replicate the exact conditions but to demonstrate the reasonableness of the hypothesised hydraulic processes. The half space was assumed to have a continuously running fracture along its left hand side and a fracture starting at the surface but terminating at 0.7 mbgl (i.e. 0.3 m below the top of the model) on its right hand side. Both fractures were discretised with a half-width equal to 1 mm. The horizontal discretisation was set to increase incrementally away from the fractures with a maximum cell width of 2 cm at the block centre as shown schematically in Figure 5.35. The vertical discretisation used was 50 x 2 cm cells.

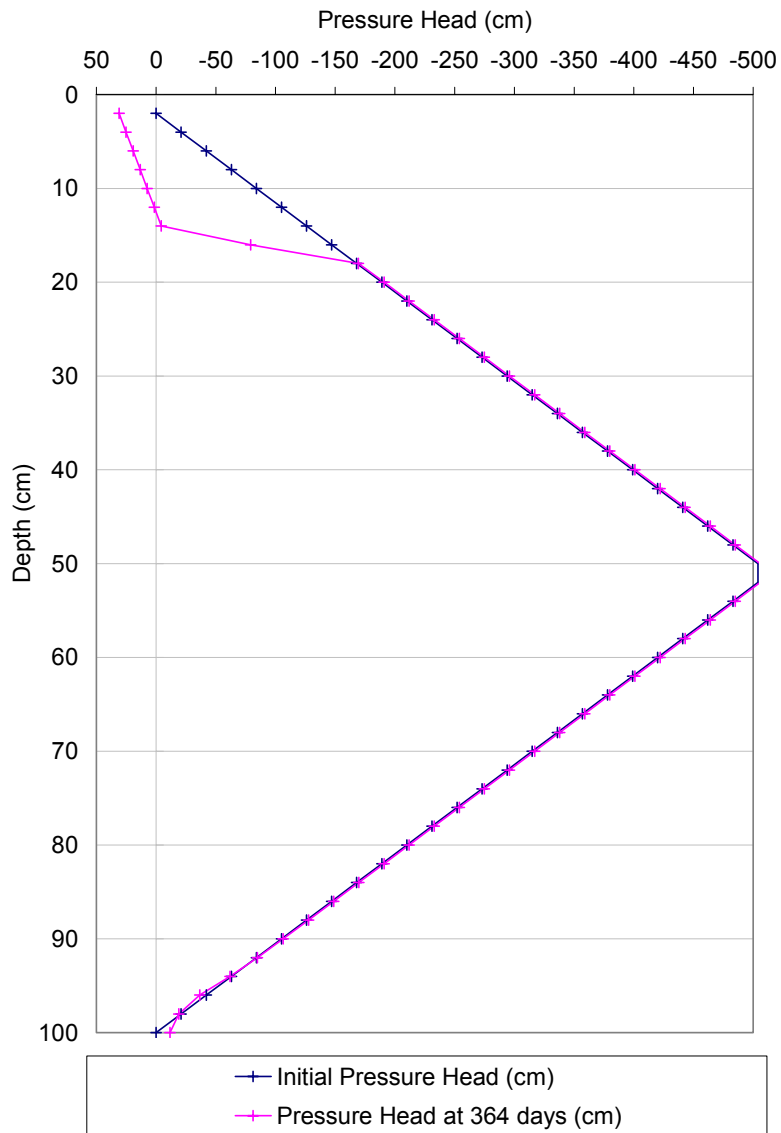


**Figure 5.34** Initial conditions and results at 364 days for 1-D single porosity model S1\_A

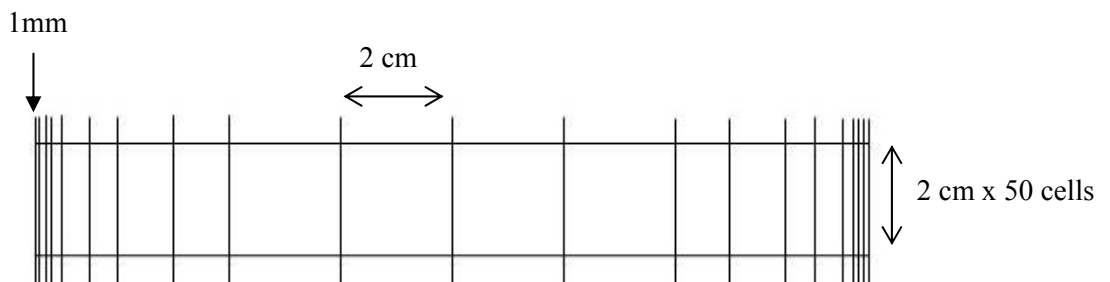


**Figure 5.35** Discretisation of model S1\_B

The initial and boundary conditions were set up exactly as for model S1\_A presented above and applied to every model column. Parameters for the till matrix were also retained. The fracture hydraulic conductivity was set to be 1000 times that of the matrix. The chosen fracture retention curve and van Genuchten parameters are shown in Figure 5.36. The form of the retention curve assumes that the fractures are dominated by relatively open pore spaces.

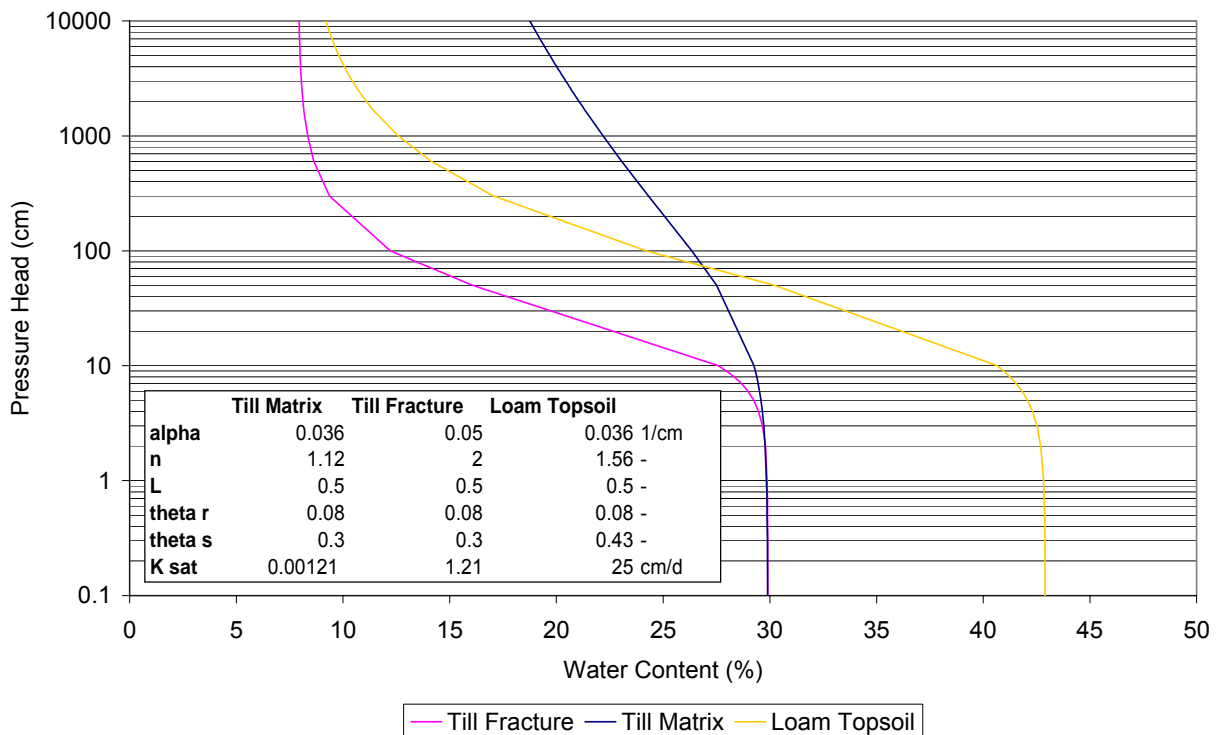


**Figure 5.36** Soil moisture characteristic curves and van Genuchten parameters for FAT3D-UNSAT models

Time steps of 1 day were run for 245 days. The resulting mean absolute volumetric error on all cells was  $2.4 \times 10^{-5} \text{ cm}^3$  and the model took 7 hours to run. The pressure head distributions at 0, 30, 60 and 90 and 150 days are shown in Figure 5.37.

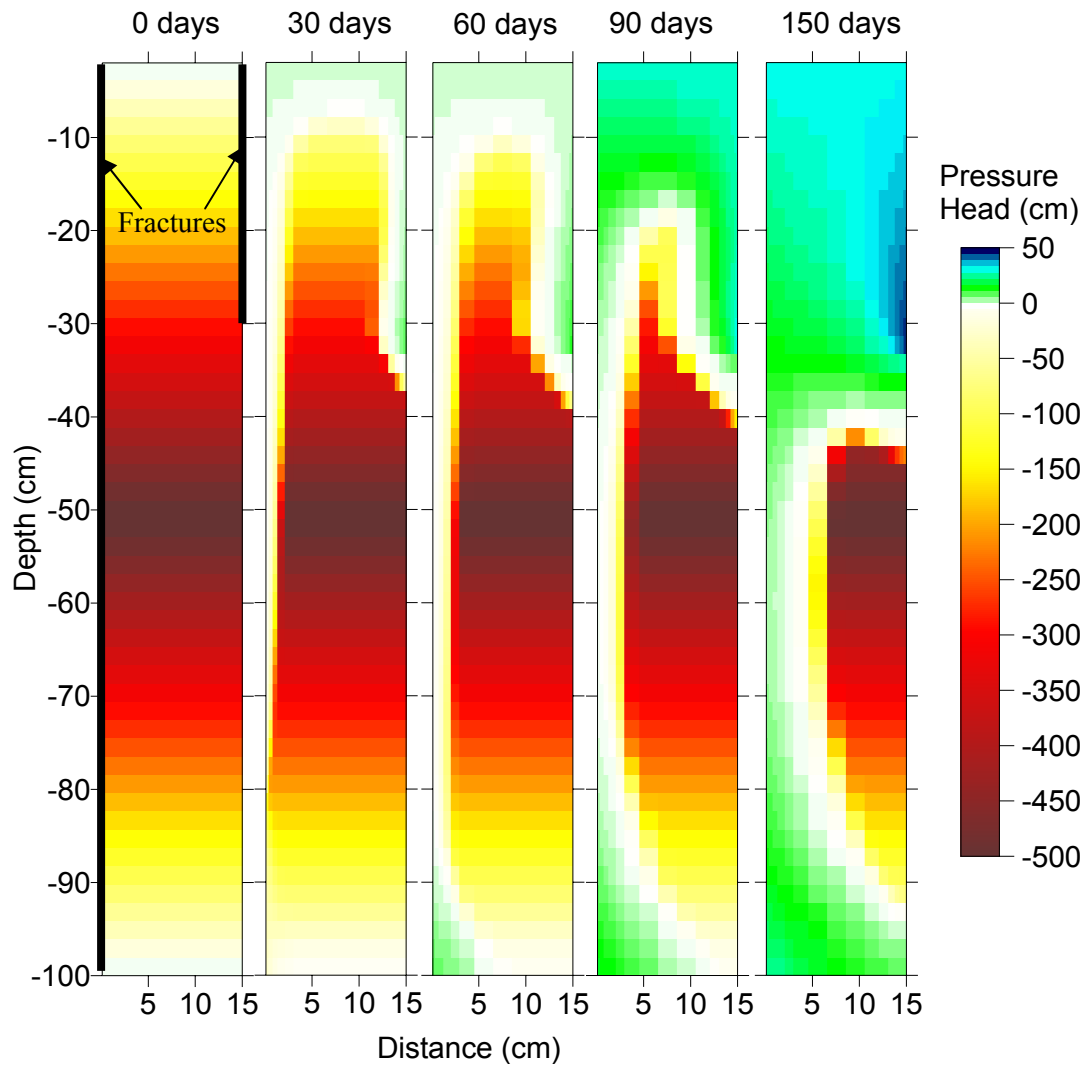


**Figure 5.37** Initial conditions and results of 2-D model S1\_B

The effects of the fractures on the wetting of the profile are clearly evident. Positive pore pressures are quickly established in the fractures and progressive wetting of the adjacent matrix can be seen. Wetting around the fracture on the right hand side of the model (closed at 30 cm depth) progresses more quickly than for the fracture on the left hand side (extends to the base of the model) as would be expected. Positive pressures take around 45 days to develop at the base of the model and then increase rapidly in line with the response of the water table inferred from the S1\_3 groundwater hydrograph.

Although the overall pattern of response is consistent with the hydraulic observations the re-saturation of the matrix progresses more slowly than suggested by the tensiometer data (S1\_T3 and S1\_T5) with large tensions persisting over a significant region even after 150 days. Alternative models were run with a variety of combinations of hydraulic parameters. It is worth commenting here that the model convergence/run-time is very sensitive to the exact parameter combinations. In particular, steeper retention curves, lower permeabilities and larger head gradients tended to lead to more unstable models. For parameter combinations which ran successfully it was found that without significantly steepening the matrix retention curve and/or increasing the matrix hydraulic conductivity it was impossible to simulate a much quicker wetting of the matrix. Significant changes to these parameters cannot be justified on the basis of existing data or literature values.

However there are other reasons why the modelled results may not seem to agree with the tensiometer data:

- i. The tensiometers do not measure at a point but give an average tension over several tens of cm<sup>3</sup> of till material (the tensiometer cups are 6 cm long and 2 cm in diameter). Furthermore they may be positioned closer to a fracture than to the block centre (in fact this is inevitable in terms of probability). The pressure response of each tensiometer is therefore highly sensitive to their position in relation to the fractures, something which is unknown. Some parts of the upper till that are subject to large suctions imposed by root extraction and are sufficiently distant from fractures might remain in a permanently unsaturated condition. Conversely if the plant root network predominantly exploits the fractures it is possible that significant drying of the centre of the till blocks does not often occur. Due to the uncertainty in the location of the

tensiometers in relation to fractures both of these situations are possible without being inconsistent with the tensiometer observations. If time and resources had allowed there would therefore have been value in excavating the tensiometers at the end of the period of monitoring to allow their locations relative to fractures to be ascertained.

- ii. The setting up of the model in two dimensions will inevitably lead to a slower wetting of the matrix blocks than we would expect for a 3-D case. This is because by representing an approximately hexagonal fracture network using a 2-D cross section the effective fracture porosity is halved. Thus the equivalent amount of fracture area per unit volume of matrix block is also halved. Modelling the 3-dimensional geometry of convergent flow into the matrix would therefore lead to significantly greater rates of re-saturation over time. The extension of the modelling to three dimensions is however a significant undertaking requiring a large amount of computer processing power and time and was not undertaken.
- iii. Flow through the variably saturated fracture network is in reality likely to be much more complex than the situation captured by the 2-D model. For example, it has already been inferred in Section 5.2.9 (by observing discontinuous seepage from fractures in the test pit) that the saturated permeability of the fractures may be highly variable. Furthermore, mechanisms of flow focussing may be significant in generating preferential flow pathways within the fracture network. Owing to the decreasing fracture intensity with depth it is likely that flow focussing will occur, for instance, in the vicinity of the intersection between the base of a closed fracture and a fracture continuing to greater depth, and around asperity contacts within fractures (Pruess

1999). Accurate simulation of the re-wetting of the matrix blocks may depend on capturing some of these processes.

Given these caveats, the 2-D model nevertheless indicates that the observed water table response at the end of the summer (and during the summer after heavy rainfall) is consistent with the proposed mechanism of preferential flow through fractures.

#### **5.4.4 1-D Equivalent Porous Media Model**

The second aim of the numerical modelling is to quantify the likely magnitude and timing of the recharge flux to the Permo-Triassic sandstone through the till.

Hydraulic disequilibrium between the matrix and fracture regions of the till is likely to be very significant during partially saturated conditions. However assuming that the till does become completely saturated during the winter, the pressure changes in the matrix in response to those in the fractures, and vice-versa, are likely to be very quick. Theoretically, daily periodic pressure changes will propagate across till matrix blocks of several tens of cm within hours. This is based on the equivalent form of Equation 4.3 for the flow of water, using a hydraulic conductivity of  $1.4 \times 10^{-10}$  m/s and a specific storage of  $1 \times 10^{-4}$  m<sup>-1</sup>. Hence under these conditions it is appropriate to model the till as a 1-D equivalent porous medium.

The variation in the hydraulic conductivity of the fracture network is likely to lead to a very variable pressure head distribution through the saturated till. Thus data from the deeper till piezometers cannot be used to derive representative vertical hydraulic gradients for flow through the till as a whole. However, since the water table is within the relatively permeable soil zone during the winter, the lateral variation in the water table is likely to be relatively low. Thus the hydraulic gradient between the water table and the base of the till may be used to derive the likely bulk flux through the till.

This approach assumes that lateral flow through the till is negligible. To test this assumption a simple analytical model has been used. If an unconfined aquifer of hydraulic conductivity  $K$ , with infinitely long fully penetrating drains at a spacing  $2a$  and an impermeable base, receives a constant recharge  $R$  then the steady state profile of the water table can be described by the following equation (Todd 1959):

$$h^2 = h_a^2 + \frac{R}{K}(a^2 - x^2) \quad (5.1)$$

where  $h_a$  is the head in the drain (relative to the impermeable base),  $h$  is the head in the aquifer (relative to the impermeable base) and  $x$  is the distance from the midway point between adjacent drains. Although the assumption of an impermeable base is not met in the case of Site 1 the equation provides a first order approximation which is nevertheless informative. For a recharge (equal to the equivalent lateral flow) of just 10 mm/a ( $3.2 \times 10^{-10}$  m/s), distance between drains of 100 m (i.e.  $a = 50$  m) and a conservatively high hydraulic conductivity of  $1 \times 10^{-7}$  m/s, it follows that the head at the midpoint between drains would need to be approximately 6.7 m above ground level for drains placed at 1 mbgl assuming flow through the upper 1.5 m of the profile. This simple model indicates that even a small amount of shallow lateral flow cannot be realistically accommodated within the till at Site 1.

It is also assumed that the PEt and rainfall for the site are adequately known. Thus the flux through the soil zone can be known with some degree of accuracy for the winter months since the problem of crop limited evaporation, often one of the greatest uncertainties in recharge modelling, can be minimised. A model was thus constructed in 1-D to simulate the position of the water table during the winter months (November to April). A soil layer 0.4 m thick was set-up with van Genuchten parameters for loamy topsoil as shown in Figure 5.36. The

top 20 cm of the soil were given a saturated water content of 0.7 to simulate the ponding of water on the uneven ground surface. Below the soil the till was assigned a constant set of parameters as defined for the till matrix as shown in Figure 5.36. The only change was made to the hydraulic conductivity which was varied in order to refine the model. The till extended to 630 cmbgl with a variable head boundary condition set equal to the head recorded by piezometer TE32. The vertical cell dimension was 5 cm and P<sub>Et</sub> and rainfall were input on a daily basis. Evaporation was assumed to occur from the topsoil only and root constants and wilting points were set at 600 and 8000 cm respectively. However, soil tension never exceeded the root constant during the modelled period and thus A<sub>Et</sub> always equalled P<sub>Et</sub>. The model was run from a starting total head of 30 cmbgl everywhere, from 20/11/04 until 30/4/05 and took several seconds to run. The results are shown in Figure 5.38 for the 'best fit' model. This case used a bulk hydraulic conductivity of 0.02 cm/d ( $2.3 \times 10^{-9}$  m/s) for the till and had a mean absolute volumetric error on all cells of  $1.4 \times 10^{-5}$  cm<sup>3</sup>. The model input and output files (run S1\_C) are given in Appendix 8.

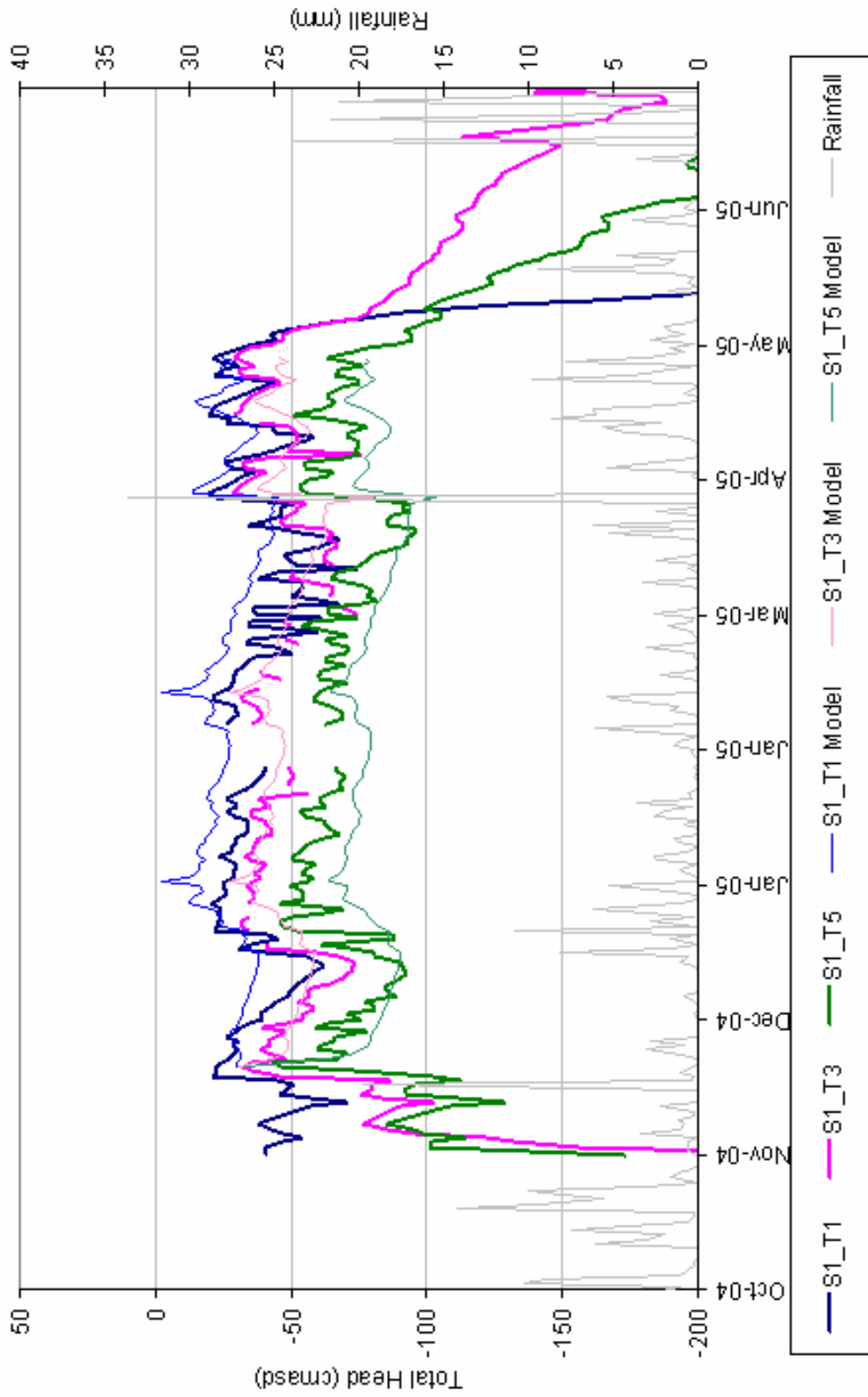


**Figure 5.38** Results of 1-D equivalent porous medium model S1\_C

The pattern of responses in the soil zone and upper till is reasonable although a smoother response is seen in the model to rainfall events than in the tensiometer data. This is likely to be due to preferential flow through macropores and fractures in the topsoil not accounted for in the model. If the hydraulic conductivity is decreased significantly from a value of around 0.02 cm/d the model overflows unrealistically. If increased the water table becomes unrealistically low. Reasonable model outputs can be reached for values in the range 0.02 +/- 0.005 cm/d. Ignoring the early time data while the initial conditions are dominant the average hydraulic gradient across the till (between the water table and heads observed in TE32) was 0.48 and recharge to the sandstone was 0.012 cm/d for the modelled period. For the 6 month winter period the recharge to the sandstone is therefore likely to have been in the range 13 to 22 mm/a. For the summer period when the water table is lower the approximate hydraulic gradient is 0.42 assuming the water table is positioned at 1.7 mbgl. If we assume that the till bulk hydraulic conductivity decreases overall with depth due to decreasing fracture intensity a maximum estimate of the recharge during this period would be calculated using a value of 0.02 cm/d. In this case the summer recharge to the sandstone is approximately 12 to 20 mm/d. This implies the total annual recharge to the sandstone is approximately 25 to 41 mm/a and is relatively constant throughout the year.

Although an estimate of recharge through the till has been reached with a possible error for the model parameterisation, the estimate is also highly dependent on the correctness of the assumption that PEt and rainfall for the site are adequately known. Uncertainties in meteorological variables were noted in Section 2.5 and are hard to quantify. For this site located in the corner of a field the proximity of trees and hedgerows may increase the rate of PEt. Furthermore the position of the hedgerow to the west of the site in the direction of the prevailing wind may mean that the incident rainfall is somewhat reduced. Both these effects

act to reduce the available water, as noted for the corner of the site using the ERT data, and may imply that the recharge has been over rather than underestimated.

An overestimation of recharge to the sandstone is also likely to have been made if the assumption of negligible lateral flow through the till is incorrect or if complete re-wetting of the till matrix blocks was not achieved by November.

It is noted that the rainfall during the modelled period was approximately 55 mm lower than the average rainfall between November and April for years since 1970. Even during this dry winter a degree of ponding was observed and the water table was often very close to the ground surface following prolonged/heavy rainfall. If recharge to the sandstone is in the range implied by the modelling then during a wetter winter runoff is likely to become more significant. Thus this process would need to be included within equivalent models for wetter years.

Although an estimate of recharge to the sandstone has been made for the year 2004 to 2005, under certain climate and abstraction scenarios this value may be very different. For instance, if the groundwater level in the sandstone in the vicinity of Site 1 was reduced due to increased groundwater abstraction during a series of wetter than average years, it is likely that the recharge through the till would increase as water would drain through the till under an increased hydraulic gradient. In this case the increased recharge would be met predominantly by a decrease in runoff. For example, if the groundwater level in the sandstone was reduced to the extent that the till drained under a unit hydraulic gradient, the recharge to the sandstone may be as high as 70 mm/a.

During a series of drier than average years, the relative rate of decline of the till water table and the sandstone piezometric level will govern the hydraulic gradient driving recharge from

the till to the sandstone. Without a longer period of monitoring it is difficult to predict how this would affect the rate of recharge to the sandstone. However, based on the understanding of the hydraulics outlined in this chapter, it is likely that as the water table declined, two positive feedback mechanisms would begin to operate to limit the rate of decline of the water table within the till. Firstly, evapotranspiration would increasingly be limited by high soil moisture deficits in the top of the soil/till profile as the water table lowered and capillary rise to the root zone was reduced. Furthermore, since water may flow to depth through preferential flow in fractures, it is likely that recharge to the water table would still occur. This process may in fact be enhanced by the widening of existing fractures or re-opening of new fractures due to prolonged drying. Secondly, due to the decrease in fracture intensity with depth the bulk hydraulic conductivity of the till may also decrease with depth, although this is far from certain given the apparent variation in fracture permeability. Hence during times of lower water table, recharge to the sandstone may be reduced slowing the rate of water table recession. The recharge to the sandstone during prolonged dry periods will therefore depend on the delicate balancing of these interacting hydraulic processes. Further monitoring and detailed modelling as suggested in Section 7.4 may help to predict the recharge response under these circumstances.

## **5.5 Conclusion**

A range of monitoring and experimental data for the site has been drawn together along with laboratory results to derive a hypothetical conceptual model of the site hydraulics in relation to groundwater recharge. The data from tensiometers and piezometers set within a robust understanding of the geology were most useful in developing an understanding of the site. The hydrochemistry data and infiltrometer and tracer test results also provided useful supporting data. The electrical methods employed in the form of TDR and ERT were

disappointing in terms of quantitative results but added some value in confirming the picture emerging from the other sources of data.

The hydraulic and hydrochemical/tracer test data are highly suggestive of the occurrence of preferential flow through the till. Furthermore, hydraulically active fractures have been observed in a test pit extending to depths of greater than 2 m. Numerical models have illustrated the features of unsaturated flow through fractured till and shown that water table responses to rainfall during the summer may feasibly occur while large tensions are present higher up the profile. Modelling has shown that such responses are impossible through the low permeability till matrix alone without a mechanism for preferential flow. Uncertainties remain as to the exact pattern of wetting and drying of the till matrix blocks due to the unknown location of tensiometer cups in relation to the fractures. Flow within the fracture system appears to be highly variable due to variations in fracture hydraulic conductivity and possible flow focussing within the unsaturated zone. An equivalent porosity model has shown that the bulk hydraulic conductivity of the till is in the range  $1.7$  to  $2.9 \times 10^{-9}$  m/s, approximately one order of magnitude higher than the till matrix permeability. This result is consistent with the range of bulk hydraulic conductivity reported for till deposits elsewhere in Shropshire (Wealthall *et al.* 1997), East Anglia (Klinck *et al.* 1996; Klinck *et al.* 1997), Denmark (Cartwright 2001) and North America (Gerber and Howard 2000). The recharge to the sandstone was likely to have been in the range 25 to 41 mm/a in 2004 to 2005 and relatively constant throughout the year. This is 2 to 3 times lower than the estimated average value for recharge through till used in the East Shropshire Permo-Triassic Sandstone Groundwater Modelling Project (Streetly and Shepley 2005). This difference is explored further in Chapter 7.

Based on the tracer test results potential travel times of contaminants to the water table may be as high as 1 cm/d. Given the uncertainty in the porosity of the hydraulically active fractures and likely significant variability in their hydraulic conductivity, the maximum potential flow velocities through the saturated till are not known. However the tritium and CFC data show that the travel time to the sandstone (at 6.3 mbgl) is less than 40 years. The presence of significant  $\text{NO}_3$  at 4.4 mbgl is also consistent with these relatively high groundwater velocities.

## **6 SITE SCALE INVESTIGATIONS 3: SITE 2 RESULTS AND MODELS**

### **6.1 Aim**

This chapter presents the results of the monitoring and investigation carried out at Site 2 using the equipment, techniques and analysis methods described in Chapter 4. Based on these results, a conceptual model of the site hydraulic processes is proposed. Results from numerical modelling undertaken to test the conceptual model and to quantify the magnitude and timing of likely recharge fluxes are then described and conclusions drawn.

### **6.2 Results**

#### **6.2.1 Geology**

The geology is known from 4 cored boreholes, from shallow augering undertaken during installation of tensiometers and TDR access tubes, and indirectly from ERT surveys.

A dark reddish brown fine to medium grained sandy topsoil (loamy sand) of 0.4 to 0.5 m thickness covers the site overlying glaciofluvial outwash material persisting to between 2.45 to 2.7 mbgl. An ERT survey oriented approximately east-west across the site is shown in Figure 6.1 and suggests that the site is located on the west side of a roughly north-south oriented channel like structure with the outwash thickening to the east. The outwash predominantly comprises well sorted medium sand with variable gravel content. Below around 1 mbgl it is grey brown in colour but above this level and below the topsoil there is a slightly cemented orange brown horizon of variable thickness. This is a zone of illuviation where iron, and most likely aluminium, oxides have accumulated into an 'iron pan' above the level of permanent saturation. Thin (<0.1 m) clay rich beds are also present in some locations above 1.5 mbgl.

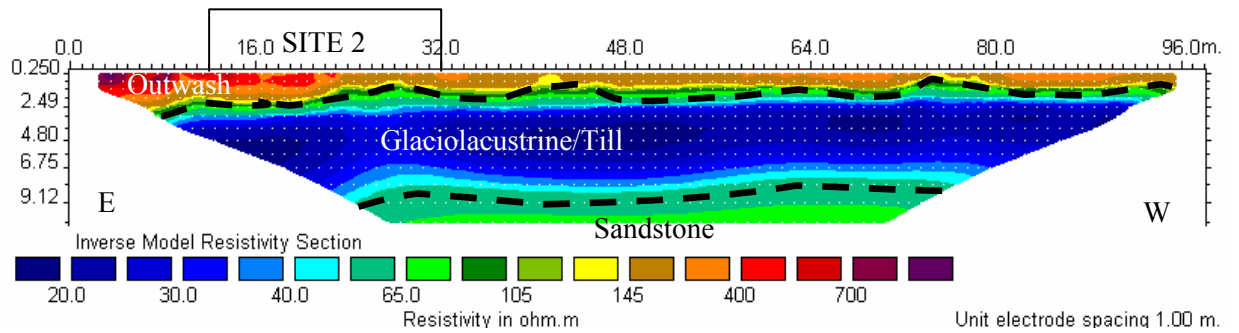


**Figure 6.1** ERT survey across Site 2

Below the glacial outwash materials lies laminated brown glaciolacustrine clay persisting to 6.7 mbgl on the east of the site but thinning to the west. The type of deposit underlying this clay varies across the site comprising layered till and glaciolacustrine sand in different combinations as indicated in Figure 6.2. Weathered slightly clayey fine to medium grained Permo-Triassic sandstone underlies the drift materials at between 7 and 8 mbgl.

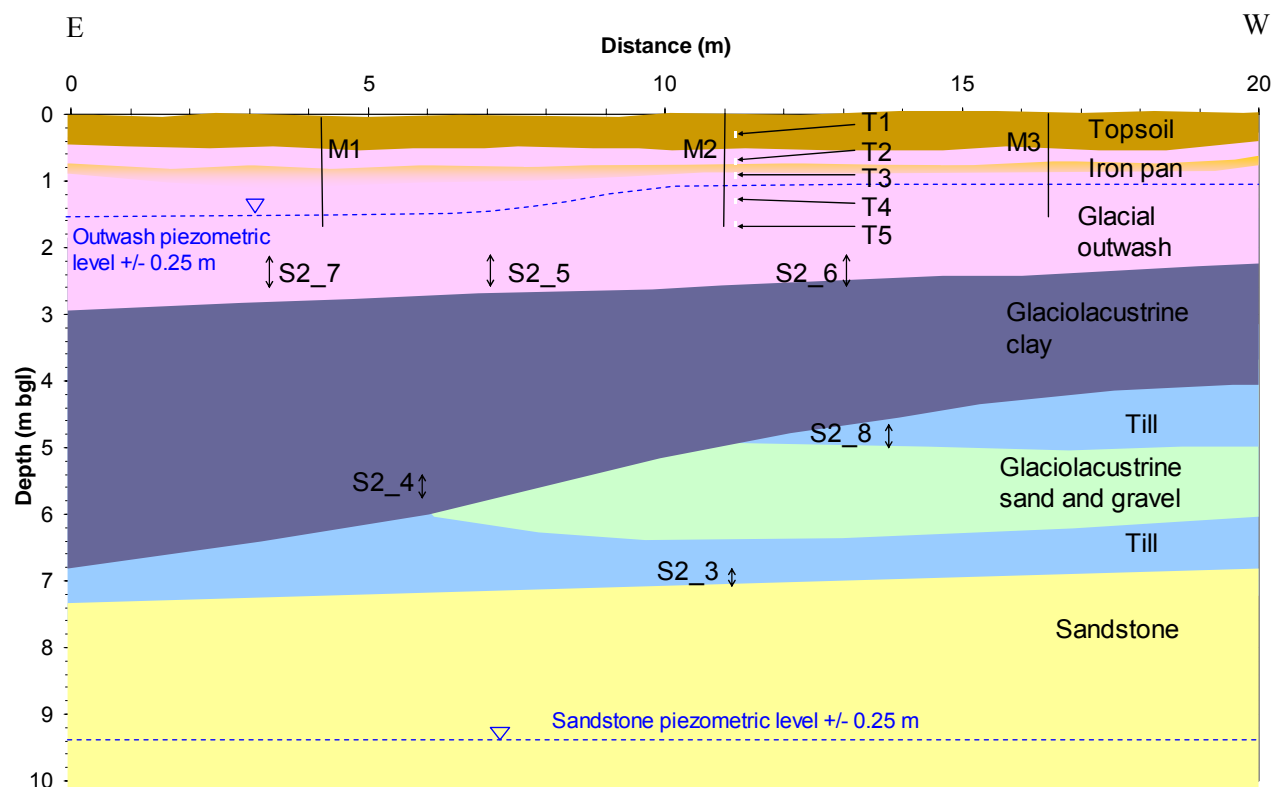


**Figure 6.2** Schematic geological cross section of Site 2

A schematic cross section is shown in Figure 6.2 to indicate the likely geometry between the different lithologies. Also shown are the monitoring locations of TDR access tubes (M1 to M3), piezometer screen intervals (S2\_3 to S2\_8) and tensiometers (T1 to T5). The depth of each installation is accurate but since the horizontal position is only approximately projected onto an east-west line across the site the figure is schematic. Each installation is however shown correctly in relation to its geological context.

### **6.2.2 Pressures**

Pressures have been recorded at three piezometers (S2\_5, S2\_6 and S2\_7) and 5 tensiometers (T1 to T5) as described in Chapter 4. Piezometers S2\_3, S2\_4 and S2\_8 were dry throughout the monitored period except during falling head tests when water was added.

The pressure heads recorded have been added to an elevation head with reference to a site datum to produce a total head. The site datum chosen was the cover of borehole S2\_3 which is near ground level.

Time series of pressure heads recorded at the tensiometers T1 to T5 are shown in Figure 6.3 for the period 8/11/04 to 13/12/04 at 5 minute intervals. Figure 6.4 shows daily average values of tensiometer pressure head for the whole monitored period. Data from the pressure transducers have been removed in cases where the pressure readings became invariable at a very low voltage, indicating that the pressure was out of range of the transducer or that the electronics had failed in some way.

Time series of total heads at the eight monitoring locations are shown in Figure 6.5. For those installations monitored by pressure transducers/data loggers daily averages have been shown. Anomalous data have again been removed.

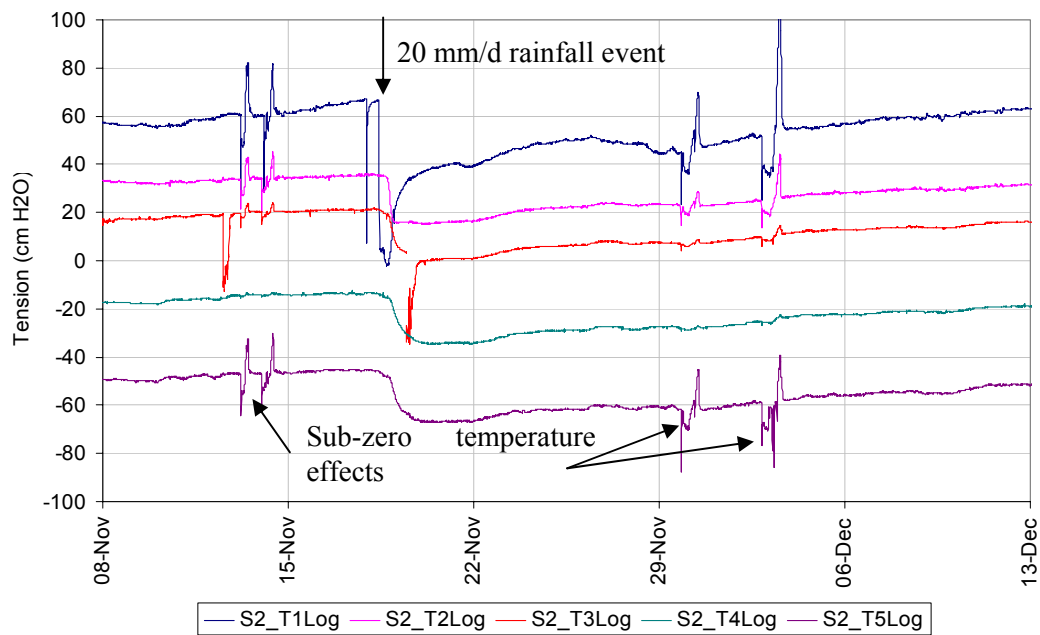


**Figure 6.3** Soil tension recorded at Site 2 tensiometers at 5 minute intervals between 8/11/04 and 13/12/04

Groundwater levels within the outwash deposits follow an annual seasonal cycle with superimposed shorter term variations in response to rainfall events. During 2004/5 levels reach an annual maximum in April and are at a minimum in September. The shorter term responses to rainfall are of a greater magnitude in S2\_6 than in S2\_5 and S2\_7. Furthermore the absolute groundwater levels are around 0.5 m higher in S2\_6 throughout the year. This in itself may explain the responsiveness of the water table at this location due to a thinner unsaturated zone and less damping of the recharge signal.

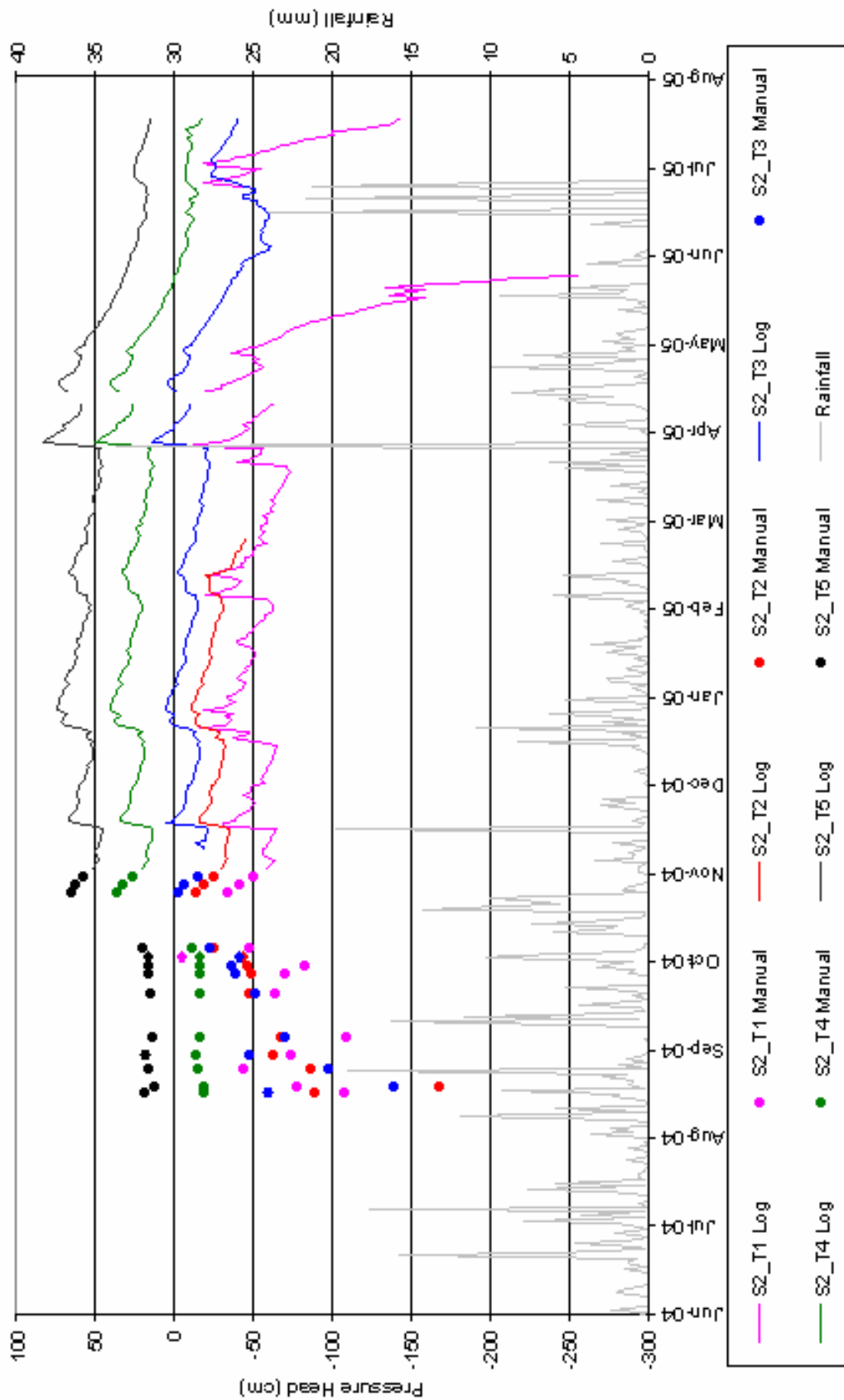


**Figure 6.4** Time series of average daily pressure heads recorded at Site 2 tensiometers

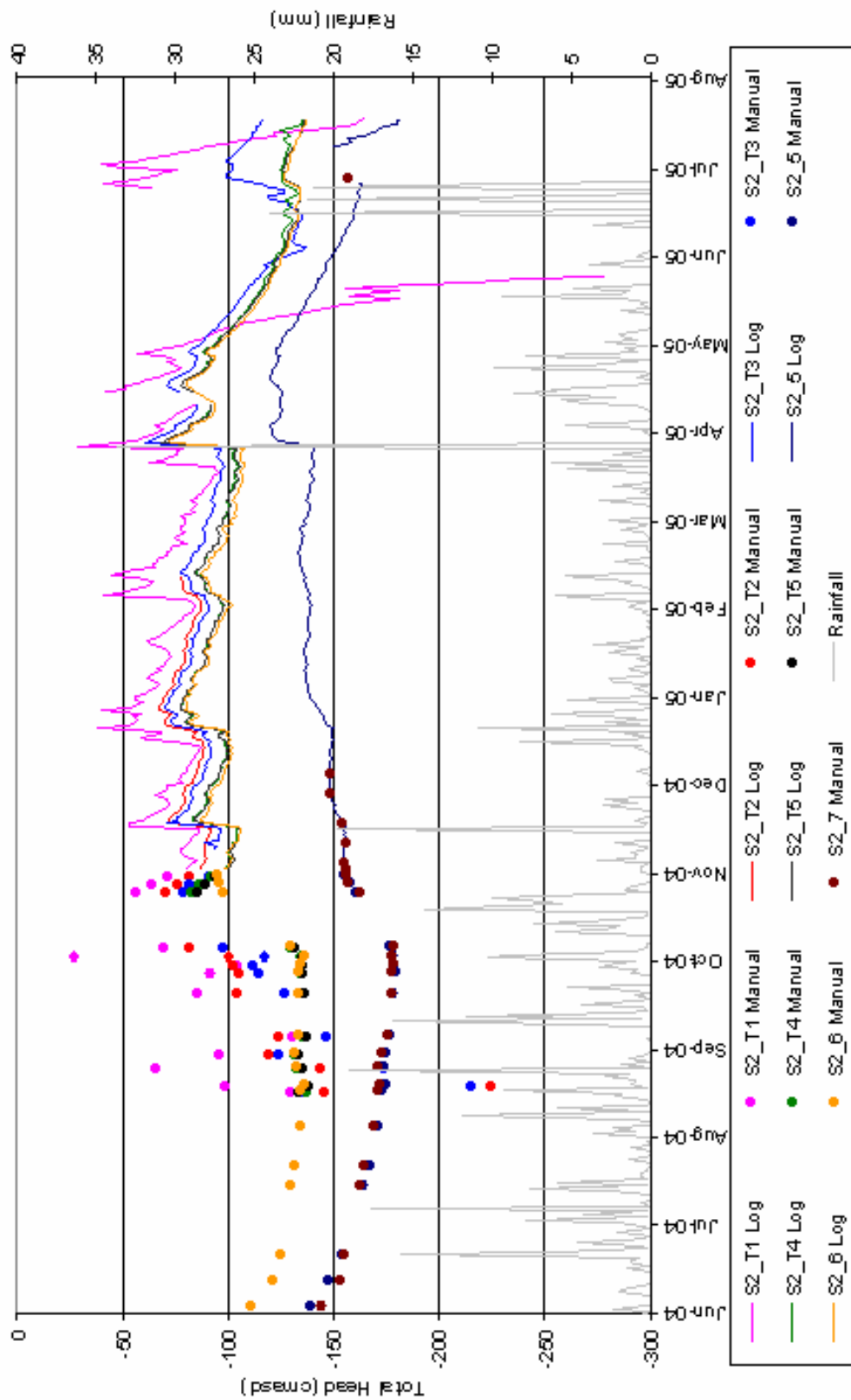


**Figure 6.5** Time series of average daily total heads recorded at Site 2 piezometers and tensiometers (cm above site datum (cmsd))

The water table recorded at the location of the tensiometer nest shows a very similar variation to that recorded in S2\_6. Water levels implied by the TDR results indicate that the water table at S2\_M1 varies in accord with piezometers S2\_5 and S2\_7 but that levels at S2\_M2 and S2\_M3 are in the higher range recorded by piezometer S2\_6 (as discussed in Section 6.2.3). Groundwater levels monitored by each tensiometer and piezometer within the outwash materials and water levels estimated (to the nearest 10 cm) from the TDR data on 6/12/04 are shown in Figure 6.6. When the spatial locations of the monitoring points are considered it is apparent that there is a zone of higher groundwater levels to the northwest of the site. The transition to a zone of lower water table is very sharp with a head difference of 0.5 m over just 5 m between the tensiometer nest and S2\_5. The hydraulic conductivity of the sandy materials encountered in all the invasive investigations of the site are likely to be in the range 0.1 to 4 m/d (see Section 6.2.5.1). Thus we might expect much smaller hydraulic gradients to persist across deposits of such (relatively high) permeability. A possible explanation is that a band of lower permeability material is present isolating the two parts of the site but that this has not been encountered during any invasive investigation. This argument is strengthened by the fact that between August and October 2004 the water level at S2\_6 had plateaued to a minimum level whereas levels in S2\_5 and S2\_7 continued to recede. This is suggestive of water in the north-western part of the site ponding against a low permeability barrier during the summer. In the winter months as water levels increase above the level of this barrier water can once more flow laterally away as indicated by the recession during winter dry periods. The plateau in the summer water levels is also strong evidence of minimal vertical flow into the glaciolacustrine clay beneath the outwash deposits.

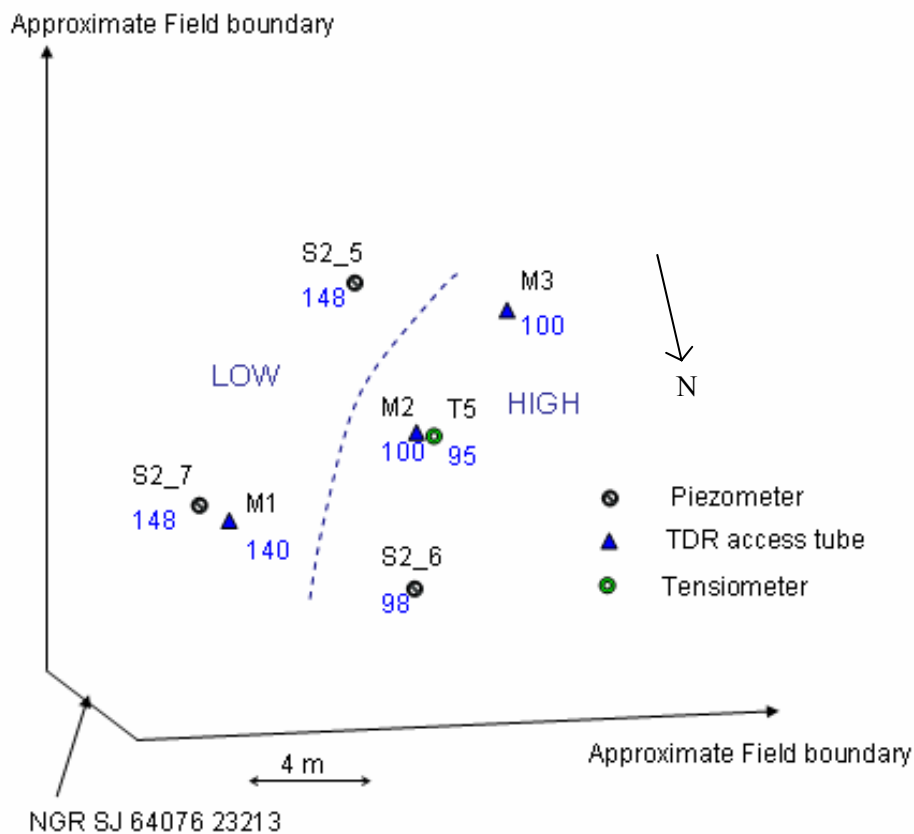


**Figure 6.6** Water table position (cm below site datum (cmbds)) within glacial outwash materials at Site 2 on 6/12/04

To test these ideas three holes were augered to a depth of 1.5 mbgl at equal intervals in between piezometer S2\_5 and TDR tube S2\_M2. A sandy clay was encountered at around 0.5 mbgl in the central hole which persisted to the base of the auger hole becoming more sandy and gravelly with depth. This deposit was not encountered in the other auger holes and appears to be very localised. If the clayey material encountered in the central auger hole is responsible for the step in the water table, it is likely that the feature is continuous. Thus it must be relatively steeply dipping since it was not encountered in the auger holes to either side. Such a deposit is unlikely to have been laid down by fluvial processes and is more likely to be a post-depositional feature caused by, for example, faulting. Faulting of Pleistocene deposits in the UK has been reported in the literature and may be caused, for instance, by the

movement or compression by moving ice (Taylor 1958), or by tension induced by the cooling of frozen ground in winter (Shotton 1965). There is no evidence of the presence of overriding ice in the area since the deposition of the outwash materials and therefore the most likely mechanism for faulting in this instance is tension induced slippage. It is possible that a modest amount of fine grained material smeared along such a fault may be sufficient to maintain the stepped water table observed at the site. However, further invasive investigations so close to the monitoring installations were not carried out to minimise interference with the site hydraulics, and without more evidence this explanation cannot be tested further.

The tensiometers generally performed well although pressure effects due to freezing of the water column occurred at times correlated with sub-zero ground temperatures. Several examples of this are shown in Figure 6.3. Two tensiometers permanently malfunctioned during the monitored period due to a failure of the electronics but the exact cause of the problem has not yet been discovered.

Between late October 2004 and early May 2005 the hydraulic gradient between all the tensiometer locations was downwards implying that recharge was occurring to the water table within the outwash deposits. During this period S2\_T4 and S2\_T5 recorded positive pressures (essentially acting as piezometers) monitoring the position of the water table whereas S2\_T1 to S2\_T3 recorded pressure heads of -70 to 20 cm. After periods of intense or persistent rainfall the pressures in each tensiometer from the surface downwards rose sequentially as the pressure wave induced by the addition of water at the ground surface travelled down the profile. The downward hydraulic gradients increase quickly after such rainfall events and then reduce slowly as the pressure heads recede during drier periods. The

response at the water table (between 0.7 to 1.0 mbgl in the winter period) is of the order of hours implying a very quick propagation of the pressure wave through the unsaturated zone.

During the spring, as temperatures began to rise and the evapotranspirative demand due to plant growth increased, tension in S2\_T1 increased very rapidly from 50 to 250 cm during May 2005 alone. Pressures in the lower tensiometers decreased more gradually meaning that an upward hydraulic gradient was induced across an increasing depth of the unsaturated zone over the beginning of the summer period in 2005. During June 2005 a series of intense rainfall events reversed this situation leading to a summer recharge event. During July and August 2004 there was also significant amount of rainfall causing wetting of the topsoil. Since the wheat crop was at full height by this time and its transpirative demand was diminishing, tensions in S2\_T1 were able to decrease significantly and the wetting of the profile began with the creation of a downward hydraulic gradient from the topsoil downwards. This wetting continued through September until a persistent downward hydraulic gradient was in place by October.

## **6.2.3 Moisture Content**

### **6.2.3.1 TDR**

As described in Chapter 4 three TDR access tubes have been installed and monitored at Site 2. During tube installation samples were taken at 10 cm intervals and gravimetric moisture contents calculated using Equation 3.2. Moisture contents by mass were converted to approximate moisture content by volume using Equation 3.7 assuming a constant bulk density of  $1500 \text{ kg/m}^3$  (measured range  $1200$  to  $1800 \text{ kg/m}^3$  - see Section 3.3.4.2). A comparison between the TDR measurements taken on the day of installation and the gravimetric values is shown in Figure 6.7. The pattern of the moisture content profiles are reasonably comparable however the TDR values are consistently higher by an average of 6% and as much as 15% by

volume. Some of this error may be due to error in the gravimetric measurement and the use of a constant bulk density. For a bulk density of  $1200 \text{ kg/m}^3$  the average discrepancy is much reduced to 3%. However if a value of  $1800 \text{ kg/m}^3$  is used the average difference is around 12%. It is concluded that the TDR reliably indicate changes in moisture content at Site 2 but that the absolute values should be treated with caution.

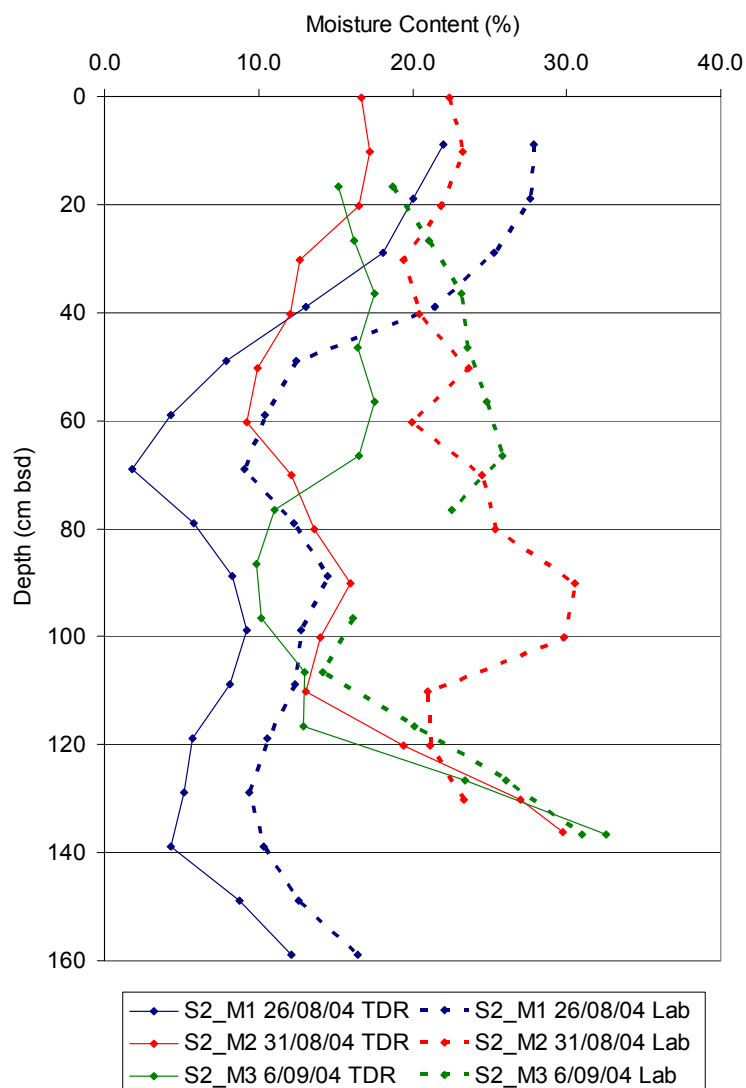


**Figure 6.7** Comparison of TDR and gravimetric moisture contents at Site 2

A selected set of approximately monthly moisture content data for each TDR access tube are shown in Figures 6.8 to 6.10 to illustrate the typical variations in moisture content.

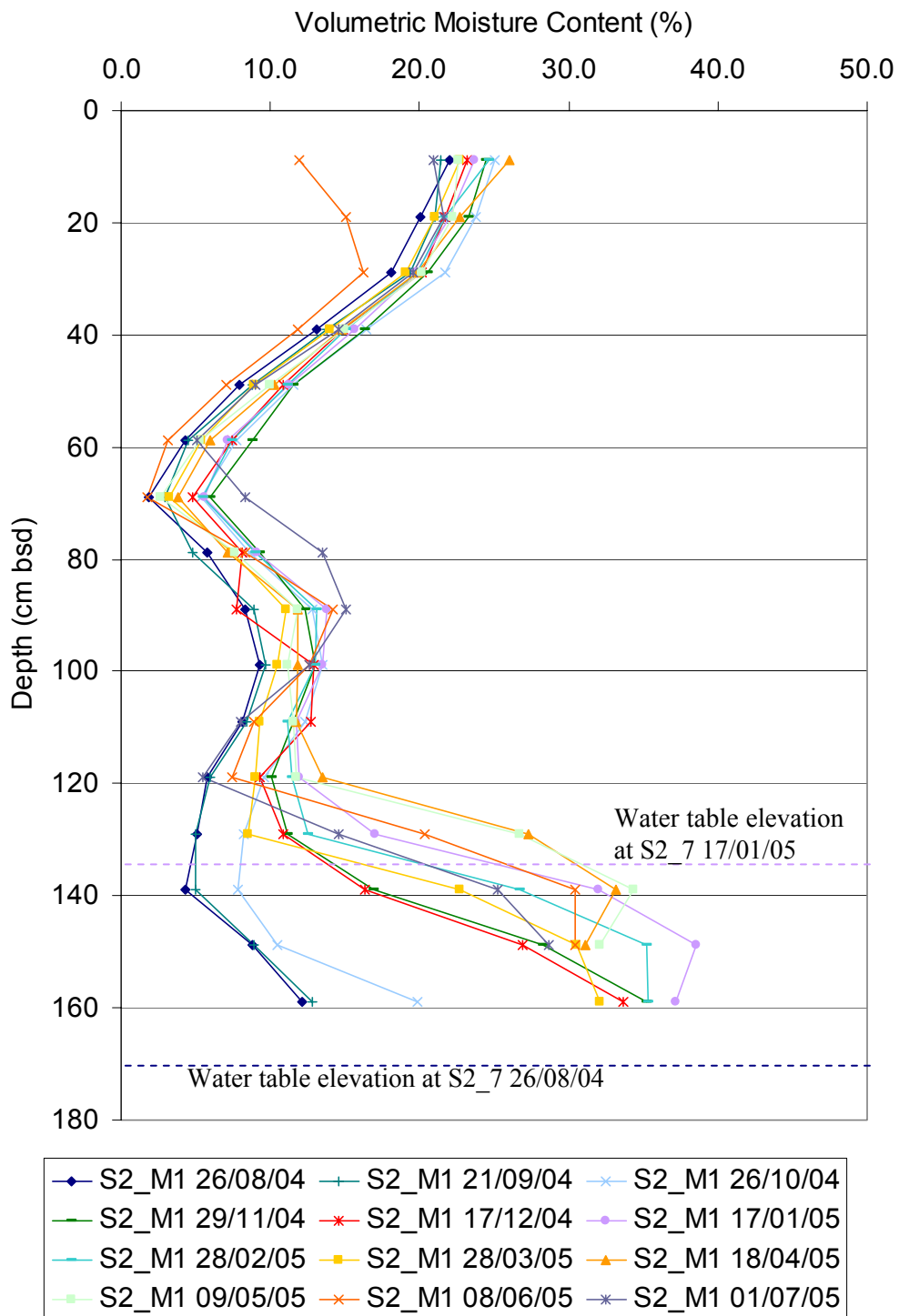


**Figure 6.8** Monthly TDR results from S2\_M1

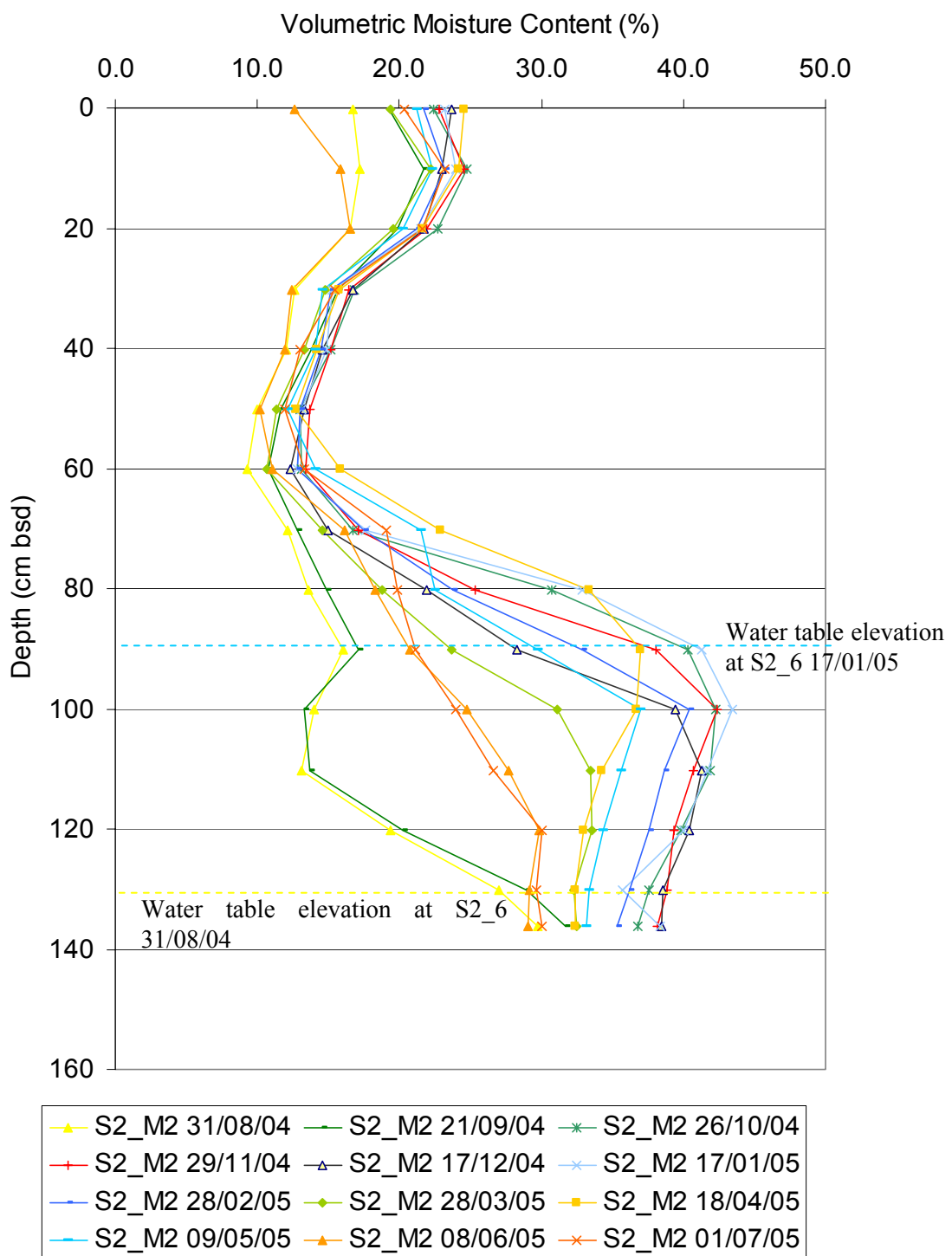


**Figure 6.9** Monthly TDR results from S2\_M2

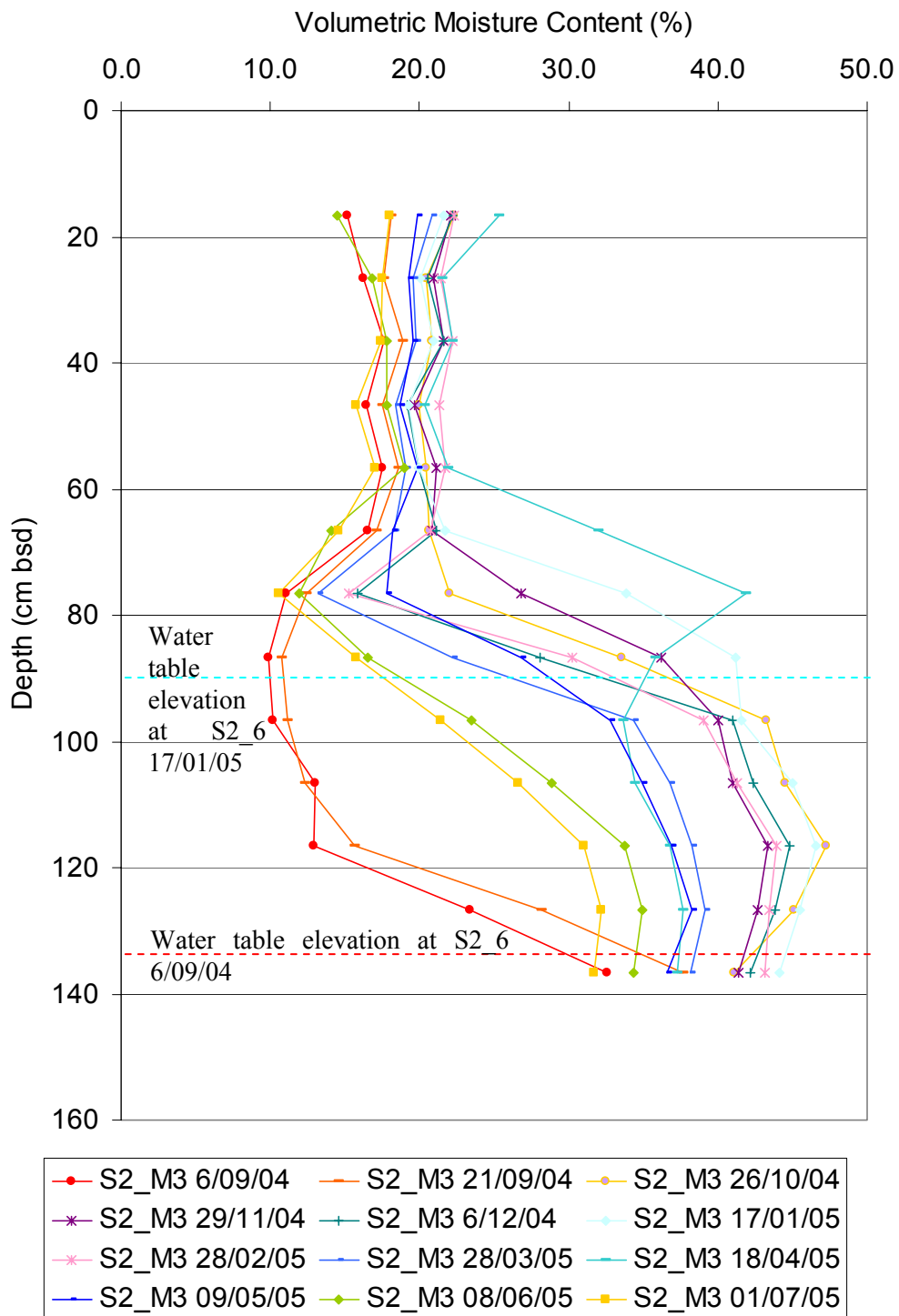


**Figure 6.10** Monthly TDR results from S2\_M3

Elevations are shown in cm below site datum (cmbds) to enable direct comparison of water table elevations with the pressure results described above in Section 6.2.2.

The pattern and magnitude of moisture content in each TDR monitoring location is very different. This is most likely due to subtle variations in grainsize distribution and hence retention properties between each location reflecting the heterogeneity of the glacial outwash materials and the derived topsoil. The changes in moisture content over time through the year, however, are similar in each location.

In the lower section of each profile the movement of the water table (shown for selected times in Figures 6.8 to 6.10) can be clearly seen to be in good agreement with the tensiometer and piezometer data presented above. As discussed previously the variation of the water table at S2\_M2 and S2\_M3 is very similar to water levels monitored by the tensiometers within the saturated zone and by piezometer S2\_6. Variations in water table elevation are also very similar between S2\_M1 and piezometers S2\_5 and S2\_7 contributing to the evidence that two zones of relatively high and low perched water are present within the glacial outwash materials at the site. Moisture contents in the zone of water table fluctuation vary between 10 and 40% by volume. Although the higher values in this range seem reasonable for the porosity of sandy materials it is likely that the lower values are significant underestimates of the actual water content as discussed above.

Above the zone of water table fluctuation but below the topsoil (top 0.5 m) only small variations of around 5% moisture content by volume are seen between the wettest and driest monitored periods. In itself this may suggest that the materials are relatively permeable so that larger head gradients (and therefore higher moisture contents) are not required to drive the downward flow of recharging water. Alternatively it may be that the magnitude of the recharge is small. Given the significant variation of water table within the outwash deposits (greater than 0.6 m) and the high hydraulic conductivity measured in the laboratory the former

hypothesis is to be favoured. The small variation in moisture content at this level in the profile may also indicate that only a low degree of evapotranspiration occurs throughout this zone.

The upper 0.5 m of the profile within the topsoil shows a large variation in moisture contents in all three monitoring locations of up to 15% by volume. This is likely to be largely due to a higher evapotranspirative demand from this zone due to the higher density of roots from the wheat and grass growing on the site during the monitored period. The higher moisture contents seen in this zone are likely to be due to the finer grained organic particles in the topsoil creating a greater abundance of smaller pore throats hence enabling greater retention of water.

Although the frequency of data collection was much lower than for the pressure data from the piezometers and tensiometers, where comparison is possible the results compare favourably. The movement of the water table has already been mentioned but responses within the unsaturated zone are also seen to vary in accord with conventional unsaturated zone flow theory. To illustrate this, a plot of tension for the upper 4 tensiometers versus soil moisture (from the nearby TDR at the equivalent depth to each tensiometer cup) is shown in Figure 6.11. The lowest tensiometer was always below the water table and therefore is not plotted. Although only a low range of tensions are available this figure shows that the relationship between soil moisture and tension is of the form expected by conventional unsaturated zone theory (Tindall and Kunkel 1999) even if there is some uncertainty over the absolute values of moisture content.

In summary the TDR measurements have proved to be a useful tool in observing the changes in moisture content at the site. However for the technique to be accurate for absolute

measurements of soil moisture a robust site specific calibration is needed for a range of materials sufficient to account for the heterogeneity of the site.

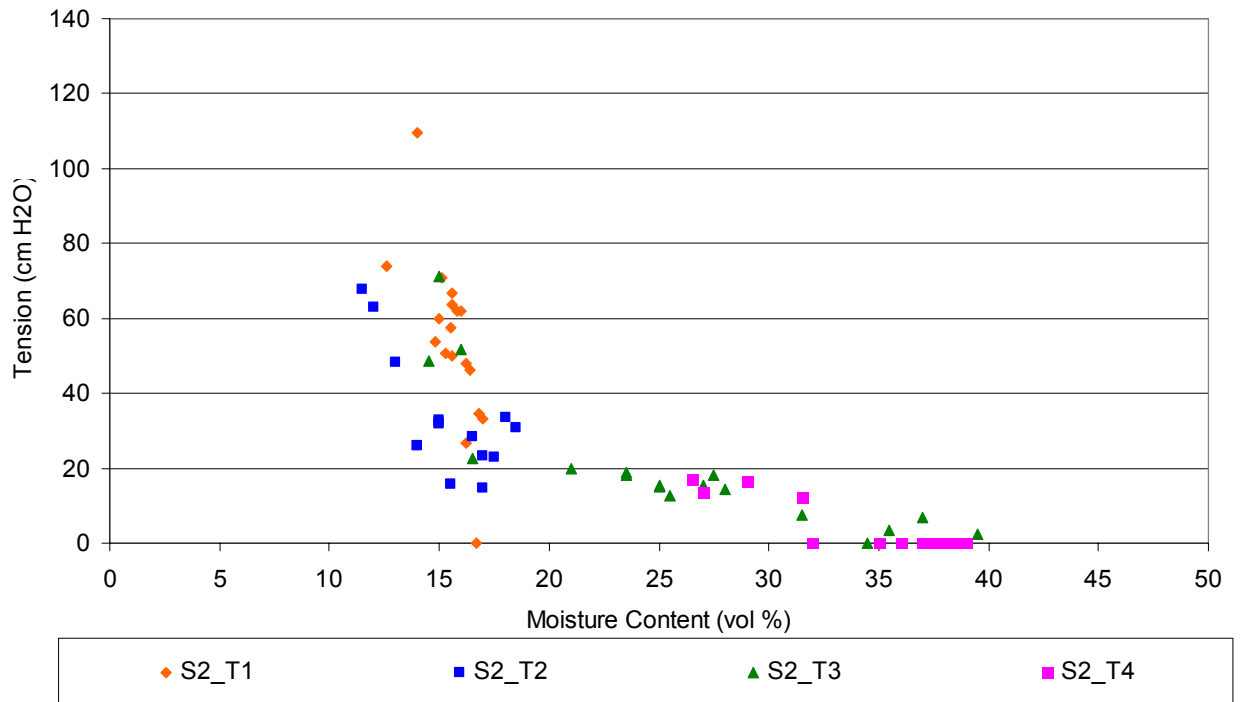


**Figure 6.11** Soil moisture (from nearby TDR) versus soil tension for Site 2 tensiometers

### 6.2.3.2 Gravimetric moisture contents from core samples

At deeper levels the moisture content distribution has been investigated using gravimetric determination from core samples using the methodology described in Section 3.2.4. The results of moisture loss (% by mass) are shown in Figure 6.12. An unquantified error associated with moisture loss during drilling and more particularly during core storage over a period of 10 days is inevitable but was minimised as far as possible by careful sealing of the cores and by keeping the cores at as low a temperature as practically possible. Thus the conclusions from these results should only be regarded as semi-quantitative.

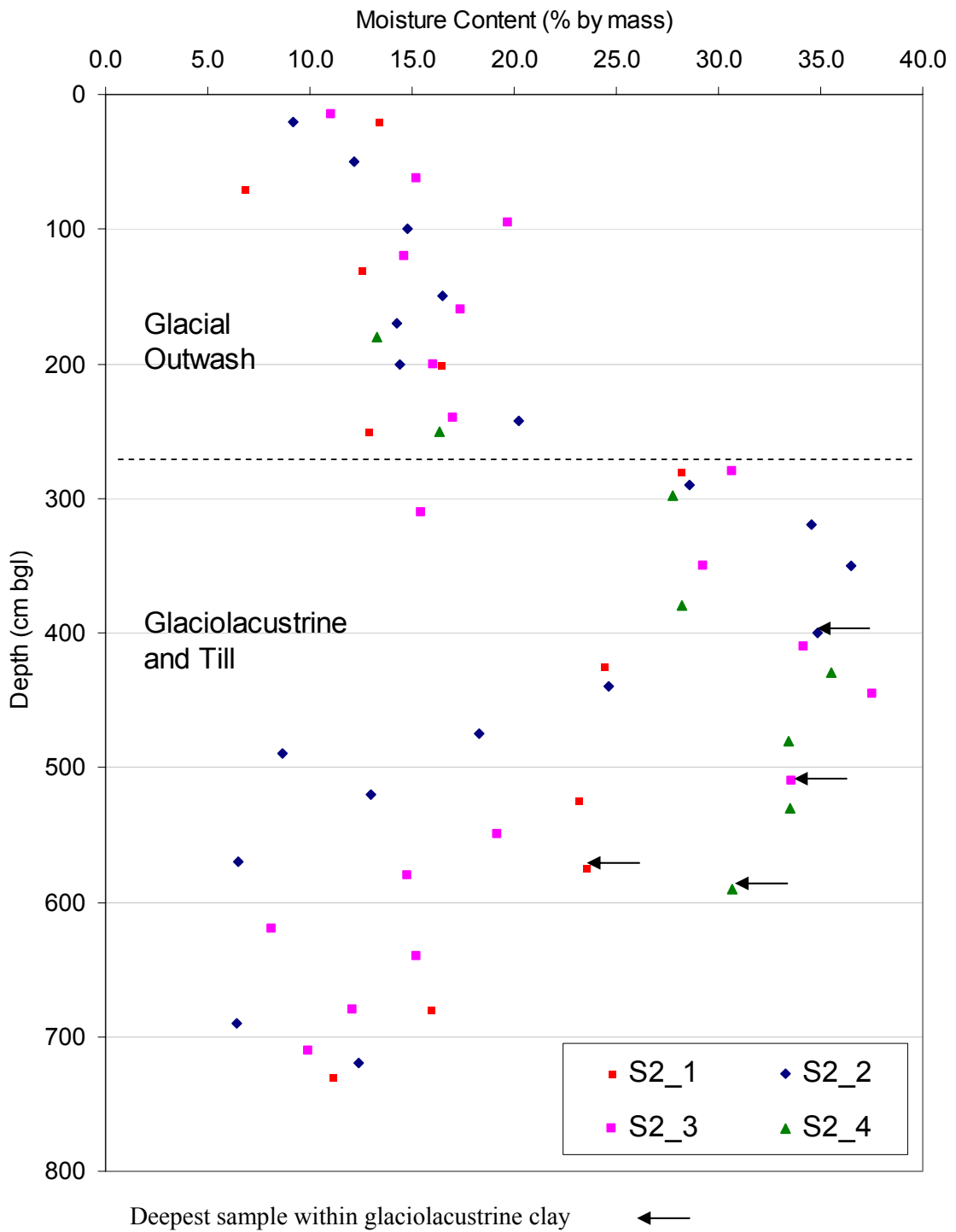


**Figure 6.12** Gravimetric moisture contents for Site 2 core samples

The upper 2.7 m of the profile within glacial outwash material shows increasing moisture contents with depth broadly in agreement with the TDR results. However, the values for

levels deeper than the water table (approximately 1.5 mbgl) are likely to be underestimates of the actual moisture content due to unavoidable loss of water while sampling saturated unconsolidated core material. Below this depth consistently high moisture contents imply that saturated conditions persist through the glaciolacustrine clay layer. Lower moisture contents are associated with till and sand layers. Since the bulk density of the till is likely to be higher than that of the glaciolacustrine materials the upper till deposit seen in S2\_2 is likely to be at or near full saturation. The results suggest that the glaciolacustrine sand layers and the lower till layer are likely to be only partially saturated.

#### **6.2.4 Infiltrometer Tests**

The results of the three double ring infiltrometer tests carried out at Site 2 (locations shown in Figure 4.2) are shown in Figure 6.13.

The results for the Test 1 and 3 are similar and although the infiltration rate does not quite reach a constant value within the timescale of the test the curve is of the expected form. At larger times the infiltration rate is likely to be around 0.1 cm/min (1.4 m/d). The departure of the results from a smooth curve may be due to heterogeneity and layering in the soil profile. Test 2 indicated a much lower rate of infiltration than Tests 1 and 3 but the rate settled to a constant value after around 30 min of around 0.01 cm/min (0.1 m/d).

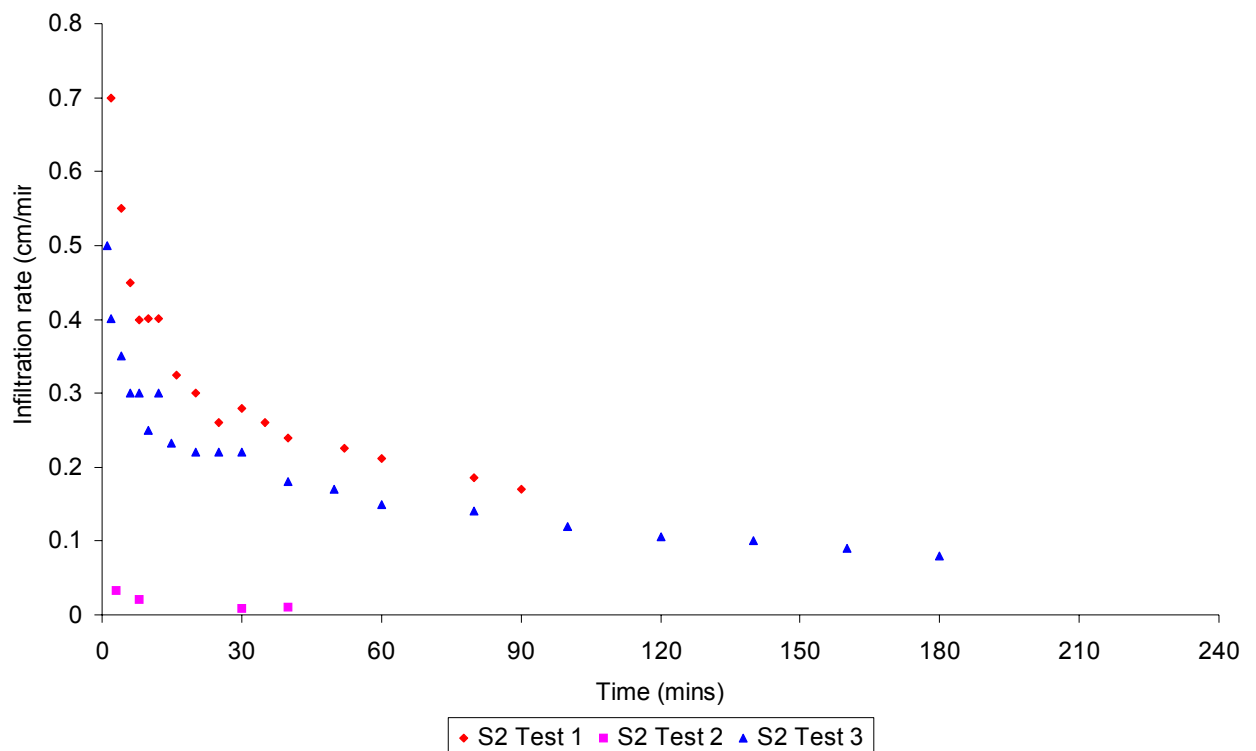


**Figure 6.13** Infiltrometer tests results for Site 2

The maximum rainfall intensity recorded during the year March 2004 to February 2005 at Oakley Folly (T17) was around 0.36 m/d (15 mm/hour) and the intensity was only greater than 6 mm/hour (0.01 cm/min) for 7 hours during this period. Assuming that the infiltration rates measured during the three tests are representative of the site it is unlikely therefore that surface ponding will be a common occurrence. This is in accord with field observations of the site over the research period indicating that even during intense rainfall events prolonged ponding (greater than a few minutes) only occurs within small areas associated with increased compaction such as wheel ruts from agricultural machinery.

## 6.2.5 Piezometer Tests

### 6.2.5.1 Glacial outwash deposits

Piezometer tests were carried out on all three piezometers screened within the glacial outwash materials. The results are plotted in Figures 6.14 to 6.16. Owing to the fast head change

observed in the test on S2\_7 only 4 data points were collected. However, straight line plots with reasonable fits were achieved in all three cases. Values of hydraulic conductivity of 0.7, 0.1 and 3.8 m/d resulted from the Hvorslev analysis for piezometers S2\_5, S2\_6 and S2\_7 respectively. Two of these values are lower than the range of vertical hydraulic conductivity derived from the constant head tests presented in Section 3.3.4.2. The most likely explanation for this is that the constant head tests overestimated the hydraulic conductivity of the samples due to density changes and other disturbance during drilling and sampling.

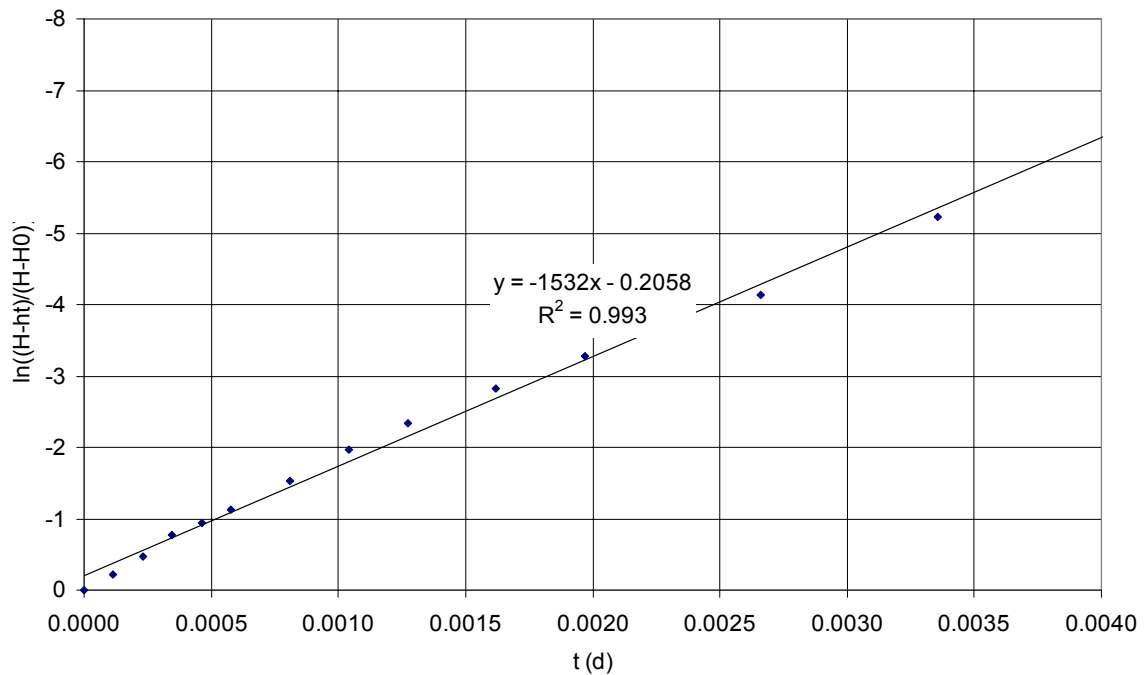


**Figure 6.14** Piezometer falling head test results for S2\_5

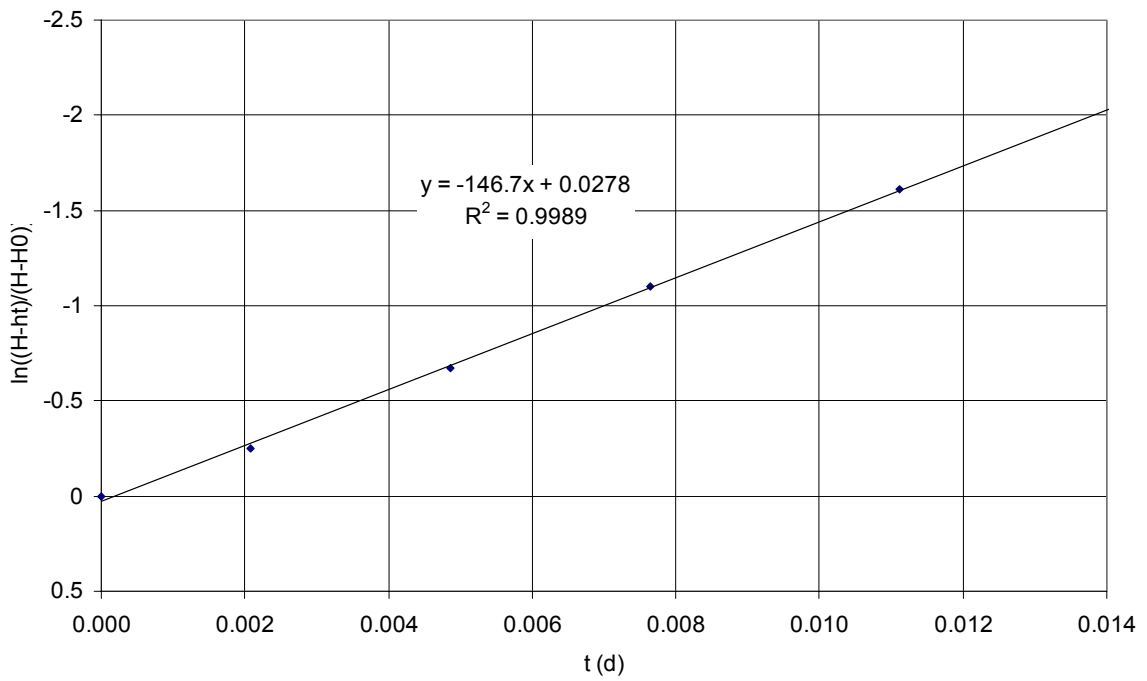


**Figure 6.15** Piezometer falling head test results for S2\_6

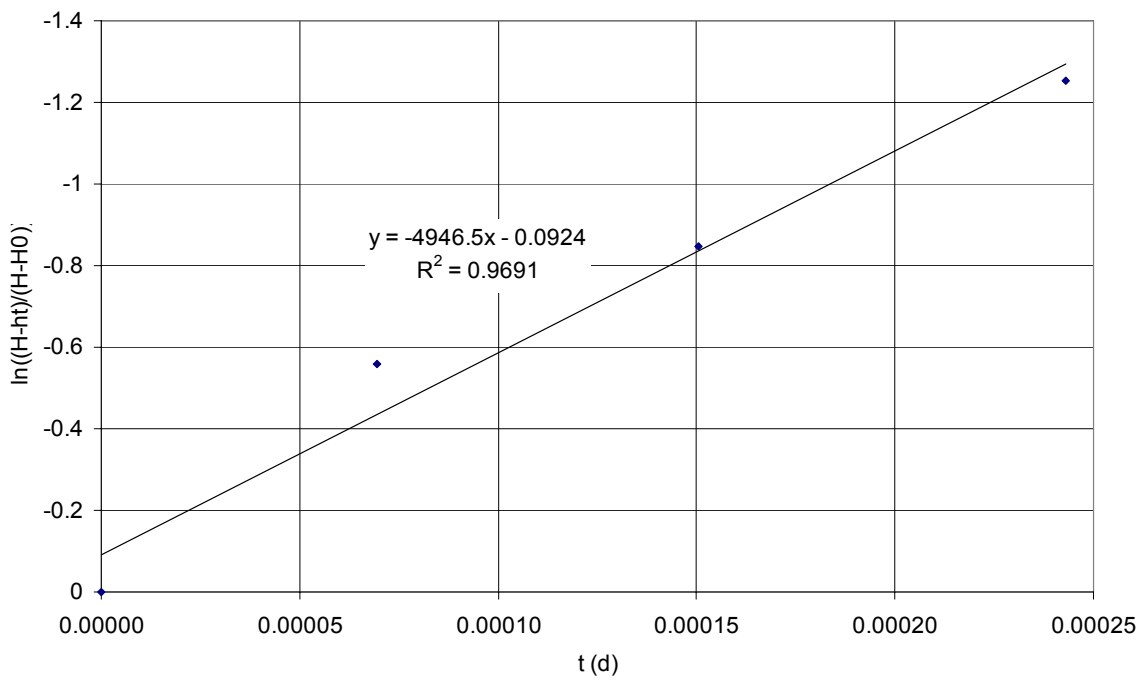


**Figure 6.16** Piezometer falling head test results for S2\_7

### 6.2.5.2 Glaciolacustrine and till

As noted above in Section 6.2.2.2 the three piezometers screened within the deeper drift below the glacial outwash deposits were dry for the period of monitoring. Falling head piezometer tests were carried out in these piezometers and for the Hvorslev analysis the initial pressure head ( $H$ ), using the base of the piezometer as a datum, was set to an estimated likely value based on modelling results presented below in Section 6.4.1.

Owing to the negative pressure head within the formation around the screen interval the gravel pack was partially saturated. As a result the head change for all three tests at early time (a few minutes) was relatively rapid until the gravel pack had become fully saturated. For later times all three tests plot in a straight line ( $R^2 > 0.98$ ) and  $\frac{L}{R} > 8$  enabling a relatively confident analysis using the Hvorslev methodology. The plots for late time are shown in Figures 6.17, 6.18 and 6.19 for piezometers S2\_3, S2\_4 and S2\_8 respectively.

Assuming  $H = 0$  the hydraulic conductivity for the test on S2\_3 is around  $3 \times 10^{-8}$  m/s. However on the basis of modelling presented below the likely maximum suction around the piezometer screen just above the till-sandstone boundary is around 100 cm. Using this value for  $H$  the hydraulic conductivity is around  $8 \times 10^{-9}$  m/s, a reasonable value for till based on the range of laboratory values given in Section 3.3.4.3.

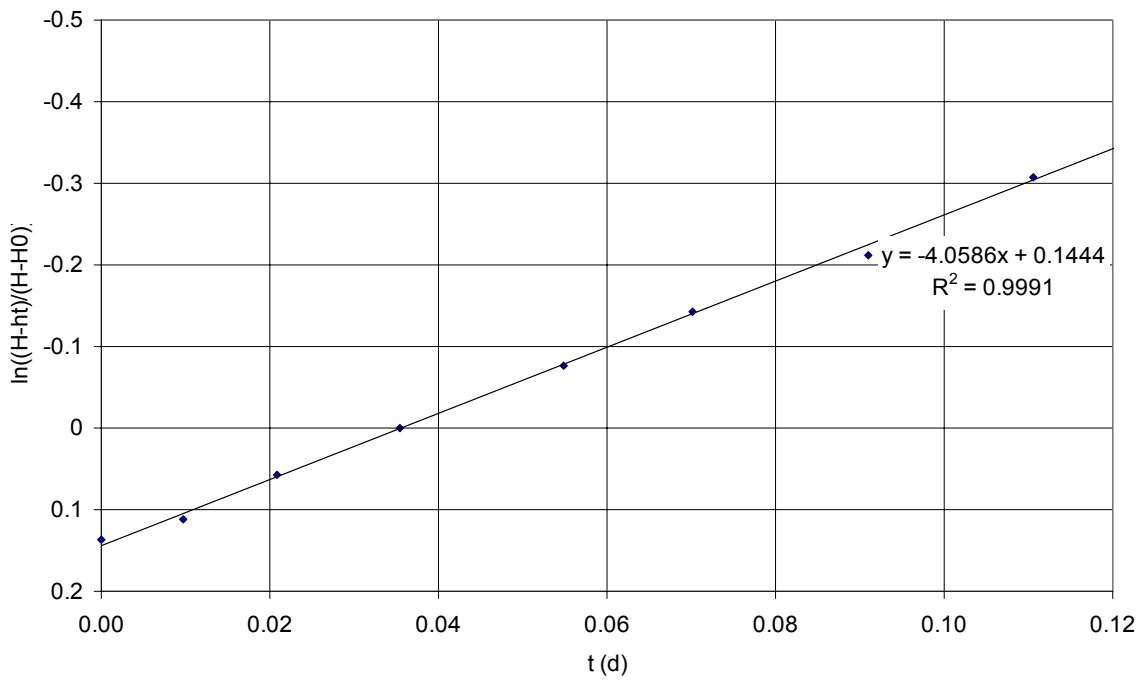


**Figure 6.17** Piezometer falling head test results for late time at S2\_3

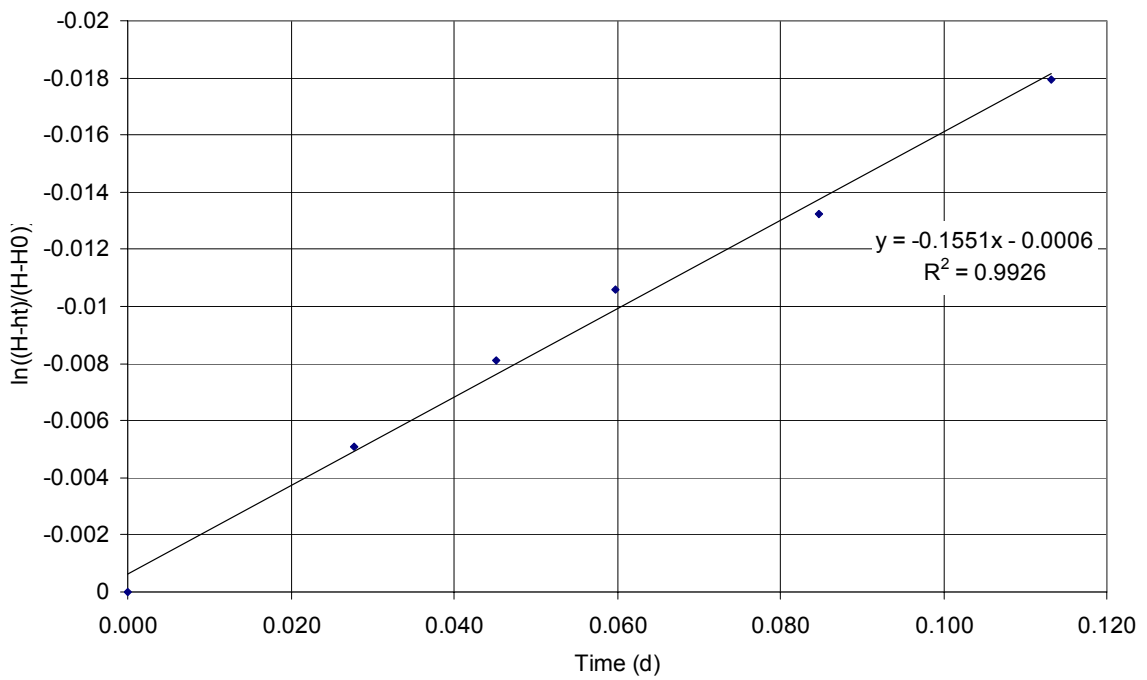


**Figure 6.18** Piezometer falling head test results for late time at S2\_4

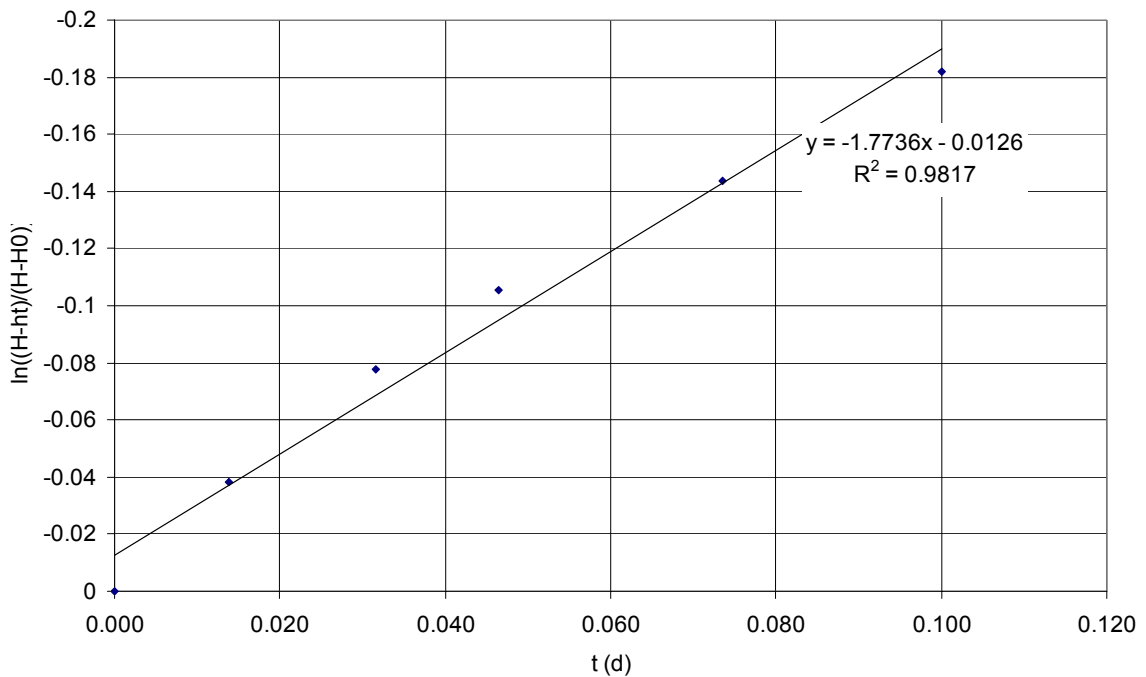


**Figure 6.19** Piezometer falling head test results for late time at S2\_8

The modelling presented below suggests that the pressure head around the piezometer screens of S2\_4 and S2\_8 is unlikely to be significantly less than zero. Assuming an initial head of zero the approximate horizontal hydraulic conductivity for the glaciolacustrine clay in which S2\_4 is installed is around  $1 \times 10^{-9}$  m/s. This is within the range of the laboratory values for this type of deposit presented in Section 3.3.4.4. The result for S2\_8 is around  $1 \times 10^{-8}$  m/s again assuming an initial head of zero. The bottom part of the piezometer screen is within a glaciolacustrine sand layer but due to a build up of sediment at the base of the piezometer tube it is uncertain how much flow occurred into this horizon during the test. It is likely that the result represents an overestimate of the hydraulic conductivity of the till in which the rest of the screened section is located.

### 6.2.6 Tracer Test

The results of tracer concentrations with depth are shown in Figure 6.20.

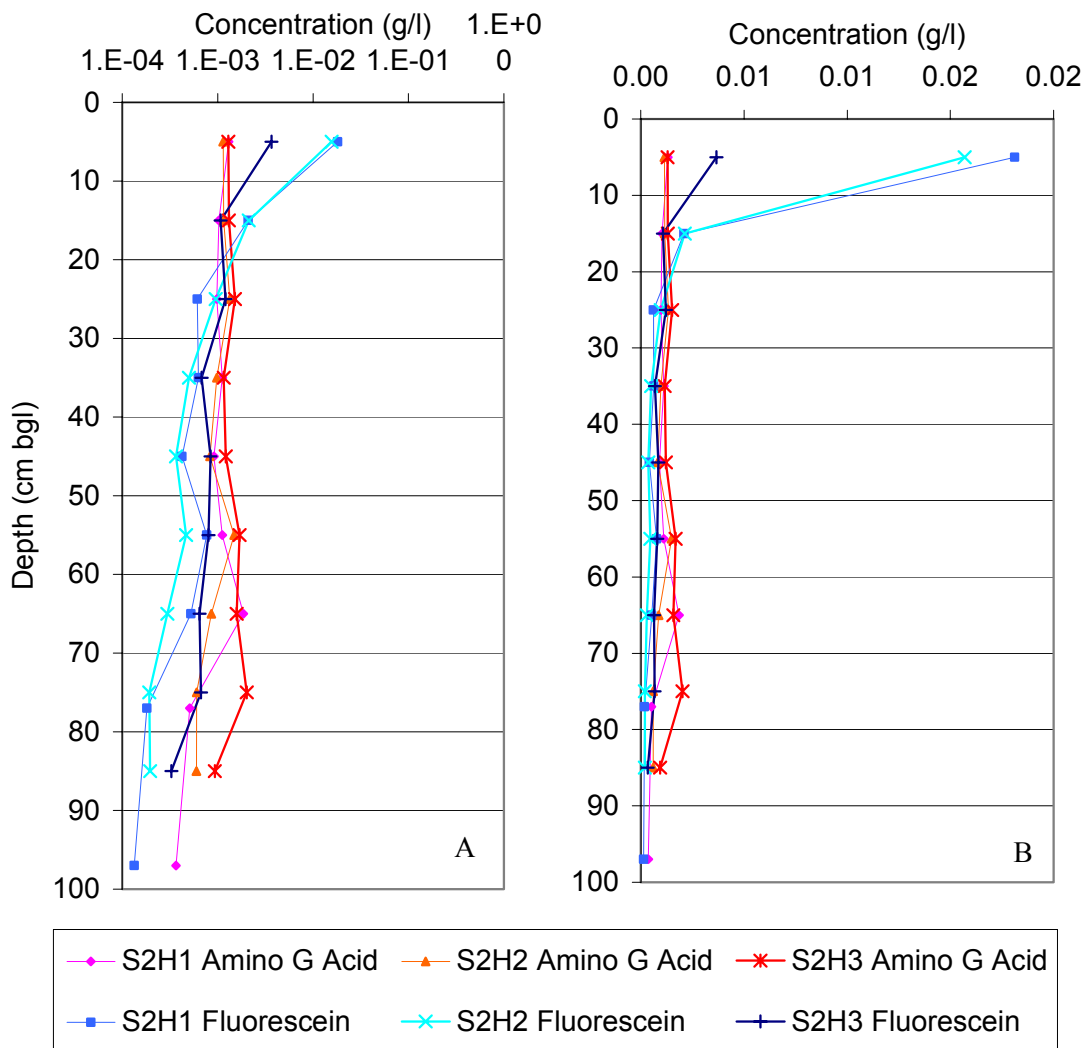


**Figure 6.20** Tracer distributions at Site 2 after 108 days (S2\_H1) and 120 days (S2\_H2 and H3) since tracer application with log (A) and linear (B) scales

As for Site 1 the results show relatively low concentrations of amino G acid throughout the profile with a variation of just 1 order of magnitude and a recovered mass of 20 to 30% of the interpolated recovery (calculated from the applied mass per unit area). Furthermore all the results are within the range of possible background fluorescence due to natural dissolved organic matter. The results for amino G acid are thus inconclusive.

The results for fluorescein show more variation with a trend of decreasing concentration between the top and bottom of the profile spanning 2 orders of magnitude. The mass recovered was between 20 and 50% of the interpolated recovery. However, it is noted that a large proportion of the retained mass is within the upper 10 cm of the profile implying that a significant proportion of the applied tracer has been retained at/near the surface layer to which it was applied.

The results can be interpreted in different ways. Firstly we might assume that vertical flow is uniform across the area of applied tracer (i.e. 'piston' or 'plug' flow). In this case the results suggest that the main 'pulse' of tracer passed through the profile prior to sampling and that the measured profile reflects the residual tracer retained due to dispersion and sorption. This scenario would require relatively large groundwater velocities through the unsaturated zone. Alternatively if non-equilibrium/preferential flow mechanisms are at work then the mass retained in the profile may be a function of a sampling bias and very different results may have been obtained if a larger number of locations within the area of applied tracer had been sampled. Numerical modelling is required to test which of these conceptual models is viable.

### **6.2.7 ERT**

Inverted ERT images for approximately monthly intervals from July 2004 to June 2005 are shown in Figure 6.21 for survey line 2W for which the most complete record is available. The presence of a low resistivity layer (<30 ohm-m) at just over 2 mbgl is consistent with the glaciolacustrine clay observed in the invasive investigations at a depth of around 2.6 mbgl. As expected from the results of the forward modelling presented in Section 4.3.6, the boundary between this lower resistivity layer and the higher resistivity materials above is significantly smoothed. This leads to uncertainty in the location of the boundary and to misleadingly low resistivity values for the lower section of the outwash materials.

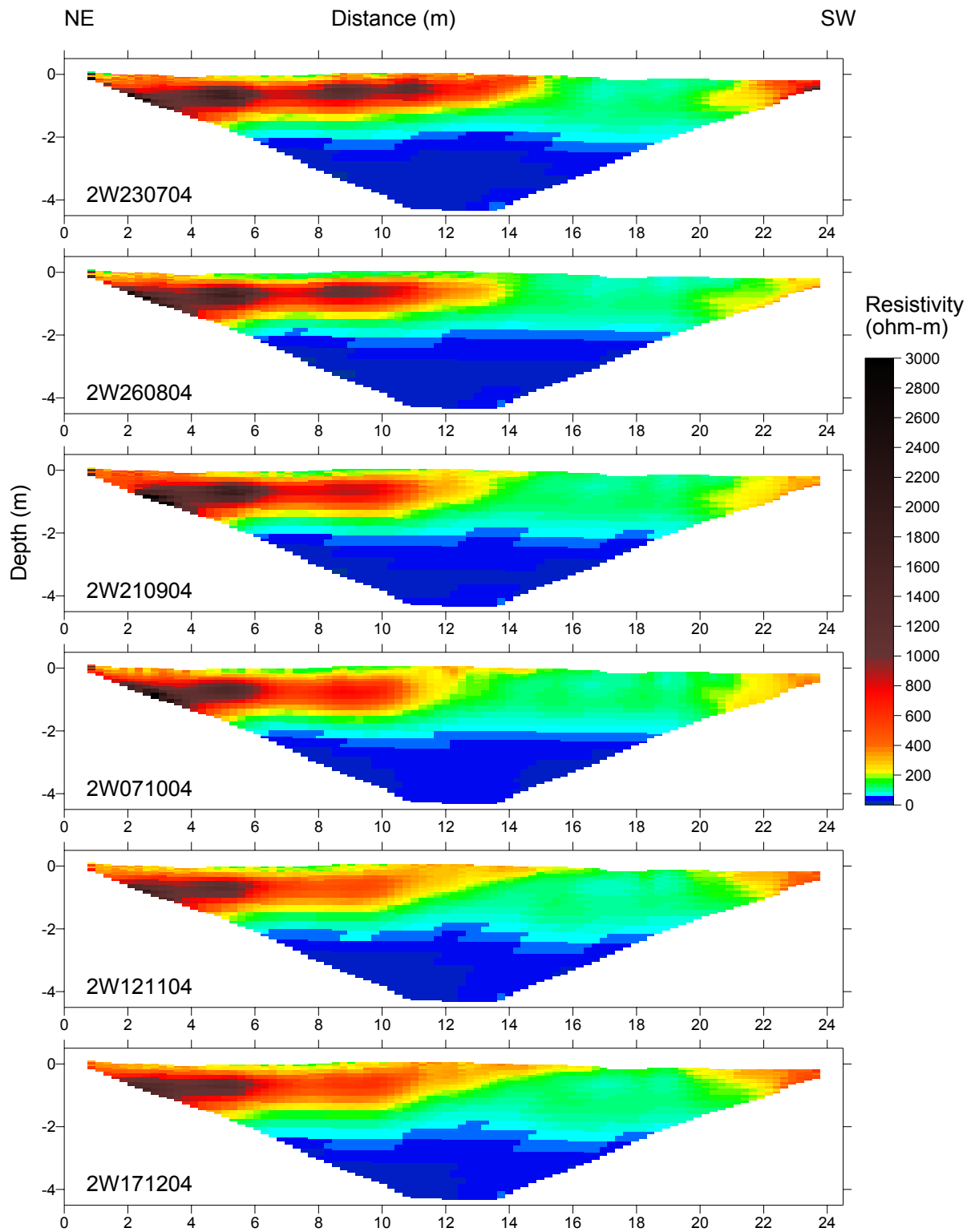


**Figure 6.21a** ERT inversions for Site 2 survey line 2W

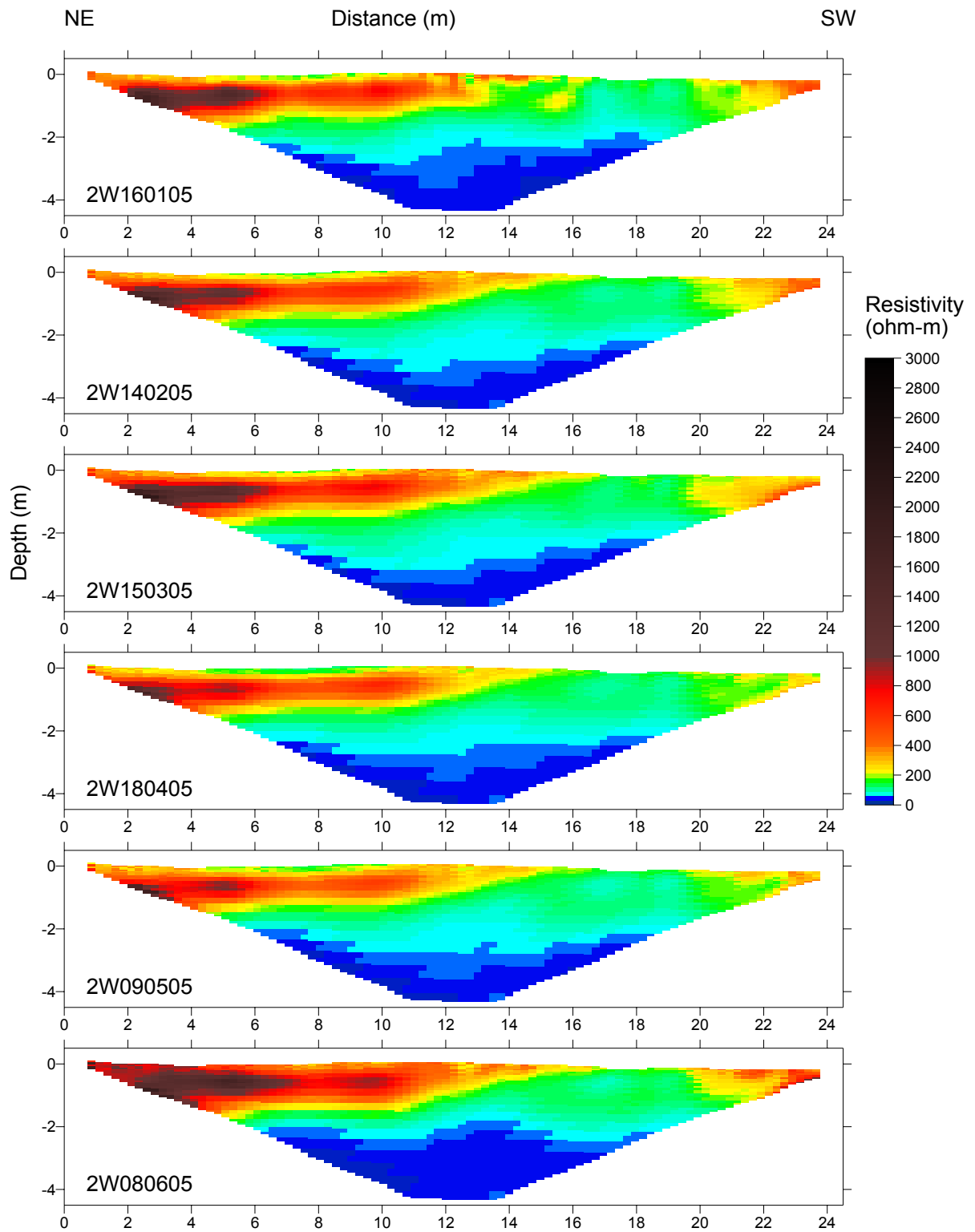


**Figure 6.21b** ERT inversions for Site 2 survey line 2W

Excluding this zone of smoothing the outwash materials vary in resistivity from approximately 80 to 3000 ohm-m although these values vary through the monitored period.

To the east of the survey line resistivity values are at a maximum but decrease steadily in a westerly direction across most of the site before increasing as the western boundary is approached. Although not shown in the figure (but included in Appendix 6) this trend is also seen in available data from survey line 2Y. Where the two survey lines cross the inverted values are very similar giving confidence in the data quality.

Difference plots between the inversion for each time interval and the inversion for 23/07/04 are shown in Figure 6.22 (i.e. resistivity on a particular date minus the resistivity on 23/07/04). Only small changes of a few tens of ohm-m are seen at depth through the year but changes in the upper 2 m of the profile are much larger ranging from approximately -1000 to 200 ohm-m. The lateral variations across the site are also significant.

A VBA script was written and implemented in Surfer Scripiter to apply a temperature correction to the data and model the moisture content using the methodology used for the forward modelling in Section 4.3.6.3 (code included in Appendix 5). The temperature and Archie parameters used were as given in Table 4.4 based on literature values for unconsolidated sands (Daily *et al.* 1992; Hagrey *et al.* 2004) with the only change being to the value of  $a$ . This was set to 0.1 to achieve a more realistic range of resistivity versus moisture content for the Site 2 data implying that the porewater resistivity is actually lower than the chosen value of 200 ohm-m. This relationship is shown in Figure 6.23. The relatively simple approach to the modelling assumes that the site is homogeneous in lithology and ignores variations in pore water salinity.

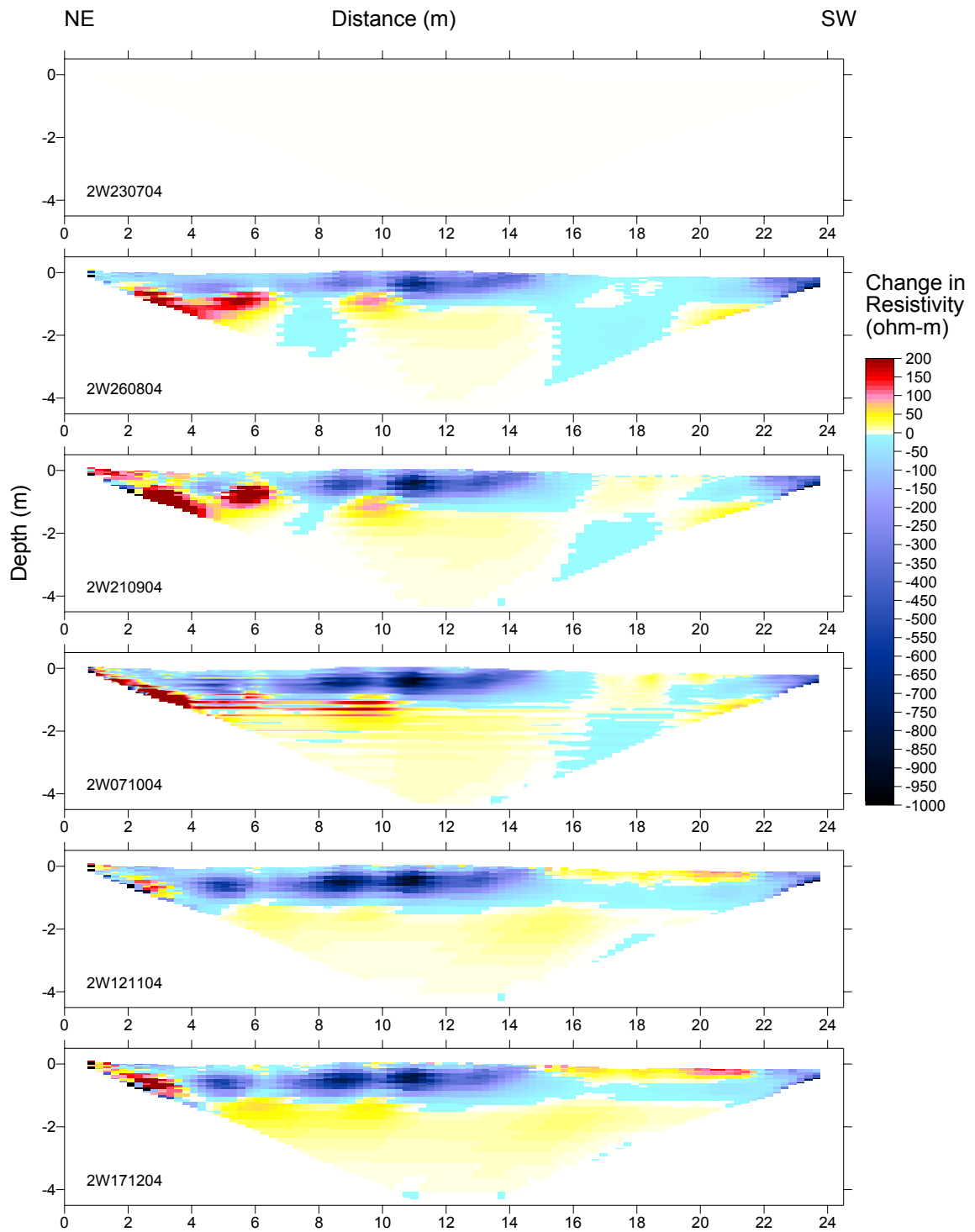


**Figure 6.22a** ERT difference from 23/07/04 for Site 2 survey line 2W (i.e. resistivity on a particular date minus the resistivity on 23/07/04)

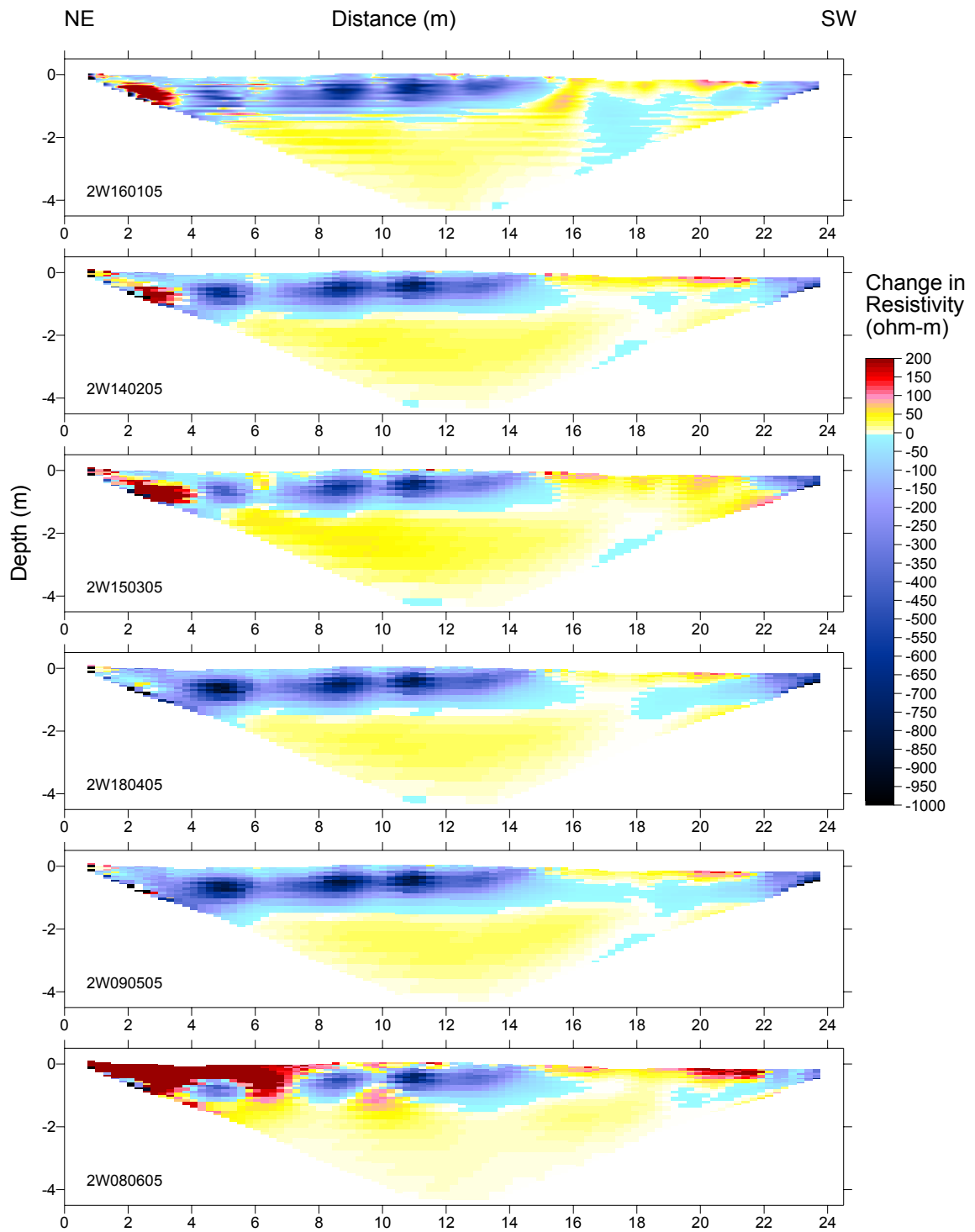


**Figure 6.22b** ERT difference from 23/07/04 for Site 2 survey line 2W (i.e. resistivity on a particular date minus the resistivity on 23/07/04)

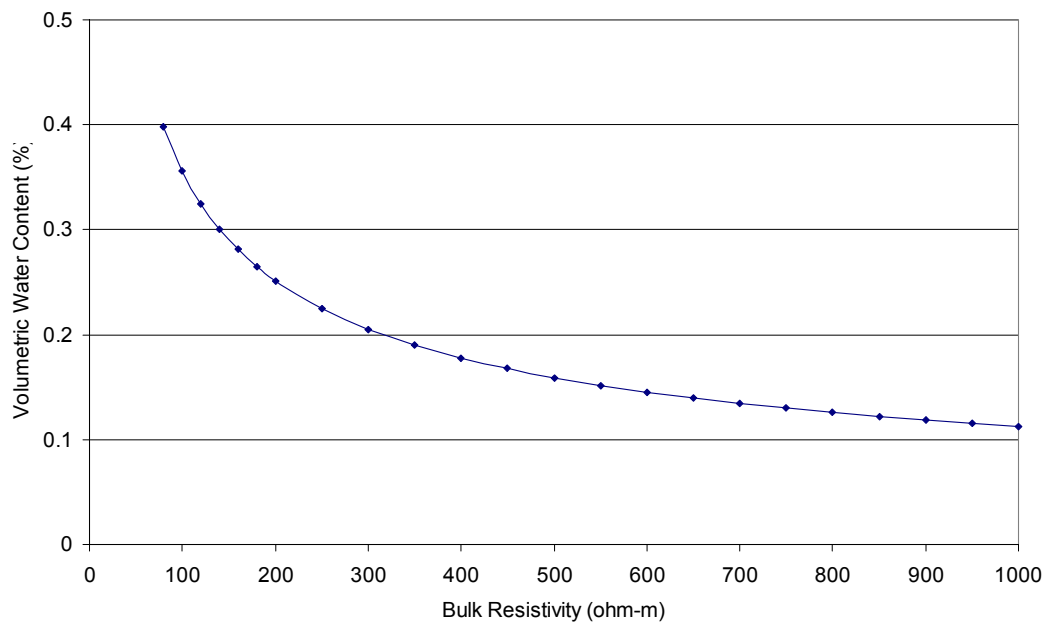


**Figure 6.23** Relationship assumed between volumetric water content and bulk resistivity based on Archie’s law for  $\varphi = 0.4$ ,  $m = 1.5$ ,  $a = 0.1$  and  $n = 2$

The results of the modelling are shown in Figure 6.24 and as differences in moisture content from 23/07/04 in Figure 6.25 (i.e. moisture content on a particular date minus the moisture content on 23/07/04). The results indicate a zone of higher water table to the west of the site consistent with the evidence presented on the basis of pressure and TDR measurements. The trend in resistivity across the site in the upper 2 m is also reflected, as would be expected, in the trend of water content from around 0.15 to 0.3 % by volume at 4 m and 18 m along the survey line respectively.

The modelled changes in water content are however disappointingly inconclusive. There is a suggestion that greater increases in moisture content may be occurring in the unsaturated zone during the winter in the central part of the site than on the periphery. However there are also decreases in water content observed below the position of the water table (1.5 +/- 0.25 mbgl for the NE half of the sections and 1.0 +/- 0.25 mbgl for the SW half) across much of the site

through the year. Significant decreases are also seen in the upper 0.5 m of the western end of the profile between summer and winter. These results are in conflict with the expectation of wetting up of the soil profile through the autumn which is seen in pressure and TDR data. This therefore casts doubt on the confidence that any expected trends seen in the results are in any way meaningful or useful for making inferences about hydraulic processes.

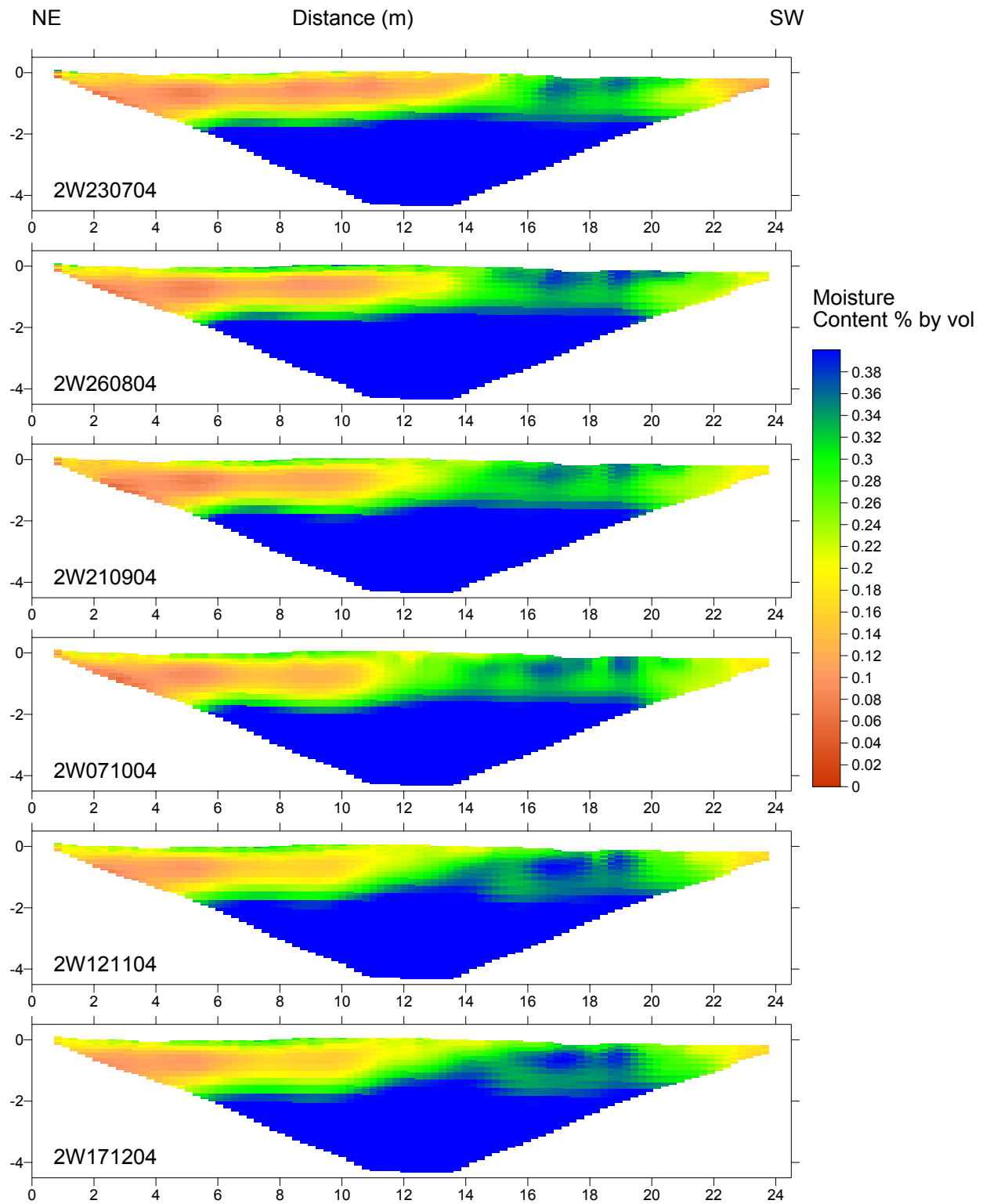


**Figure 6.24a** ERT inverted moisture content for Site 2 survey line 2W

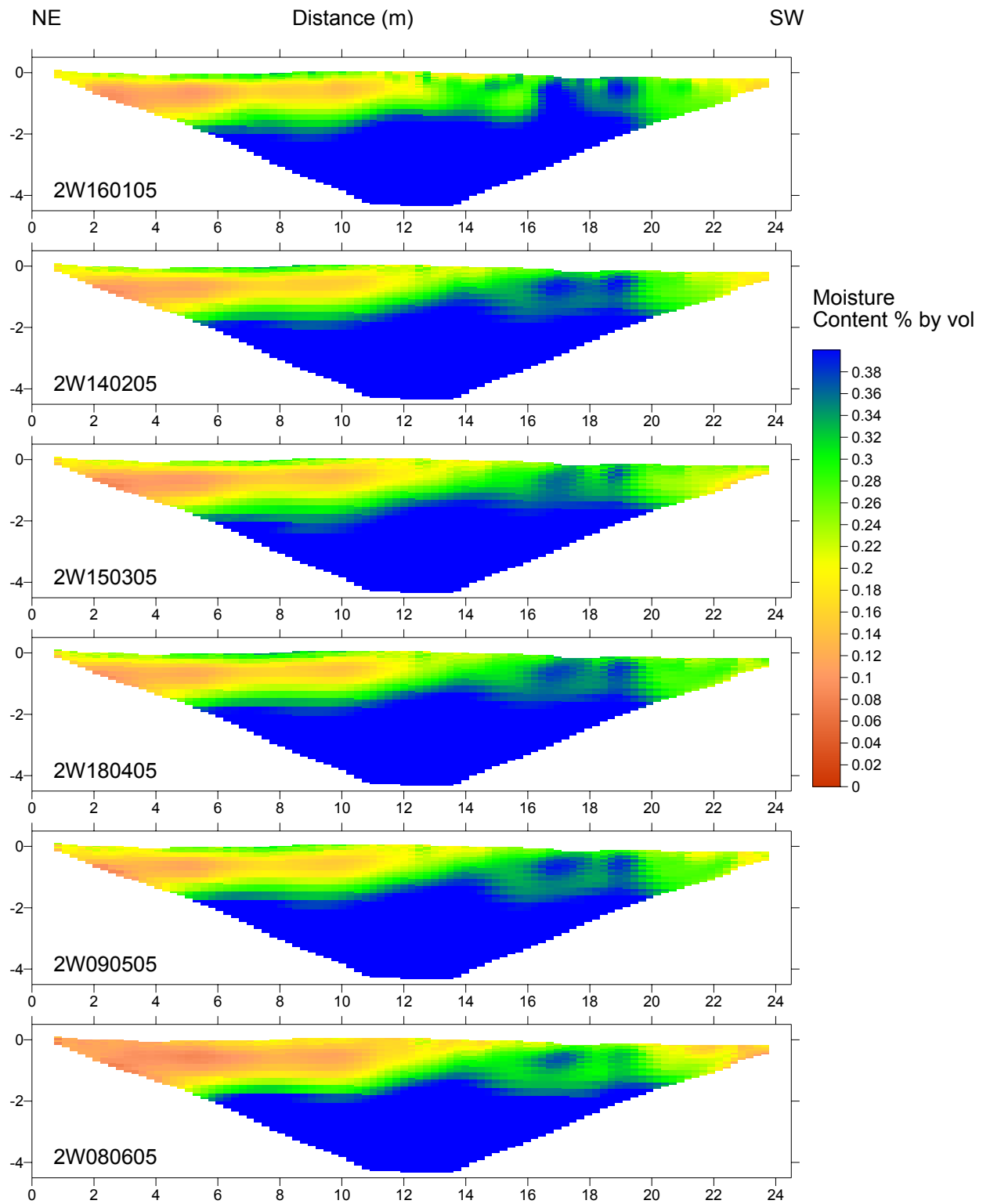


**Figure 6.24b** ERT inverted moisture content for Site 2 survey line 2W

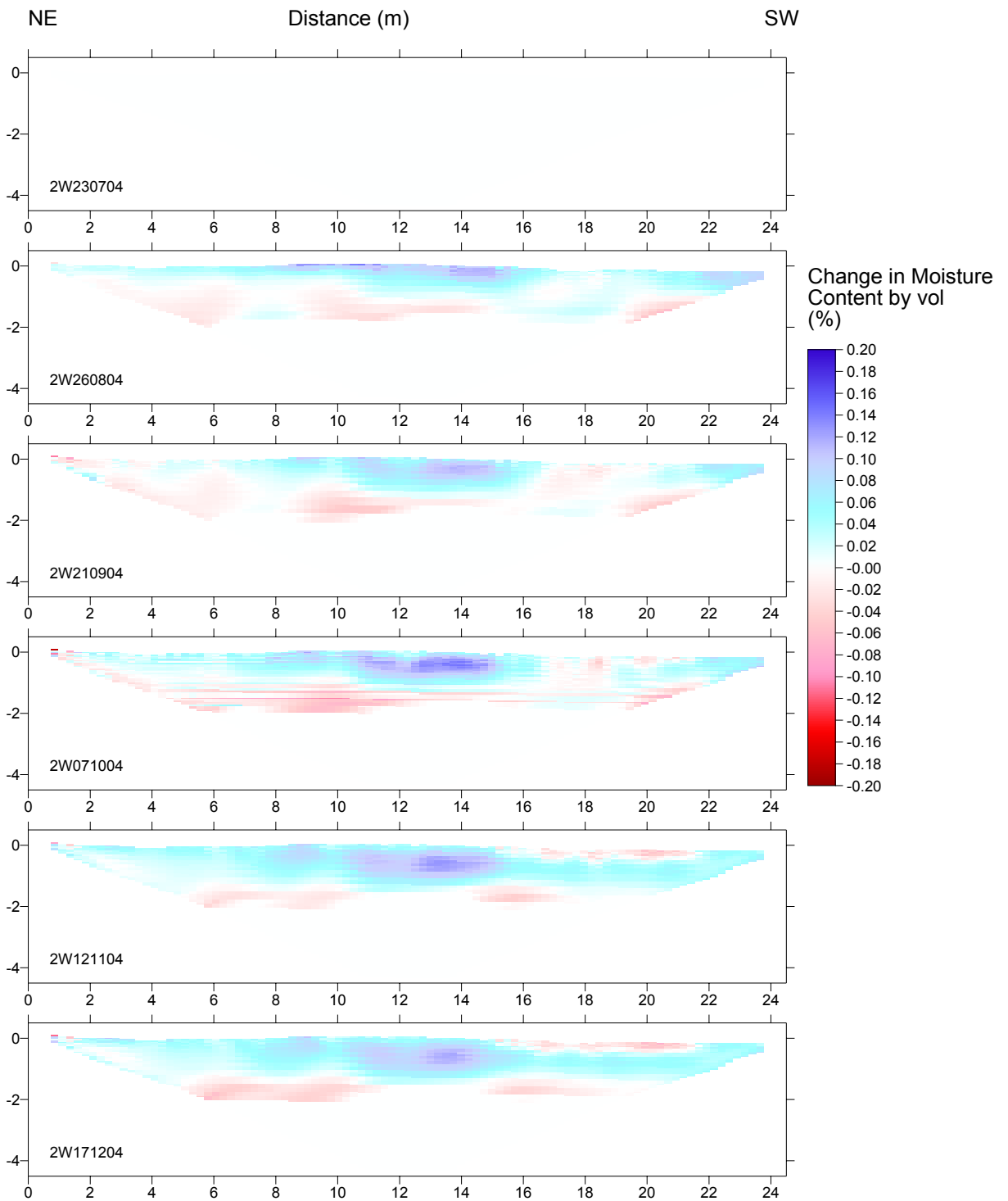


**Figure 6.25a** ERT inverted moisture content changes from 23/07/04 for Site 2 survey line 2W (i.e. moisture content on a particular date minus the moisture content on 23/07/04)

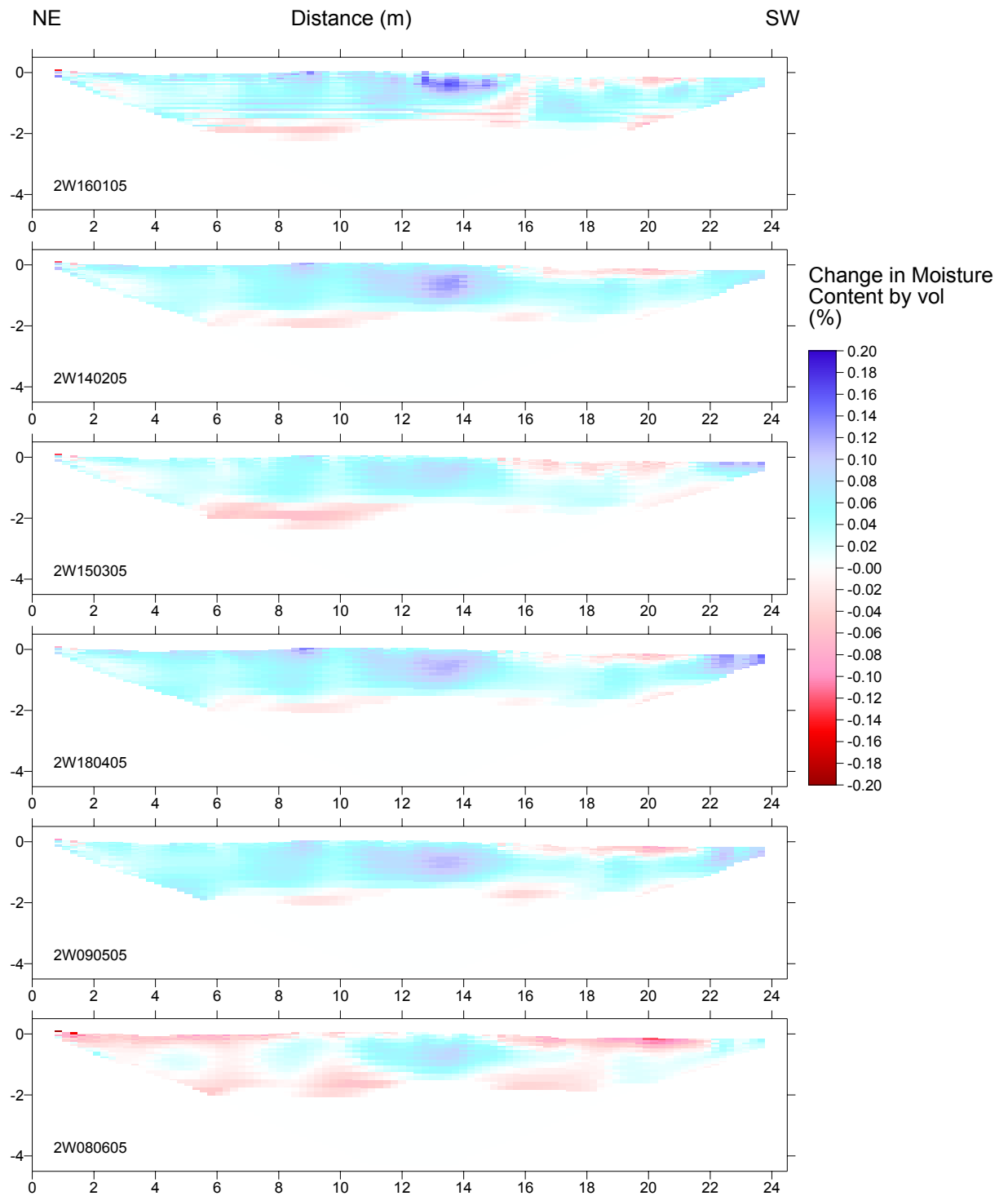


**Figure 6.25b** ERT inverted moisture content changes from 23/07/04 for Site 2 survey line 2W (i.e. moisture content on a particular date minus the moisture content on 23/07/04)

The models were re-run a number of times using a variety of parameter combinations for the temperature correction and Archie's law. However it was found that an improvement in one particular area of the model was always countered by decreased realism in other areas.

There are several reasons why the approach taken may have failed. Variations in pore water salinity due to agricultural spreading and spraying as well as natural variations due to precipitation/evaporation effects have not been taken into account. Sufficient data are not available to include this effect in a meaningful way but its influence is known to be potentially significant (Rein *et al.* 2004). Furthermore the variations in the relationship between temperature, and more particularly moisture content, and lithology are unlikely to be as simple as that described by Archie's Law. In particular the role of clay minerals in the conduction of charge has been ignored. These relationships are likely to vary with lithology which is known from invasive investigations to vary significantly within the outwash materials encountered at the site.

Hence although very useful for defining the geometry and potential lithological variations within the site the time series ERT method has not added significantly to the understanding of the site hydraulic processes. It is possible that with a significant and focussed additional data collection effort and the application of much more sophisticated equivalent porous medium modelling techniques that more useful and quantitative information might be generated. This is a significant undertaking and not within the scope of this research. For the purposes of this thesis it is enough to highlight some of the shortcomings of the technique and to rely more heavily on other types of data.

### **6.2.8 Tritium Analysis**

Samples of glaciolacustrine clay from S2\_1 (taken from 3.5 to 4.0 mbgl) and S2\_3 (taken from 4.00 to 4.25 mbgl and 4.25 to 4.47 mbgl) were sent for tritium analysis and were found to have tritium activities of  $9.5 \pm 0.5$ ,  $7.4 \pm 0.5$  and  $5.6 \pm 0.4$  T.U. respectively. A possible explanation for the decreasing tritium activity with depth is that the values represent a diffusion front with only minimal advection. Since the tritium concentration in precipitation has been highly variable over the last 50 years and that it is also subject to radioactive decay, modelling is needed to test this hypothesis. This follows in Section 6.4.2. However, first it is necessary to outline the conceptual model of the site hydraulics.

### **6.3 Conceptual Model of Hydraulic Processes**

The data and analysis presented so far in this chapter enable a picture of the hydraulic processes contributing to recharge at the site to be pieced together.

The infiltration capacity of the soil is likely to be high enough to accommodate precipitation from all but the most severe storms. Near surface runoff is therefore likely to be minimal for this reason and also given the relatively flat topography of the site. A small degree of surface ponding does occur after heavy rainfall within the wheel ruts of agricultural machinery which cut across the SW corner of the site presumably due to the decreased permeability of the near surface soils due to compaction.

A perched water table is present across the site within moderately permeable glacial outwash materials which persist to around 2.6 mbgl above a relatively impermeable glaciolacustrine clay unit. These deposits are laterally and vertically heterogeneous in terms of lithology and this is reflected in spatial variations in electrical properties and derived moisture contents within the unsaturated zone. Coarser and drier materials are generally found to the east of the

site becoming finer and moister to the west. The level of the water table appears to be delineated into two zones with a persistent head difference of around 0.5 m, levels being higher to the north-west. This is thought to be due to the presence of a band of low permeability material hydraulically isolating the two parts of the site, possibly caused by faulting.

Pressure and moisture content responses in the unsaturated zone suggest that significant recharge only occurs to the upper water table while downward hydraulic gradients persist and moisture contents are relatively high. This mostly occurs in the autumn and winter but also is seen after particularly heavy summer rainfall in late June 2005. The water table recedes following an exponential pattern during periods when it is assumed that lateral/vertical discharge exceeds the recharge flux. During the spring and summer when evapotranspiration is higher, significant soil moisture deficits accumulate and upward hydraulic gradients persist throughout the unsaturated zone for much of the time. Any precipitation which infiltrates before being evaporated is stored within the unsaturated zone with little or no pressure response seen at the water table. Hence summer recharge is generally very low (with the exception noted above). During the later part of the summer the upper water table ceases to recede suggesting that vertical flow into the glaciolacustrine clay beneath is very low and that the recession at times of higher water levels is predominantly due to lateral drainage. The ultimate destination of this lateral discharge has not been investigated and may be to field drains or perhaps to infiltration to the sandstone aquifer at some distance from the site in the manner described in Section 3.4 C.

The very quick response of the water table to precipitation, particularly in the northwest of the site, suggests that under certain conditions preferential flow processes may be occurring.

Thus it is uncertain to what extent recharge may be effectively modelled using a single porosity model implementing the Richards equation in 1-D. This will be tested below using numerical flow models.

It has already been hypothesised that only a small amount of water flows vertically into the glaciolacustrine deposits lying below the upper glacial outwash materials. Further evidence for this comes from the tritium results which are suggestive of a transport regime with a minimal advective component. Furthermore piezometer tests failed to yield hydraulic conductivities significantly higher than those measured in the laboratory. This result suggests that matrix flow is dominant and that no preferential flow pathways exist at least at the scale of, or finer than, the scale of the piezometer tests. A low flux through the glaciolacustrine clay of the order of the vertical hydraulic conductivity of the matrix therefore implies a low recharge of just a few mm/a to the underlying sandstone at the site. Due to the low diffusivity of the clay the variability in recharge throughout the year is likely to be very low. The presence of partially saturated sand/till layers and the unsaturated zone of the sandstone beneath may serve to increase the hydraulic gradient across the clay and therefore increase the flux. These hypotheses will be investigated with the use of numerical models presented below.

## **6.4 Numerical Models**

### **6.4.1 Variable Saturation Model of Glaciolacustrine, Till and Sandstone Deposits**

It was noted in Section 6.2.5 that several of the piezometers screened within glaciolacustrine and till deposits at Site 2 were dry throughout the monitoring period. Furthermore, after water had been added to the piezometers for falling head tests the piezometers then dried out completely. It is therefore concluded that negative pressure heads are present in the profile at the locations of the piezometer screen intervals. Partial saturation of the glaciolacustrine

sands and lower till also seems likely based on the gravimetric moisture content data presented above. Since there is a perched water table above the glaciolacustrine clay, at first sight it might be intuitive to think that positive pressure heads would prevail throughout the profile. However since the sandstone underlying the drift has an unsaturated zone of approximately 2 m there may be sufficient suction at the transition of the drift sandstone interface to cause negative pore pressures higher up the drift profile.

To test this hypothesis a steady state 1-D model was constructed using HYDRUS-1D Version 2.0 (Simunek *et al.* 1998), a public domain software package for simulating the one-dimensional movement of water, heat and multiple solutes in variably-saturated media. The assumptions underlying the modelling approach are essentially identical to those for FAT3D-UNSAT given in Appendix 7.

A model was set up with a constant pressure head of 135 cm at the top to represent the average level of the perched water table within the outwash deposits above the top of the glaciolacustrine clay layer. A constant pressure head was also set at the base of the model equal to zero to represent the water table in the sandstone lying on average 6.8 m below the top of the glaciolacustrine clay layer. For simplicity the model was set up using a single set of flow parameters for the upper layer (representing the drift) approximating a low permeability clay with van Genuchten parameters as predicted by the Rosetta database (Schaap *et al.* 2001), for a deposit comprising 13% clay and 87% silt. Rosetta is a computer program for estimating soil hydraulic parameters with hierarchical pedotransfer functions and a database of values for a large range of material types is included with the HYDRUS-1D model. The pedotransfer function approach is well documented and aims, with various degrees of success, to derive realistic soil moisture characteristics from easily obtainable data such as soil texture

without having to go through expensive and time consuming laboratory procedures to derive the characteristics directly (Clapp and Hornberger 1978; Carsel and Parrish 1988; Wosten *et al.* 1995; Alphen *et al.* 2001; Wagner *et al.* 2001).

The hydraulic conductivity was set to  $1.4 \times 10^{-10} \text{ ms}^{-1}$  equal to the median vertical hydraulic conductivity of the glaciolacustrine clay measured in the laboratory. This upper model layer is 4.9 m thick. For the lower layer van Genuchten parameters were taken from Digges La Touche (1998) for a fine to medium grained sandstone. The parameters used are given in Table 6.1. Initial heads were set to vary linearly between a pressure head of 135 cm at the top of the model to 0 cm at the base.

The model was run until a steady state was reached with a pressure head tolerance of 0.01 cm and a water content tolerance of  $1 \times 10^{-5}$ . The mass balance error was 0.64%. Model run files are given in Appendix 9 (model run s2lower1).

Parameter	Glaciolacustrine clay and till	Glaciolacustrine sand layer	Permo-Triassic sandstone
$\alpha \text{ (cm}^{-1}\text{)}$	0.008	0.01	0.15
n (-)	1.6	4.9	2.7
L (-)	0.5	0.5	0.5
$\theta_r \text{ (-)}$	0.06	0.01	0.04
$\theta_s \text{ (-)}$	0.4	0.3	0.4
K (m/s)	1.4E-10	3.82E-06	8.1E-05

**Table 6.1** Van Genuchten parameters used in variably saturated models of the lower part of the Site 2 drift profile

The results are shown in Figure 6.26 and indicate that negative pressure heads are likely to persist in the lower 0.5 m of the drift profile.

Since across some of Site 2 a sandy horizon is encountered between the glaciolacustrine clays and the lower till, a second model was constructed to investigate the effects of a sand layer within the profile. This layer was added between 2.4 and 2.9 m below the top of the model with Van Genuchten parameters for a sand based on the Rosetta database (Schaap *et al.* 2001) and a saturated hydraulic conductivity of 700 cm/d. In all other regards the model was identical to the two layer model. The model parameters are shown in Table 6.1 and model results in Figure 6.26. The mass balance error was 0.27%. Model run files are given in Appendix 9 (model run s2lower2).

The results show the effect of the sand layer in reducing the pressure head within this layer and causing negative pressure heads to persist to within 30 cm above the layer. This occurs as the fixed flux through the model requires a much smaller head gradient within the high permeability sand than within the low permeability clays causing the large change in pressure head across the sand layer. In addition the presence of the sand layer causes the flux through the model to increase from 5.8 mm/a to 7.2 mm/a.

A transient model was also run for the 2 layer case with a sinusoidally varying upper and lower pressure head with a period of a year and an amplitude of 0.25 m, a realistic seasonal variation in water level for both the outwash and the sandstone at this location. Over the model run of 25 years the resulting model flux settles into a sinusoidal pattern varying between 5.5 and 6.0 mm/a in phase with the boundary variations (i.e. maximum in boundary head coinciding with maximum flux). The mass balance error was 0.003%. Model run files are given in Appendix 9 (model run s2lower3).

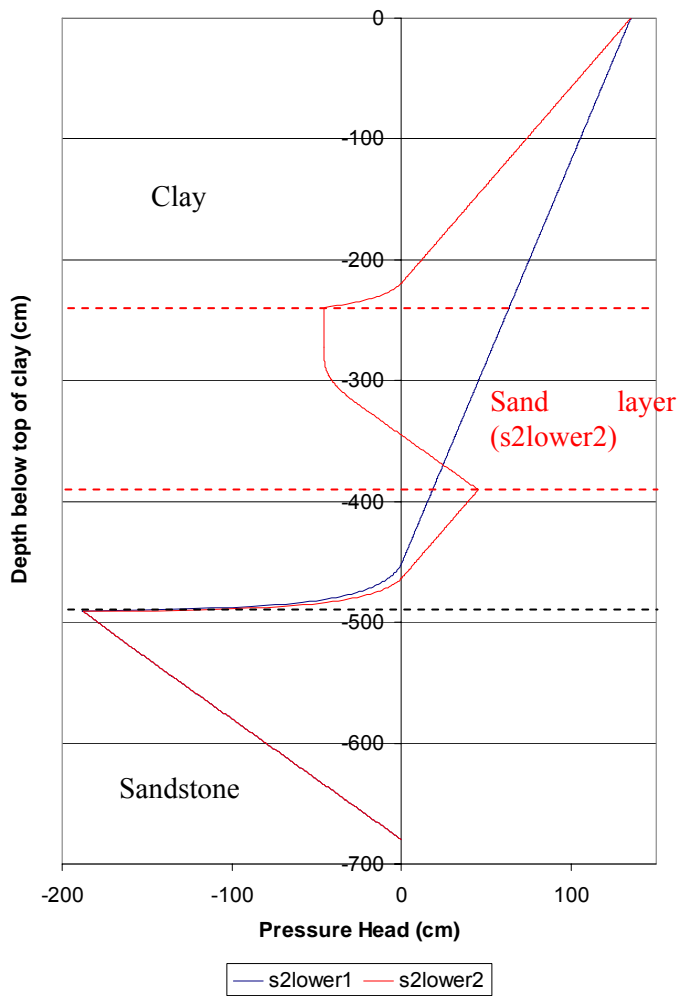


**Figure 6.26** Results of 1-D variably saturated models of the lower part of the Site 2 drift profile

These results confirm that the occurrence of dry piezometers within the drift profile is to be expected where the piezometers are screened within a few tens of cm of a sandy horizon or the sandstone itself. With reference to Figure 6.2 this explains the dryness of piezometers S2\_3 and S2\_8 which have part of the screened section adjacent to the sandstone and glaciolacustrine sand layer respectively.

However, explaining the dryness of S2\_4 is still problematic as this piezometer is screened within glaciolacustrine clay between 5.55 and 5.95 mbgl. The sandstone is likely to be

reached at a depth of 7.5 mbgl based on other borehole logs at the site (this particular borehole was only drilled to 6.0 mbgl) and no sand layer is present within the drift profile at this location. A possible explanation is that the sand layers present in boreholes S2\_2 and S2\_3, at around the elevation of the S2\_4 screen section, pinch out in the vicinity of S2\_4, close enough to reduce the pressure head to below zero.

To see how close a sand layer might have to be to have this effect a 10 m wide 2-D model was set up using the code FAT3D-UNSAT (described in Appendix 7). Identical parameters to the three layer 1-D model were used but with the sand layer only present across the right hand 4 m and a horizontal to vertical hydraulic conductivity ratio of 10:1 for all layers. The model was run until a steady state was reached and the resulting average mass balance error was less than 0.01%. The resulting pressure head distribution is shown in Figure 6.27.

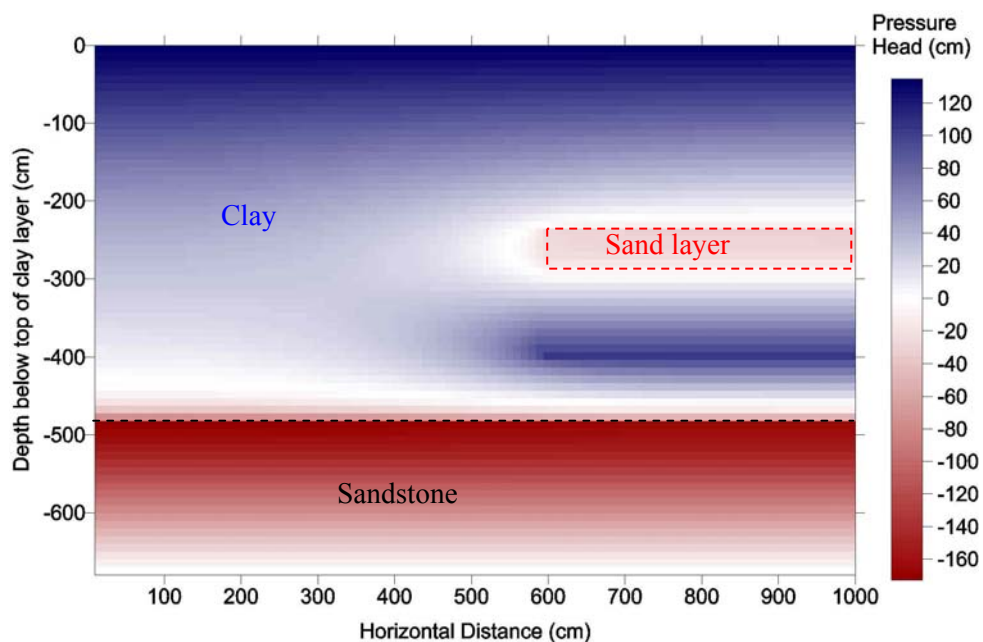


**Figure 6.27** Results of a 2-D variably saturated model of the lower part of the Site 2 drift profile

This indicates that the negative pressure head may extend greater than 0.5 m laterally away from a sand layer for these model conditions.

It is concluded that the presence of dry piezometers is consistent with the conceptual model of flow presented for the site.

#### **6.4.2 Model of Tritium Transport in Clay**

A model was needed to test the hypothesis of slow matrix flow through the glaciolacustrine clay implied by the tritium data.

It has been shown above that conditions in the top of the glaciolacustrine clay layer are likely to be saturated due to a perched water table in the outwash deposits above. MODFLOW (McDonald and Harbaugh 1984) was used to model steady groundwater flow in 1-D through a 2.5 m 50 cell column using a uniform grid and fixed head boundaries at top and bottom. As shown by the variably saturated modelling above, the pressure heads at the top and bottom of the glaciolacustrine clay layer are approximately 135 cm and -185 cm respectively. Given that the thickness of the clay is around 490 cm this equates to a hydraulic gradient of approximately 1.65. This hydraulic gradient was set using constant head boundaries and with a hydraulic conductivity of  $1.4 \times 10^{-10} \text{ ms}^{-1}$  the resulting flux was 7.3 mm/a. The gradient and flux are consistent with the results of the steady state variably saturated zone models presented in Section 6.4.1. The criterion for convergence was set to 0.001 m.

MT3DMS (Zheng and Wang 1999) was then used to model the transport of tritium for advection, dispersion, diffusion and radioactive decay. The tritium source term was a variable concentration boundary at the top of the model based on a best estimate of the historic atmospheric tritium concentration. This assumes that the input of tritium to the clay layer is approximately equal to the value of tritium found in precipitation. This is a reasonable

assumption given the high permeability of the outwash materials above the clay resulting in low groundwater travel times from the ground surface to the top of the clay in contrast to the long (50 years) duration of the model. The historic record of tritium in rainwater is very limited for the UK but a reasonable amount of data are available for stations in Ireland and the Netherlands. Available data from the Global Network of Isotopes in Precipitation (GNIP) data for the UK region is shown in Figure 6.28 along with the average, minimum and maximum source term time series used for input to the model. The source term was discretised on a yearly basis for input to the model.

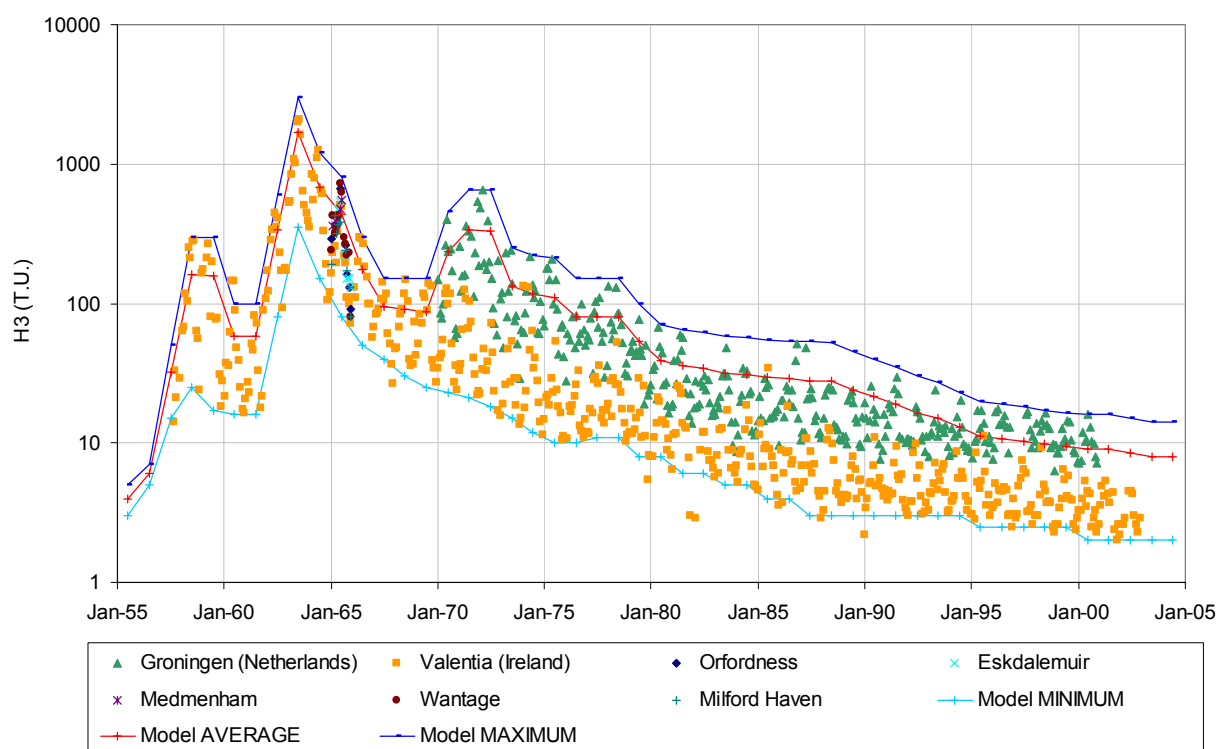


**Figure 6.28** Historic data for tritium in precipitation for the UK area. Data courtesy of IAEA (2004) Isotope Hydrology Information System (ISOHIS) Database: <http://isohis.iaea.org>.

A dispersivity of 0.05 m was assumed based on the equation of Xu and Eckstein (1995) for an average flow length of 2 m. The tritium half life of 12.3 years was used to control radioactive decay (Freeze and Cherry 1979) and the diffusion co-efficient for tritium was set to  $4.32 \times 10^{-6}$

$5 \text{ m}^2/\text{d}$  based on laboratory tests on a clay till (D'Astous *et al.* 1989). The assumed porosity was 0.4. These parameters were used in the baseline Run 1. The method of characteristics (MOC) solution scheme was considered most appropriate to the problem in order to minimise numerical dispersion. The model was run from 1955 to 2004 with transport time steps of 0.1 d and a concentration change criterion for convergence of  $1 \times 10^{-8}$  T.U.

A number of additional model runs were then carried out to investigate the sensitivity of the model to the input parameters. Runs 2 and 3 used the same parameters as Run 1 but with the maximum and minimum source terms respectively. Runs 4, 5 and 6 are identical to Runs 1, 2 and 3 respectively but with the flux increased by a factor of 10 to 73 mm/a (by increasing  $K$  to  $1.4 \times 10^{-9} \text{ ms}^{-1}$ ). Figure 6.29 presents the results alongside the measured data. Mass balance errors ranged from 0.05% to 0.39% with an average of 0.17%. Model input and output data are included in Appendix 9 with naming convention trit1\_“Run Number”.

The results suggest that the uncertainty in the source term is very significant. Thus a reasonable model fit is possible using the baseline parameters and a source term somewhere in between the average (Run 1) and the maximum (Run 2). When the flux is increased by a factor of ten (Runs 4 to 6) the fit becomes very poor as, for 2 of the 3 cases, modelled concentrations of tritium increase with depth instead of decreasing over the depth range of the samples.

The main implication of the results is that the model is consistent with the observed data for a low groundwater flux case but becomes inconsistent at significantly higher fluxes. This confirms the conceptual model of very slow groundwater flow through the glaciolacustrine clays underlying Site 2 and a small contribution of just several mm/a recharge to the underlying sandstone aquifer.

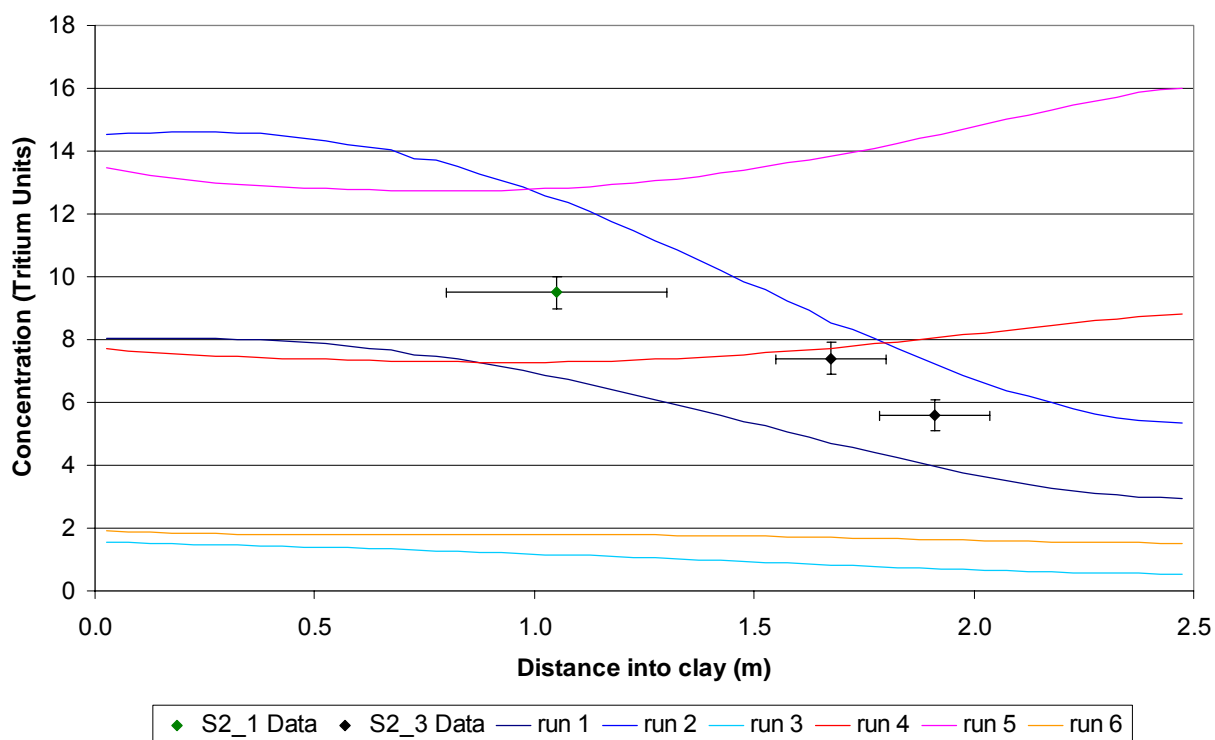


**Figure 6.29** Predicted tritium distribution within the glaciolacustrine clay for all model runs at the time of drilling (2004)

### 6.4.3 Model of Outwash Deposits

#### 6.4.3.1 HYDRUS model

In order to test the conceptual model of recharge to the glacial outwash deposits at Site 2 a single porosity Hydrus-1D model was constructed. The model was based on the observations made at the location of the tensiometer nest within the zone of relatively high water table. In this instance HYDRUS-1D version 3.0 was used (Simunek *et al.* 2005).

The option of ‘horizontal drains’ was chosen for the lower boundary condition located at 2.5 mbgl at the top of the glaciolacustrine clay layer. This in effect assumes that all drainage is lateral and that the clay is impermeable. This is a reasonable assumption given the low flux of just a few mm per year likely to be flowing vertically into the clay as discussed above which is within the likely error of the fluxes in the model output. Flow into the drains is

controlled by the following equation assuming the drains are located in a homogeneous soil profile above an impervious layer:

$$q_{drain} = \frac{4K_h h_{dr}^2}{L_{dr}^2} + \frac{h_{dr}}{\gamma_{entr}} \quad (6.1)$$

where  $q_{drain}$  is the drain discharge rate per unit surface area [ $LT^{-1}$ ],  $K_h$  is the horizontal saturated hydraulic conductivity,  $h_{dr}$  is the water table height above the drain at the midpoint between the drains, i.e. the hydraulic head taken from the model needed for calculating subsurface flow into the drains [L],  $L_{dr}$  is the drain spacing [L] and  $\gamma_{entr}$  is the entrance resistance into the drains [T]. This function seems reasonable to use as it will result in a recession curve of the form observed in the water table at Site 2. However, during model development it became apparent that the model was insensitive to the parameter  $\gamma_{entr}$  and the model would run even for  $\gamma_{entr}=0$ , for which a floating point error should presumably result. This matter has been taken up with the model developers but with no response to date. For the present purpose the model behaved as expected for variations in the parameters governing the first term on the right hand side of Equation 6.1 and seemed to give the desired drainage needed to simulate the observed piezometric responses. The co-ordinate of the bottom of the drainage was set to the position of the water table in September 2004. A value of 5000 cm for  $L_{dr}$  was found to be most effective for fitting the model.

The upper boundary was modelled using the atmospheric boundary condition with surface layer option including the options for root water uptake and root growth. A daily time series of rainfall was aggregated from data for Peplow Home Farm (431312) and Bowling Green (T10) (see Section 2.5.1) for the modelled time period of 1/1/2004 to 30/6/05. Daily PET values calculated from data for Oakley Folly (T17) (see Section 2.5.2) were set equal to inputs

to the model of either potential evaporation ( $E_p$ ) or potential transpiration ( $T_p$ ). Evaporation from the soil surface was used when bare soil was considered dominant during the autumn/winter period (16 August to 15 March) before vegetation had emerged. During the growing season (16 March to 15 August) transpiration was used with evaporation from the soil surface considered to be negligible. For the 2004 growing season Site 2 was under winter wheat. The wheat was harvested by hand in mid-August and for the rest of the modelled period wild vegetation was allowed to re-establish itself and in time became dominated by grass and weeds. The transpiration model chosen was that of Feddes (1978) which calculates root water uptake ( $S$ ) by the following equation:

$$S = \alpha b T_p \quad (6.2)$$

where  $\alpha$  is a prescribed dimensionless function of the soil water pressure head ( $0 \leq \alpha \leq 1$ ) and  $b$  is a normalised water uptake distribution with depth. For this model water uptake is considered to be close to zero near saturation ( $h_0$ ) (due to root growth being hampered by deficient aeration) but optimal between some small value of soil tension ( $h_1$ ) and a limiting point ( $h_2$ ). For tensions greater than  $h_2$  water uptake decreases linearly with tension until a wilting point is reached ( $h_3$ ) and water uptake ceases. The parameter  $h_2$  is also a function of  $T_p$  since water uptake may become limiting at lower soil tensions for higher transpiration rates. This is implemented by designating values of  $h_2$  ( $h_2H$  and  $h_2L$ ) for threshold values of  $T_p$  ( $T_pH$  and  $T_pL$ ). For the root growth model it is assumed that the actual root depth is the product of the maximum rooting depth ( $L_m$ ) and a classical Verhulst-Pearl logistic growth function (see Simunek, van Genuchten *et al.* (2005) for details) based on a user defined growth rate calculated from designated values of root depth ( $L_i$ ) and time ( $R_i$ ). An initial rooting depth ( $L_i$ ), initial root growth time ( $R_i$ ), harvest time ( $R_h$ ) and an exponential depth

distribution co-efficient ( $DD$ ) are required from the user. The value of  $DD$  controls the rate of exponential decay of the water uptake distribution with depth ( $b$ ).

Since HYDRUS-1D only allows the user to input data for one growing season at a time, two models were run back to back. The first run (s2upper1) for the whole of 2004 used root parameters for wheat (Wesseling *et al.* 1991) shown in Table 6.2. The second run (s2upper2) used initial heads from the last day of the first run and ran until 30/6/05 with root parameters for grass (Taylor and Ashcroft 1972) also shown in Table 6.2.

Due to the uncertainty in absolute moisture contents from the TDR data it was decided to derive van Genuchten parameters for the model using the relationship between the gravimetric moisture contents at the site of TDR tube M2 and associated tensions measured by the adjacent tensiometers. These limited data are shown in Figure 6.30. Based on the lithological evidence from augering TDR tube M2 it was decided that three types of material would be needed in the model. A topsoil layer from 0 to 50 cmbgl overlies a sandy outwash material (Outwash 1) to the base of the model at 250 cmbgl. A lower permeability layer has been placed from 92 to 118 cmbgl (Outwash 2) as the PSD analyses show a significant rise in the proportion of silt and clay size particles coincident with a distinct zone of higher gravimetric moisture content shown in Figure 6.7. The van Genuchten parameters assigned to each layer are shown in Figure 6.30. The number of model nodes used was 1001 at a regular spacing of 2.5 mm.

Parameter	Symbol	Unit	s2upper1 (wheat)	s2upper2 (grass)
Pressure at saturation	$h_0$	cm	0	0
Anaerobis point	$h_1$	cm	1	1
Limiting tension at $T_pH$	$h_2H$	cm	500	300
Limiting tension at $T_pL$	$h_2L$	cm	900	1000
Wilting point	$h_3$	cm	16000	16000
$T_p$ for $h_2H$	$T_pH$	cm/d	0.5	0.5
$T_p$ for $h_2L$	$T_pL$	cm/d	0.1	0.1
Maximum root depth	$L_m$	cm	100	100
Root depth at $R_t$	$L_t$	cm	100	100
Time $L_t$ reached	$R_t$	d	183	183
Initial root depth	$L_i$	cm	0.01	0.01
Time of initial root growth	$R_i$	d	75	75
Harvest time	$R_h$	d	228	228
Exponential depth distribution coefficient	$DD$	$d^{-1}$	0.105	0.105

**Table 6.2** Root zone parameters for model s2upper 1 and s2upper2

The initial conditions for the model were a pressure head of 170 cm at the model base decreasing linearly to -100 cm at the top of the model. This approximates a water table at 80 cmbgl which is a reasonable assumption for the site in mid-winter conditions. Monitoring data do not begin until June 2004 and continue for a calendar year until the end of the model. The criteria for convergence were set to 0.0001 for moisture content and 0.1 cm for pressure

head. Mass balances were kept to less than 0.1%. The run time for the models was of the order of tens of seconds. The model input and output files for runs S2lower1 to 4 are given in Appendix 9.

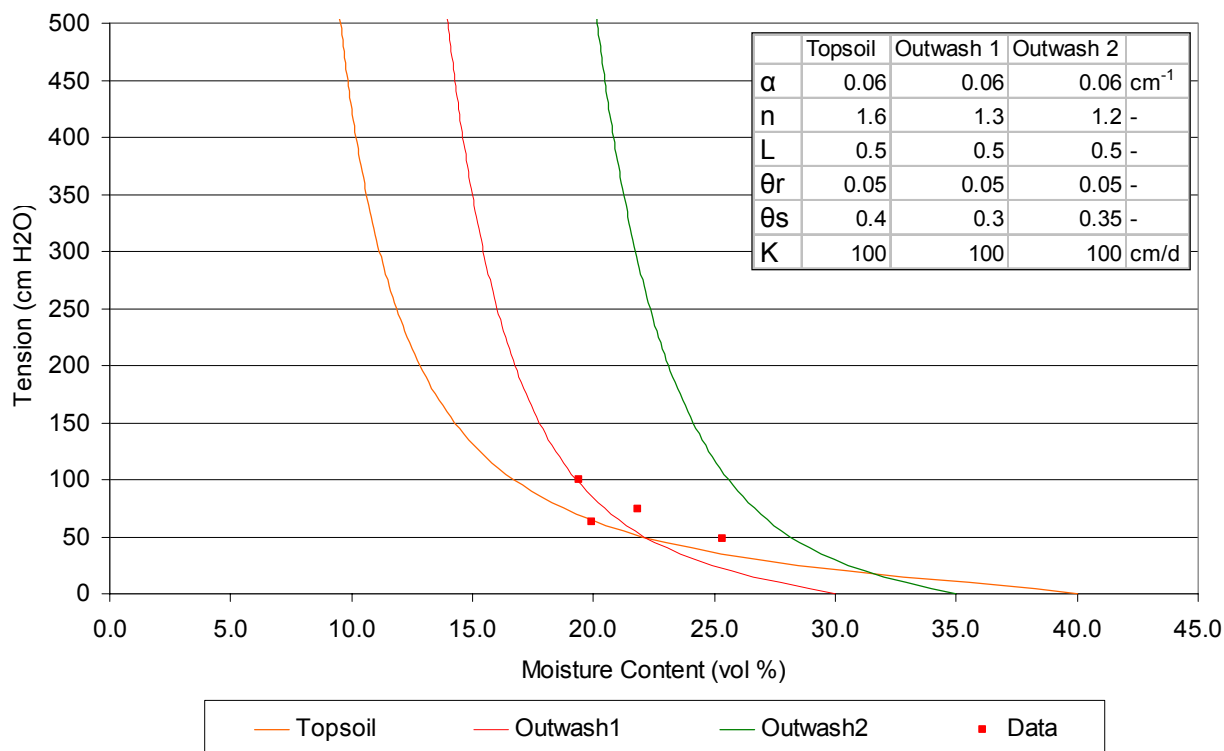


**Figure 6.30** Soil moisture characteristic curves for models s2upper1 and s2upper2

Several model runs were carried out to achieve a reasonable parameterisation of the drainage function. Once this was acceptable it was found that the model was not accurately simulating the wetting of the profile in September 2004 and in June 2005 leading to unreasonably low pressure heads throughout the winter of 2004-2005. In order to achieve a better fit to the data crop coefficients ( $K_c$ ) were used to limit the PE<sub>t</sub> during the mid to late summer period. This approach is common practice in implementing the FAO approach to recharge estimation (FAO 1998; Hulme *et al.* 2001). For the wheat crop during 2004  $K_c$  was set to 0.35 from 1/7/04 to 25/7/04 during which time the wheat would have reached its maximum rooting depth, and set to zero between the onset of senescence at 25/7/04 and harvest on 15/8/04. A

value of  $K_c$  of 0.2 was used for the mature grass from 1/6/05 until the end of the model run. These  $K_c$  values are reasonable based on the available literature for crop timing and development in Shropshire (Streetly *et al.* 2002). Multiplying the PEt by the  $K_c$  value limited the amount of late summer transpiration to allow a more realistic wetting of the profile.

The model results are shown in Figure 6.31 against calibration targets of monitored pressure heads at the 5 tensiometers. Due to the uncertainty in the absolute moisture content in the TDR dataset it was not possible to also refine the model against observed moisture content changes.

The general form of the pressure responses is reasonable and captures well the plateau in the water table during the summer 2004, the wetting of the profile into autumn 2004 and the variations in the water table during the winter 2004-2005. However the modelled recovery of the water levels during June 2005 is still too slow even using the low  $K_c$  values during this time. Furthermore there is a persistent lag in the modelled water table response of several days. A number of further model runs were carried out to try and resolve these issues with little success. Some improvement in the lag was possible only by using unrealistically steep soil moisture characteristic curves (i.e. low values of the van Genuchten  $n$  parameter implying very high retention) but this is not conceptually justifiable. Reducing the time increment to enable hourly changes in the rainfall inputs made little difference. Increasing the permeability of the deposits led to increased evaporation from the water table bringing pressures persistently too low. If the drainage rate was much slower the entire profile became saturated during the winter months. Hence it was decided that the model results for the combination of parameters displayed in Figure 6.31 was the 'best fit' achievable given the constraint of physically realistic parameters.

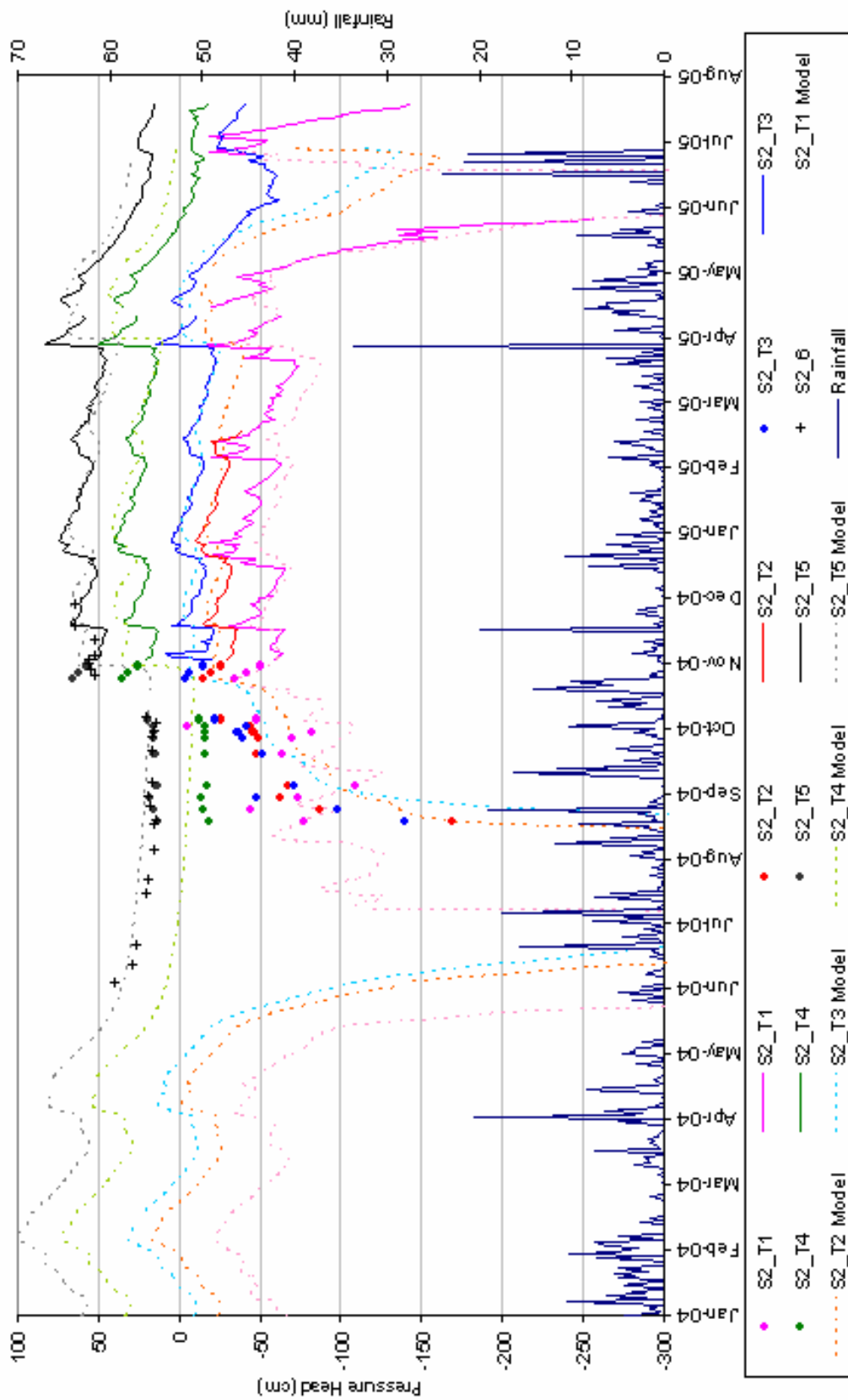


**Figure 6.31** Results of models s2upper1 and s2upper2

The modelling suggests that a significant amount of recharge to and drainage from the shallow glacial outwash material occurred during the modelled period. During 2004 rainfall less evapotranspiration (total available water (TAW)) amounted to 129 mm with 114 mm of lateral flow occurring. During the period of calibration data between July 2004 and June 2005 these values were 188 mm and 77 mm respectively. The large difference between the TAW and lateral flow in this case is due to the large soil moisture deficit accumulated during the summer of 2004. This led to a relatively large increase in unsaturated zone water storage hence restricting the amount of lateral flow occurring.

It is important that it is shown that this amount of lateral flow is physically realistic given the limited room for lateral head differences due to the presence of such a shallow water table. The simple analytical model described by Equation 5.1 in Section 5.4.4 is useful in this regard. For a recharge of 120 mm/a ( $3.3 \times 10^{-4}$  m/d), distance between drains of 100 m (i.e.  $a = 50$  m) and a hydraulic conductivity of 1 m/d it follows that the head at the midpoint between drains would need to be approximately 0.7 mbgl for drains placed at 1.5 mbgl assuming the outwash materials are 2.5 m thick. This is a reasonable value given the field conditions and suggests, given the simple nature of the model, that this amount of lateral flow could be accommodated by drainage flow within the outwash materials at Site 2.

The results also suggest that by using HYDRUS-1D with realistic parameters for the soil hydraulic characteristics it is not possible to model the very quick response of the water table to rainfall. This suggests that the flow mechanisms within the unsaturated zone cannot be simulated by the 1-D Richards equation alone and that preferential flow processes are likely to be in operation. As noted in Section 1.4.5 a range of such processes have been described in the literature such as flow through macropores, development of flow instabilities due to

heterogeneity or water repellency or funnelling of flow due to the presence of sloping soil layers. For the case of Site 2 the particular preferential processes occurring unfortunately cannot be ascertained on the basis of data collected for this thesis alone. This is a matter for further research, more on which will be said in Section 7.4. It was however noted in Section 6.2.2 that the water table response in S2\_5 and S2\_7 was much slower than that at S2\_6 and at the site of the tensiometers. It was suggested that this is likely to be due to smoothing of the pressure signal due to the presence of a thicker unsaturated zone. To test this idea the model was run again (s2upper3 for 2004 and s2upper4 for 2005) with a lower drainage base level (at 200 cmbgl) and with a lower water table as an initial condition (at 130 cmbgl). All other parameters were held constant since the aim was not to achieve a good model fit in this instance but to test how much smoothing occurs in the model for an increase in unsaturated zone thickness of around 0.5 m. The result is shown in Figure 6.32 alongside observed heads at S2\_5. The degree of smoothing in the model results is reasonable for the lower magnitude precipitation events during the winter of 2004-2005 but the observed water table rises are significantly faster than the modelled response for events larger than approximately 20 mm/d.

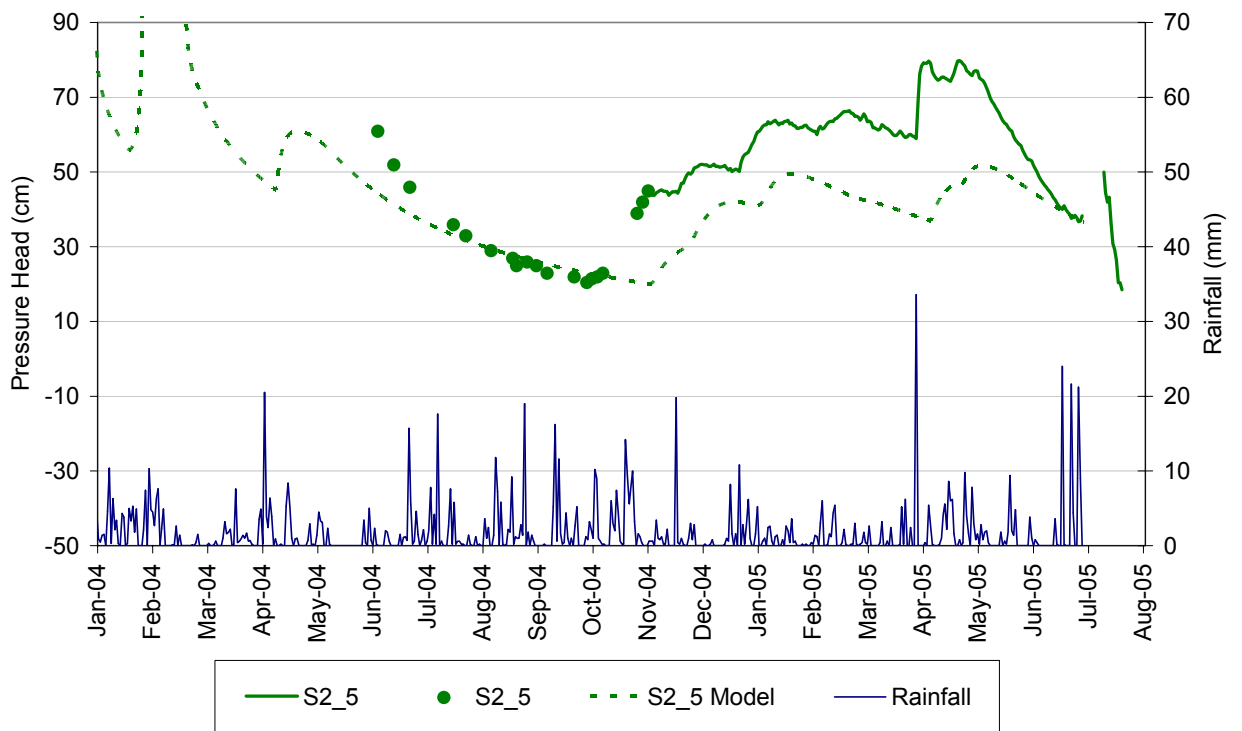


**Figure 6.32** Results of models s2upper3 and s2upper4

Hence in combination, the model results suggest that preferential flow may be more significant at shallower depths in the profile. This may be due to instabilities in the wetting front enhanced by textural changes on the irregular interface between the topsoil and coarser outwash material it overlies. Furthermore the results also suggest that preferential flow may only be significant deeper in the profile during higher intensity rainfall events. For low intensity rainfall, dis-equilibrium between preferential pathways and the ‘matrix’ may be short lived and redistribution of water may lead to the appearance of homogeneous flow at greater depths. In contrast during heavy sustained rainfall dis-equilibrium during the early stages may lead to enhanced flow to greater depths although as time passes the infiltration process would be expected to show more homogeneous characteristics (Zhou *et al.* 2002). However, in addition to being driven by vertical flow from above, it should be noted that the

rapid response of the deeper water table may also be due to the propagation of lateral pressure variations from adjacent areas where the water table is more responsive.

#### **6.4.3.2 Soil moisture balance model**

A common approach to recharge estimation particularly for groundwater modelling purposes is the use of soil moisture balance models such as Penman-Grindley or FAO to calculate recharge. The generated recharge is then modified in a variety of ways in the presence of drift materials to estimate recharge to the groundwater model and lateral flow to surface water and/or runoff recharge. For purposes of comparison with the moderately complex HYDRUS-1D model a relatively simple soil moisture balance model was therefore created.

It is noted that the FAO method is very similar to the Penman-Grindley method but derives the ‘root constant’ and ‘wilting point’ from physically based parameters and implements a linear decrease in the slope of the AEt/PEt function rather than a simple step function used by the original Grindley model. However, many of the parameters required for this approach are difficult to estimate. The Penman-Grindley model is much simpler to parameterise than the FAO model and has therefore been used here.

A VBA code was written and implemented within a Microsoft Excel spreadsheet (included in Appendix 9). Daily rainfall and PEt inputs were identical to those used for the HYDRUS-1D model presented in Section 6.4.3.1. The code reads the required inputs from the spreadsheet, calculates AEt and recharge on a daily basis and writes these values back to the spreadsheet. Formulas in the spreadsheet then modify the recharge to the glacial outwash to calculate recharge through the glaciolacustrine deposits to the sandstone beneath and lateral flow to drainage by the following method. Each day the amount of recharge is added to a store representing water held in the outwash deposits above the glaciolacustrine layer. The

simulated head in the outwash material ( $h$ ) is equal to the amount of water in the store divided by the specific yield of the material ( $S$ ). The value of recharge through the clay to the sandstone is assigned to the value of a prescribed daily recharge limit as long as enough water is present in the store. Lateral flow is generated by multiplying the remaining water in the store by a linear decay constant ( $\eta$ ) and the time step length (in this case 1 day), as shown in Equation 6.5. The amount of water in the store on the next day is then equal to the recharge to the outwash the next day less the recharge to the sandstone and the lateral flow generated on the current day. In this way a time series of values for recharge to the sandstone, lateral flow to drains and a simulated groundwater level can be realised.

It is noted that the linear decay constant can be related to aquifer parameters in the following manner. The case is considered of a one-dimensional aquifer of constant transmissivity ( $T$ ) and storage co-efficient ( $S$ ). If a recharge mound with initial maximum head  $h_0$  at a distance  $x = L$  and constant head conditions at  $x = 0$  and  $x = 2L$  is allowed to decay, the head,  $h$ , at time  $t$  will be governed by the following equation (Erskine and Papaioannou 1997):

$$h = h_0 e^{-\eta t} \quad (6.3)$$

where  $\eta = \frac{\pi^2 T}{4SL^2}$  (6.4)

If a linear decay constant is implemented in the manner described above it follows that:

$$h_t = h_{t-1}(1 - \eta t) \quad (6.5)$$

Since for small  $\eta t$ ,  $e^{-\eta t} \approx 1 - \eta t$  Equations 6.3 and 6.5 are directly comparable and the linear decay constant can be derived from aquifer parameters via Equation 6.4.

For the first run (PG1) root constants ( $C$ ) and wilting points ( $D$ ) for arable land use were taken from those used in a groundwater modelling study of the West Midlands Permo-Triassic Sandstone (Soley *et al.* 1998). These are shown in Table 6.3. A value of 0.07 for the specific yield of the outwash deposits was derived using the soil moisture characteristic curve for ‘Outwash 1’ used in the HYDRUS-1D model described above. Values for  $T$  and  $L$  of  $5 \text{ m}^2/\text{d}$  and 100 m respectively gave a linear decay constant for lateral flow of  $0.018 \text{ d}^{-1}$ . The daily recharge limit through the glaciolacustrine clay was set to  $0.014 \text{ mm/d}$  ( $5 \text{ mm/a}$ ) and datum to which groundwater levels would recede was set to 1.3 mbgl. The model was run from 1/1/2004 until 30/6/05 with an initial condition of zero soil moisture deficit, a reasonable assumption for this time of year.

The simulated groundwater level and soil moisture deficit (SMD) within the outwash deposits for model run PG1 are shown in Figure 6.33. Assessment of the model fit was again carried out against observations made at the site of the tensiometers (S2\_T5). The magnitude of the water level variations during November 2004 to February 2005 are reasonable suggesting that the model behaves well during ‘wet’ conditions and that the values chosen for the aquifer parameters are reasonable. However the large water table rise during October 2004 and March 2005 are greatly underestimated suggesting a deficiency in the modelled processes. In order to improve the model fit a second model run was carried out (PG2). The root constants were severely reduced for the late summer and winter periods in order to reduce the AEt and SMD during the times of poor model fit. There is some justification for this as during these times bare soil was dominant and AEt would have been limited by the evaporative capacity of the soil. Reducing the root constants is conceptually equivalent to the method of reducing the  $K_c$  values below 1 during these times in the HYDRUS-1D models presented in Section 6.4.3.1 above. The values used are shown in Table 6.3.

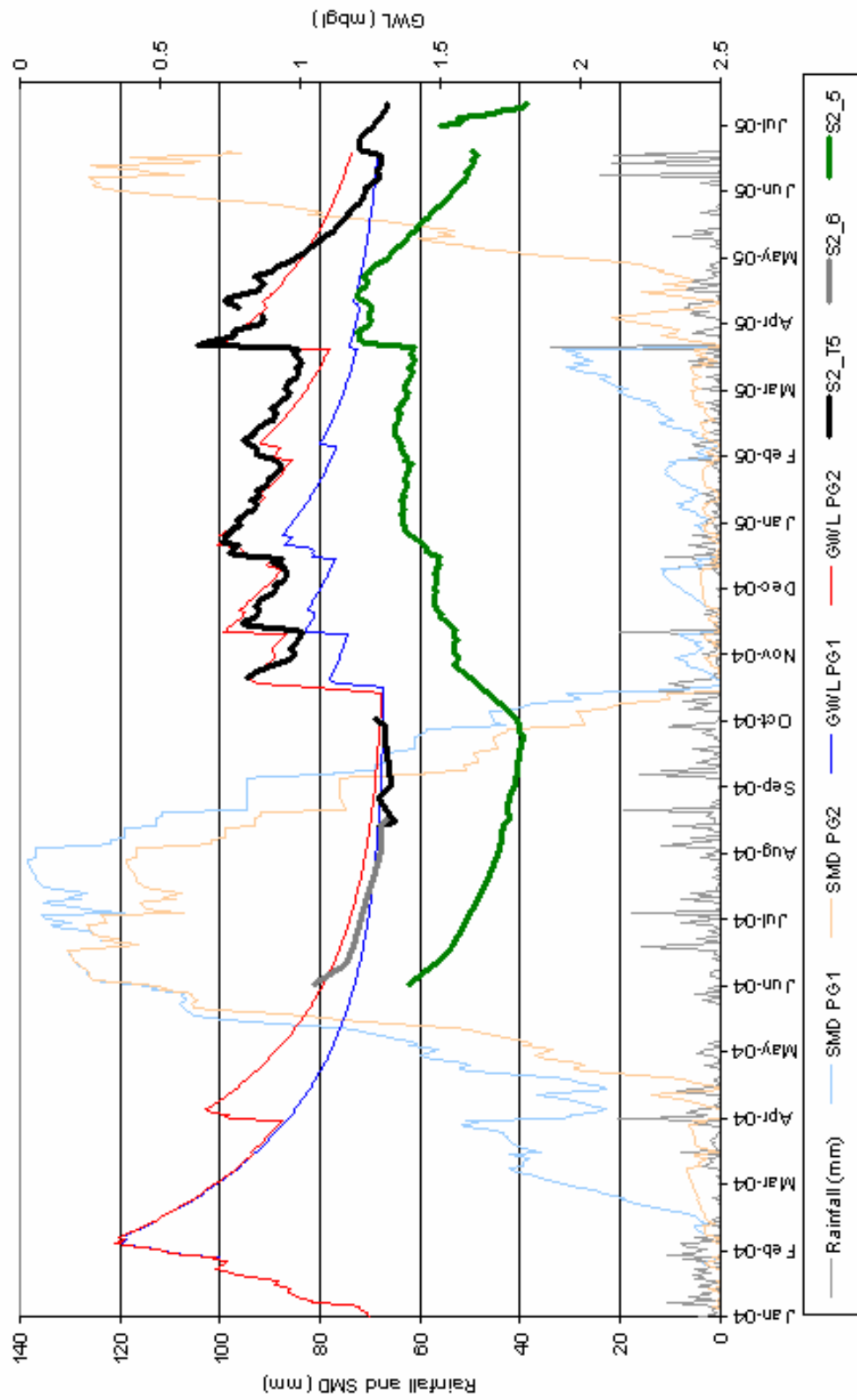


**Figure 6.33** Results of models PG1 and PG2

	<b>Model PG1</b>		<b>Model PG2</b>	
<b>Month</b>	<b>C (mm)</b>	<b>D (mm)</b>	<b>C (mm)</b>	<b>D (mm)</b>
<b>Jan</b>	50	75	3	75
<b>Feb</b>	55	75	3	75
<b>Mar</b>	65	90	5	90
<b>Apr</b>	80	120	80	120
<b>May</b>	105	150	105	150
<b>Jun</b>	125	195	125	195
<b>Jul</b>	135	200	115	200
<b>Aug</b>	80	90	0	90
<b>Sep</b>	55	60	0	60
<b>Oct</b>	45	50	0	50
<b>Nov</b>	45	50	3	50
<b>Dec</b>	45	50	3	50

**Table 6.3** Root constant and wilting points for models PG1 and PG2 (mm)

The results of model run PG2 are given in Figure 6.33 and show a greatly improved model fit to water levels recorded by S2\_T5. This is actually a better representation of the water table response than that produced by the much more complex HYDRUS-1D model. In this case since water surplus to evaporative demand is allowed to recharge the water table instantaneously for times of zero SMD the quick response of the water table is more accurately reproduced. This equates to a highly simplified preferential flow model during winter conditions. It is noted that since no smoothing is applied to the recharge signal in generating the simulated water table that the model fails to simulate heads accurately for the

part of the site with a deeper water table represented on Figure 6.33 by the hydrograph for S2\_5.

For this model run the recharge to the sandstone aquifer is a steady 5 mm/a. Values for rainfall less AEt, recharge to the outwash deposits and lateral discharge are 151 mm, 124 mm and 121 mm respectively for the year of calibration data between July 2004 and June 2005. The values differ markedly from those for the 'best fit' HYDRUS-1D model presented above in Section 6.4.3.1. The main differences stem from a greater soil moisture deficit building up in the profile during summer 2004 in the HYDRUS-1D model which means that AEt is lower than for PG2. Hence although a greater amount of water is available for recharge, the amount of lateral discharge simulated by the HYDRUS-1D model is lower than that for PG2.

## **6.5 Conclusion**

A range of monitoring and experimental data for the site has been drawn together along with laboratory results to derive a hypothetical conceptual model of the site hydraulics in relation to groundwater recharge. The data from tensiometers and piezometers set within a robust understanding of the geology derived from invasive and ERT investigations were most useful in developing an understanding of the site. The tritium data and infiltrometer tests also provided useful supporting data. The electrical methods employed in the form of TDR and time series ERT were disappointing in terms of quantitative results but added some value in confirming the emerging understanding of the site.

The conceptual model hypotheses of the site hydraulic processes presented in Section 6.3 have been tested and largely verified using numerical models presented in Section 6.4.

The recharge to the perched water table within the glacial outwash deposits is likely to have been of the order of 150 mm/a for the period July 2004 to June 2005 occurring predominantly

in the autumn and winter period although a significant recharge event also occurred in June 2005. The observed hydraulic response is inconsistent with flow governed by the 1-D Richards equation and preferential flow processes enabling rapid flow of water through the profile are likely to be occurring. Preferential flow appears to be more significant at shallow depths and during more intense precipitation events. Recharge to the Permo-Triassic sandstone is likely to be just a few mm/a, due to the low permeability of the intervening glaciolacustrine deposits, and to occur at a more or less constant rate throughout the year. A significant flux of water is thus thought to drain laterally from the site within the glacial outwash deposits. The destination of this water is currently unknown but may flow to field drains (known to exist within 50 m of the site) or recharge the Permo-Triassic sandstone at some distance from the site where glaciolacustrine clay deposits are no longer present to restrict deeper infiltration. The amount of lateral flow has been shown to be physically realistic given the presence of such a shallow water table.

# **7 CONCLUSIONS AND RECOMMENDATIONS**

## **7.1 Introduction**

It was stated in Chapter 1 that this thesis aims to further the understanding of hydraulic processes governing recharge through glacial drift at a range of scales. It is believed that this has been achieved and conclusions at the subcatchment, local and site scale have been made in this regard at the end of Chapters 2, 3 and 5/6 respectively. This chapter completes the thesis by drawing together the main findings of the research, discussing their implications and transferability, giving an appraisal of the research strategy and contribution, and making recommendations for further research.

## **7.2 Discussion of Main Findings**

### **7.2.1 Site Scale (cm to 10s m)**

#### **7.2.1.1 Till**

Chapter 5 showed that hydraulic and hydrochemical/tracer test data are highly suggestive of the occurrence of preferential flow through lodgement till. Furthermore, near-vertical hydraulically active fractures have been observed in a test pit extending to depths of greater than 2 m. These are thought to have been derived through processes of desiccation and/or freeze thaw on the basis of the observed decrease in fracture intensity with depth. The fractures are commonly infilled with sediment (often fine grained calcareous material or sand) that appears to have been derived from weathered clasts within the till.

Numerical models have illustrated the features of unsaturated flow through fractured till and shown that water table responses to rainfall during the summer may feasibly occur while large tensions are present higher up the profile. Modelling has shown that such responses are impossible through the low permeability till matrix alone without a mechanism for preferential flow. Uncertainties remain as to the exact pattern of wetting and drying of the till

matrix blocks due to the unknown location of tensiometer cups in relation to the fractures. Flow within the fracture system appears to be highly variable due to variations in fracture hydraulic conductivity and, possibly, flow focussing within the unsaturated zone.

An equivalent porosity model has shown that the bulk hydraulic conductivity of the till (6 m thick at Site 1) is in the range  $1.7$  to  $2.9 \times 10^{-9}$  m/s, approximately one order of magnitude higher than the till matrix permeability. The recharge to the sandstone is likely to have been in the range 25 to 41 mm/a in 2004 to 2005 and relatively constant throughout the year. Based on the tracer test results, potential travel times of contaminants to the water table may be as high as 1 cm/d. Given the uncertainty in the porosity of the hydraulically active fractures and likely variability in their hydraulic conductivity, the maximum potential flow velocities through the saturated till are not known. However the environmental tracer data show that the travel time to the sandstone (at 6.3 mbgl) is less than 40 years.

#### **7.2.1.2 Glaciofluvial outwash**

Observed hydraulic responses within glacial outwash have been shown, in Chapter 6, to be inconsistent with flow governed by the 1-D Richards equation. It is likely that preferential flow is occurring which appears to be more significant at shallow depths and during more intense precipitation events. Recharge to the water table within the outwash deposits is likely to have been of the order of 150 mm/a for 2004 to 2005 occurring predominantly, but not exclusively, in the autumn and winter. Significant lateral flow through shallow glacial outwash materials has been inferred, caused by perching of water on underlying low permeability glaciolacustrine materials. The destination of the lateral flow may mostly be to field drains. However, it is possible that aquifer recharge may be enhanced where the underlying clays pinch out, due to the subsequent infiltration of lateral subsurface flows.

An interesting case of a stepped water table has been observed. At a field site around 20 m across, two discrete zones of relatively high and low water level occur within glacial outwash (sand and gravel) with a head difference of 0.5 m between them. The step in the water table occurs across a distance of just a few metres. The two parts of the site appear to be hydraulically isolated from each other by a low permeability barrier of unknown origin (possibly related to faulting) which was not delineated by invasive investigation.

#### **7.2.1.3 Glaciolacustrine deposits**

It has been shown in Chapter 6, on the basis of hydraulic observations and tritium age dating, that laminated glaciolacustrine clays only a few metres thick may restrict vertical flow to the sandstone aquifer to just a few mm/a. The recharge is likely to be more or less constant throughout the year.

#### **7.2.1.4 Time series ERT**

It has been shown in Chapters 5 and 6 that temperature effects on resistivity in the near subsurface can be very significant (Cuthbert *et al.* 2004). Furthermore, a forward model presented in Chapter 4 indicates that applying a post-inversion temperature correction is a reasonable approach to dealing with such effects where the relationship between the material resistivity and temperature is adequately known. In the example given in Chapter 4, the use of a time series of ERT surveys has not enabled a realistic quantitative appraisal of moisture content changes to be made. This is due to uncertainties in the relationships between temperature, and more particularly, moisture content and lithology for the range of glacial materials encountered at Site 2. In the case of till underlying Site 1, as described in Chapter 5, the laboratory relationships between temperature, moisture content and resistivity have been defined to some extent (Russell and Barker 2005). However the ERT method is of limited use in assessing moisture content changes in the till. This is because the resistivity does not

change significantly at moisture contents observed in the field, except where extreme drying occurs in the shallow soil zone. The time series ERT method has however been useful for qualitatively describing spatial differences in shallow moisture content changes at the fieldsites.

#### **7.2.1.5 Representativeness of site scale results**

Although a detailed picture has emerged of the hydraulics operating at the two fieldsites, some consideration needs to be given as to how representative the sites are for the wider Potford Brook catchment.

Site 1 is situated near the centre of a large (for this catchment) patch of continuous till which thins towards its margins. The till is just over 6 m thick at Site 1 but the till is not known to be thicker than 10 m anywhere in the catchment. Furthermore, the evidence from the local scale investigations presented in Chapter 3 indicates that the till is relatively homogeneous on the scale of 10s to 100s m. As such the site may be fairly representative in terms of hydraulic processes occurring in other till covered areas across the catchment. However, it is likely that as the till thickness and lithology varies, the degree and style of fracturing and weathering will also vary to some extent. The hydraulic relationship to the sandstone aquifer also changes, for instance where the piezometric level is well below the base of the till in the northwest of the catchment. Thus the magnitude and timing of recharge is likely to be significantly different from place to place.

As would be expected due to their depositional processes, glaciolacustrine and glaciofluvial deposits appear to be more variable in terms of thickness, extent and lithology across the catchment, in comparison to till deposits. Hence the degree to which Site 2 is representative may be limited to the style rather than the magnitude of the hydraulic responses.

Sites 1 and 2 are located within the context of local scale conceptual models E and B respectively (summarised below in Section 7.2.2). However, the results of the site scale investigations also inform an understanding of the processes involved in models A, C and D.

Thus, further similar studies as conducted at Sites 1 and 2 would be worthwhile to test the variability in hydraulic functioning in other parts of the catchment and to focus on other conceptual model situations.

### **7.2.2 Local Scale (10s m to km)**

The detailed geometry of the drift in different parts of the catchment has been described at the local scale in Chapter 3. The results show the strength of the ERT method for such investigation when supplemented by a degree of borehole control (Cuthbert *et al.* 2004) and highlight the inadequacy of existing drift mapping for understanding the local scale drift structure. Aside from the drift structural aspects, another interesting feature of the ERT surveys is the variation in resistivity associated with the root zones of large trees.

A limited laboratory investigation into the core-scale hydraulic properties of the main drift types (till, glaciofluvial outwash and glaciolacustrine deposits) has produced results consistent with literature values.

On the basis of the local scale investigations a series of conceptual recharge scenarios have been proposed as follows:

**A** In some areas glacial outwash deposits directly overlie the sandstone aquifer and predominantly comprise sands and gravels. Such deposits are likely to have relatively high vertical hydraulic conductivities and provide little barrier to the downward movement of recharging water.

**B** In many locations low permeability layers, such as till, glaciolacustrine clays or finer grade outwash material, underlie more permeable glacial outwash deposits. Where such layers are laterally persistent, lateral flow at the interface will occur resulting in discharge to drains, watercourses or seepage/riparian areas.

**C** Where low permeability layers are laterally discontinuous, water flowing laterally within the overlying layer may recharge the aquifer some distance away from where it infiltrated.

**D** Where the interface between the upper permeable layer and the underlying low permeability deposit is uneven, water may pond in hollows at the boundary providing a reservoir from which recharge can occur slowly through underlying deposits during much of the year.

**E** Where till directly overlies the aquifer (a thin covering of outwash or head may also be present) the recharge will depend on the bulk permeability of the deposits and the hydraulic gradient between the till water table and the aquifer piezometric surface. The bulk permeability is likely to vary with lithology and the depth/degree of fracturing. Where the till is thin and highly fissured, the bulk vertical hydraulic conductivity is likely to be much greater than that of the matrix allowing significant amounts of recharge to the underlying aquifer.

**F** In areas where the till is patchy and at the till margins, water running off clayey soils overlying the till may run on to more permeable deposits and recharge the aquifer in these locations.

*G* Agricultural land drains are present in many areas and in some cases discharge to soakaways cut through the till into the weathered top of the sandstone aquifer. Thus water can bypass the low permeability till below and recharge the aquifer directly via these drains.

Owing to the limited coverage of the ERT surveys carried out for this research (see Figure 3.5) it is not yet possible to map the distribution of the conceptual models into ‘domains’ of applicability over more than a fraction of the Potford Brook catchment. Further work to extend such mapping and to find quicker ways of mapping the distribution of conceptual domains is currently being carried out under a wider LOCAR project at the University of Birmingham.

### **7.2.3 Catchment Scale (km to 10s km)**

Chapter 2 presented the major components of the hydrologic functioning of the Potford Brook catchment. Compared to many other catchments in the UK, data availability and quality are very good and yet prior to this research there was major uncertainty in regard to the distribution and magnitude of recharge. More detailed investigation at the local and site scale, as has been carried out for this thesis, is beyond the scope of most regional water resource modelling studies. However, in many cases acceptable refinement of such models against regional targets can be achieved using ‘black-box’ recharge models which give the desired recharge and flow outputs for historic model calibration without requiring knowledge of the local scale processes. A recent water resources modelling study of the Tern catchment by the Environment Agency is one such example (Streetly and Shepley 2005). This model suggests that the average recharge through areas mapped as till covered in the Potford Brook catchment may be approximately 90 mm/a in comparison to 240 mm/a for drift free areas. However, based on the fieldwork presented in Chapter 3 which was carried out within a single conceptual recharge domain of the Environment Agency model (‘Sandstone aquifer with clay

Drift'), at least 7 distinct hydraulic processes are thought to be occurring at the local scale. It is not possible, on the basis of this research alone, to judge the accuracy of the Environment Agency estimate since the site scale quantification of recharge has not covered all of these hydraulic processes. Given that the estimate for recharge through till given in Chapter 5 was around 25 to 41 mm/a, the Environment Agency estimate seems quite high. However, recharge is likely to be higher in some of the area mapped as till due to runoff-runon processes and in areas where the till is thinner and/or more highly fractured. Until more is known about the degree to which runoff-runon processes can increase recharge locally, a more complete appraisal of the Environment Agency estimate is not possible.

It remains to be seen whether when significant changes, for example due to climate change or new abstractions, are made to a hydrological system that regional recharge models not informed by the processes operating at the local scale, will produce a correct response. Furthermore some of the local and site scale recharge models proposed imply markedly reduced travel times for contaminant migration to the underlying aquifer than would be expected for slow vertical percolation through low permeability drift materials. Hence for making decisions about aquifer protection it is crucial that an understanding of the local scale processes is developed to inform decisions that have, in many cases, to be based on existing mapping and data from widely spaced boreholes.

### **7.3 Appraisal of Research Methodology and Contribution**

#### **7.3.1 Methodology**

The approach of progressive scale refinement used for the research was, in many ways, very effective. The study at the sub-catchment scale highlighted the present uncertainty of the distribution and magnitude of recharge through the drift and the importance of a better understanding for sustainable water resource management. The local scale investigations

were critical in choosing suitable locations for the detailed fieldsites, enabled the detail of the drift geometry to be realised and provided a firm context for the site scale field studies. A weakness of the approach was that the research effort had to be spread across the scales so that limited time was available to probe more deeply where particularly interesting results were obtained. Further work in some of these areas is recommended in Section 7.4.

The approach of applying a range of different techniques to the fieldsites also worked very well. In particular, the combination of hydraulic monitoring and the use of tracers proved to be successful where the use of one method in isolation may have left much greater uncertainty in the hypothesised flow mechanisms.

### **7.3.2 Contribution**

As discussed in Section 1.5, existing studies of drift hydraulics have tended to focus on either the shallow soil zone and issues concerning unsaturated flow, or the deeper saturated zone and issues concerning aquifer recharge. This thesis makes a significant and original contribution by giving a holistic consideration of the problem of recharge through drift from the ground surface to the aquifer. More particularly the thesis presents some of the first direct evidence of hydraulically active fractures in glacial tills in Britain and, to this author's knowledge, the first quantification of the recharge flux through glaciolacustrine clay deposits. Similar conceptual recharge pathways have been inferred in other studies based on the interpolation of borehole logs and outcrop data (e.g. Gerber *et al.* 2001). However, the application of ERT in deriving continuous structural models of glacial drift is an internationally original contribution to the hydrogeological literature.

The research approach fits with that of a wider LOCAR project entitled "Towards a Methodology for Determining the Pattern and Magnitude of Recharge Through Drift

Deposits.” This thesis contributes to the aims of that project by developing an understanding of the important hydraulic processes at the site and local scale to support the quantitative modelling of recharge across all spatial scales. These results will be combined with those of detailed geological and geostatistical modelling of drift distribution and structure, and numerical upscaling, currently being undertaken by BGS and the University of Birmingham. The initial approach taken to the problem of upscaling has been to use variably saturated 2-D models encompassing several local scale conceptual models to simulate the aggregated recharge response for the sandstone (Mackay *et al.* 2005). It is hoped that further development of such models integrated with geostatistical structural models will enable more confident modelling of recharge through drift at the regional scale.

A better understanding of recharge is an important part of sustainable catchment management both in terms of water quantity and quality. Thus the findings of the research directly contribute to the aims of the LOCAR programme which is studying the interconnections between aquatic ecology, surface hydrology, groundwater and earth surface processes. In this regard it is important that the results of this study are in some way transferable to other drift covered areas so that such in depth studies are not needed for every catchment. The results of this research, both in terms of core-scale and site scale hydraulic parameters (as noted in Chapters 3 and 5), are within the range of literature values reported for other drift covered areas of the UK and also other parts of the world (e.g. Scandinavia and North America). Thus, where similar geological deposits are encountered it is reasonable to assume that there is a degree of transferability in terms of the hydraulic processes. An appreciation of the style and scale of depositional and post-depositional processes has been shown to be important. A difficult question is how much investigation is necessary to be confident in transferring ideas derived in one area and applying them to another. Furthermore, can correlations be found

between micro scale processes and measurable macroscopic properties that can be used to map out zones where specific processes are occurring? These are matters for further research and it is hoped that the wider LOCAR project into recharge through drift can go some way to answering them.

A series of conference papers have been produced during the period of research based on the data presented in this thesis. These are given in Appendix 10.

#### **7.4 Recommendations**

By considering the limitations of the thesis, recommendations for future work become apparent:

- Owing to the time constraints of the project not all of the hydraulic processes/pathways identified in Chapter 3 were studied using detailed site investigation. Two potentially important processes thus remain to be studied in detail as follows:
  - i. Runoff-runon recharge in areas of patchy till/glaciolacustrine clay, at the scale of 10s to 100s m
  - ii. Recharge occurring some distance away from the point of infiltration due to the flow of water through permeable outwash deposits overlying laterally discontinuous till/glaciolacustrine clay
- The significance of preferential flow has been identified in unsaturated till and glaciofluvial outwash deposits. Some regional water resource models already include 'bypass flow' in order to generate sufficient recharge to model the catchment water balance adequately. However the ways in which this process has been modelled and

parameterised is often difficult to justify. Further research into this issue is necessary to enable such processes to be modelled in a defensible way.

- Further data collection is required in order to understand fully the process of wetting and drying of till matrix blocks and to investigate more adequately the properties of the till fractures. An extension of the modelling of till fracture flow presented in Chapter 5 could then be carried out to explore the sensitivity of the wetting and drying of matrix blocks to the 3-D block geometry and to investigate the significance of flow focussing. Further understanding of these processes and increased knowledge of the fracture properties will be essential to developing a robust understanding of the movement of solutes through the till necessary for decisions regarding aquifer vulnerability and to adequately model the hydraulic behaviour of the till during prolonged dry periods.
- The influence of plant rooting depths and distributions on the drying of the upper parts of the till profile would also be a useful subject for further research. Of particular interest is the extent to which plant roots exploit the fractures within the till and therefore cause preferential drying, and how this affects the fracture permeability and the development of the fracture network over time.
- Although ERT has been used to good effect for mapping the structure of the drift deposits, the success of geophysical methods (ERT and TDR) for monitoring changes in water content has been limited. Further research is needed to find ways of making quantitative hydrological judgements from such geophysical methods without the need for onerous site specific calibrations.
- To resolve the uncertainties with the applied tracer experiment within the till, an integrated experiment is recommended whereby the tracer experiment is repeated but the patch is

excavated after 6 months. Samples of till could then be taken directly from the faces of the test pit to compare the tracer movement in the fractures and the matrix while minimising the possibility of cross contamination.

## REFERENCES

- Allen, J. R. L. (1983). "Studies in Fluvial Sedimentation - Bars, Bar-Complexes and Sandstone Sheets (Low-Sinuosity Braided Streams) in the Brownstones (L-Devonian), Welsh Borders." *Sedimentary Geology* 33(4): 237-293.
- Alphen, B. J., H. W. G. Booltink and J. Bouma (2001). "Combining pedotransfer functions with physical measurements to improve the estimation of soil hydraulic properties." *Geoderma* 103: 133-147.
- Anderson, M. P. (1989). "Hydrogeologic Facies Models to Delineate Large-Scale Spatial Trends in Glacial and Glaciofluvial Sediments." *Geological Society of America Bulletin* 101(4): 501-511.
- Archie, G. E. (1942). "The electrical resistivity log as an aid in determining some reservoir characteristics." *Trans. Am. Inst. Min. Metall. Pet. Eng.* 146: 54-67.
- Artimo, A., J. Makinen, R. C. Berg, C. C. Abert and V. P. Salonen (2003). "Three-dimensional geologic modeling and visualization of the Virttaankangas aquifer, southwestern Finland." *Hydrogeology Journal* 11(3): 378-386.
- Aspiron, U. and T. Aigner (1999). "Towards realistic aquifer models: a three-dimensional georadar case study of quaternary gravel deltas (Singen Basin, SW Germany)." *Sedimentary Geology* 129(3-4): 1-24.
- Baker, A. (2002). "Fluorescence properties of some farm wastes: implications for water quality monitoring." *Water Research* 36: 189-195.
- Baker, A. and J. Lamont-Black (2001). "Fluorescence of dissolved organic matter as a natural tracer of groundwater." *Ground Water* 39(5): 745-750.
- Baker, A. C. (1994). *The measurement of hydraulic and solute transport parameters in clays*. PhD Thesis, School of Earth Sciences, University of Birmingham.
- Bennett, M. R. and N. F. Glasser (1996). *Glacial Geology: Ice Sheets and Landforms*. Chichester, England, Wiley.
- Beres, M., P. Huggenberger, A. G. Green and H. Horstmeyer (1999). "Using two- and three-dimensional georadar methods to characterize glaciofluvial architecture." *Sedimentary Geology* 129: 1-24.
- Beven, K. (1991). *Modeling preferential flow: an uncertain future?* Preferential Flow, Chicago, Illinois, U. S., American Society of Agricultural Engineers. 1-11.
- Beven, K. and P. Germann (1982). "Macropores and Water Flow in Soils." *Water Resources Research* 18(5): 1311-1325.

BGS (2001). *The hydrochemistry of the Tern Catchment, Shropshire*. British Geological Survey. CR/01/131.

Binley, A., G. Cassiani, R. Middleton and P. Winship (2002). "Vadose zone flow model parameterisation using cross-borehole radar and resistivity imaging." *Journal of Hydrology* 267: 147-159.

Bloomfield, J. (1994). *Unconsolidated Sedimentary Aquifers: Review No 5 - The Use of Laboratory Techniques in the Characterization of Unconsolidated Sedimentary Aquifer Physical Properties*. Keyworth, Nottingham, British Geological Survey. BGS Technical Report WC/94/62.

Bonell, M. (1972a). "The application of the auger hole method in Holderness Drift." *Journal of Hydrology* 16: 125-146.

Bonell, M. (1972b). "An assessment of the possible factors contributing to well level fluctuations in Holderness Boulder Clay, East Yorkshire." *Journal of Hydrology* 16: 361-368.

Bonell, M. (1973). "Time lag response in boulder clay wells." *Nordic Hydrology* 4(86-104).

Bonell, M. (1976). "Some comments on the association between saturated hydraulic conductivity and texture of Holderness boulder clay." *Catena* 3: 77-90.

Bonell, M. (1978). *An evaluation of shallow groundwater movement in a small Boulder Clay covered catchment in Holderness*. University of Hull. Miscellaneous Series No. 18.

Boulton, G. S. and M. A. Paul (1976). "The influence of genetic processes on some geotechnical properties of glacial tills." *Quarterly Journal of Engineering Geology* 9: 159-194.

Boulton, G. S. and P. Worsley (1965). "Late Weichselian Glaciation in the Cheshire-Shropshire Basin." *Nature* 207: 704-706.

Boyce, J. I. and N. Eyles (2000). "Architectural element analysis applied to glacial deposits: Internal geometry of a late Pleistocene till sheet, Ontario, Canada." *Geological Society of America Bulletin* 112(1): 98-118.

Bradbury, C. G. and K. R. Rushton (1998). "Estimating runoff-recharge in the Southern Lincolnshire Limestone catchment, UK." *Journal of Hydrology* 211(1-4): 86-99.

Bridge, D. McC., A. J. Humpage, H. Sheppard, M. Lelliott and M. Garcia-Bajo (2002). *East Shropshire Permo-Triassic Sandstone Groundwater Modelling Project. Task 1: Geological Framework Study*. BGS, Environment Agency. CR/02/176.

Bullister, J. L. and R. F. Weiss (1988). "Determination of CC13F and CC12F2 in seawater and air." *Deep-Sea Research* 35: 839-853.

- Bunch, M. A., R. Mackay, J. H. Tellam and P. Turner (2004). "A model for simulating the deposition of water-lain sediments in dryland environments." *Hydrology and Earth System Sciences* 8: 122-134.
- Cain, S. F., G. A. Davis, S. P. Loheide and J. J. Butler (2004). "Noise in pressure transducer readings produced by variations in solar radiation." *Ground Water* 42(6): 939-944.
- Carsel, R. F. and R. S. Parrish (1988). "Developing joint probability distributions of soil water retention characteristics." *Water Resources Research* 24(5): 755-769.
- Carslaw, H. S. and J. C. Jaeger (1959). *Conduction of heat in solids*, Oxford University Press.
- Cartwright, D. J. (2001). *Using hydraulic testing to determine transport properties of a fractured clay aquitard*. MSc Project Report, Department of Geological Sciences, University College London.
- Catt, J. A. (1986). *Soil and Quaternary Geology: A Handbook for Field Scientists*. New York, Oxford University Press.
- Christy, A. D., L. A. McFarland and D. Carey (2000). "The use of test pits to investigate fracturing and glacial stratigraphy in tills and other unconsolidated materials." *Ohio Journal of Science* 100(3-4): 100-106.
- Clapp, R. B. and G. M. Hornberger (1978). "Empirical equations for some hydraulic properties." *Water Resources Research* 14(4): 601-604.
- Corrigan, C. A., H. E. Jamieson and V. H. Remenda (2001). "Fracture wall cements and coatings from two clayey till aquitards." *Ground Water* 39(5): 786-794.
- Cravens, S. J. and L. C. Ruedisili (1987). "Water-Movement in Till of East-Central South-Dakota." *Ground Water* 25(5): 555-561.
- Cuthbert, M. O., R. Mackay, J. H. Tellam and A. J. Humpage (2004). *Local and regional scale controls on recharge in a drift covered catchment*. Groundwater Flow Understanding: from local to regional scales, IAH XXXIII Congress, Zacatecas, Mexico, IAH. T513, 1-4.
- Cuthbert, M. O., E. J. F. Russell, R. D. Barker and R. Mackay (2004). *The effect of seasonal temperature variations on the resistivity of glacial till*. Near Surface 2004 - 10th European Meeting of Environmental and Engineering Geophysics, Utrecht, The Netherlands, EAGE. PO32 1-4.
- Cuthbert, M. O. and R. W. N. Soley (2000). *Data Presentation and Analysis for the Sheriffhales Groundwater Augmentation Trial in the Upper River Worfe*. Entec UK Ltd.
- Daily, W., A. Ramirez, D. Labrecque and J. Nitao (1992). "Electrical-resistivity tomography of vadose water-movement." *Water Resources Research* 28(5): 1429-1442.

- D'Astous, A. Y., W. W. Ruland, J. R. G. Bruce, J. A. Cherry and R. W. Gillham (1989). "Fracture effects in the shallow groundwater zone in weathered Sarnia-area clay." *Canadian Geotechnical Journal* 26: 43-56.
- de Marsily, G., F. Delay, V. Teles and M. T. Schafmeister (1998). "Some current methods to represent the heterogeneity of natural media in hydrogeology." *Hydrogeology Journal* 6(1): 115-130.
- Digges La Touche, S. (1998). *Unsaturated flow in the Triassic sandstones of the United Kingdom*. PhD Thesis, School of Earth Sciences, University of Birmingham.
- Durner, W. (1994). "Hydraulic conductivity estimation for soils with heterogeneous pore structure." *Water Resources Research* 30(2): 211-223.
- Ekes, C. and E. J. Hickin (2001). "Ground penetrating radar facies of the paraglacial Cheekye Fan, southwestern British Columbia, Canada." *Sedimentary Geology* 143(3-4): 199-217.
- Erskine, A. D. and A. Papaioannou (1997). "The use of aquifer response rate in the assessment of groundwater resources." *Journal of Hydrology* 202: 373-391.
- Evet, S., J.-P. Laurent, P. Cepuder and C. Hignett (2002). *Neutron scattering, capacitance, and TDR soil water content measurements compared on four continents*. 17th WCSS, Thailand. 1021 1-10.
- Eyles, N. and J. A. Sladen (1981). "Stratigraphy and Geotechnical Properties of Weathered Lodgement Till in Northumberland, England." *Quarterly Journal of Engineering Geology* 14(2): 129-141.
- FAO (1998). *Crop Evapotranspiration - Guidelines for computing crop water requirements*. *FAO Irrigation and drainage paper 56*. Rome, Food and Agriculture Organisation of the United Nations.
- Feddes, R. A., P. J. Kowalik and H. Zaradny (1978). *Simulation of field water use and crop yield*. Wageningen, Netherlands, Centre for Agricultural Publishing and Documentation.
- Finch, J. (1999). *Post drought soil water recharge*. Institute of Hydrology. National Groundwater and Contaminated Land Centre Project NC/06/12.
- Fletcher, S. W. (1976). *Geology, groundwater tables, and soil moisture content variations at Hodnet Heath*. Environment Agency.
- Fogg, G. E. (1986). "Groundwater flow and sand body interconnectedness in a thick, multiple aquifer system." *Water Resources Research* 22: 679-694.
- Fox, M. (2003). *Assessing the relationship between resistivity and moisture content at an unsaturated zone test site*. MSc Project Report, School of Geography, Earth and Environmental Sciences, University of Birmingham.

- Fraser, G. S. and J. M. Davis (1998). *Hydrogeological Models of Sedimentary Aquifers*. Tulsa, Oklahoma, US, SEPM.
- Fredericia, J. (1990). "Saturated hydraulic conductivity of clayey Tills and the role of fractures." *Nordic Hydrology* 21: 119-132.
- Freeze, R. A. and J. A. Cherry (1979). *Groundwater*. Englewood Cliffs, New Jersey, Prentice-Hall.
- Fuller, R. M., G. M. Smith, J. M. Sanderson, R. A. Hill and A. G. Thomson (2002). "The UK Land Cover Map 2000: construction of a parcel-based vector map from satellite images." *Cartographic J* 39: 15-25.
- Fullwood, J. (2005). *Personal Communication*
- Gale, S. J. and P. G. Hoare (1991). *Quaternary Sediments*, Belhaven Press, London, UK.
- Garrick, H. (2003). *The impact of groundwater abstraction on the Potford and Platt surface water catchment, Tern catchment, Shropshire*. MSc Project Report, Department of Earth Sciences, University of Birmingham.
- Gerber, R. E., J. I. Boyce and K. W. F. Howard (2001). "Evaluation of heterogeneity and field-scale groundwater flow regime in a leaky till aquitard." *Hydrogeology Journal* 9(1): 60-78.
- Gerber, R. E. and K. Howard (2000). "Recharge through a regional till aquitard: Three-dimensional flow model water balance approach." *Ground Water* 38(3): 410-422.
- Gerke, H. H. and J. M. Kohne (2004). "Dual-permeability modelling of preferential bromide leaching from a tile-drained glacial till agricultural field." *Journal of Hydrology* 289: 239-257.
- Gerke, H. H. and M. T. van Genuchten (1993a). "A dual porosity model for simulating the preferential movement of water and solutes in structured porous media." *Water Resources Research* 29(2): 305-319.
- Gerke, H. H. and M. T. van Genuchten (1993b). "Evaluation of a first-order water transfer term for variably saturated dual-porosity flow models." *Water Resources Research* 29(4): 1225-1238.
- Gerke, H. H. and M. T. van Genuchten (1996). "Macroscopic representation of structural geometry for simulating water and solute movement in dual-porosity media." *Advances in Water Resources* 19(6): 343-357.
- Goode, D. J., Busenberg, Eurybiades, L. N. Plummer, A. M. Shapiro and D. A. Vroblesky (1997). *CFC degradation under anaerobic water table conditions in glacial drift at Mirror Lake New Hampshire*. Geological Society of America 1997 Annual Meeting, 20-23 October 1997, Salt Lake City, Utah, GSA Abstracts with Programs, vol. 29, no.6, p.77.

- Griffiths, D. H. and R. D. Barker (1993). "Two dimensional resistivity imaging and modelling in areas of complex geology." *Journal of Applied Geophysics* 29(211-226).
- Grisak, G. E., J. A. Cherry, Vonhof and J. P. Blumele (1976). Hydrogeologic and hydrochemical properties of fractured till in the interior plains region. *Glacial Till*. R. F. Legget, Roy Soc Can Spec Pub. 12: 304-335.
- Hagrey, S. A., R. Meissner, U. Werban, W. Rabbel and A. Ismaeil (2004). "Hydro-, bio-geophysics." *The Leading Edge* July 2004(670-674).
- Haldorsen, S. and J. Kruger (1990). "Till genesis and hydrogeological properties." *Nordic Hydrology* 21: 81-94.
- Harden, H. S., J. P. Chanton, J. B. Rose, D. E. John and M. E. Hooks (2003). "Comparison of sulfur hexafluoride, fluorescein and rhodamine dyes and the bacteriophage PRD-1 in tracing subsurface flow." *Journal of Hydrology* 277: 100-115.
- Hazen, A. (1911). "Discussion of "Dams on Soil Foundations"." *Trans. Amer. Soc. Civil Engrs.* 73: 199.
- Heathcote, J. A., R. T. Lewis and R. W. N. Soley (2003). "Rainfall routing to runoff and recharge for regional groundwater resource models." *Quarterly Journal of Engineering Geology and Hydrogeology* 37(2): 113-130.
- Heathcote, J. A. and J. W. Lloyd (1984). "Groundwater chemistry in southeast Suffolk (U.K.) and its relation to Quaternary geology." *Journal of Hydrology* 75(1-4): 143-165.
- Heinz, J., S. Kleinedam, G. Teutsch and T. Aigner (2003). "Heterogeneity patterns of Quaternary glaciofluvial gravel bodies (SW-Germany): application to hydrogeology." *Sedimentary Geology* 158: 1-23.
- Hendry, M. J. (1988). "Hydrogeology of Clay Till in a Prairie Region of Canada." *Ground Water* 26(5): 607-614.
- Hendry, M. J., C. J. Kelln, L. I. Wassenar and J. Shaw (2004). "Characterising the hydrogeology of a complex clay-rich aquitard system using detailed vertical profiles of the stable isotopes of water." *Journal of Hydrology* 293: 47-56.
- Hillel, D. (1987). "Unstable flow in layered soils: a review." *Hydrological Processes* 1: 143-147.
- Hinton, M. J., S. L. Schiff and M. C. English (1993). "Physical-Properties Governing Groundwater-Flow in a Glacial Till Catchment." *Journal of Hydrology* 142(1-4): 229-249.
- Hiscock, K. M. (1993). "The Influence of Pre-Devensian Glacial Deposits on the Hydrogeochemistry of the Chalk Aquifer System of North Norfolk, UK." *Journal of Hydrology* 144(1-4): 335-369.

- Hiscock, K. M. (2005). *Hydrogeology, Principles and Practice*. Oxford, Blackwell.
- Holman, I. P., T. M. Hess, P. B. Leeds-Harrison, R. C. Palmer and I. Truckell (2002). *Investigating the effects of land drainage activities on natural recharge to groundwater*. Environment Agency. R&D Technical Report W6-076/TR.
- Hulme, P. (2002). *Groundwater Resources Modelling: Guidance Notes and Template Project Brief (Version 1)*. Environment Agency. R&D Guidance Notes W213.
- Hulme, P. and e. al (2002). *Groundwater Resources Modelling: Guidance notes and template project brief*. Environment Agency. R&D Guidance Notes W213.
- Hulme, P., K. R. Rushton and S. Fletcher (2001). *Estimating recharge in UK catchments. Impact of Human Activity on Groundwater Dynamics (Proceedings of a symposium held during the Sixth IAHS Scientific Assembly at Maastricht, The Netherlands, July 2001)*, Maastricht, The Netherlands, IAHS. 33-42.
- Humpage, A. J. (2005). *Personal communication*
- Hvorslev, M. J. (1951). "Time lag and soil permeability in groundwater observations." *U.S. Army Corps Engrs. Waterways Exp. Sta. Bull.* 36.
- IoH (1989). *Flow Regimes from Experimental and Network Data (FRIEND)*, NERC, UK.
- Iversen, B. V., P. van de Keur and H. Vosgerau (2004). *Relating lithofacies to hydrofacies: two-dimensional hydrological modelling in the vadose zone of glaciofluvial deposits*. Abstracts Volume of EGU General Assembly, Nice, France, EGS. EGU04-A-05429.
- Jackson, D. and K. R. Rushton (1987). "Assessment of Recharge Components for a Chalk Aquifer Unit." *Journal of Hydrology* 92(1-2): 1-15.
- Jacob, C. E. (1940). "On the flow of water in an elastic artesian aquifer." *Trans. Amer. Geophysical Union* 21: 574-586.
- Jakobsen, P. R. and K. E. S. Klint (1999). "Fracture distribution and occurrence of DNAPL in a clayey lodgement till." *Nordic Hydrology* 30(4/5): 285-300.
- Jansson, C. and P.-E. Jansson (2003). *Preferential water flow in a glacial till soil*. Abstracts Volume of EGS-AGU-EUG Joint Assembly, Nice, France, EGS. EAE03-A-10309.
- Jenssen, P. D. (1990). "Methods for measuring the saturated hydraulic conductivity of Tills." *Nordic Hydrology*: 95-106.
- Jones, L., T. Lemar and C.-T. Tsai (1992). "Results of two pumping tests in Wisconsin age weathered till in Iowa." *Ground Water* 30(4): 529.
- Kasnavia, T., D. Vu and D. A. Sabatini (1999). "Fluorescent dye and media properties affecting sorption and tracer selection." *Ground Water* 37(3): 376-381.

- Keller, C. K., G. Vanderkamp and J. A. Cherry (1986). "Fracture Permeability and Groundwater-Flow in Clayey Till near Saskatoon, Saskatchewan." *Canadian Geotechnical Journal* 23(2): 229-240.
- Keller, C. K., G. Vanderkamp and J. A. Cherry (1988). "Hydrogeology of 2 Saskatchewan Tills .1. Fractures, Bulk Permeability, and Spatial Variability of Downward Flow." *Journal of Hydrology* 101(1-4): 97-121.
- Keller, C. K., G. Vanderkamp and J. A. Cherry (1989). "A Multiscale Study of the Permeability of a Thick Clayey Till." *Water Resources Research* 25(11): 2299-2317.
- Khanzode, R. M., S. K. Vanapalli and D. G. Fredland (2002). "Measurement of soil-water characteristic curves for fine-grained soils using a small-scale centrifuge." *Canadian Geotechnical Journal* 39: 1209-1217.
- Klinck, B. A., J. A. Barker, D. J. Noy and G. P. Wealthall (1996). *Mechanisms and rates of recharge through glacial till: Experimental and modelling studies from a Norfolk site*. British Geological Survey. Fluid Processes Series Technical Report WE/96/1.
- Klinck, B. A., P. N. Hopson, A. N. Morigi, A. J. Bloodworth, S. D. J. Inglethorpe, D. C. Entwistle and G. P. Wealthall (1997). *The hydrogeological classification of superficial clay: the hydrogeological characterisation of glacial Till in East Anglia*. Environment Agency. R&D Technical Report W28.
- Klint, K. E. S. and P. Gravesen (1999). "Fractures and biopores in Weichselian clayey till aquitards at Flakkebjerg, Denmark." *Nordic Hydrology* 30(4/5): 267-284.
- Kohne, J. M., B. P. Mohanty, J. Simunek and H. H. Gerke (2004). "Numerical evaluation of a second-order water transfer term for variably saturated dual-permeability models." *Water Resources Research* 40: W07409.
- Koltermann, C. E. and S. M. Gorelick (1996). "Heterogeneity in sedimentary deposits: A review of structure- imitating, process-imitating, and descriptive approaches." *Water Resources Research* 32(9): 2617-2658.
- Kruseman, G. P. and N. A. de Ridder (1990). *Analysis and Evaluation of Pumping Test Data*. Wageningen, The Netherlands, ILRI.
- Kung, K.-J. S. (1990a). "Preferential Flow in a Sandy Vadose Zone: 2. Mechanism and Implications." *Geoderma* 46: 59-71.
- Kung, K.-J. S. (1990b). "Preferential Flow in a Sandy Vadose Zone: 1. Field Observation." *Geoderma* 46: 51-58.
- Laurent, J.-P. (2002). *Field comparison of neutron and TDR "Trime-Tube" probes on four sites*. Progress report 2001-2002 contract 11195/FAO.

- Lerner, D. N., A. S. Issar and I. Simmers, Eds. (1990). *Groundwater Recharge: A guide to understanding and estimating natural recharge*. International Contributions to Hydrogeology, Verlag Heinz Heise.
- Liu, H. H., G. S. Bodvarsson and S. Finsterle (2002). "A note on unsaturated flow in two-dimensional fracture networks." *Water Resources Research* 38(9): 1176.
- Liu, H. H., C. B. Haukwa, C. F. Ahlers, G. S. Bodvarsson, A. L. Flint and W. B. Guertal (2003). "Modeling flow and transport in unsaturated fractured rock: an evaluation of the continuum approach." *Journal of Contaminant Hydrology* 62-63: 173-188.
- Lloyd, J. W. (1980). "The importance of drift deposit influences on the hydrogeology of major British aquifers." *J. Inst. Water Eng. Sci.* 34: 346-356.
- Lloyd, J. W. (1983). Hydrogeological investigations in glaciated terrains. *Glacial Geology: An introduction for engineers and earth scientists*. Ed. N. Eyles. Toronto, Canada, Pergamon Press: 349-368.
- Lloyd, J. W., D. Harker and R. A. Baxendale (1981). "Recharge Mechanisms and Groundwater-Flow in the Chalk and Drift Deposits of Southern East-Anglia." *Quarterly Journal of Engineering Geology* 14(2): 87-96.
- Lloyd, J. W. and K. M. Hiscock (1990). Importance of drift deposits in influencing chalk hydrogeology. *Chalk*. London, Thomas Telford.
- Loke, M. H. (2002). RES2DMOD ver. 3.01: Rapid 2D resistivity forward modelling using the finite difference and finite element methods.
- Loke, M. H. (2004). RES2DINV ver. 3.54: Rapid 2D resistivity and I-P inversion using the least-squares method.
- Loke, M. H. and R. D. Barker (1995). "Least Squares Deconvolution of Apparent Resistivity Pseudosections." *Geophysics* 42: 1682-1690.
- Loke, M. H. and R. D. Barker (1996a). "Rapid Least Squares Inversion of Apparent Resistivity Pseudosections by a Quasi-Newton Method." *Geophysical Prospecting* 44: 131-152.
- Loke, M. H. and R. D. Barker (1996b). "Practical Techniques for 3D Resistivity Surveys and Inversion." *Geophysical Prospecting* 44: 499-523.
- Mackay, R. and P. E. O'Connell (1991). Statistical methods of characterizing hydrogeological parameters. *Applied Groundwater Hydrology: A British Perspective*. Eds. R. A. Downing and W. B. Wilkinson. Oxford, Clarendon Press: 217-242.
- Mackay, R., M. O. Cuthbert, H. Ash and J. H. Tellam (2005). Towards an up-scaled model of aquifer recharge through glacial drift deposits, Shropshire, UK. Model Care 2005 Conference Proceedings, The Hague, The Netherlands.

Marks, R. J., W. G. Darling, A. R. Lawrence and A. G. Hughes (2001). *Recharge through drift: progress report*. British Geological Survey. IR/01/049.

Marks, R. J., A. R. Lawrence, E. J. Whitehead, J. E. Cobbing, W. G. Darling and A. G. Hughes (2004). *Recharge to the Chalk aquifer beneath thick till deposits in East Anglia*. British Geological Survey. IR/04/007.

Marthaler, H. P. (1983). "A pressure transducer for field tensiometers." *Soil Sci. Soc. Am. J.* 47: 624-627.

Mase, C. W., J. A. Cherry, L. D. McKay and A. J. A. Unger (1990). *Hydrogeology of desiccated fractured clays*. American Geophysical Union Fall Meeting, San Francisco, California, U.S.

McDonald, D. M. J. (1996). *Estimating groundwater recharge through glacial till at Bacon Hall, Shropshire*. British Geological Survey. WD/95/22.

McDonald, M. G. and A. W. Harbaugh (1984). *A modular three-dimensional finite difference groundwater flow model*. USGS.

McKay, L. D., J. A. Cherry and R. W. Gillham (1993). "Field Experiments in a Fractured Clay Till .1. Hydraulic Conductivity and Fracture Aperture." *Water Resources Research* 29(4): 1149-1162.

McKay, L. D. and J. Fredericia (1995). "Distribution, origin and hydraulic influence of fractures in a clay-rich glacial deposit." *Canadian Geotechnical Journal* 32: 957-975.

McKay, L. D., J. Fredericia, M. Lenczewski, J. Morthorst and K. E. S. Klint (1999). "Spatial variability of contaminant transport in a fractured till, Avedore Denmark." *Nordic Hydrology* 30(4/5): 333-360.

McMillan, A. A. and J. H. Powell (1999). BGS rock classification scheme, volume 4: *Classification of artificial (man-made) ground and natural superficial deposits applications to geological maps and datasets in the UK*: British Geological Survey, Research Report RR-99-04

McMillan, A. A., J. A. Heathcote, B. A. Klinck, M. G. Shepley, C. P. Jackson and P. J. Degnan (2000). "Hydrogeological characterisation of the onshore Quaternary sediments at Sellafield using the concept of domains." *Quarterly Journal of Engineering Geology* 33: 301-323.

Miall, A. D. (1984). *Principles of Sedimentary Basin Analysis*. New York, Springer-Verlag.

Michot, D., Y. Benderitter, A. Dorigny, B. Nicoulland, D. King and A. Tabbagh (2003). "Spatial and temporal monitoring of soil water content with an irrigated corn crop cover using surface electrical resistivity tomography." *Water Resources Research* 39(5): 1138.

- Morris, D. G. and R. W. Flavin (1990). *A Digital Terrain Model for Hydrology*. 4th International Symposium on Spatial Data Handling, Zurich.
- Mualem, Y. (1976). "A new model for predicting the hydraulic conductivity of unsaturated porous media." *Water Resources Research* 12(3): 513-522.
- Neuman, S. P. and D. A. Gardner (1989). "Determination of Aquitard Aquiclude Hydraulic Properties from Arbitrary Water-Level Fluctuations by Deconvolution." *Ground Water* 27(1): 66-76.
- Nielson, D. R., M. T. van Genuchten and J. W. Biggar (1986). "Water flow and solute transport processes in the unsaturated zone." *Water Resources Research* 22(9): 89S-108S.
- Nilsson, B., R. C. Sidle, K. E. Klint, C. E. Boggild and K. Broholm (2001). "Mass transport and scale-dependent hydraulic tests in a heterogeneous glacial till-sandy aquifer system." *Journal of Hydrology* 243: 162-179.
- Nyborg, M. R. (1989). "A model for the relationship between the hydraulic conductivity and primary sedimentary structures of Till." *Nordic Hydrology* 20: 137-152.
- Omoti, U. and A. Wild (1979). "Use of fluorescent dyes to mark the pathways of solute movement through soils under leaching conditions: 1. Laboratory experiments." *Soil Science* 128(1): 28-33.
- Ortega-Guerrero, A., D. L. Rudolph and J. A. Cherry (1999). "Analysis of long-term land subsidence near Mexico City: Field investigations and predictive modeling." *Water Resources Research* 35(11): 3327-3341.
- Oster, H., C. Sonntag and M. K. O. (1996). "Groundwater age dating with chlorofluorocarbons." *Water Resources Research* 37: 2989-3001.
- Parker, B. L., J. A. Cherry and S. W. Chapman (2004). "Field study of TCE diffusion profiles below DNAPL to assess aquitard integrity." *Journal of Contaminant Hydrology* 74(1-4): 197-230.
- Philip, J. R. (1967). "The theory of absorption in aggregated media." *Aust. J. Soil. Res.* 6: 1-19.
- Pruess, K. (1999). "A mechanistic model for water seepage through thick unsaturated zones in fractured rocks of low matrix permeability." *Water Resources Research* 35(4): 1039-1051.
- Ragab, R., J. Finch and R. Harding (1997). "Estimation of groundwater recharge to chalk and sandstone aquifers using simple soil models." *Journal of Hydrology* 190: 19-41.
- Rein, A., R. Hoffman and P. Dietrich (2004). "Influence of natural time-dependent variations of electrical conductivity on DC resistivity measurements." *Journal of Hydrology* 285: 215-232.

- Remenda, V. H., G. vanderKamp and J. A. Cherry (1996). "Use of vertical profiles of delta O-18 to constrain estimates of hydraulic conductivity in a thick, unfractured aquitard." *Water Resources Research* 32(10): 2979-2987.
- Richards, L. A. (1931). "Capillary conduction of liquids in porous mediums." *Physics* 1: 318-333.
- Robins, N. S. (1998). Recharge: the key to groundwater pollution and aquifer vulnerability. *Groundwater Pollution, Aquifer Recharge and Vulnerability*. Ed. N. S. Robins. London, Geological Society, Special Publications.
- Rodda, J. C. (1967). "The systematic error in rainfall measurement." *Journal of the Institute of Water Engineers* 21: 173-177.
- Rodda, J. C. and S. W. Smith (1986). "The significance of the systematic error in rainfall measurement for assessing wet deposition." *Atmospheric Environment* 20(5): 1059-1064.
- Ross, P. J. and K. R. J. Smettem (2000). "A simple treatment of physical non-equilibrium water flow in soils." *Soil Sci. Soc. Am. J.* 64: 1926-1930.
- Rowe, P. W. (1972). "The relevance of soil fabric to site investigation practice." *Geotechnique* 22(2): 195-300.
- Ruland, W. W., J. A. Cherry and S. Fenestra (1991). "The Depth of Fractures and Active Groundwater-Flow in a Clayey Till Plain in Southwestern Ontario." *Ground Water* 29(3): 405-417.
- Rushton, K. R. (1975). "Aquifer analysis of the Lincolnshire Limestone using mathematical models." *Journal of the Institution of Water Engineers and Scientists* 29: 373-388.
- Rushton, K. R. (2000). Recharge Estimation in British Aquifers: A Review by Ken Rushton for the Environment Agency. National Groundwater and Contaminated Land Centre, Solihull, UK, Environment Agency.
- Rushton, K. R., M. W. Kawecki and F. C. Brassington (1988). "Groundwater Model of Conditions in Liverpool Sandstone Aquifer." *Journal of the Institution of Water and Environmental Management* 2(1): 67-84.
- Rushton, K. R. and C. Ward (1979). "The estimation of groundwater recharge." *Journal of Hydrology* 41: 345-361.
- Russell, E. J. F. and R. D. Barker (2004). *Variation of clay resistivity with moisture loss*. Near Surface 2004 - 10th European Meeting of Environmental and Engineering Geophysics, Utrecht, The Netherlands, EAGE. PO56 1-4.
- Russell, E. J. F. and R. D. Barker (2005). "Electrical properties of clay in relation to moisture loss." Submitted to *Near Surface Geophysics*.

- Sage, R. C. and J. W. Lloyd (1978). "Drift deposit influences on the Triassic Sandstone aquifer of NW Lancashire as inferred by hydrochemistry." *Quarterly Journal of Engineering Geology* 11(3): 209-218.
- Scanlon, B. R., R. W. Healy and P. G. Cook (2002). "Choosing appropriate techniques for quantifying groundwater recharge." *Hydrogeology Journal* 10(1): 18-39.
- Schaap, M. G., F. J. Leij and M. T. van Genuchten (2001). "Rosetta: a computer program for estimating soil hydraulic parameters with hierarchical pedotransfer functions." *Journal of Hydrology* 251: 163-176.
- Schmugge, T. J., T. J. Jackson and H. L. McKim (1980). "Survey of methods for soil moisture determination." *Water Resources Research* 16(6): 961-979.
- Schumacher, W. (1864). *Die Physik des Bodens*. Berlin.
- Schwartz, F. W. and H. Zhang (2003). *Fundamentals of Groundwater*. New York, John Wiley and Sons.
- Sears, R. (1998). The British Nuclear Fuels Drigg low-level waste site characterisation programme. *Groundwater Pollution, Aquifer Recharge and Vulnerability*. Ed. N. S. Robins. London, Geological Society, London, Special Publications.
- Shotton, F. W. (1965). "Normal faulting in British Pleistocene deposits." *Quarterly Journal of the Geological Society of London* 121: 419-434.
- Simunek, J., N. J. Jarvis, M. T. van Genuchten and A. Gardenas (2003). "Review and comparison of models for describing non-equilibrium and preferential flow and transport in the vadose zone." *Journal of Hydrology* 272: 14-35.
- Simunek, J., M. Sejna and M. T. van Genuchten (1998). *The HYDRUS-1D software package for simulating the one-dimensional movement of water, heat and multiple solutes in variably-saturated media (Version 2.0)*. U. S. Salinity Laboratory, Agricultural Research Centre, U. S. Department of Agriculture.
- Simunek, J., M. T. van Genuchten and M. Sejna (2005). *The HYDRUS-1D software package for simulating the one-dimensional movement of water, heat and multiple solutes in variably-saturated media (Version 3.0)*. Department of Environmental Sciences, University of California Riverside.
- Smart, P. L. and I. M. S. Laidlaw (1977). "An evaluation of some fluorescent dyes for water tracing." *Water Resources Research* 13(1): 15-33.
- Smith, R. E., K. R. J. Smettem, P. Broadbridge and D. A. Woolhiser (2002). *Infiltration theory for hydrologic applications*. Washington, American Geophysical Union.

Soley, R. W. N. and J. A. Heathcote (1998). Recharge through the drift: a study of contrasting Chalk catchments near Redgrave Fen, UK. *Groundwater Pollution, Aquifer Recharge and Vulnerability*. Ed. N. S. Robins, Geological Society, London, Special Publications.

Soley, R. W. N., K. J. Hudson and J. S. Sutton (1998). *West Midlands Permo-Triassic Sandstones Water Resources Study*. Entec UK Ltd on behalf of the Environment Agency.

Spears, D. A. and M. J. Reeves (1975). "The influence of superficial deposits on groundwater quality in the Vale of York." *Quarterly Journal of Engineering Geology* 8(4): 255-269.

SRA (1972). *Shropshire Groundwater Investigation: First Report*. Severn River Authority.

SRA (1974). *Shropshire Groundwater Investigation: Second Report*. Severn River Authority.

SRA (1976). *Determination of the unconfined storage coefficient for the Triassic sandstones of the Tern development area*. Severn River Authority.

Streetly, M. (2005). *Personal communication*

Streetly, M. and M. G. Shepley (2002). *East Shropshire Permo-Triassic Sandstone Groundwater Modelling Project. Task 2: Literature Review*. Environment Agency. CR/02/176.

Streetly, M. and M. G. Shepley (2005). *East Shropshire Permo-Triassic Sandstone Groundwater Modelling Project. Task 8: Final Report*. Environment Agency. CR/02/176.

Streetly, M., H. Streetly and C. Hamilton (2002). *East Shropshire Permo-Triassic Sandstone Groundwater Modelling Project. Task 3: Water Balance Study*. Environment Agency. CR/02/176.

Streetly, M. and C. Young (2004). *East Shropshire Permo-Triassic Sandstone Groundwater Modelling Project. Task 6: Development and Refinement of Groundwater Model*. Environment Agency. CR/02/176.

STWA (1980a). *Shropshire Groundwater Scheme Soil Moisture Monitoring - Main Report*. Severn Trent Water Authority.

STWA (1980b). *Shropshire Groundwater Scheme Soil Moisture Monitoring - Technical Annexes*. Severn Trent Water Authority.

STWA (1981). *Shropshire Groundwater Scheme Soil Moisture Monitoring - Final Summary Report*. Severn Trent Water Authority.

STWA (1982). *Shropshire Groundwater Scheme Technical Annex 1: Soil Survey*. Severn Trent Water Authority.

- Taylor, B. J. (1958). "Cemented shear-planes in the Pleistocene Middle Sands of Lancashire and Cheshire." *Proceedings of the Yorkshire Geological Society* 31: 359-366.
- Taylor, S. A. and G. M. Ashcroft (1972). *Physical Edaphology*. San Francisco, California, Freeman and Co.
- Thomas, G. S. P. (1989). "The Late Devensian glaciation along the western margin of the Cheshire-Shropshire lowland." *Journal of Quaternary Science* 4(2): 167-181.
- Tindall, J. A. and J. R. Kunkel (1999). *Unsaturated zone hydrology for scientists and engineers*. New Jersey, Prentice Hall.
- Todd, D. K. (1959). *Ground Water Hydrology*. New York, John Wiley and Sons Inc.
- Trudgill, S. T. (1987). "Soil water dye tracing, with special reference to the use of Rhodamine WT, Lissamine FF and Amino G Acid." *Hydrological Processes* 1: 149-170.
- University of Birmingham (1981). Final Report to the North West Water Authority. Saline Groundwater Investigation: Phase 1 Lower Mersey Basin.
- van der Kamp, G. (2001). "Methods for determining the in-situ hydraulic conductivity of shallow aquitards - an overview." *Hydrogeology Journal* 9(1): 5-16.
- van Genuchten, M. T. (1980). "A closed-form equation for predicting the hydraulic conductivity of unsaturated soils." *Soil Sci. Soc. Am. J.* 44: 892-898.
- Villholth, K. G. and K. H. Jensen (1998b). "Flow and transport processes in a macroporous subsurface-drained glacial till soil II. Model analysis." *Journal of Hydrology* 207: 121-135.
- Villholth, K. G., K. H. Jensen and J. Fredericia (1998a). "Flow and transport processes in a macroporous subsurface-drained glacial till soil I. Field investigations." *Journal of Hydrology* 207: 98-120.
- Visvalingham, M. (1974). "Well-point techniques and the shallow water table in boulder clay." *Journal of Soil Science* 25(4): 505-516.
- Vries, J. J. and I. Simmers (2002). "Groundwater recharge: an overview of processes and challenges." *Hydrogeology Journal* 10(1): 5-17.
- Wagner, B., V. R. Tarnawski, V. Hennings, U. Muller, G. Wessolek and R. Plagge (2001). "Evaluation of pedo-transfer functions for unsaturated soil hydraulic conductivity using an independent data set." *Geoderma* 102: 275-297.
- Walker, J. P., G. R. Willgoose and J. D. Kalma (2004). "In situ measurements of soil moisture: a comparison of techniques." *Journal of Hydrology* 293: 85-99.
- Walley, W. J. and P. D. Hedges (1979). *The effect of groundwater drawdown upon available soil moisture*. University of Aston.

Wealthall, G. P., A. Brandon, S. D. J. Inglethorpe and D. C. Entwistle (1997). *The hydrogeological characterisation of glacial till and glacio-lacustrine sediments in Shropshire*. British Geological Survey. R&D Technical Report W29.

Wesseling, J. G., J. A. Elbers, P. Kabat and B. J. van den Broek (1991). *SWATRE: instructions for input, Internal Note*. Winand Staring Centre.

Wheater, H. S. and D. J. Sherratt (1983). *Shropshire Groundwater Recharge Estimation*. Imperial College.

Whittaker, J. E. (2004). *Personal Communication*

Williams, R. (1967). "The influence of joints on the movement of groundwater through glacial till." *Journal of Hydrology* 5: 163-170.

Wills, L. J. (1924). "The development of the Severn valley in the neighbourhood of Ironbridge and Bridgnorth." *Quarterly Journal of the Geological Society of London* 80: 274-314.

Worsley, P. (1975). An appraisal of the Glacial Lake Lapworth concept. *Environment, Man and Economic Change*. Eds. A. D. M. Philips and B. J. Turton. London, Longman: 90-118.

Wosten, J. H. M., P. A. Finke and M. J. W. Jansen (1995). "Comparison of class and continuous pedotransfer functions to generate soil hydraulic characteristics." *Geoderma* 66: 227-237.

Xu, M. and Y. Eckstein (1995). "Use of a weighted least squares method in evaluation of the relationship between dispersivity and field scale." *Ground Water* 33: 905-908.

Yates, E. M. and F. Moseley (1967). A Contribution to the Glacial Geomorphology of the Cheshire Plain. The Institute of British Geographers Transactions and Papers.

Zheng, C. and P. P. Wang (1999). *MT3DMS: A modular three-dimensional multispecies transport model for simulation of advection, dispersion and chemical reactions of contaminants in groundwater systems; Documentation and user guide*. U.S. Army Corps of Engineers, Contract Report SERDP-99-1.

Zhou, Q. Y., J. Shimada and A. Sato (2002). "Temporal variations of the three dimensional rainfall infiltration process in heterogeneous soil." *Water Resources Research* 38(4): 1030.

# APPENDICES

The Appendices for the thesis are as follows:

**Appendix 1** Baseflow Separation Code

**Appendix 2** Geological Logs of Core Material

**Appendix 3** Core Photographs and Auger Hole Logs

**Appendix 4** Input and Output Files for ERT Forward Model

**Appendix 5** Scripts for ERT Time Series Processing

**Appendix 6** ERT Time Series Images for Survey Lines 1B and 2Y

**Appendix 7** Introduction to FAT3D-UNSAT

**Appendix 8** Site 1 Model Input and Output Files

**Appendix 9** Site 2 Model Input and Output Files

**Appendix 10A** List of conference papers based on research for the thesis

**Appendix 10B** Conference papers based on research for the thesis

Appendices 1, 3 to 6 and 8 to 10B are included on a CD in the sleeve attached to the back cover of the thesis. Each appendix is filed in a separate folder which includes a 'README' file (e.g. README\_Appendix1.txt). This file lists the directory structure of, and briefly describes each file contained within, the relevant appendix.

A second CD labelled 'Supplementary Data' is also included with the thesis. This includes a digital form of data presented in the thesis, and various supplementary data not included in the thesis but which may be of interest to other researchers working in this field of study or geographical area.

Appendices 2, 7 and 10A, the only printed appendices, now follow in turn.

## **APPENDIX 2**

### **GEOLOGICAL LOGS OF CORE MATERIAL**

Geological logs are presented for the following cores:

**S1\_1** (4 pages)

**S1\_2** (4 pages)

**S1\_3** (2 pages)

**S2\_1** (4 pages)

**S2\_2** (4 pages)

**S2\_3** (4 pages)

**S2\_4** (3 pages)

# APPENDIX 7

## INTRODUCTION TO FAT3D-UNSAT

### DESCRIPTION

#### Authorship

FAT3D-UNSAT was written by Professor Rae Mackay of the University of Birmingham (Hydrogeology Group, Department of Earth Sciences).

#### Function

FAT3D-UNSAT models numerically the movement of water in the unsaturated zone in a soil/geological profile. The soil can be heterogeneous. Suitable boundary conditions have to be applied at the top and bottom of the modelled profile. Excess water applied at the top boundary can pond on the soil surface. Evaporation from bare ground and a vegetated surface can be modelled. At this stage, vegetative uptake is specified by an extraction function.

#### Conceptual Components

FAT3D-UNSAT makes certain assumptions about the physical system that require explanation in order to make best use of the code. These are listed below:

All soils are assumed to possess a single porosity with respect to flow (i.e. a porous medium model).

- Transitions between soil properties are assumed to be abrupt.

- Flow in the pores is assumed to be Darcian with the hydraulic conductivity modified only by the moisture content in the pores.
- Hysteresis in the variation of pore water pressure and hydraulic conductivity with soil moisture content is ignored.
- The soil water is assumed to be isothermal, and incompressible.
- The soil grains are assumed to be rigid and static.
- All air in the profile is assumed to have a constant pressure equal to the atmospheric pressure.
- Barometric effects are ignored.
- All chemical and biological processes are ignored.
- Flow is three dimensional and hydraulic properties are permitted to be anisotropic with the major and minor axes aligned with the finite difference mesh axes.
- Air is assumed to be entirely displaced during the wetting up of the soil to saturation.

## **MATHEMATICAL MODEL**

The mathematical model adopts the 3D equivalent of Richards' equation for soil water flow, which is based on the mass balance and Darcy's Law. Richards' equation can be written as follows:

$$\frac{d}{dx} \left( K_x \frac{dh}{dx} \right) + \frac{d}{dy} \left( K_y \frac{dh}{dy} \right) + \frac{d}{dz} \left( K_z \frac{dh}{dz} \right) + \frac{dK}{dz} + q_s + C(h_b - h) = \frac{d\theta}{dh} \frac{dh}{dt} \quad (1)$$

where:

$K_i$  = hydraulic conductivity in the  $i$ 'th orientation, which depends only on the moisture

content  $K_i = K_i(\theta)$  [LT<sup>-1</sup>]

$z$  = elevation above datum.. Positive is upwards [L]

$h$  = pressure head in the water which depends on the moisture content  $h(\theta)$  [L]

$\theta$  = moisture content [-]

$q_s$  = source or sink flows per unit volume [1/T]

$h_b$  = boundary head [L]

$C$  = boundary head conductance [1/LT]

When the soil is unsaturated the pressure head is less than zero, when the pressure head is greater than equal to zero the soil is saturated.

The soil moisture characteristic equations  $K(\theta)$  and  $h(\theta)$  are those developed by van Genuchten and are written as follows:

The saturation of the soil is given by

$$s = \frac{(\theta - \theta_r)}{(\theta_s - \theta_r)} \quad (2)$$

where

$s$  = degree of saturation ( $0 \leq s \leq 1$ ) [-]

$\theta$  = moisture content [-]

$\theta_s$  = saturated moisture content [-]

$\theta_r$  = residual moisture content [-]

The permeability of the soil is given by

$$K(s) = K_{sat} s^{1/2} \left( 1 - \left( 1 - s^{n/(n-1)} \right)^{(n-1)/n} \right)^2 \quad (3)$$

where

$K_{sat}$  = Saturated hydraulic conductivity [LT-1]

$n$  = van Genuchten shape parameter [-]

The tension head (the negative of the pressure head) is given by

$$\psi(s) = \frac{\left( s^{-1/m} - 1 \right)^{1/n}}{\alpha} \quad (4)$$

where

$\psi(s)$  = the tension characteristic =  $-h(s)$  [L]

$m = (n-1)/n$  = van Genuchten shape parameter [-]

$\alpha$  = van Genuchten Scale parameter

Equation 1 is solved subject to appropriate initial and boundary conditions.

Initial conditions can be defined in terms of either moisture content or pressure head as follows:

$$h(x,y,z,t) \quad [\{x,y,z\} \in R, t=0]$$

$$\theta(x,y,z,t) \quad [\{x,y,z\} \in R, t=0]$$

where

$R$  = modelled region [L]

Boundary conditions can be specified as time dependent pressure head, seepage, or flux at any point in the model domain. Ponding can be permitted to take place on cells or excess moisture on cells corresponding to the ground surface can be controlled to runoff from the modelled region.

Units are only required to be standard SI units. All parameters adopt the same units.

## **NUMERICAL MODEL**

A block centred finite difference approximation is applied with variable dimensions permitted in the three cell directions. Cells in the 3D volume can be omitted from the modelled region,  $R$ , by assigning a material code of zero.

The method of solution is by Newton Raphson iteration to account for the non-linearity of the flow balance equation. The general form of the Newton Raphson scheme is as follows:

$$\sum_{i=1}^{NCELLS} \frac{dR_i}{dh_j} \Delta h_j = -R_j \dots [1 \leq j \leq NCELLS] \quad (5)$$

where

$h_j$  = the unknown pressure head on the node centre of the cell j of the grid.

$\Delta h_j$  = pressure head correction for cell j for current iteration.

$R_j$  = the residual flow imbalance in cell j. at the start of current iteration

Equation set 5 is repetitively solved until the following convergence criterion is met or the maximum number of iterations allowed is exceeded (MAXIT):

$$\sum_{j=1}^{NCELLS} |R_j| \leq tol \quad (6)$$

where

$tol$  = tolerance on the global flow imbalance.

Timestepping is controlled by the model to vary between a given minimum and maximum depending on the degree of non-linearity of the problem. If for a given timestep, convergence is not achieved according to Equation 6 within the specified number of iterations, the timestep is reduced by a factor, RMPDN and the head changes for the timestep are recalculated. The timestep is not allowed to fall below a specified minimum timestep, TMIN. When convergence is achieved for a given timestep the next timestep is increased by a factor, RMPUP, up to the maximum timestep length, TMAX.

The model will terminate if convergence cannot be achieved at the minimum timestep.

As the timestepping is not known a priori the output of data for given timepoints is achieved by the model adjusting the timesteps to ensure that the heads for each of the specified output times are calculated at the correct time point.

Boundary conditions for the model are entered assuming a piece wise constant variation. Boundary conditions are entered for a set of specified times spanning the required period of simulation. The minimum number of condition time points for any simulation is 2. Boundary condition data are entered similarly for both the top and bottom boundaries.

Hydraulic data are defined through a set of material types and the codes (>0) for the material types are distributed over the model cells as required for the problem specified. Boundary and initial conditions are entered at the start of the model run and may be updated at the end of timeblocks or the end of timesteps. If updating does not take place the condition data from the previous timestep is assumed to apply.

## **INPUT/OUTPUT**

To facilitate operation of the code an Excel Workbook has been developed that controls the input to, execution and output from the model. The data entry on each of the sheets are identified clearly on the sheet and require no additional explanation other than the information provided in this manual. The spreadsheet can be used to import data from the model output files in time and transect format for each of the components of the water balance on a cell or cells.

# APPENDIX 10A

## LIST OF CONFERENCE PAPERS BASED ON THE RESEARCH FOR THE THESIS

Cuthbert, M. O., Mackay, R., Lawrence, A. R. and Peach, D. 2003. *Understanding regional and local scale hydraulic processes controlling recharge through drift*. Geophysical Research Abstracts Volume 5, EGS-AGU-EUG Joint Assembly 2003, EAE03-A-12910.

Cuthbert, M. O., Mackay, R., and Barker, R. D. 2004. *The use of electrical resistivity tomography (ERT) in deriving recharge models for a drift covered catchment*. Geophysical Research Abstracts Volume 6, EGU General Assembly 2004, EGU04-A-05080.

Cuthbert, M. O., E. J. F. Russell, R. D. Barker and R. Mackay (2004). *The effect of seasonal temperature variations on the resistivity of glacial till*. Near Surface 2004 - 10th European Meeting of Environmental and Engineering Geophysics, Utrecht, The Netherlands, EAGE. PO32 1-4.

Cuthbert, M. O., R. Mackay, J. H. Tellam and A. J. Humpage (2004). *Local and regional scale controls on recharge in a drift covered catchment*. Groundwater Flow Understanding: from local to regional scales, IAH XXXIII Congress, Zacatecas, Mexico, IAH. T513, 1-4.

Mackay, R., M. O. Cuthbert, H. Ash and J. H. Tellam (2005). *Towards an up-scaled model of aquifer recharge through glacial drift deposits, Shropshire, UK*. Model Care 2005 Conference Proceedings, The Hague, The Netherlands.